United States
Environmental Protection
Agency
Air

Office of Air Quality
Planning and Standards
Research Triangle Park, NC 27711

EPA-454/R-98-012
May 1998

GUIDANCE FOR USING CONTINUOUS MONITORS IN $PM_{2.5}$ MONITORING NETWORKS

GUIDANCE FOR USING CONTINUOUS MONITORS IN $PM_{2.5}$ MONITORING NETWORKS

May 29, 1998

PREPARED BY

John G. Watson[1]
Judith C. Chow[1]
Hans Moosmüller[1]
Mark Green[1]
Neil Frank[2]
Marc Pitchford[3]

PREPARED FOR

Office of Air Quality Planning and Standards
U.S. Environmental Protection Agency
Research Triangle Park, NC 27711

[1]Desert Research Institute, University and Community College System of Nevada, PO Box 60220, Reno, NV 89506
[2]U.S. EPA/OAQPS, Research Triangle Park, NC, 27711
[3]National Oceanic and Atmospheric Administration, 755 E. Flamingo, Las Vegas, NV 89119

DISCLAIMER

The development of this document has been funded by the U.S. Environmental Protection Agency, under cooperative agreement CX824291-01-1, and by the Desert Research Institute of the University and Community College System of Nevada. Mention of trade names or commercial products does not constitute endorsement or recommendation for use. This draft has not been subject to the Agency's peer and administrative review, and does not necessarily represent Agency policy or guidance.

ABSTRACT

This guidance provides a survey of alternatives for continuous *in-situ* measurements of suspended particles, their chemical components, and their gaseous precursors. Recent and anticipated advances in measurement technology provide reliable and practical instruments for particle quantification over averaging times ranging from minutes to hours. These devices provide instantaneous, telemetered results and can use limited manpower more efficiently than manual, filter-based methods. Commonly used continuous particle monitors measure inertial mass, mobility, electron attenuation, light absorption, and light scattering properties of fine particles. Sulfur and nitrogen oxides monitors can detect sulfate and nitrate particles when the particles are reduced to a sulfur- or nitrogen-containing gas. The measurement principles, as well as the operating environments, differ from those of the $PM_{2.5}$ Federal Reference Method (FRM), and these differences vary between monitoring locations and time of year. These variations are caused by the different properties quantified by a wide array of measurement methods, modification of the aerosol by the sampling and analysis train, and differences in calibration methods. When the causes of these discrepancies are understood, they can be used advantageously to determine where and when: 1) equivalence with FRMs is expected; 2) mathematical adjustments can be made to obtain a better correlation; and 3) differences can be related to a specific particle or source characteristic.

TABLE OF CONTENTS

Page

Disclaimer ii

Abstract iii

Table of Contents iv

List of Tables vii

List of Figures viii

List of Acronyms xi

1. INTRODUCTION 1-1
   1.1 Continuous Particle Monitors and Air Pollution 1-1
   1.2 Federal Reference and Equivalent Methods 1-3
   1.3 Relevant Documents 1-4

2. MEASURED PARTICLE PROPERTIES 2-1
   2.1 Particle Size Distribution 2-1
   2.2 Chemical Composition 2-5
   2.3 Particle Interactions with Light 2-15
   2.4 Mobility 2-16
   2.5 Beta Attenuation 2-16
   2.6 Summary 2-18

3. CONTINUOUS PARTICLE MEASUREMENT METHODS 3-1
   3.1 Mass and Mass Equivalent 3-1
      3.1.1 Tapered Element Oscillating Microbalance (TEOM®) 3-1
      3.1.2 Piezoelectric Microbalance 3-12
      3.1.3 Beta Attenuation Monitor (BAM) 3-13
      3.1.4 Pressure Drop Tape Sampler (CAMMS) 3-14
   3.2 Visible Light Scattering 3-14
      3.2.1 Nephelometer 3-14
      3.2.2 Optical Particle Counter (OPC) 3-19
      3.2.3 Condensation Nuclei Counter (CNC) 3-19
      3.2.4 Aerodynamic Particle Sizer (APS) 3-20
      3.2.5 LIght Detection And Ranging (LIDAR) 3-22
   3.3 Visible Light Absorption 3-23
      3.3.1 Aethalometer and Particle Soot/Absorption Photometer 3-24
      3.3.2 Photoacoustic Spectroscopy 3-25
   3.4 Electrical Mobility 3-26
      3.4.1 Electrical Aerosol Analyzer (EAA) 3-26
      3.4.2 Differential Mobility Particle Sizer (DMPS) 3-26

TABLE OF CONTENTS (continued)

Page

3.5 Chemical Components....3-27
3.5.1 Single Particle Mass Spectrometers....3-27
3.5.2 Carbon Analyzer....3-28
3.5.3 Sulfur Analyzer....3-29
3.5.4 Nitrate Analyzer....3-30
3.5.5 Multi-Elemental Analyzer....3-31
3.5.5.1 Streaker....3-31
3.5.5.2 DRUM....3-31
3.6 Precursor Gases....3-32
3.6.1 Ammonia Analyzer....3-32
3.6.2 Nitric Acid Analyzer....3-33
3.6.3 Fourier Transform Infrared (FTIR) Spectroscopy....3-33
3.6.4 Other Nitric Acid Instruments....3-34
3.7 Summary....3-35

4. MEASUREMENT PREDICTABILITY, COMPARABILITY, AND EQUIVALENCE....4-1
4.1 Measurement Comparability....4-3
4.2 Measurement Predictability....4-15
4.2.1 Particle Light Scattering and $PM_{2.5}$ Concentration....4-15
4.2.2 Particle Light Absorption and Elemental Carbon Concentration....4-17
4.2.3 Mass Concentration and Optical Measurements....4-21
4.3 Summary....4-29

5. USES OF CONTINUOUS PM MEASUREMENTS....5-1
5.1 Diurnal Variations....5-2
5.2 Wind Speed and PM Relationships....5-4
5.3 Source Directionality....5-8
5.4 Receptor Zones of Representation and Source Zones of Representation....5-19
5.5 Summary....5-19

6. CONTINUOUS PARTICLE MONITORING IN $PM_{2.5}$ NETWORKS....6-1
6.1 $PM_{2.5}$ Network Site Types....6-1
6.2 Federal Reference and Equivalent Methods....6-2
6.3 Potential Tolerances for FEM and CAC Monitor Designation....6-4

7. REFERENCES....7-1

APPENDIX A: CONTINUOUS MEASUREMENT DATA SETS....A-1
A.1 Southern California Air Quality Study (SCAQS)....A-1
A.2 1995 Integrated Monitoring Study (IMS95)....A-2
A.3 1997 Southern California Ozone Study (SCOS97) – North American Research Strategy for Tropospheric Ozone (NARSTO)....A-2

TABLE OF CONTENTS (continued)

Page

A.4 San Joaquin Valley Compliance Network A-3
A.5 Imperial Valley/Mexicali Cross Border PM_{10} Transport Study A-4
A.6 Washoe County (Nevada) Compliance Network A-5
A.7 Las Vegas PM_{10} Study A-5
A.8 Northern Front Range Air Quality Study (NFRAQS) A-6
A.9 Mount Zirkel Visibility Study A-7
A.10 Robbins Particulate Study A-8
A.11 Birmingham (Alabama) Compliance Network A-8
A.12 Mexico City Aerosol Characterization Study A-8

LIST OF TABLES

		Page
Table 2-1	Measured Aerosol Concentrations for the 19 Regions in the IMPROVE Network from March 1988 to February 1991	2-12
Table 3-1	Summary of Continuous Monitoring Technology	3-2
Table 3-2	Operating Characteristics of Commercially Available Nephelometers	3-17
Table 3-3	Comparison of Condensation Nuclei Counter Specifications	3-22
Table 4-1	Test Specifications for $PM_{2.5}$ Equivalence to Federal Reference Method	4-2
Table 4-2	Collocated Comparisons between Continuous and Filter-Based $PM_{2.5}$ or PM_{10} Monitors from Recent Aerosol Characterization Studies	4-6
Table 4-3	$PM_{2.5}$ Mass Scattering Efficiency (m^2/g) as a Function of Relative Humidity (%)	4-18
Table 4-4	Relationships between Optical Measurements and PM Concentrations	4-22
Table 5-1	Cross-Border Fluxes at the Calexico Site	5-12
Table 5-2	Distibution of Hourly PM_{10} and SO_2 Concentrations at Robbins, IL, as a Function of Wind Speed and Wind Direction	5-15

LIST OF FIGURES

		Page
Figure 2-1	Particle size range of aerosol properties and measurement instruments – application range of aerosol instruments.	2-2
Figure 2-2	Size range of aerosol properties.	2-3
Figure 2-3	Example of particle number, surface area, and volume size distribution in the atmosphere.	2-4
Figure 2-4	Representative mass size distribution with measured particle size fractions and dominant chemical components.	2-6
Figure 2-5	Changes in liquid water content of sodium chloride, ammonium nitrate, ammonium sulfate, and a combination of compounds at different relative humidities.	2-9
Figure 2-6	Fraction of total nitrate as particulate ammonium nitrate at different temperatures for various relative humidities and ammonia/nitrate molar ratios.	2-11
Figure 2-7	Ammonium sulfate particle scattering efficiency as a function of particle diameter.	2-17
Figure 2-8	Particle absorption efficiencies as a function of elemental carbon particle diameter for several densities (first number in legend), real and imaginary indices of refraction (second and third numbers in legend).	2-17
Figure 3-1	Particle scattering efficiency (σ_{sp}) as function of particle diameter for silica particles (δ = 2.2 g/cm^3, n = 1.46 at 550 nm) and monochromatic green light (λ = 550 nm).	3-19
Figure 4-1	Collocated comparisons of 24-hour-averaged TEOM and BAM with high-volume SSI for PM_{10} measurements acquired in Central California between 1988 and 1993.	4-4
Figure 4-2	Collocated comparison of 24-hour-averaged TEOM and high-volume SSI PM_{10} during winter and summer at the Bakersfield and Sacramento sites in Central California between 1988 and 1993.	4-5
Figure 4-3	Collocated comparison of three-hour $PM_{2.5}$ SFS with $PM_{2.5}$ TEOM at the Bakersfield site, as well as $PM_{2.5}$ and PM_{10} SFS with BAM at the Chowchilla site in California's San Joaquin Valley between 12/09/95 and 01/06/96.	4-8

LIST OF FIGURES (continued)

		Page
Figure 4-4	Collocated comparisons of 24-hour PM_{10} with BAM versus high-volume SSI, medium-volume SFS, low-volume dichotomous, and mini-volume portable samplers in Imperial Valley, CA, between 03/13/92 and 08/29/93.	4-10
Figure 4-5	Collocated comparisons of 24-hour-averaged PM_{10} BAM versus SFS and portable samplers in Las Vegas Valley, NV, between 01/03/95 and 01/28/96.	4-12
Figure 4-6	Collocated comparison of 6- and 12-hour PM_{10} BAM versus SFS in north Denver, CO, during winter and summer 1996.	4-13
Figure 4-7	Collocated comparison of 24-hour PM_{10} BAM versus high-volume SSI and dichotomous samplers in southeastern Chicago, IL, between 10/12/95 and 09/30/96.	4-14
Figure 4-8	Relationship between hourly particle light scattering (b_{sp}) measured by nephelometer and ambient relative humidity in San Joaquin Valley, CA, between 12/09/95 and 01/06/96.	4-16
Figure 4-9	Relationship between $PM_{2.5}$ light absorption (b_{ap}) measured by densitometer on Teflon-membrane filter and elemental carbon measured by thermal/optical reflectance on a co-sampled quartz-fiber filter for three-hour samples acquired in San Joaquin Valley, CA, between 12/09/95 and 01/06/96.	4-19
Figure 4-10	Relationship between filter-based $PM_{2.5}$ SFS elemental carbon (measured by thermal/optical reflectance on quartz-fiber filter) and aethalometer black carbon on three-hour samples acquired in the San Joaquin Valley between 12/09/95 and 01/06/96.	4-20
Figure 5-1	Winter weekday and weekend patterns in PM_{10} concentrations during summer (April to September 1995) and winter (October 1995 to March 1996) periods at a mixed light industrial/suburban site in the Las Vegas Valley, NV.	5-3
Figure 5-2	Weekday and weekend patterns for 50th percentile PM_{10} concentrations at the City Center and East Charleston (Microscale) urban center sites and Bemis/Craig and Walter Johnson urban periphery sites during Winter 1995 in the Las Vegas Valley, NV.	5-5
Figure 5-3	Diurnal variations of hourly BAM PM_{10} concentrations at a monitoring site in Calexico, CA, near the U.S./Mexico border during 03/12/92 to 08/29/93.	5-6

LIST OF FIGURES (continued)

		Page
Figure 5-4	Relationships between BAM PM_{10} and wind speed for northerly flow.	5-7
Figure 5-5	Relationships between BAM PM_{10} and wind speed for southerly flow.	5-7
Figure 5-6	Distribution of hourly BAM PM_{10} as a function of wind speed at 14 meteorological sites in the Las Vegas Valley, NV, monitoring network between 01/01/95 and 01/31/96.	5-9
Figure 5-7	Relationship between hourly averaged wind speed and PM_{10} concentrations at a North Las Vegas, NV, site (Bemis) during the period of 04/08/95 to 04/09/95.	5-10
Figure 5-8	Distribution of hourly PM_{10} concentrations as a function of wind speed at a southeastern Chicago, IL, site (Eisenhower) during the first three quarters of 1996.	5-11
Figure 5-9	PM_{10} concentrations at the 20th, 50th, and 80th percentiles at a southeastern Chicago, IL, site (Eisenhower) during the first three quarters of 1996.	5-13
Figure 5-10	Hourly $PM_{2.5}$ elemental concentrations (ng/m^3) at three southeastern Chicago, IL, sites near Robbins, IL, averaged by wind sector for one week apiece during the first three calendar quarters of 1996.	5-16
Figure 5-11	Five-minute-average aethalometer black carbon measurements at a downtown (MER) site and a suburban (PED) site in Mexico City.	5-20

LIST OF ACRONYMS

°C	degrees Celsius
µg	microgram
µm	micron or micrometer
ACPM	Ambient Carbon Particulate Monitor
ACS	American Chemical Society
AIRS	Aerometric Information Retrieval System
AMTIC	Ambient Monitoring Technology Information Center
APNM	Automated Particle Nitrate Monitor
APS	Aerodynamic Particle Sizer
ASTM	American Society for Testing Materials
ATOFMS	Aerosol Time Of Flight Mass Spectrometry
b_{abs}	light absorption
BAM	Beta Attenuation Monitor
b_{ap}	particle light absorption
BC	black carbon
b_{ext}	light extinction
b_{sp}	particle light scattering
CAC	Correlated Acceptable Continuous
CAMMS	Continuous Ambient Mass Monitoring System
CFR	Code of Federal Regulations
CIMS	Chemical Ionization Mass Spectrometry
CMZ	Community Monitoring Zone
CNC	Condensation Nuclei Counter

LIST OF ACRONYMS (continued)

CO	carbon monoxide
CO_2	carbon dioxide
COH	Coefficient Of Haze
CORE	Community-Oriented site (or COmmunity-REpresentative site)
DIAL	DIfferential Absorption Lidar
DIC	DIChotomous sampler
DMPS	Differential Mobility Particle Sizer
DOAS	Differential Optical Absorption Spectroscopy
DRUM	Davis Rotating-drum Universal-size-cut Monitoring impactor
EAA	Electrical Aerosol Analyzer
EC	elemental carbon
FEM	Federal Equivalent Method
FPD	Flame Photometric Detector
FRM	Federal Reference Method
FTIR	Fourier Transform InfraRed spectroscopy
H_2SO_4	sulfuric acid
HNO_3	nitric acid
IC	Ion Chromatography
IMPROVE	Interagency Monitoring of PROtected Visual Environments
km	kilometer
L/min	liter per minute
LAMMS	Laser Microprobe Mass Spectrometer
LED	Light Emitting Diode

LIDAR	LIght Detecting And Ranging
LPFF	Laser Photolysis Fragment Fluorescence
m	meter
m^3	cubic meter
mm	millimeter
Mm^{-1}	inverse megameters
MPA	Metropolitan Planning Area
MS	Mass Spectrometry
MSA	Metropolitan Statistical Area
mW	milliwatt
NAAQS	National Ambient Air Quality Standards
NAMS	National Air Monitoring Stations
Nd:YAG	Neodymium Yttrium Aluminum Garnet
NFRAQS	Northern Front Range Air Quality Study [Colorado]
NH_3	ammonia
NH_4^+	ammonium
NH_4HSO_4	ammonium bisulfate
NH_4NO_3	ammonium nitrate
$(NH_4)_2SO_4$	ammonium sulfate
NIST	National Institute for Standards and Technology
nm	nanometer
NO_2	nitrogen dioxide
NO_3^-	nitrate

LIST OF ACRONYMS (continued)

NO_X	nitrogen oxides
NPS	National Park Service
OAQPS	Office of Air Quality Planning and Standards [U.S. Environmental Protection Agency]
OC	organic carbon
OPC	Optical Particle Counter
ORD	Office of Research and Development [U.S. Environmental Protection Agency]
PALMS	Particle Analysis by Laser Mass Spectrometry
PM	suspended Particulate Matter
PM_{10}	suspended Particulate Matter with aerodynamic diameters less than 10 microns (µm)
$PM_{2.5}$	suspended Particulate Matter with aerodynamic diameters less than 2.5 microns (µm)
ppb *or* ppbv	parts per billion volume
ppt *or* pptv	parts per trillion volume
PSAP	Particle Soot/Absorption Photometer
RH	Relative Humidity
RSMS	Rapid Single-particle Mass Spectrometer
S	sulfur
SLAMS	State/Local Air Monitoring Stations
SMPA	Scanning Mobility Particle Analyzer
SO_2	sulfur dioxide
$SO_4^=$	sulfate
SPM	Special Purpose Monitor
SSI	Size-Selective Inlet

LIST OF ACRONYMS (continued)

TDLAS	Tunable Diode Laser Absorption Spectroscopy
TEOM	Tapered Element Oscillating Microbalance
TSP	Total Suspended Particles
U.S. EPA	U.S. Environmental Protection Agency
WINS	Well Impactor Ninety-Six $PM_{2.5}$ inlet

1. INTRODUCTION

This guidance describes available continuous monitoring methods for suspended particles. Some of these methods are candidates for Correlated Acceptable Continuous (CAC) monitors that might be used in parallel with filter-based samplers to reduce sampling frequencies for $PM_{2.5}$ (fraction of particles with aerodynamic diameters less than 2.5 µm) (U.S. EPA, 1997a, 1997b). The guidance describes: 1) properties of suspended particles that can be measured; 2) available devices to measure these properties over durations of one-hour or less; 3) conditions under which continuous monitor measurements might or might not be correlated with or predictors of filter-based particle concentrations; and 4) how continuous measurements can be used to attain a variety of monitoring objectives.

The relevant NAAQS are (U.S. EPA, 1997c, 1997d):

- Twenty-four hour average $PM_{2.5}$ not to exceed 65 µg/m^3 for a three-year average of annual 98th percentiles at any population-oriented monitoring site in a Metropolitan Planning Area (MPA).

- Three-year annual average $PM_{2.5}$ not to exceed 15 µg/m^3 at a single community-oriented monitoring site or for the spatial average of eligible community exposure sites in a MPA.

- Twenty-four hour average PM_{10} (particles with aerodynamic diameters less than 10 µm) not to exceed 150 µg/m^3 for a three-year average of annual 99th percentiles at any site in a monitoring area.

- Three-year average of three annual average PM_{10} concentrations not to exceed 50 lµg/m^3 at any site in a monitoring area.

This section states the background, federally specified monitoring methods, and objectives of this continuous monitoring guidance document. Section 2 describes the chemical and physical properties of particulate matter (PM) that are measured by different continuous monitoring techniques. Section 3 specifies the measurement principles, averaging periods, detection limits, and potential uses of existing continuous monitoring instruments. Section 4 examines available collocated comparisons between continuous particle monitors and filter samplers to determine the degree to which they are correlated in different environments. Section 5 provides guidance and examples for using continuous $PM_{2.5}$ measurements to address source/receptor relationships. Section 6 describes how continuous particle monitors might be used in $PM_{2.5}$ networks to supplement filter measurements. Cited references and resources that provide more detail on specific topics are assembled in Section 7. Data bases, assembled from collocated filter and continuous $PM_{2.5}$ and PM_{10} measurements in past air quality studies, are provided in Appendix A.

1.1 Continuous Particle Monitors and Air Pollution

Continuous particle measurements have been made since the early days of air pollution monitoring. The British Smoke Shade measurement was established as a

continuous monitoring device in London during the 1920s to quantify the darkening of filter material as air was drawn through it (Brimblecombe, 1987; Thornes, 1978). It evolved into a more automated and reproducible particle concentration measurement during the ensuing decades (Hill, 1936; Ingram and Golden, 1973). In the United States, the principle of light absorption by particles was implemented in the form of Coefficient of Haze (COH) measured by the American Iron and Steel Industry's paper tape sampler (Hemeon et al., 1953; ASTM, 1985; Herrick et al., 1989).

In these early measurements, visible light (generated by an incandescent bulb) was transmitted through (or reflected from in the case of the British Smoke method) a section of filter paper before and after ambient air is drawn through it. The optical density of the particle deposit was determined from the logarithm of the ratio of intensities measured on the filter with and without the deposit. In its most advanced implementation, a clean portion of a filter tape was periodically moved into the sampling position, thereby allowing diurnal variations (typically hourly averages) in particle concentrations to be recorded. While these methods provide a good measure of light absorption by suspended particles (Edwards et al., 1984), they do not account for the portion of aerosol mass that does not absorb light (Ball and Hume, 1977; Barnes, 1973; Waller, 1963; Waller et al., 1963; Lee et al., 1972; Lodge et al., 1981). The particle size collection characteristics of the British Smoke Shade sampler were not understood until the late 1970s (McFarland, 1979), when the instrument was found to collect particles with aerodynamic diameters less than ~ 5 µm.

In spite of this specificity to light absorbing aerosol, the original epidemiological associations between particles and health were established from these light absorption measurements. Several of these health associations were used to justify the previous TSP (Total Suspended Particles, particles with aerodynamic diameters less than 30 µm) (U.S. Dept. HEW, 1969; Hemeon, 1973) and PM_{10} NAAQS (U.S. EPA, 1982, 1987). These early continuous measurements illustrate that a variety of particle indicators, including particle mass and light absorption, can be associated with health end-points even though their measured quantities are not the same. More recent health studies (U.S. EPA, 1996; Vedal, 1997) confirm positive correlations between a variety of particle indicators, several of which derive from continuous measurement methods, and health end-points.

Continuous *in-situ* monitors have been used to acquire consecutive hourly-averaged concentrations of mass, mass surrogates, chemical components, and precursor gases. Continuous monitors contrast with "manual" measurements that draw air through an absorbing substrate or filter medium that retains atmospheric pollutants for later laboratory analysis. Since the promulgation of NAAQS in the early 1970s, continuous monitors have been used to measure sulfur dioxide, nitrogen dioxide, carbon monoxide, and ozone gases. Suspended particles, however, have typically been measured by filtration with subsequent laboratory weighing or chemical analysis (Chow and Watson, 1998a).

Three continuous PM_{10} monitors based on inertial mass (R&P Tapered Element Oscillating Microbalance, U.S. EPA, 1990) and electron absorption (Andersen Instruments and Wedding and Associates Beta Attenuation Monitors, U.S. EPA, 1990, 1991) have been designated as equivalent methods that can be used to determine compliance with the PM_{10} NAAQS. The PM_{10} equivalence designation (U.S. EPA, 1987) results from wind-tunnel test

specifications for the PM_{10} inlet and collocated sampling with filter-based PM_{10} reference methods at different test locations. Subsequent comparisons of these continuous monitors with each other and with filters show very good and very poor agreement, mostly depending on the aerosol being sampled (e.g., Allen et al., 1997; Arnold et al., 1992; Meyer et al., 1992; Shimp, 1988; Tsai and Cheng, 1996; van Elzakker and van der Muelen, 1989).

New $PM_{2.5}$ monitoring regulations (40 CFR 58, Appendix D, Section 2.8.1.3.8) require continuous $PM_{2.5}$ monitors to be operated in large U.S. metropolitan areas. These regulations (40 CFR Section 58.13) also define a "CAC" monitor as an optional $PM_{2.5}$ analyzer that can be used to supplement a $PM_{2.5}$ reference or equivalent sampler at community-oriented (CORE) monitoring sites to reduce sampling frequency from daily to every third day (U.S. EPA, 1997b). This alternative sampling approach is intended to provide state and local agencies with additional flexibility in designing and operating $PM_{2.5}$ networks.

The potential uses of CAC measurements are to: 1) reduce site visits and network operation costs; 2) identify the need to increase sampling frequency with a $PM_{2.5}$ reference or equivalent method in order to make better comparisons to the $PM_{2.5}$ NAAQS; 3) evaluate telemetered concentrations in real-time to issue alerts or to implement periodic control strategies (e.g., burning bans, no-drive days); 4) evaluate diurnal variations in human exposures to outdoor air; 5) define zones of representation of monitoring sites and zones of influence of pollution sources; and 6) understand the physics and chemistry of high $PM_{2.5}$ and PM_{10} concentrations.

Unless a continuous analyzer is designated as an equivalent method, its data cannot be used to determine NAAQS compliance. However, the potential discrepancies between continuous PM and manual measurements can be determined. This will permit selection of acceptable continuous methods that can be correlated with a federal reference or equivalent method.

1.2 Federal Reference and Equivalent Methods

The revised PM NAAQS represent a major change from previous standards in terms of the size fraction being measured, the averaging of concentrations over space and time, the monitoring methods used, and network design strategies. Federal Reference Method (FRM) or Federal Equivalent Method (FEM) samplers are to be used in $PM_{2.5}$ compliance monitoring networks (i.e., State and Local Air Monitoring Stations [SLAMS] and National Ambient Monitoring Stations [NAMS]). Interagency Monitoring of Protected Visual Environments (IMPROVE) samplers may also be used at regional background or regional transport sites in lieu of FRMs or FEMs. Continuous monitors can be tested and classified as Class III FEM for compliance monitoring.

Sampler design, performance characteristics, and operational requirements for the $PM_{2.5}$ FRM are specified in 40 CFR part 50, Appendix L; 40 CFR part 53, Subpart E; and 40 CFR part 58, Appendix A (U.S. EPA, 1997a-d). The $PM_{2.5}$ FRM is intended to acquire deposits over a 24-hour period on a Teflon-membrane filter from air drawn at a controlled flow rate through the Well Impactor Ninety Six (WINS) $PM_{2.5}$ inlet. The inlet and size

separation components, filter types, filter cassettes, and internal configurations of the filter holder assemblies are specified by design, with drawings and manufacturing tolerances published in 40 CFR part 53 (U.S. EPA, 1997b). Other sampler components and procedures (such as flow rate control, operator interface controls, exterior housing, data acquisition) are specified by performance characteristics, with specific test methods to assess that performance.

Federal Equivalent Methods (FEMs) are divided into several classes in order to encourage innovation and provide monitoring flexibility. Class I FEMs meet nearly all FRM specifications, with minor design changes that permit sequential sampling without operator intervention and different filter media in parallel or in series. Flow rate, inlets, and temperature requirements are identical for FRMs and Class I FEMs. Particles losses in flow diversion tubes are to be quantified and must be in compliance with Class I FEM tolerances specified in 40 CFR part 53, Subpart E (U.S. EPA, 1997b).

Class II FEMs include samplers that acquire 24-hour integrated filter deposits for gravimetric analysis, but that differ substantially in design from the reference-method instruments. These might include dichotomous samplers, high-volume samplers with $PM_{2.5}$ size-selective inlets, and other research samplers. More extensive performance testing is required for Class II FEMs than for FRMs or Class I FEMs, as described in 40 CFR part 53, Subpart F (U.S. EPA, 1997b).

Class III FEMs include samplers that do not qualify as Class I or Class II FEMS. This category is intended to encourage the development of and to permit the evaluation of new monitoring technologies that increase the specificity of $PM_{2.5}$ measurements or decrease the costs of acquiring a large number of measurements. Class III FEMs may be filter-based integrated samplers or filter- or non-filter-based *in-situ* continuous or semi-continuous samplers. Test procedures and performance requirements for Class III candidate instruments will be determined on a case-by-case basis. Performance criteria for Class III FEMs will be restrictive because equivalency to reference methods must be demonstrated over a wide range of particle size distributions and aerosol compositions.

1.3 Relevant Documents

This continuous particle monitoring guidance is complemented by other U.S. EPA documents:

- Guidance for Network Design and Optimum Site Exposure for $PM_{2.5}$ and PM_{10} – Draft Version 3. Prepared under a cooperative agreement between U.S. EPA Office of Air Quality Planning and Standards, Research Triangle Park, NC, and Desert Research Institute, Reno, NV. December 15, 1997 (Watson et al.,1997a).

- Guideline on Speciated Particulate Monitoring, Draft 2. Prepared under a cooperative agreement between U.S. EPA Office of Air Quality Planning and Standards, Research Triangle Park, NC, and Desert Research Institute, Reno, NV. February 9, 1998 (Chow and Watson, 1998a).

- Prototype $PM_{2.5}$ Federal Reference Method Field Studies Report – An EPA Staff Report. U.S. EPA Office of Air Quality Planning and Standards, Las Vegas, NV. July 9, 1997 (Pitchford et al., 1997).

- Revised Requirements for Designation of Reference and Equivalent Methods for $PM_{2.5}$ and Ambient Air Quality Surveillance for Particulate Matter – Final Rule. 40 CFR part 58. *Federal Register*, **62**(138):38830-38854. July 18, 1997 (U.S. EPA, 1997a).

- Revised Requirements for Designation of Reference and Equivalent Methods for $PM_{2.5}$ and Ambient Air Quality Surveillance for Particulate Matter – Final Rule. 40 CFR part 53. *Federal Register*, **62**(138):38763-38830. July 18, 1997 (U.S. EPA, 1997b).

- National Ambient Air Quality Standards for Particulate Matter – Final Rule. 40 CFR part 50. *Federal Register*, **62**(138):38651-38760. July 18, 1997 (U.S. EPA, 1997c).

- National Ambient Air Quality Standards for Particulate Matter; Availability of Supplemental Information and Request for Comments – Final Rule. 40 CFR part 50. *Federal Register*, **62**(138):38761-38762. July 18, 1997 (U.S. EPA, 1997d).

2. MEASURED PARTICLE PROPERTIES

Particles in the atmosphere vary in size, chemical composition, and optical properties. Airborne particle diameters range over five orders of magnitude, from a few nanometers to around 100 micrometers. Aerodynamic diameter (the diameter of spherical particles with equal settling velocity and unit density of 1 g/cm^3) is used in aerosol technology to characterize air filtration, instrument performance, and respiratory deposition. Except for spherical particles of unit density, the actual diameter or geometric mean diameter (which accounts for actual particle density and shape factors) is smaller than the commonly referenced aerodynamic diameter.

Different aerosol monitoring techniques have been developed to measure aerosol properties in different size ranges. As shown in Figure 2-1, aerosol sizes between 0.001 and 100 µm can be quantified with continuous or manual aerosol sampling instruments (Hinds, 1982; Willeke and Baron, 1993). Figure 2-2 illustrates the particle size ranges that can be measured in terms of aerosol number, surface area, volume and mass size distribution, mode of aerosol, inhalation properties, deposition mechanism, and optical features. This section discusses the chemical, physical (e.g., mobility), and optical (e.g., light scattering, light absorption) properties of aerosol.

2.1 Particle Size Distribution

Particle size is one of the key parameters in determining emission sources, atmospheric processes, formation mechanisms, deposition/removal processes, visibility impairment, as well as interactions with the human respiratory system and associated health effects. Aerosol particle sizes are often characterized by their size distributions. Figure 2-3 displays the multi-modal particle characteristics of the aerosol number, surface area, and volume distributions. Size distributions like these have been found under a wide range of environmental and emissions conditions.

The number of particles in the atmosphere can often exceed 10^7 or 10^8 for each cubic centimeter of urban or non-urban air. The top panel of Figure 2-3 shows that the largest number of particles is in the nuclei or ultrafine size fraction with particle diameters less than 0.1 µm. The number distribution exhibits a bimodal feature that peaks at ~0.02 and ~0.1 µm. Ultrafine particles are often observed near emission sources and possess a very short lifetime, with a duration of less than one hour. Ultrafine particles rapidly condense on or coagulate with larger particles or serve as nuclei for fog or cloud droplets, forming particles in the accumulation mode (0.08 to ~2 µm).

There is increasing concern regarding the potential health effects associated with inhalation of ultrafine particles. Phalen et al. (1991) showed that lung deposition peaks at 60% for ~0.03 µm particles. These high deposition levels in the upper respiratory system may aggravate symptoms of rhinitis, allergies, and sinus infections, and are associated with acute mortality (Oberdörster et al., 1995; Finlay et al., 1997). Continuous instruments that can measure particle number concentrations include the condensation nuclei counter

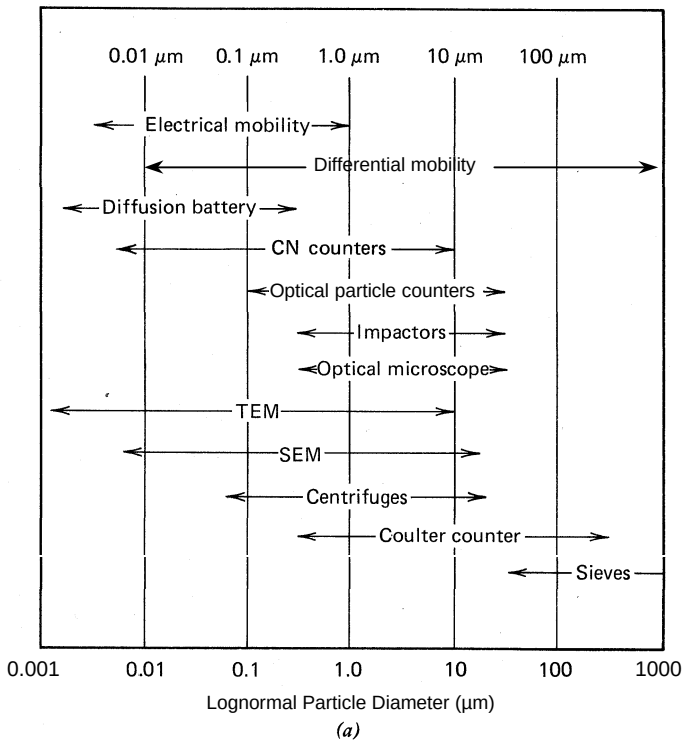

Figure 2-1. Particle size range of aerosol properties and measurement instruments – application range of aerosol instruments (modified from Hinds, 1982).

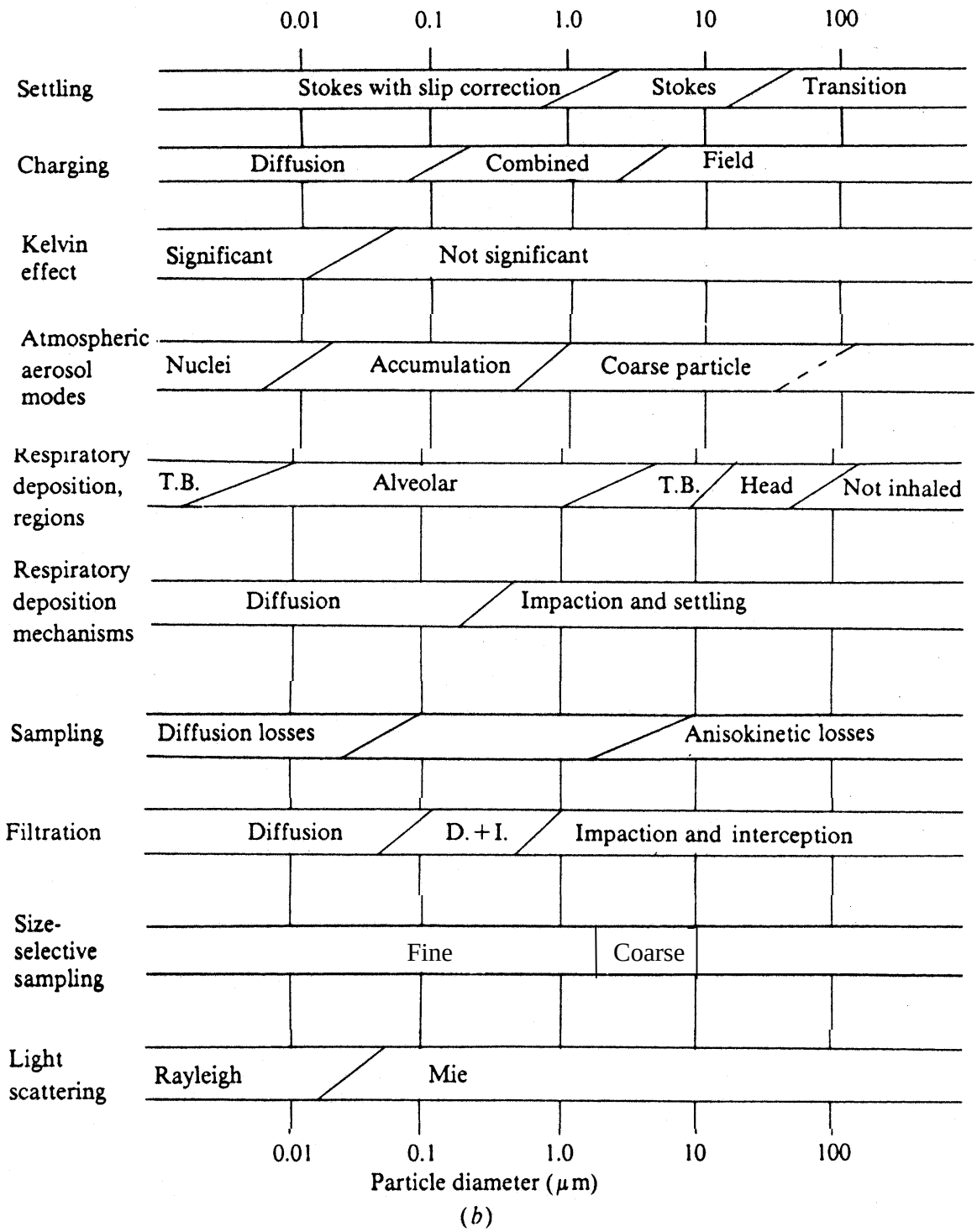

Figure 2-2. Size range of aerosol properties (modified from Hinds, 1982).

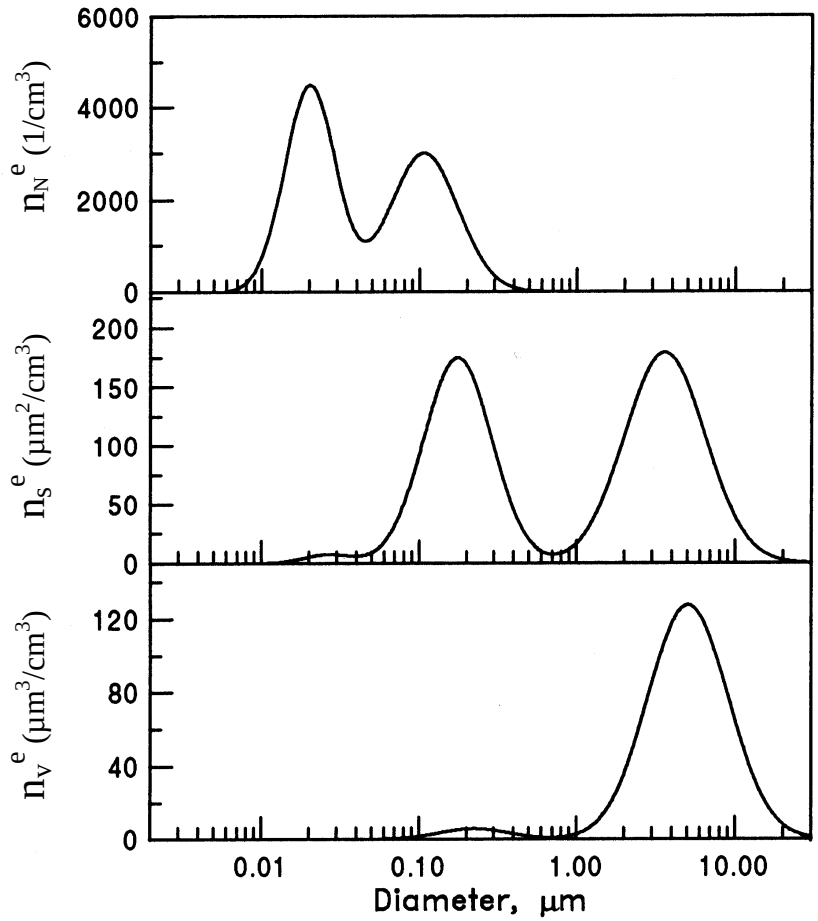

Figure 2-3. Example of particle number, surface area, and volume size distribution in the atmosphere (based on Seinfeld and Pandis, 1997).

(Pollak and Metnieks, 1959; Cheng, 1993), aerosol particle sizer (Wilson and Liu, 1980; Baron et al., 1993), differential mobility analyzer (Yeh, 1993), diffusion battery (Fuchs, 1964; Cheng, 1993), electrical aerosol analyzer (Whitby and Clark, 1966), and optical particle counter (Hodkinson, 1966; Whitby and Vomela, 1967; Sloane et al., 1991).

The surface area distribution in the middle panel of Figure 2-3 also exhibits a bimodal feature that peaks at ~0.2 and ~1.3 µm. These particles, classified as accumulation range (0.08 to ~2 µm), result from the coagulation of ultrafine particles, from condensation of volatile species, from gas-to-particle conversion, and from finely ground dust particles. Particles in the accumulation mode scatter and absorb light more efficiently than the larger particles.

Particle surfaces are directly exposed to body fluids following inhalation or ingestion. Potentially toxic trace metals and organic gases can be adsorbed onto these surfaces. Characterizing the physics and chemistry of airborne particle surfaces is needed to understand the biomechanisms of exposed populations. Electron spectroscopy (Lodge, 1989), electron probe microanalysis (Wernish, 1985), and time-of-flight mass spectrometry (Prather et al., 1994) are applied for particle surface analysis.

Most aerosol measurements report integrals of the mass size distribution as shown in Figure 2-4. Note that the nucleation and accumulation ranges constitute the $PM_{2.5}$ size fraction. The majority of sulfuric acid, ammonium bisulfate, ammonium sulfate, ammonium nitrate, organic carbon, and elemental carbon is found in this size range. Particles larger than 2.5 µm are called "coarse" particles; they result from grinding activities and are dominated by materials of geological origin. Pollen and spores are also found in the coarse mode.

Several continuous monitors measure chemical components dominating the accumulation mode, such as the sulfur analyzer (e.g., Allen et al., 1984; Benner and Stedman, 1989, 1990), automated nitrate analyzer (Hering, 1997), *in-situ* carbon analyzer (Turpin et al., 1990a, 1990b; Turpin and Huntzicker, 1991; Rupprecht et al., 1995), and time-of-flight mass spectrometer (Nordmeyer and Prather, 1994; Prather et al., 1994). Continuous monitors that measure precursor gases (gases that transform into particles in the atmosphere), including the ammonia analyzer (e.g., Rapsomanikis et al., 1988; Genfa et al., 1989; Harrison and Msibi, 1994) and nitric acid analyzer (e.g., Burkhardt et al., 1988), can also be used to address gas-to-particle transformation processes in the atmosphere.

2.2 Chemical Composition

Particle mass has been the primary property measured for compliance with PM standards, mainly due to its practicality and cost-effectiveness. Epidemiological studies have shown a relationship between increased ambient particle concentrations and adverse health outcomes (U.S. EPA, 1996; Vedal, 1997). Attempts have been made to attribute observed associations to specific compounds of airborne particles. The relative abundances of chemical components in the atmosphere closely reflect the characteristics of emission sources. These chemical compositions need to be quantified in order to establish causality between exposure and health effects. Major chemical components of $PM_{2.5}$ or PM_{10} mass in

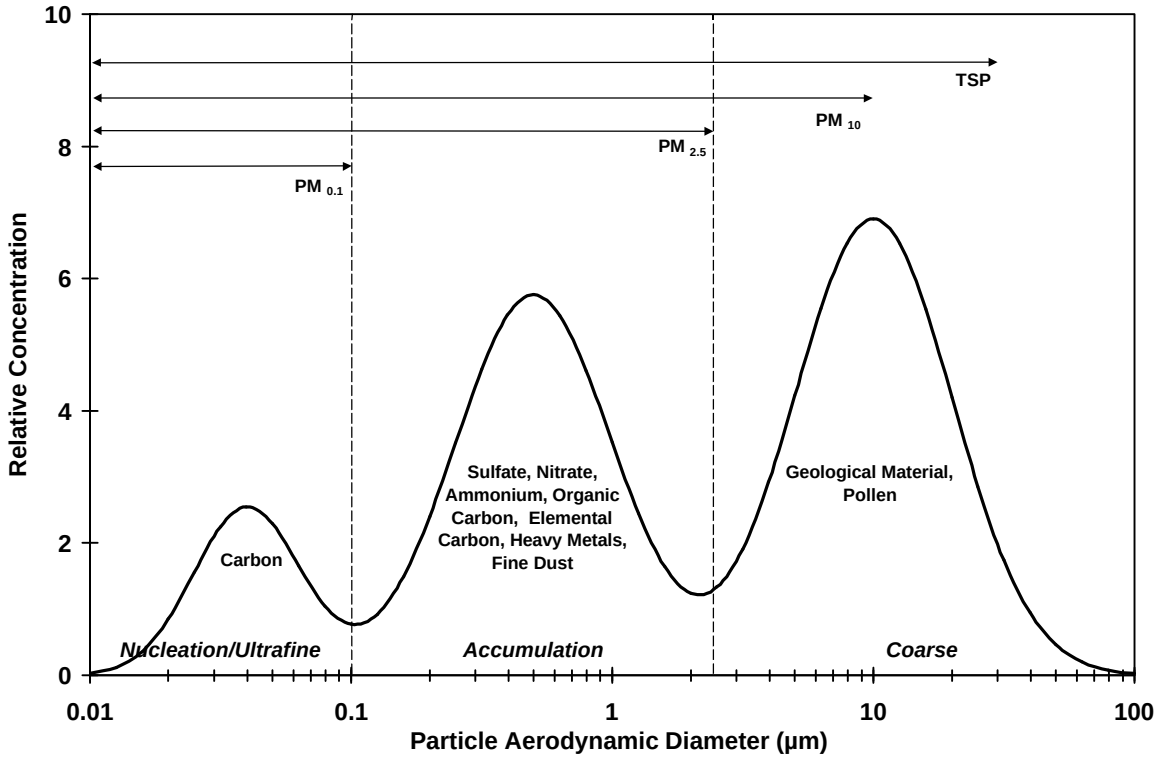

Figure 2-4. Representative mass size distribution with measured particle size fractions and dominant chemical components.

urban and non-urban areas consist of nitrate, sulfate, ammonium, carbon, geological material, sodium chloride, and liquid water:

- **Nitrate:** Ammonium nitrate (NH_4NO_3) is the most abundant nitrate compound, resulting from a reversible gas/particle equilibrium between ammonia gas (NH_3), nitric acid gas (HNO_3), and particulate ammonium nitrate. Because this equilibrium is reversible, ammonium nitrate particles can easily evaporate in the atmosphere, or after they have been collected on a filter, owing to changes in temperature and relative humidity (Stelson and Seinfeld, 1982a, 1982b; Allen et al., 1989). Sodium nitrate ($NaNO_3$) is found in the $PM_{2.5}$ and coarse fractions near sea coasts and salt playas (e.g., Watson et al., 1994b) where nitric acid vapor irreversibly reacts with sea salt (NaCl).

- **Sulfate:** Ammonium sulfate ($(NH_4)_2SO_4$), ammonium bisulfate ($(NH_4HSO_4$), and sulfuric acid (H_2SO_4) are the most common forms of sulfate found in atmospheric particles, resulting from conversion of gases to particles. These compounds are water-soluble and reside almost exclusively in the $PM_{2.5}$ size fraction. Sodium sulfate (Na_2SO_4) may be found in coastal areas where sulfuric acid has been neutralized by sodium chloride (NaCl) in sea salt. Though gypsum (Ca_2SO_4) and some other geological compounds contain sulfate, these are not easily dissolved in water for chemical analysis. They are more abundant in the coarse fraction than in $PM_{2.5}$, and are usually classified in the geological fraction.

- **Ammonium:** Ammonium sulfate ($(NH_4)_2SO_4$), ammonium bisulfate (NH_4HSO_4), and ammonium nitrate (NH_4NO_3) are the most common compounds. The sulfate compounds result from irreversible reactions between sulfuric acid and ammonia gas, while the ammonium nitrate can migrate between gases and particle phases (Watson et al., 1994a). Ammonium ions may coexist with sulfate, nitrate, and hydrogen ions in small water droplets. While most of the sulfur dioxide and oxides of nitrogen precursors of these compounds originate from fuel combustion in stationary and mobile sources, most of the ammonia derives from living beings, especially animal husbandry practiced in dairies and feedlots.

- **Organic Carbon:** Particulate organic carbon consists of hundreds, possibly thousands, of separate compounds. The mass concentration of organic carbon can be accurately measured, as can carbonate carbon, but only about 10% of specific organic compounds that it contains have been measured. Vehicle exhaust (Rogge et al., 1993a), residential and agricultural burning (Rogge et al., 1998), meat cooking (Rogge et al., 1991), fuel combustion (Rogge et al., 1993b, 1997), road dust (Rogge et al., 1993c), and particle formation from heavy hydrocarbon (C_8 to C_{20}) gases (Pandis et al., 1992) are the major sources of organic carbon in $PM_{2.5}$. Because of this lack of molecular specificity, and owing to the semi-volatile nature of many carbon compounds, particulate "organic carbon" is operationally defined by the sampling and analysis method.

- **Elemental Carbon:** Elemental carbon is black, often called "soot." Elemental carbon contains pure, graphitic carbon, but it also contains high molecular weight, dark-colored, non-volatile organic materials such as tar, biogenics, and coke. Elemental carbon usually accompanies organic carbon in combustion emissions with diesel exhaust (Watson et al., 1994c) being the largest contributor.

- **Geological Material:** Suspended dust consists mainly of oxides of aluminum, silicon, calcium, titanium, iron, and other metals oxides (Chow and Watson, 1992). The precise combination of these minerals depends on the geology of the area and industrial processes such as steel-making, smelting, mining, and cement production. Geological material is mostly in the coarse particle fraction (Houck et al., 1990), and typically constitutes ~50% of PM_{10} while only contributing 5 to 15% of $PM_{2.5}$ (Chow et al., 1992a; Watson et al., 1994b).

- **Sodium Chloride:** Salt is found in suspended particles near sea coasts, open playas, and after de-icing materials are applied. Bulk sea water contains 57±7% chloride, 32±4% sodium, 8±1% sulfate, 1.1±0.1% soluble potassium, and 1.2±0.2% calcium (Pytkowicz and Kester, 1971). In its raw form (e.g., deicing sand), salt is usually in the coarse particle fraction and classified as a geological material (Chow et al., 1996). After evaporating from a suspended water droplet (as in sea salt or when resuspended from melting snow), it is abundant in the $PM_{2.5}$ fraction. Sodium chloride is often neutralized by nitric or sulfuric acid in urban air where it is often encountered as sodium nitrate or sodium sulfate (Pilinis et al., 1987).

- **Liquid Water:** Soluble nitrates, sulfates, ammonium, sodium, other inorganic ions, and some organic material (Saxena and Hildemann, 1997) absorb water vapor from the atmosphere, especially when relative humidity exceeds 70% (Tang and Munkelwitz, 1993). Sulfuric acid absorbs some water at all humidities. Particles containing these compounds grow into the droplet mode as they take on liquid water. Some of this water is retained when particles are sampled and weighed for mass concentration. The precise amount of water quantified in a $PM_{2.5}$ depends on its ionic composition and the equilibration relative humidity applied prior to laboratory weighing.

The liquid water and ammonium nitrate compositions of suspended particles are especially important for continuous particle monitors. These are both volatile substances that migrate between the gas and particle phase depending on the composition, temperature, and relative humidity of the atmosphere. The presence of ionic species (such as sulfate and nitrate compounds) enhances the liquid water uptake of suspended particles, as shown in Figure 2-5. The sharp rise in liquid water content at relative humidities between 55% and 75% is known as deliquescence. The humidities at which soluble particles take on liquid water depend on the chemical mixture and temperature, as explained in the caption to Figure 2-5.

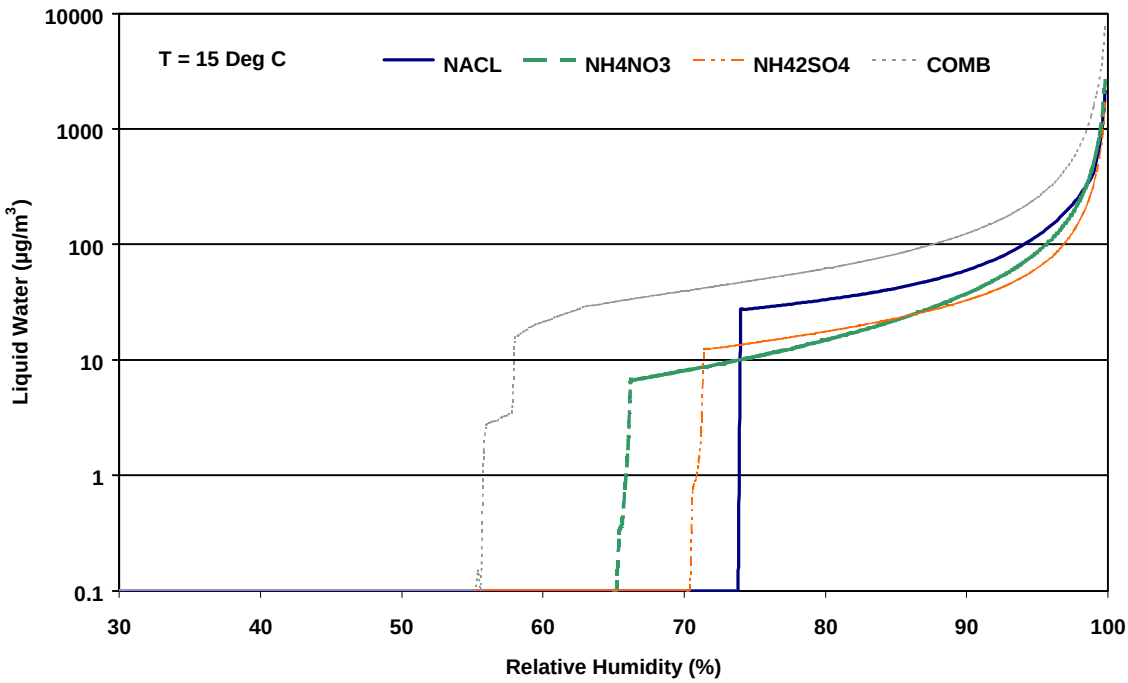

Figure 2-5. Changes in liquid water content of sodium chloride, ammonium nitrate, ammonium sulfate, and a combination of compounds at different relative humidities. These curves were generated from the SCAPE aerosol equilibrium model (Kim et al., 1993a; 1993b; Kim and Seinfeld, 1995; Meng et al., 1995). The "NACL" case is for 3.83 µg/m^3 of sodium ion and 6.24 µg/m^3 of gas phase hydrochloric acid (HCl). The "NH4NO3" case is for 10 µg/m^3 of gas phase nitric acid (HNO_3) and 10 µg/m^3 of gas phase sulfuric acid (H_2SO_4). At a temperature of 15 degrees Celsius, solid ammonium nitrate (NH_4NO_3) is present for the lower relative humidities. SCAPE shows a deliquescence relative humidity of 66.2%, within 4% of the measured value of 62% for 25 degrees Celsius (Pruppacher and Klett, 1978). The "NH42SO4" case is for 10 µg/m^3 of gas phase ammonia (NH_3) and 10 µg/m^3 of H_2SO_4; there is sufficient ammonia to neutralize the available sulfate, and the gas-phase constituents are in equilibrium with solid-phase ammonium sulfate for the lower relative humidities. The deliquescence point of around 80% is expected (Tang et al., 1977a, 1977b). The "COMB" (combination) case consists of 10 µg/m^3 of equivalent HNO_3 and H_2SO_4, 20 µg/m^3 of equivalent NH_3, 3.83 µg/m^3 of sodium ion, and 6.24 µg/m^3 of equivalent HCl. SCAPE yields solid-phase sodium sulfate, ammonium sulfate, ammonium chloride, and ammonium nitrate for the lower humidities, with a deliquescence relative humidity for the mixture of approximately 57%. This is in agreement with the fact that the deliquescence point for a mixture lies below the minimum deliquescence points for the individual salts (Wexler and Seinfeld, 1991; Kim and Seinfeld, 1995), and is in agreement with a deliquescence relative humidity of 56% found by Tang (1980) for a mixture of 45% by weight NH_4NO_3 and 55% by weight $(NH_4)_2SO_4$.

Figure 2-6 shows how the fraction of nitrate in the particle phase changes with temperature, relative humidity, and the amount of excess ammonia in the atmosphere. These curves were generated from the same equilibrium model used to examine liquid water content in Figure 2-5. Atmospheric particle nitrate can occur in atmospheric aerosol particles as solid ammonium nitrate or as ionized ammonium nitrate in particles containing water. In both the solid and ionized forms, ammonium nitrate is in equilibrium with gas-phase nitric acid and ammonia. In Figure 2-6, the total sulfate concentration was set to 5 μg/m^3 of equivalent H_2SO_4, and the total nitrate concentration was set to 20 μg/m^3 of equivalent HNO_3. The total ammonia concentration was varied to simulate different ammonium enrichment regimes, and this is indicated in the legends as the molar ratio of total available ammonia to the available sulfate and nitrate. When this "ion ratio" is unity, there is exactly enough ammonium ion available to neutralize all available nitric and sulfuric acid.

For fixed relative humidity, increasing temperature decreases the particle nitrate fraction and decreasing temperature increases the particle nitrate fraction. As temperatures approach 0 °C, nearly all of the nitrate is in the particle phase, limited only by the availability of ammonia. For higher temperatures, increasing relative humidity increases the particle nitrate fraction. When there is sufficient ammonia present with 30% relative humidity, more than 90% of the nitrate is in the particle phase for temperatures less than 20 °C. More than half of the particle nitrate is gone at temperatures above 30 °C, and all of it disappears at temperatures above 40 °C.

This has several implications for nitrate measurement by continuous monitors. Particle nitrate concentrations are probably low in warm, arid environments, so it will not be a large fraction of $PM_{2.5}$ and will not influence mass measurements by continuous particle monitors. However, ammonium nitrate can be a large fraction of $PM_{2.5}$ in cool, moist climates. Continuous monitors that require air streams to be heated from temperatures exceeding 20 °C will cause ammonium nitrate in the sample to volatilize, thereby eliminating that portion of the PM mass from detection.

PM concentration and chemical composition vary in time and space due to changes in emission density, meteorology, and terrain features. Table 2-1 illustrates seasonal variations of $PM_{2.5}$ in different regions of the IMPROVE network for the three years between March 1988 and February 1991 (Malm et al., 1994). Only the Washington, DC site is situated in an urban area, with the regional-scale background represented by the other areas.

Although $PM_{2.5}$ mass concentrations were similar among different seasons, the $PM_{2.5}$ chemical composition varied considerably with time of year at the Washington, DC site. Ammonium sulfate concentrations were higher in summer (8.6 μg/m^3, accounting for 51% of $PM_{2.5}$ mass) and lower in winter (5.4 μg/m^3, 33.2% of $PM_{2.5}$ mass). In contrast, ammonium nitrate concentrations were lower in summer (1.2 μg/m^3, accounting for 7.4% of $PM_{2.5}$ mass) and higher in winter (3.4 μg/m^3, accounting for 20.9% of $PM_{2.5}$ mass).

$PM_{2.5}$ mass from the Appalachian Mountains region shows marked seasonal differences, with 6.5 μg/m^3 during winter and 16.6 μg/m^3 during summer. These seasonal differences are driven by ammonium sulfate levels, which ranged from 3.0 μg/m^3 (46% of

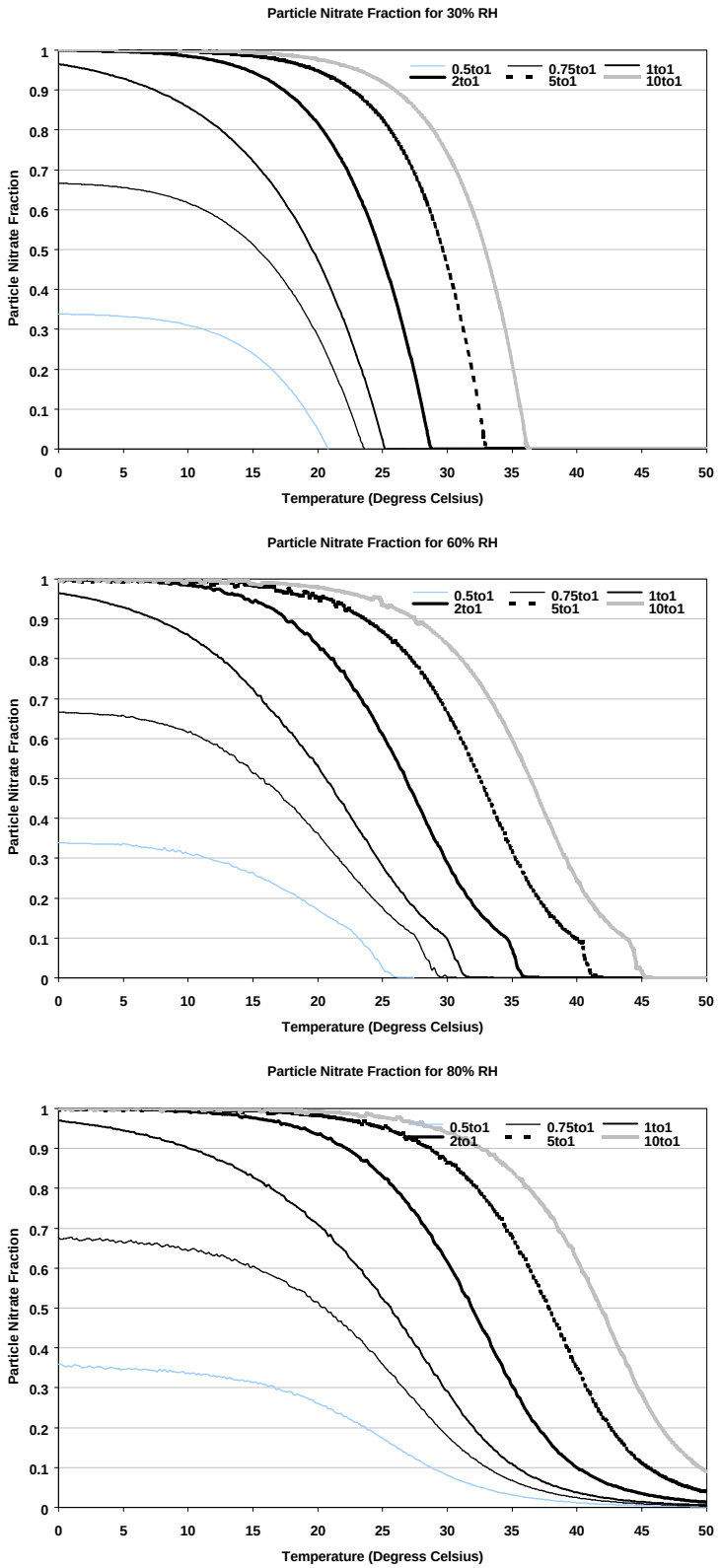

Figure 2-6. Fraction of total nitrate as particulate ammonium nitrate at different temperatures for various relative humidities and ammonia/nitrate molar ratios.

Table 2-1
Measured Aerosol Concentrations for the 19 Regions[a] in the IMPROVE Network from March 1988 to February 1991[b]

	Aerosol Concentration in µg/m^3 (Percent Mass)						
Season	Fine Mass	Ammonium Sulfate	Nitrate	Organics	Elemental Carbon	Soil	Coarse Mass
			Alaska				
Winter	1.6	0.7 (42.1)	0.1 (6.2)	0.6 (36.5)	0.1 (3.4)	0.2 (11.8)	4.0
Spring	2.4	0.9 (39.5)	0.1 (3.1)	0.7 (30.5)	0.1 (2.3)	0.6 (24.6)	3.9
Summer	2.7	0.5 (20.7)	0.0 (1.2)	1.5 (57.9)	0.1 (3.2)	0.4 (16.9)	5.4
Autumn	1.2	0.4 (32.1)	0.1 (4.3)	0.6 (49.2)	0.1 (4.9)	0.1 (9.5)	3.2
Annual	1.9	0.6 (32.6)	0.1 (3.3)	0.9 (43.9)	0.1 (3.3)	0.3 (17.0)	4.2
			Appalachian				
Winter	6.5	3.0 (45.8)	0.8 (12.8)	2.0 (31.3)	0.4 (6.2)	0.3 (3.8)	3.1
Spring	10.6	6.0 (56.8)	0.8 (7.9)	2.7 (25.1)	0.5 (4.4)	0.6 (5.8)	4.5
Summer	16.6	10.5 (63.5)	0.3 (2.0)	4.4 (26.5)	0.5 (2.9)	0.8 (5.1)	11.2
Autumn	9.7	5.6 (58.0)	0.5 (4.9)	2.7 (28.1)	0.5 (5.0)	0.4 (4.0)	5.5
Annual	10.9	6.3 (58.0)	0.6 (5.7)	3.0 (27.2)	0.5 (4.2)	0.5 (4.8)	6.2
			Boundary Waters				
Winter	5.2	2.0 (38.0)	1.4 (27.4)	1.4 (27.0)	0.2 (3.8)	0.2 (3.9)	3.2
Spring	5.4	2.6 (48.7)	0.4 (6.8)	1.8 (32.6)	0.2 (3.6)	0.4 (8.3)	5.1
Summer	6.2	2.2 (35.8)	0.1 (2.1)	3.1 (50.6)	0.3 (4.2)	0.5 (7.3)	8.2
Autumn	4.3	1.6 (37.9)	0.4 (10.1)	1.8 (40.9)	0.2 (4.6)	0.3 (6.6)	5.8
Annual	5.3	2.0 (38.9)	0.6 (11.0)	2.1 (39.5)	0.2 (4.1)	0.3 (6.5)	5.7
			Cascades				
Winter	3.8	0.6 (14.6)	0.1 (3.5)	2.6 (67.2)	0.5 (12.0)	0.1 (2.7)	2.9
Spring	5.2	1.4 (26.7)	0.2 (4.7)	2.7 (53.2)	0.5 (8.8)	0.3 (6.7)	3.1
Summer	6.7	2.4 (35.7)	0.4 (6.1)	3.0 (45.1)	0.5 (8.1)	0.3 (5.0)	4.6
Autumn	5.3	1.3 (24.6)	0.2 (3.7)	3.1 (58.7)	0.5 (9.7)	0.2 (3.3)	3.9
Annual	5.1	1.3 (25.7)	0.2 (4.5)	2.8 (55.7)	0.5 (9.5)	0.2 (4.5)	3.5
			Colorado Plateau				
Winter	2.9	0.9 (33.0)	0.5 (13.1)	1.1 (37.3)	0.2 (6.1)	0.3 (10.5)	3.2
Spring	3.4	0.9 (27.9)	0.2 (7.0)	1.0 (29.9)	0.1 (2.6)	1.1 (32.6)	5.3
Summer	4.1	1.3 (31.9)	0.2 (4.3)	1.6 (39.0)	0.2 (4.2)	0.9 (20.6)	6.4
Autumn	3.2	1.2 (36.3)	0.1 (4.6)	1.2 (38.4)	0.2 (5.0)	0.5 (15.7)	3.7
Annual	3.4	1.1 (31.9)	0.2 (7.2)	1.2 (36.3)	0.2 (4.3)	0.7 (20.3)	4.7
			Central Rockies				
Winter	2.0	0.5 (27.8)	0.2 (11.2)	0.9 (45.1)	0.1 (3.18)	0.3 (12.2)	3.0
Spring	3.4	0.9 (27.6)	0.3 (7.8)	1.1 (32.0)	0.1 (2.1)	1.1 (30.5)	4.3
Summer	4.8	1.0 (24.0)	0.1 (3.2)	2.4 (48.7)	0.2 (4.6)	0.9 (19.4)	7.5
Autumn	2.9	0.8 (27.9)	0.1 (4.5)	1.3 (45.4)	0.1 (4.3)	0.5 (18.0)	4.0
Annual	3.3	0.8 (25.8)	0.2 (5.9)	1.5 (43.7)	0.1 (3.9)	0.7 (20.7)	4.8
			Central Coast				
Winter	5.6	0.9 (16.8)	1.9 (29.3)	2.3 (44.7)	0.4 (6.3)	0.2 (2.9)	7.7
Spring	4.2	1.4 (33.6)	0.8 (18.7)	1.5 (36.5)	0.2 (4.1)	0.3 (7.1)	9.3
Summer	4.5	1.9 (43.4)	0.8 (17.1)	1.4 (31.5)	0.1 (2.9)	0.2 (5.0)	10.7
Autumn	5.7	1.4 (24.2)	1.0 (16.3)	2.7 (47.9)	0.4 (6.9)	0.3 (4.7)	7.8
Annual	5.0	1.4 (28.5)	1.1 (21.1)	1.9 (40.3)	0.3 (5.2)	0.2 (4.8)	8.9

Table 2-1 (continued)
Measured Aerosol Concentrations for the 19 Regions[a] in the IMPROVE Network from March 1988 to February 1991[b]

	Aerosol Concentration in µg/m^3 (Percent Mass)						
Season	Fine Mass	Ammonium Sulfate	Nitrate	Organics	Elemental Carbon	Soil	Coarse Mass
			Florida				
Winter	5.5	2.4 (43.3)	0.7 (12.5)	1.9 (34.0)	0.4 (6.9)	0.2 (3.2)	8.5
Spring	7.7	3.8 (48.5)	0.9 (11.2)	2.1 (27.4)	0.3 (3.7)	0.7 (9.2)	8.0
Summer	9.1	2.5 (27.1)	0.5 (5.9)	3.0 (33.3)	0.3 (3.4)	2.7 (30.2)	13.6
Autumn	6.9	3.1 (45.8)	0.5 (7.8)	2.3 (33.3)	0.4 (6.2)	0.5 (6.9)	8.6
Annual	7.1	2.9 (40.9)	0.7 (9.2)	2.3 (31.9)	0.4 (5.0)	0.9 (13.0)	9.6
			Great Basin				
Winter	1.1	0.3 (25.9)	0.1 (12.3)	0.5 (48.0)	0.0 (1.4)	0.1 (12.3)	1.0
Spring	2.4	0.5 (22.1)	0.1 (5.9)	0.9 (35.6)	0.0 (I. 1)	0.9 (35.3)	3.7
Summer	4.5	0.7 (14.9)	0.1 (2.5)	1.7 (38.8)	0.1 (2.2)	1.9 (41.6)	8.2
Autumn	3.1	0.6 (17.7)	0.1 (4.6)	1.4 (44.5)	0.1 (2.6)	1.0 (30.6)	5.1
Annual	2.8	0.5 (18.3)	0.1 (4.7)	1.1 (40.1)	0.1 (2.0)	1.0 (34.9)	5.0
			Hawaii				
Winter	4.0	2.8 (70.8)	0.1 (1.6)	0.9 (22.9)	0.1 (2.4)	0.1 (2.4)	3.0
Spring	3.6	2.5 (67.8)	0.1 (2.2)	0.8 (22.1)	0.1 (1.8)	0.2 (6.1)	7.4
Summer	1.6	0.9 (56.7)	0.1 (5.3)	0.5 (30.6)	0.0 (2.6)	0.1 (4.8)	10.3
Autumn	3.4	2.5 (72.0)	0.1 (1.6)	0.8 (22.1)	0.1 (2.0)	0.1 (2.3)	9.3
Annual	3.2	2.2 (68.5)	0.1 (2.2)	0.7 (23.4)	0.1 (2.1)	0.1 (3.7)	8.1
			Northeast				
Winter	6.6	3.3 (50.6)	0.8 (11.4)	1.8 (27.8)	0.5 (7.2)	0.2 (3.0)	3.1
Spring	6.1	3.6 (58.5)	0.4 (7.1)	1.5 (24.4)	0.3 (5.3)	0.3 (4.6)	4.1
Summer	8.6	4.5 (52.4)	0.3 (4.0)	3.0 (35.1)	0.4 (4.9)	0.3 (3.6)	6.7
Autumn	5.6	3.0 (53.5)	0.4 (7.1)	1.6 (29.4)	0.4 (6.6)	0.2 (3.5)	4.1
Annual	6.7	3.6 (53.5)	0.5 (7.2)	2.0 (29.8)	0.4 (5.9)	0.2 (3.7)	4.5
			Northern Great Plains				
Winter	3.4	1.2 (34.5)	0.6 (16.6)	1.1 (31.7)	0.1 (3.6)	0.5 (13.6)	3.9
Spring	5.0	1.9 (38.6)	0.6 (11.8)	1.3 (26.7)	0.1 (2.4)	1.0 (20.5)	6.0
Summer	5.6	1.8 (32.1)	0.2 (2.9)	2.2 (39.5)	0.2 (3.2)	1.2 (22.3)	9.7
Autumn	4.0	1.2 (30.0)	0.2 (5.2)	1.5 (37.1)	0.1 (3.6)	1.0 (24.1)	5.8
Annual	4.5	1.5 (34.0)	0.4 (8.5)	1.5 (33.9)	0.1 (3.1)	0.9 (20.6)	6.3
			Northern Rockies				
Winter	5.3	1.0 (18.6)	0.6 (10.6)	3.0 (56.7)	0.5 (9.4)	0.3 (4.8)	2.5
Spring	4.6	1.1 (23.3)	0.2 (5.2)	2.4 (52.2)	0.3 (6.7)	0.6 (12.5)	4.2
Summer	5.4	0.9 (17.1)	0.2 (3.1)	3.0 (54.5)	0.3 (6.1)	1.0 (19.2)	9.2
Autumn	6.7	0.9 (12.8)	0.3 (4.3)	4.3 (64.7)	0.6 (9.4)	0.6 (8.8)	5.7
Annual	5.5	1.0 (17.7)	0.3 (5.7)	3.1 (57.3)	0.4 (7.9)	0.6 (11.4)	5.5
			Southern California				
Winter	4-6-	0.5 (11.3)	2.2 (47.8)	1.2 (26.2)	0.2 (5.3)	0.4 (9.4)	4.2
Spring	13.6	1.7 (12.2)	6.9 (51.1)	3.2 (23.5)	0.6 (4.2)	1.2 (8.9)	9.8
Summer	13.8	2.4 (17.2)	4.6 (33.4)	4.2 (30.6)	0.8 (5.7)	1.8 (13.1)	15.2
Autumn	8.1	1.1 (13.4)	3.1 (38.6)	2.0 (24.3)	0.4 (5.1)	1.5 (18.6)	13.2
Annual	9.8	1.4 (13.9)	4.2 (43.0)	2.5 (25.9)	0.5 (4.9)	1.2 (12.3)	10.4

Table 2-1 (continued)
Measured Aerosol Concentrations for the 19 Regions[a] in the IMPROVE Network from March 1988 to February 1991[b]

	Aerosol Concentration in µg/m^3 (Percent Mass)						
Season	Fine Mass	Ammonium Sulfate	Nitrate	Organics	Elemental Carbon	Soil	Coarse Mass
			Sonora Desert				
Winter	3.2	1.2 (38.6)	0.3 (8.6)	1.1 (34.6)	0.2 (5.2)	0.4 (13.0)	3.3
Spring	4.4	1.2 (26.5)	0.3 (6.9)	1.3 (29.8)	0.1 (2.9)	1.5 (33.9)	7.5
Summer	5.6	2.1 (37.7)	0.2 (3.8)	1.8 (33.0)	0.2 (3.2)	1.2 (22.3)	7.6
Autumn	4.5	1.7 (37.5)	0.2 (3.7)	1.7 (37.1)	0.2 (5.1)	0.8 (16.5)	5.8
Annual	4.4	1.5 (35.4)	0.3 (5.5)	1.5 (33.4)	0.2 (4.1)	0.9 (21.6)	6.0
			Sierra Nevada				
Winter	2.5	0.4 (14.9)	0.7 (27.1)	1.1 (46.7)	0.1 (4.2)	0.2 (7.2)	2.1
Spring	4.3	1.0 (24.2)	0.6 (14.3)	1.7 (29.4)	0.2 (4.0)	0.8 (18.1)	4.8
Summer	7.2	1.7 (23.4)	0.6 (8.0)	3.6 (49.6)	0.5 (6.7)	0.9 (12.2)	7.0
Autumn	4.4	0.9 (20.6)	0.6 (13.2)	2.1 (48.3)	0.3 (6.5)	0.5 (11.4)	5.3
Annual	4.5	1.0 (21.7)	0.6 (13.6)	2.1 (46.4)	0.3 (5.6)	0.6 (12.7)	4.7
			Sierra-Humboldt				
Winter	1.7	0.2 (14.2)	0.1 (7.2)	1.0 (56.6)	0.1 (6.6)	0.3 (15.4)	2.9
Spring	3.0	0.6 (18.6)	0.2 (8.2)	1.4 (48.5)	0.1 (4.8)	0.6 (19.9)	2.9
Summer	4.0	0.7 (18.2)	0.2 (4.7)	2.2 (55.1)	0.3 (6.5)	0.6 (15.5)	5.6
Autumn	2.8	0.4 (15.5)	0.1 (3.5)	1.7 (59.9)	0.2 (7.4)	0.4 (13.7)	2.7
Annual	2.9	0.5 (17.1)	0.2 (5.7)	1.6 (54.7)	0.2 (6.3)	0.5 (16.2)	3.7
			Washington D.C.				
Winter	16.3	5.4 (33.2)	3.4 (20.9)	4.9 (29.9)	2.0 (12.4)	0.6 (3.6)	30.1
Spring	16.8	7.3 (43.6)	2.6 (15.5)	4.2 (24.9)	1.7 (10.1)	1.0 (5.9)	10.2
Summer	16.7	8.6 (51.4)	1.2 (7.4)	4.4 (26.1)	1.6 (9.8)	0.9 (5.3)	13.5
Autumn	15.3	6.6 (43.3)	1.6 (10.5)	4.4 (28.5)	2.0 (12.8)	0.8 (4.9)	8.4
Annual	16.2	6.9 (42.4)	2.2 (13.8)	4.5 (27.5)	1.8 (11.4)	0.8 (4.9)	16.4
			West Texas				
Winter	3.6	1.5 (40.6)	0.2 (6.2)	1.1 (31.4)	0.1 (3.8)	0.6 (18.0)	5.1
Spring	6.4	2.2 (33.6)	0.3 (4.7)	1.7 (26.1)	0.2 (2.5)	2.1 (33.0)	10.4
Summer	6.6	2.5 (38.7)	0.3 (4.7)	1.7 (25.9)	0.1 (2.0)	1.9 (28.7)	7.4
Autumn	4.8	2.3 (46.8)	0.2 (3.4)	1.4 (29.1)	0.2 (3.5)	0.8 (17.2)	7.0
Annual	5.4	2.1 (39.3)	0.3 (4.7)	1.5 (27.6)	0.1 (2.8)	1.4 (25.6)	7.5

[a] IMPROVE and NPS/IMPROVE protocol sites according to 1a Region:

Alaska
- Denali National Park

Appalachian Mountains
- Great Smoky Mountains National Park
- Shenandoah National Park

Boundary Waters
- Isle Royale National Park
- Voyageurs National Park

Cascade Mountains
- Mount Rainier National Park

Central Rocky Mountains
- Bridger Wilderness Area
- Great Sand Dunes National Monument
- Rocky Mountain National Park
- Weminuche Wilderness Area
- Yellowstone National Park

Coastal Mountains
- Pinnacles National Monument
- Point Reyes National Seashore
- Redwood National Park

Colorado Plateau
- Arches National Park
- Bandelier National Monument
- Bryce Canyon National Park
- Canyonlands National Park
- Grand Canyon National Park
- Mesa Verde National Park
- Petrified Forest National Park

Florida
- Everglades

Great Basin
- Jarbidge Wilderness Area

Hawaii
- Hawaii Volcanoes National Park

Northeast
- Acadia National Park

Northern Great Plains
- Badlands National Monument

Northern Rocky Mountains
- Glacier National Park

Sierra Nevada
- Yosemite National Park

Sierra-Humboldt
- Crater Lake National Park
- Lassen Volcanoes National Park

Sonoran Desert
- Chiricahua National Monument
- Tonto National Monument

Southern California
- San Gorgonio Wilderness Area

Washington, D.C.
- Washington, D.C.

West Texas
- Big Bend National Park
- Guadalupe Mountains National Monument

(IMPROVE=Interagency Monitoring of Protected Visual Environments; NPS=National Park Service)

[b] Based on Malm et al. (1994).

$PM_{2.5}$ mass) in winter to 10.5 μg/m^3 (64% of $PM_{2.5}$ mass) in summer. The region represented by the San Gorgonio site in Southern California also reported significant seasonal $PM_{2.5}$ differences of 4.6 μg/m^3 during winter, 13.6 μg/m^3 during spring, and 13.8 μg/m^3 during summer. Spring and summer $PM_{2.5}$ concentrations were driven by nitrate concentrations, which were 2 to 3 times higher than during fall and winter. This site lies along one of the ventilation pathways for California's South Coast Air Basin which produces copious quantities of ammonium nitrate particles (Solomon et al., 1989; Chow et al., 1994a, 1994b).

In the IMPROVE network, carbonaceous aerosol accounts for 20% to 50% of $PM_{2.5}$, with elevated concentrations found during summer, reflecting possible contributions from photochemical conversion of heavy hydrocarbon gases to particles. Crustal components were also major $PM_{2.5}$ components at these regionally representative sites, accounting for 20% to 30% of $PM_{2.5}$ mass in the southwest and northwest.

Relative abundances of particulate chemical components in urban areas often differ from the data presented in Table 2-1 due to the superposition of urban emissions on top of regional background and particles transported from upwind sources. Chow et al. (1998a) shows that $PM_{2.5}$ organic carbon is enriched in residential neighborhoods during cold winter periods, reflecting contributions from home heating and vehicle exhaust, especially cold starts. Elevated nitrate concentrations are often found during the fall and winter owing to lower temperatures and higher humidities, as described above.

2.3 Particle Interactions with Light

Visibility degrades when particle concentrations increase, but the nature of this degradation has a complex dependence on particle properties and the atmosphere (Watson and Chow, 1994). Visible light occupies a region of the electromagnetic spectrum with wavelengths between 400 nm and 700 nm, similar to particle diameters in the accumulation mode. Light falling on an object is reflected and absorbed as a function of its wavelength. Light reflected from an object is transmitted through the atmosphere where its intensity is attenuated when it is scattered and absorbed by gases and particles. The sum of these scattering and absorption coefficients yields the extinction coefficient (b_{ext}) expressed in units of inverse megameters ($Mm^{-1}=1/10^6$ m). Typical extinction coefficients range from ~10 Mm^{-1} in pollution-free air to ~1,000 Mm^{-1} in extremely polluted air (Trijonis et al., 1988). The inverse of b_{ext} corresponds to the distance (in 10^6 m) at which the original intensity of transmitted light is reduced by approximately two-thirds.

Light is scattered when diverted from its original direction by matter (Malm, 1979). The presence of atmospheric gases such as oxygen and nitrogen limits horizontal visual range to ~400 km and obscures many of the attributes of a target at less than half of this distance. This "Rayleigh scattering" in honor of the scientist who elucidated this phenomena, is the major component of light extinction in areas where pollution levels are low, has a scattering coefficient of ~10 Mm^{-1}, and it can be accurately estimated from temperature and pressure measurements (Edlen, 1953; Penndorf, 1957).

Light is also scattered by particles suspended in the atmosphere, and the efficiency of this scattering per unit mass concentration is largest for particles with sizes comparable to the wavelength of light (~500 nm), as shown in Figure 2-7 for an ammonium sulfate particle. Note the rapid change in scattering efficiency in the region between 0.1 and 1 μm that makes light scattering measurements very sensitive to small changes in particle size within this region. The degree to which particles scatter light depends on their size, shape, and index of refraction (which depends on their chemical composition). Each $\mu g/m^3$ of pure ammonium sulfate or ammonium nitrate typically contributes 2 to 6 Mm^{-1}. Each $\mu g/m^3$ of soil particles less than 2.5 μm in aerodynamic diameter contributes ~ 1 Mm^{-1}. The sizes of most crustal particles are several times the typical wavelengths of light and each $\mu g/m^3$ of these particles with diameters >2.5 μm contributes ~0.5 Mm^{-1} to extinction (White et al., 1994).

Light is absorbed in the atmosphere by nitrogen dioxide (NO_2) gas, by black carbonaceous particles (Horvath, 1993a, 1993b), and by non-transparent geological material. Each $\mu g/m^3$ of nitrogen dioxide contributes ~0.17 Mm^{-1} of extinction at ~550 nm wavelengths (Dixon, 1940), so NO_2 concentrations in excess of 60 $\mu g/m^3$ (30 ppbv) are needed to exceed Rayleigh scattering. This contribution is larger for shorter wavelengths (e.g., blue light) and smaller for longer wavelengths (e.g., red light). Black carbon particles are seldom found in emissions from efficient combustion sources, although they are abundant in motor vehicle exhaust, fires, and residential heating emissions. Figure 2-8 shows that the absorption efficiency of elemental carbon particles has a complex relationship to particle size and assumptions about the particle composition. For the majority of particle types, Figure 2-8 shows that the theoretical scattering efficiency is substantially lower than that estimated from ambient measurements, which are usually in the range of 5 to 20 m^2/g (Hitzenberger and Puxbaum, 1993; Jennings and Pinnick, 1980).

2.4 Mobility

A particle's mobility is defined as the ratio of particle velocity to the force that accelerates the particle to that velocity. Mobility is related to mass by Newton's first law, stating that its mass is equal to the force applied divided by the particles acceleration. A constant velocity is easier to measure than a velocity that is changing during acceleration. For this reason, detection devices submit individual particles to a force, usually aerodynamic or electrostatic, for a short time period, then remove that force to measure the particle velocity. They may also apply a force that counteracts the resistance of air to bring a particle to a constant velocity; this force depends on the size and shape of the particle.

2.5 Beta Attenuation

Electrons (or "beta rays") having kinetic energies less than 1 million electron volts collide with atoms they encounter, while higher energy electrons interact with the atomic shell or the atomic nucleus. These collisions cause incremental losses in electron energy that is somewhat proportional to the number of collisions. When a stream of electrons with a given energy distribution is directed across a thin layer of material, the transmitted energy is exponentially attenuated as the thickness of the sample, or the number and types of atoms it encounters, increases.

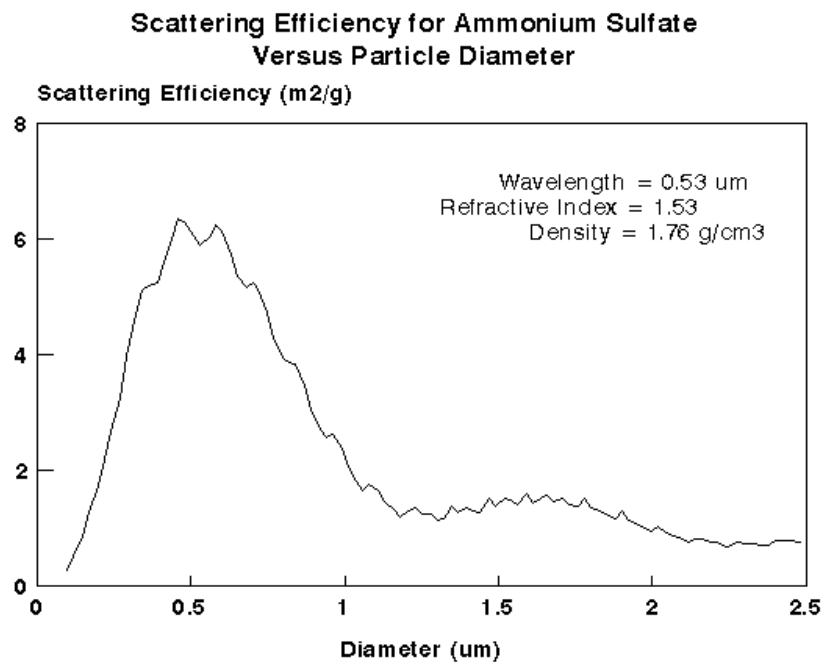

Figure 2-7. Ammonium sulfate particle scattering efficiency as a function of particle diameter. Note that the highest efficiency corresponds to particle sizes near the peak of the accumulation mode.

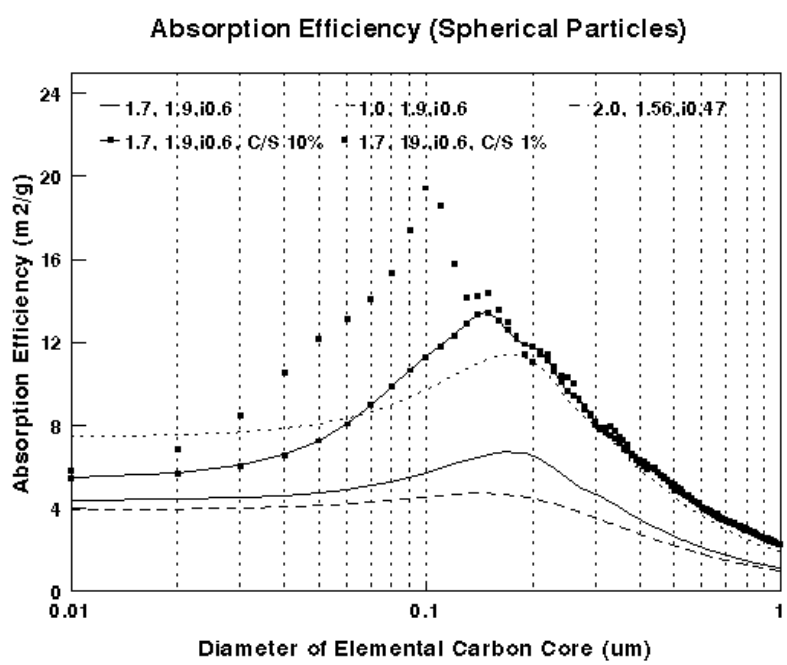

Figure 2-8. Particle absorption efficiencies as a function of elemental carbon particle diameter for several densities (first number in legend), real and imaginary indices of refraction (second and third numbers in legend). First three cases are for pure elemental carbon. Fourth and fifth cases are for 10% and 1% carbon as the core of a sulfate particle.

Beta ray attenuation is not the same for all atoms and varies with the ratio of atomic number to atomic mass of each atom. Different elements in ambient air will have different attenuation properties, so the relationship between attenuation and mass is not exact. Jaklevic et al. (1981) show that the ratio of atomic number to mass for most of the atoms in suspended particles is reasonably constant, with the exception of hydrogen.

2.6 Summary

Suspended particles are present in a large number of particle sizes and chemical compositions. These vary from place to place and time to time, especially between the eastern and western United States and between winter and summer. Some of the chemical components of suspended particles, particularly water and ammonium nitrate, are in equilibrium with gas-phase concentrations. This equilibrium changes with temperature, relative humidity, and precursor gas concentrations. Particle mobility, light absorption, and light scattering properties are also functions of chemical composition, size, and shape. These particle properties must be considered, and to some extent defined, when different measurement principles incorporated in filter-based and continuous *in-situ* monitors are applied to their quantification.

3. CONTINUOUS PARTICLE MEASUREMENT METHODS

This section surveys continuous *in-situ* instruments that measure different properties of suspended particles. Instrument specifications, measurement properties, detection thresholds, typical averaging times, development status, potential uses, and maintenance needs are discussed when this information is available. Continuous monitors are classified by the properties that they measure with respect to: 1) mass (i.e., inertial mass, beta-ray attenuation, pressure drop); 2) interactions with light (i.e., particle light scattering, particle light absorption); 3) mobility (i.e., electrical mobility, aerodynamic mobility); 4) chemical components (i.e., single particle characteristics, nitrate, carbon, sulfur, and other elements); and 5) precursor gases (i.e., ammonia, nitric acid). Table 3-1 shows that there are several approaches to measuring the same properties as well as multiple providers for these instruments. Instrument descriptions given here are brief, with emphasis on their applicability to $PM_{2.5}$ and PM_{10} measurements. More detail is given by Baron et al. (1993), Gebhart (1993), Rader and O'Hern (1993), Williams et al. (1993), and Pui and Swift (1995), as well as in the cited references and the bibliography in Section 7.

3.1 Mass and Mass Equivalent

Particle mass is determined by its inertia, by its electron attenuation properties, and by the decrease in pressure across small pores in a filter. Four different types of mass measurement monitors are discussed in the following subsections.

3.1.1 Tapered Element Oscillating Microbalance (TEOM®)

The TEOM® (Patashnick and Hemenway, 1969; Patashnick, 1987; Patashnick and Rupprecht, 1991; Rupprecht et al., 1992) draws air through a hollow tapered tube, with the wide end of the tube fixed, while the narrow end oscillates in response to an applied electric field. The narrow end of the tube carries the filter cartridge. The sampled air stream passes from the sampling inlet, through the filter and tube, to a flow controller. The tube-filter unit acts as a simple harmonic oscillator with

$$\omega = (k/m)^{0.5} \tag{3-1}$$

where: ω = the angular frequency,
k = the restoring force constant, and
m = the oscillating mass.

As particles are collected on the filter, the oscillating mass changes and results in a change of the oscillating frequency. An electronic control system maintains the tapered tube in oscillation and continuously measures this oscillating frequency and its changes. To calibrate the system, the restoring force constant (k in Equation 3-1) is determined by placing a gravimetrically determined calibration mass on the filter and recording the frequency change due to this mass.

Table 3-1
Summary of Continuous Monitoring Technology

Instrument	Quantity Measured	Methodology
I. Mass and Mass Equivalent		
Tapered Element Oscillating Microbalance (TEOM) [y] (Patashnick and Hemenway, 1969; Patashnick, 1987; Patashnick and Rupprecht, 1991; Meyer et al., 1992; Rupprecht et al., 1992; Allen et al., 1997)	Particle mass. Detection limit ~ 5 $\mu g/m^3$ for a five minute average.	Particles are continuously collected on a filter mounted on the tip of a glass element which oscillates in an applied electric field. The glass element is hollow, with the wider end fixed; air is drawn through the filter and through the element. The oscillation of the glass element is maintained based on the feedback signal from an optical sensor. The resonant frequency of the element decreases as mass accumulates on the filter, directly measuring inertial mass. The typical signal averaging period is 10 minutes. Temperatures are maintained at a constant value, typically 30°C or 50°C, to minimize thermal expansion of the tapered element.
Piezoelectric Microbalance [d] (Olin and Sem, 1971); Sem et al., 1977; Fairchild and Wheat, 1984; Bowers and Chuan, 1989; Ward and Buttry, 1990; Noel and Topart, 1994)	Particle mass. Detection limit ~ 10 $\mu g/m^3$ for a one minute average.	Particles are deposited by inertial impaction or electrostatic precipitation onto the surface of a piezoelectric quartz crystal disk. The natural resonant frequency of the crystal decreases as particle mass accumulates. The changing frequency of the sampling crystal is electronically compared to a clean reference crystal, generating a signal that is proportional to the collected mass. The reference crystal also allows for temperature compensation.
Beta Attenuation Monitor (BAM) [i,af] (Nader and Allen, 1960; Spurny and Kubie, 1961; Lilienfeld and Dulchinos, 1972; Husar, 1974; Cooper, 1975; Lilienfeld, 1975; Sem and Borgos, 1975; Cooper, 1976; Macias, 1976; Jaklevic et al., 1981; Courtney et al., 1982; Klein et al., 1984; Wedding and Weigand, 1993; Speer et al., 1997)	Particle mass. Detection limit ~ 5 $\mu g/m^3$ for a one hour average	Beta rays (electrons with energies in the 0.01 to 0.1 MeV range) are attenuated according to an approximate exponential (Beer's Law) function of particulate mass, when they pass through deposits on a filter tape. Automated samplers utilize a continuous filter tape, first measuring the attenuation through the unexposed segment of tape to correct for blank attenuation. The tape is then exposed to ambient sample flow, accumulating a deposit. The beta attenuation measurement is repeated. The blank-corrected attenuation readings are converted to mass concentrations, with averaging times as short as 30 minutes.
Pressure Drop Tape Sampler (CAMMS) [k,ag] (Babich et al., 1997)	Particle mass. Detection linit ~ 2 $\mu g/m^3$ for a one hour average	CAMMS (continuous ambient mass monitor system) measures the pressure drop across a porous membrane filter (Fluoropore). For properly chosen conditions, the pressure drop is linearly correlated to the particle mass deposited on the filter.

Table 3-1 (continued)
Summary of Continuous Monitoring Technology

Instrument	Quantity Measured	Methodology
II. Visible Light Scattering		
Nephelometer [c,n,p,r,x,y,aa] (Mie, 1908; Koschmieder, 1924; Beuttell and Brewer, 1949; Ahlquist and Charlson, 1967, 1969; Charlson et al., 1967, 1968, 1969; Quenzel, 1969a, 1969b; Horvath and Noll, 1969; Borho, 1970; Ensor and Waggoner, 1970; Garland and Rae, 1970; Heintzenberg and Hänel, 1970; Rae and Garland, 1970; Rae, 1970a; Rae, 1970b; Ruppersberg, 1970; Covert et al., 1972; Ensor et al., 1972; Thielke et al., 1972; Bhardwaja et al., 1973; Heintzenberg and Quenzel, 1973a; Heintzenberg and Quenzel, 1973b; Rabinoff and Herman, 1973; Bhardwaja et al., 1974; Charlson et al., 1974a, 1974b; Quenzel et al., 1975; Heintzenberg, 1975, 1978; Heintzenberg and Bhardwaja, 1976; Harrison, 1977a, 1977b, 1979; Sverdrup and Whitby, 1977; Bodhaine, 1979; Heintzenberg and Witt, 1979; Heintzenberg, 1980; Mathai and Harrison, 1980; Waggoner and Weiss, 1980; Wiscombe, 1980; Harrison and Mathai, 1981; Johnson, 1981; Malm et al., 1981; Ruby and Waggoner, 1981; Waggoner et al., 1981; Winkler et al., 1981; Larson et al., 1982; Hasan and Lewis, 1983; Heintzenberg and Bäcklin, 1983; Waggoner et al., 1983; Hitzenberger et al., 1984; Gordon and Johnson, 1985; Rood et al., 1985, 1987; Ruby, 1985; Wilson et al., 1988; Barber and Hill, 1990; Trijonis et al., 1990; Bodhaine et al., 1991; Sloane et al., 1991; Nyeki et al., 1992; Optec Inc., 1993; Eldering et al., 1994; Horvath and Kaller, 1994; White et al., 1994; Mulholland and Bryner, 1994; Lowenthal et al., 1995; Anderson et al., 1996; Heintzenberg and Charlson, 1996; Watson et al., 1996; Rosen et al., 1997; Anderson and Ogren, 1998; Moosmüller et al., 1998)	*In-situ*, integrated light scattering from particles and gases; a direct estimate of the aerosol light-scattering coefficient, b_{scat}; lower detection limit ~ 1 Mm^{-1} for a ten minute average.	Ambient gases and particles are continuously passed through an optical chamber; the chamber is generally in the form of a long cylinder illuminated from one side, perpendicular to the long axis of the chamber. The light source is located behind a lambertian diffuser and illuminates the aerosol at visible wavelengths. Light is scattered by particles in the chamber over angles ranging from 0° to 180°; mounted behind a series of baffles, a photomultiplier tube located at one end of the chamber detects and integrates the light scattered over about 9° to 171°. The light detected by the photomultiplier is usually limited by filters to wavelengths in the 500 to 600 nm range, corresponding to the response of the human eye. The instrument is calibrated by introducing gases of known index of refraction, which produce a known scattered energy flux. (For this purpose, halocarbon gases must now be replaced by non-ozone-reactive alternatives.) A typical signal averaging period is about 2 minutes.

Table 3-1 (continued)
Summary of Continuous Monitoring Technology

Instrument	Quantity Measured	Methodology
Optical Particle Counter/Size Spectrometer [j,u,v,aa] (Gucker et al., 1947a, 1947b; Gucker and Rose, 1954; Whitby and Vomela, 1967; Whitby and Liu, 1968; Liu et al., 1974c; Heintzenberg, 1975, 1980; Hindman et al., 1978; Mäkynen et al., 1982; Chen et al., 1984; Robinson and Lamb, 1986; van der Meulen and van Elzakker, 1986; Wen and Kasper, 1986; Buettner, 1990; Gebhart, 1991; Hering and McMurry, 1991; Kaye et al., 1991; Sloane et al., 1991; Eldering et al., 1994; Kerker, 1997; Fabiny, 1998)	Number of particles in the 0.1 to 50 µm size range.	Light scattered by individual particles traversing a light beam is detected at various angles; these signals are interpreted in terms of particle size via calibrations.
Condensation Nuclei (CN) Counter [aa] (Liu and Pui, 1974; Sinclair and Hoopes, 1975; Bricard et al., 1976; Agarwal and Sem, 1980; Liu et al., 1982; Miller and Bodhaine, 1982; Bartz et al., 1985; Ahn and Liu, 1990; Noone and Hansson, 1990; Su et al., 1990; Zhang and Liu, 1990; Keston et al., 1991; McDermott et al., 1991; Stolzenburg and McMurry, 1991; Zhang and Liu, 1991; Saros et al., 1996)	Number of nucleating particles (particles in the ~0.003 to 1 µm size range).	Particles are exposed to high supersaturations (150% or greater) of a working fluid such as alcohol; droplets are subsequently nucleated, allowing detection of the particles by light scattering.
Aerodynamic Particle Sizer [aa] (Wilson and Liu, 1980; Kasper, 1982; Chen et al., 1985; Baron, 1986; Chen and Crow, 1986; Griffiths et al., 1986; Wang and John, 1987; Ananth and Wilson, 1988; Brockmann et al., 1988; Wang and John, 1989; Brockmann and Rader, 1990; Chen et al., 1990; Cheng et al., 1990, 1993; Lee et al., 1990; Rader et al., 1990; Heitbrink et al., 1991; Marshall et al., 1991; Heitbrink and Baron, 1992; Peters et al., 1993)	Number of particles in different size ranges.	Parallel laser beams measure the velocity lag of particles suspended in accelerating air flows.

Table 3-1 (continued)
Summary of Continuous Monitoring Technology

Instrument	Quantity Measured	Methodology
LIDAR [e,f,h,l,s,t] (Hitschfeld and Bordan, 1954; Fiocco et al., 1971; Fernald, 1972; Melfi, 1972; Rothe et al., 1974; Cooney, 1975; Woods and Jolliffe, 1978; Klett, 1981; Aldén et al., 1982; Browell, 1982; Browell et al., 1983; Measures, 1984; Force et al., 1985; McElroy and Smith, 1986; Ancellet et al., 1987, 1989; Edner et al., 1988; Galle et al., 1988; Alvarez II et al., 1990; Beniston et al., 1990; de Jonge et al., 1991; Grund and Eloranta, 1991; Ansmann et al., 1992; Kölsch et al., 1992; McElroy and McGown, 1992; Milton et al., 1992; She et al., 1992; Whiteman et al., 1992; Kovalev, 1993, 1995; Moosmüller et al., 1993; Gibson, 1994; Kempfer et al., 1994; Kovalev and Moosmüller, 1994; Piironen and Eloranta, 1994; Zhao et al., 1994; Grant, 1995; Toriumi et al., 1996; Evans et al., 1997; Hoff et al., 1997; Moosmüller and Wilkerson, 1997)	Range resolved atmospheric backscatter coefficient (cm^2/steradian) and gas concentrations.	A short laser pulse is sent into the atmosphere, backscattered light from gas and aerosols is detected as a function of time of flight for the light pulse. This results in a range resolved measurement of the atmospheric backscatter coefficient if extinction is properly accounted for. Special systems which separate molecular and aerosol scattering have an absolute calibration and extinction and backscatter ratio can be retrieved. Differential absorption lidars use multiple wavelengths and utilize the wavelength dependent absorption of atmospheric gases to retrieve their range resolved concentrations.
III. Visible Light Absorption		
Aethalometer [m,z] (Hansen et al., 1984, 1988, 1989; Rosen et al., 1984; Hansen and Novakov, 1989, 1990; Hansen and McMurry, 1990; Hansen and Rosen, 1990; Parungo et al., 1994; Pirogov et al., 1994)	Light absorption, reported as concentration of elemental carbon. Detection limit ~ 0.1 $\mu g/m^3$ black carbon for a one minute average.	Ambient air is continuously passed through a quartz-fiber filter tape. Light-absorbing particles such as black carbon cause attenuation of a light beam. By assuming that all light-absorbing material is black carbon, and that the absorption coefficient of the black carbon is known and constant, the net attenuation signals can be converted into black carbon mass concentrations. The time resolution of the aethelometer is on the order of a fraction of a minute depending on ambient black carbon concentration.
Particle Soot/Absorption Photometer (PSAP) [x] (Bond et al., 1998; Quinn et al., 1998)	Light absorption detection limit ~0.2 Mm^{-1} for a five-minute average. For an absorption efficiency of 10 m^2/g, this would correspond to 20 ng/m^3 of black carbon.	The PSAP produces a continuous measurement of absorption by monitoring the change in transmittance across a filter (Pallflex E70-2075W) for two areas on the filter, a particle deposition area and a reference area. A light emitting diode (LED) operating at 550 nm, followed by an Opal glass serves as light source. The absorption reported by the PSAP is calculated with a nonlinear equation correcting for the magnification of absorption by the filter medium and for response nonlinearities as the filter is loaded.

Table 3-1 (continued)
Summary of Continuous Monitoring Technology

Instrument	Quantity Measured	Methodology
Photoacoustic Spectroscopy [g,ag] (Bruce and Pinnick, 1977; Pao, 1977; Terhune and Anderson, 1977; Lin and Campillo, 1985; Adams, 1988; Adams et al., 1989, Arnott et al., 1995; Petzold and Niessner, 1995, 1996; Bijnen et al., 1996; Moosmüller and Arnott, 1996; Moosmüller et al., 1997; Arnott et al., 1998; Moosmüller et al., 1998)	Light absorption, reported as black carbon. Detection limit ~ 50 ng/m^3 for a ten-minute average.	Ambient air is aspirated through a resonant chamber, where it is illuminated by modulated (chopped) laser light at a visible wavelength (e.g., 514.5 nm). Light-absorbing particles, principally elemental carbon, absorb energy from the laser beam and transfer it as heating of the surrounding air. The expansion of the heated gas produces a sound wave at the same frequency as the laser modulation. This acoustic signal is detected by a microphone; its signal is proportional to the amount of absorbed energy. The illumination must be carefully chosen to avoid atmospheric gaseous absorption bands.
IV. Electrical Mobility		
Electrical Aerosol Analyzer (EAA) [aa] (Whitby and Clark, 1966; Liu et al., 1974a, 1974b; Liu and Pui, 1975; Helsper et al., 1982)	Number of particles in the sub-micrometer size range (~ 0.01 to 1.0 μm).	Particles are collected according to their size-dependent mobilities in an electric field. The collected particles are detected by their deposition of charge in an electrometer.
Differential Mobility Particle Sizer (DMPS) [aa] (Knutson and Whitby, 1975a, 1975b; Hoppel, 1978; Alofs and Balakumar, 1982; Hagen and Alofs, 1983; Fissan et al., 1983; ten Brink et al., 1983; Kousaka et al., 1985; Reineking and Porstendörfer, 1986; Wang and Flagan, 1990; Reischl, 1991; Winklmayr et al., 1991; Zhang et al., 1995; Birmili et al., 1997; Endo et al., 1997)	Number of nucleating particles in different size ranges (~ 0.01 to 1.0 μm size range).	Particles are classified according to their mobility in an electric field, which is a function of their size; a condensation nuclei counter then counts the population in a size "bin".

Table 3-1 (continued)
Summary of Continuous Monitoring Technology

Instrument	Quantity Measured	Methodology
V. Chemical-Specific Particle Monitors		
Single Particle Mass Spectrometer (RSMS, PALMS, ATOFMS) [ad,ae,af,ag] (Thomson and Murphy, 1993; Mansoori et al., 1994; Murphy and Thomson, 1994, 1995; Noble et al., 1994; Nordmeyer and Prather, 1994; Prather et al., 1994; Carson et al., 1995; Johnston and Drexler, 1995; Mansoori et al., 1996; Neubauer et al., 1996; Noble and Prather, 1996, 1997, 1998; Salt et al., 1996; Carson et al., 1997; Gard et al., 1997, 1998; Liu et al., 1997; Middlebrook, 1997; Murphy and Thomson, 1997a, 1997b; Murphy et al., 1997, 1998; Silva and Prather, 1997; Thomson et al., 1997; Murphy and Schein, 1998)	Particle sizes and single particle compositions.	Particles in air are introduced into successively lower-pressure regions and acquire high velocities due to gas expansion. Particle size is evaluated by laser light scattering. The particles then enter a time-of-flight mass spectrometer.
Ambient Carbon Particulate Monitor (ACPM) [y] (Turpin et al., 1990a, 1990b; Chow et al., 1993a; Rupprecht et al., 1995)	Concentrations of organic and elemental carbon. Detection limit ~ 0.2 $\mu g/m^3$ for a two hour average.	Measurement of carbon particulate by automatic thermal CO_2method. The carbon collected in a high-temperature impactor oxidized at elevated temperatures after sample collection is complete. A CO_2 meter measures the amount of carbon released as result of sample oxidation. OC and EC can be speciated by volatizing OC at an intermediate temperature.
Sulfur Analyzer, Flame Photometric Detection (FPD) [k,ag] (Dagnall et al., 1967; Stevens et al., 1969, 1971; Farwell and Rasmussen, 1976; Cobourn et al., 1978; Durham et al., 1978; Huntzicker et al., 1978; Kittelson et al., 1978; Jaklevic et al., 1980; Mueller and Collins, 1980; Tanner et al., 1980; Camp et al., 1982; Benner and Stedman, 1989, 1990)	Sulfur dioxide and sulfate. Detection limit ~ 0.1 $\mu g/m^3$ for a one hour average.	Sulfur species are combusted in a hydrogen flame, creating excited sulfur dimers (S_2*). Fluorescence emission near 400 nm is detected by a photomultiplier. The photomultiplier current is proportional to the concentration of sulfur in all species. Four out of five FPD systems agreed to within ± 5% in a one-week ambient sampling intercomparison.

Table 3-1 (continued)
Summary of Continuous Monitoring Technology

Instrument	Quantity Measured	Methodology
Nitrate Analyzer, Automated Particle Nitrate Monitor (APNM) [a,y,ag] (Winkler, 1974; Roberts and Friedlander, 1976; Hering and Friedlander, 1982; Stein et al., 1994; Yamamoto and Kosaka, 1994; Hering, 1997; Chow and Watson, 1998b; Chow et al., 1998b; Hering, 1998; Hering and Stolzenburg, 1998; Norton et al., 1998)	Particle Nitrate. Detection limit ~ 0.5 $\mu g/m^3$ for a 12-minute average.	Particle collection by impaction followed by flash vaporization and detection of the evolved gases in a chemiluminescent NO_x analyzer.
Streaker [w] (Hudson et al., 1980; Bauman et al., 1987; Annegarn et al., 1990; Chow, 1995)	$PM_{2.5}$ and PM_{10} elemental composition.	Particles are collected on two impaction stages and a Nuclepore polycarbonate-membrane after-filter followed by particle-induced x-ray emission (PIXE) analysis for multielements.
Davis Rotating-Drum Universal-Size-Cut Monitoring Impactor (DRUM) [ac] (Raabe et al., 1988; Pitchford and Green, 1997)	Size-fractionated elemental composition from 0.07 µm to 15 µm in diameter for eight size ranges.	Particles are collected on grease-coated mylar substrates that cover the outside circular surface of eight clock-driven slowly rotating cylinders or drums (one for each stage). Mylar substrates are submitted for focused-beam particle-induced x-ray emission (PIXE) analysis of multielements.
VI. Precursor Gas Monitors		
Ammonia Analyzer, Chemiluminescence [z] (Breitenbach and Shelef, 1973; Braman et al., 1982; Keuken et al., 1989; Langford et al., 1989; Wyers et al., 1993; Sorensen et al., 1994; Chow et al., 1998b; Jaeschke et al., 1998)	Ammonia concentration. Detection limit ~ 10 ppb.	Ammonia concentrations are measured by first removing oxides of nitrogen, then oxidizing ammonia to nitrogen oxide by thermal oxidation at high temperature for detection by chemiluminescence.
Ammonia Analyzer, Fluorescence [b,q] (Abbas and Tanner, 1981; Rapsomanikis et al., 1988; Genfa et al., 1989; Harrison and Msibi, 1994)	Ammonia concentration. Detection limit ~ 0.1 ppb.	Sampled ammonia is removed from the airstream by a diffusion scrubber, dissolved in a buffered solution, and reacted with o-phtaldialdehyde and sulfite. The resulting i-sulfonatatoisoindole fluoresces when excited with 365 nm radiation, and the intensity of the 425 nm emission is monitored for quantification. The diffusion scrubber might be modified to pass particles while excluding ammonia gas to continuously quantify ammonium ions.

Table 3-1 (continued)
Summary of Continuous Monitoring Technology

Instrument	Quantity Measured	Methodology
Other ammonia analyzers[ag] (Appel et al., 1988; Rooth et al., 1990; Wiebe et al., 1990; Williams et al., 1992; Sauren et al., 1993; Schendel et al., 1990; Platt, 1994; Mennen et al., 1996)	Ammonia concentration.	Other, less established methods to measure ammonia include photoacoustic spectroscopy, vacuum ultraviolet/photofragmentation laser-induced fluorescence, Differential Optical Absorption Spectroscopy (DOAS) in the ultraviolet DIfferential Absorption Lidar (DIAL, see section 3.2.5), and Fourier Transform Infrared (FTIR) spectroscopy (see section 3.6.3).
Nitric Acid Analyzer [ag] (Ripley et al., 1964; Kelly et al., 1979, 1990; Burkhardt et al., 1988; Fox et al., 1988; Hering et al., 1988; Fehsenfeld et al., 1990; Gregory et al., 1990; Harrison, 1994; Harrison and Msibi, 1994)	Nitric acid concentration. Detection limit ~ 0.1 ppb for a 5-minute average.	Nitric acid can be reduced to NO_2 prior to detection by the chemiluminescent and luminol methods.
Long Path Fourier Transform Infrared Spectroscopy (FTIR) [o] (White, 1976; Tuazon et al., 1978; Doyle et al., 1979; Tuazon et al., 1980; Tuazon et al., 1981; Hanst et al., 1982; Biermann et al., 1988; Hanst and Hanst, 1994)	Nitric acid and ammonia concentrations. Detection limit ~ 4 ppb for nitric acid and ~ 1.5 ppb for ammonia for a 5-minute average.	Long path absorption spectroscopy. A path length of more than 1 km is folded into a 25-m long White cell.
Tunable Diode Laser Absorption Spectroscopy (TDLAS) [ab] (Schiff et al., 1983; Anlauf et al., 1985, 1988; Harris et al., 1987; Fox et al., 1988; Hering et al., 1988; Mackay et al., 1988; Schmidtke et al., 1988; Fehsenfeld et al., 1998)	Nitric acid concentation. Detection limit ~ 0.3 ppb for a 5-minute average.	Nitric acid concentrations are measured by high spectral resolution diode laser spectroscopy in the mid-infrared spectral region. The sample is introduced into a reduced pressure White cell to reduce pressure broadening and increase the path length.
Mist Chamber[ag] (Talbot et al., 1990)	Nitric acid concentrations. Detection limit ~ 0.01 ppb for a 10-minute average.	The mist chamber method samples nitric acid by efficiently scrubbing it from the atmosphere in a refluxing mist chamber followed by analysis of the scrubbing solution for NO_3^- by ion chromatography. A sensitivity of 10 pptv for a 10-minute integration period has been reported.

Table 3-1 (continued)
Summary of Continuous Monitoring Technology

Instrument	Quantity Measured	Methodology
Laser-Photolysis Fragment-Fluorescence (LPFF)[ag] (Papenbrock and Stuhl, 1991)	Nitric acid concentrations. Detection limit ~ 0.1 ppb for a 15-minute average.	Nitric acid concentrations have also been measured with the Laser-Photolysis Fragment-Fluorescence (LPFF) Method, which irradiates the air sample with ArF laser light (193 nm) resulting in the photolysis of nitric acid. The resulting hydroxyl radical (OH) emits fluorescence at 309 nm which is taken as a measure of the nitric acid mixing ratio in air. A sensitivity of 0.1 ppbv and a time constant of 15 minutes limited by surface ad- and desorption have been reported. An intercomparison of this technique with a denuder technique was also reported.
Chemical Ionization Mass Spectrometry (IMS)[ag] (Huey et al., 1998; Mauldin et al., 1998; Fehsenfeld et al., 1998)	Nitric acid concentrations. Detection limit ~ 0.005 ppb for a 10-second average.	Chemical Ionization Mass Spectrometry (CIMS) has been used for the sensitive (few pptv) and fast (second response) measurement of atmospheric nitric acid concentrations. Reagent ions formed by an ion source are mixed with the sampled air and react selectively with nitric acid. The ionic reaction product is detected with a mass spectrometer. Two different CIMS instruments have been described and compared with an older, more established filter pack technique.

Table 3-1 (continued)
Summary of Continuous Monitoring Technology

[a] Aerosol Dynamics Inc.
2329 Fourth Street
Berkeley, CA 94710
Tel.: 510-649-9360
Fax: 510-649-9260

[b] Advanced Pollution Instrumentation Inc.
6565 Nancy Ridge Dr.
San Diego, CA 92121
Tel.: 619-657-9800
Fax: 619-657-9816
email: api@cts.com

[c] Belfort Instrument Company
727 South Wolfe Street
Baltimore, MD 21231
Tel.: 410-342-2626
Fax: 410-342-7028
e-mail: belfortin@aol.com
www: http://www.belfortinst.com

[d] California Measurements Inc.
150 E. Montecito Ave.
Sierra Madre, CA 91024
Tel.: 818-355-3361
Fax: 818-355-5320

[e] Coherent Technologies Inc.
655 Aspen Ridge Drive
Lafayette, CO 80306
Tel.: 303-604-2000
e-mail: milton@ctilidar.com

[f] Corning OCA Corporation
Applied Optics
7421 Orangewood Avenue
P. O. Box 3115
Garden Grove, CA 92842-3115
Tel.: 714-895-1667
Fax: 714-891-4356
e-mail: clemensesa@corning.com
www: http://www.oca.com/lidar.htm

[g] Desert Research Institute
Energy & Environmental Engineering
P.O. Box 60220
Reno, NV 89506
Tel.: 702-677-3194
Fax: 702-677-3157
www: http://www.dri.edu

[h] Elight Laser Systems GmbH
Potsdamer Straße 18A
D-14513 Teltow
Germany
Tel.: 49-3328-430-112
Fax: 49-3328-430-115
e-mail: 100276.3673@compuserve.com

[i] Graseby-Andersen
500 Technology Court
Smyrna, GA 30082-5211
Tel.: 770 319 9999
Fax: 770 319 0336
e-mail: nutech@graseby.com
www: http://www.graseby.com

[j] Grimm Technologies
9110 Charlton Place
Douglasville, GA 30135
Tel.: 770-577-0853
Fax: 770-577-0955

[k] Harvard University
School of Public Health
665 Huntington Ave.
Boston, MA 02115
www: http://www.hsph.harvard.edu

[l] Kayser-Threde GmbH
Wolfratshauser Straße 48
D-81379 München
Germany
Tel.: 49-89-724-95-0
Fax: 49-89-724-95-291
e-mail: fy@kayser-threde.de
www: http://www.kayser-threde.de

[m] Magee Scientific Company
1829 Francisco Street
Berkeley, CA 94703
Tel.: 510-845-2801
Fax: 510-845-7137
e-mail: Aethalometers@MageeSci.com
www: http://www.mageesci.holowww.com:80/

[n] Met One Instruments
1600 Washington Blvd.
Grants Pass, OR 97526
Tel.: 541-471-7111
Fax: 541-471-7116

[o] Midac Corporation
17911 Fitch Ave.
Irvine, CA 92714
Tel.: 714-660-8558
Fax: 714-660-9334

[p] MIE Inc.
7 Oak Park
Bedford, MA 01730
Tel.: 617-275-1919
Fax: 617-275-2121

[q] Opsis Inc.
1165 Linda Vista, Suite 112
San Marcos, CA 92069
Tel.: 760-752-3005
Fax: 760-752-3007

[r] Optec, Inc.
199 Smith Street
Lowell, MI 49331
Tel.: 616-897-9351
Fax: 616-897-8229
e-mail: OptecInc@aol.com
www: optecinc.com

[s] Optech Inc.
100 Widcat Road
North York, Ontario M3J 2Z9
Canada
Tel.: 416-661-5904
Fax: 416-661-4168

[t] ORCA Photonics Systems Inc.
14662 NE 95th St.
Redmond, WA 98052
Tel.: 425-702-8706
Fax: 425-702-8806
e-mail: info@willows.orcaphoton.com
www: http://www.orcaphoton.com/

[u] Palas GmbH
Gresbachstr. 3b
D-76229 Karlsuhe
Germany
Tel.: 721-962-13-0
Fax: 721-962-13-33
www: http://gitverlag.com/laborjahrbuch/pis/Palas/default.html

[v] Particle Measuring Systems Inc.
1855 South 57th Court
Boulder, CO 80301
Tel.: 303-443-7100
Fax: 303-449-6870

[w] PIXE Analytical Laboratories
P.O. Box 2744
Tallahassee, FL 32316
Tel.: 904-574-6469 or 800-700-7494

[x] Radiance Research
535 N.W. 163rd St.
Seattle, WA 98177
Tel.: 206-546-4859
Fax: 206-546-8425
e-mail: radiance@cmc.net

Table 3-1 (continued)
Summary of Continuous Monitoring Technology

[y] Rupprecht & Patashnick Co.
25 Corporate Circle
Albany, NY 12203
Tel.: 518-452-0065
Fax: 518-452-0067
email: info@rpco.com
www: http://www.rpco.com

[z] Thermo Environmental Instruments (TEI)
8 West Forge Parkway
Franklin, MA 02038
Tel.: 508-520-0430
Fax: 508-520-1460

[aa] TSI Inc.
Particle Instruments Division
P.O. Box 64394
St. Paul, MN 55164
Tel.: 612-490-2833
Fax: 612-490-3860
e-mail: particle@tsii.com
www: http://www.tsi.com

[ab] Unisearch Associates Inc.
222 Snidercroft Road
Concord, Ontario
Tel.: 905-669-3547
Fax:905-669-8652

[ac] University of California
Air Quality Group
Crocker Nuclear Laboratory
Davis, CA 95616

[ad] University of California
Dept. of Chemistry
Riverside, CA 92521
www: http://www.ucr.edu

[ae] University of Delaware
Dept. of Mechanical Engineering
Newark, DE 19716
www: http://www.udel.edu

Because the restoring force constant k is a function of temperature, the sampling apparatus (tapered tube, filter) and sampled air are kept at a constant temperature. The default value for this temperature setting is usually 50 °C to prevent the measurement of particle-bound water. Filter lifetimes are usually two to four weeks. After a filter change, the new filter is equilibrated for one-half to one hour prior to acquiring data.

In ambient particulate applications, the R&P TEOM® operates with an initial filter mass of about 50 mg and a deposited aerosol mass of no greater than 10 mg. It is capable of operating with flow rates through the filter from 0.5 to 5 L/min, with a typical flow rate of 3 L/min. The R&P TEOM® ambient particulate monitor provides for averaging times from 10 minutes to 24 hours and is available with a choice of sample inlets for TSP, PM_{10}, $PM_{2.5}$, or $PM_{1.0}$ (particles with aerodynamic diameters less than 1 µm) monitoring. Collocated TEOM instruments have reported a precision of ±2.8 µg/m^3 for hourly averaged PM_{10} concentrations and ±5.1 µg/m^3 for 10-minute-averaged PM_{10} concentrations.

The default 50 °C temperature prevents water vapor condensation and provides a standard sample condition, but it volatilizes most of the ammonium nitrate and some of the volatile organic compounds in atmospheric particles. As a consequence, monitored sites and seasons having high levels of ammonium nitrate and/or organic particulate mass do not always yield a reasonable correspondence between time-integrated TEOM® and collocated filter measurements (Allen et al., 1997). All instruments that apply high temperature pre-conditioning, not just the TEOM®, are affected by this phenomena.

Large fluctuations in the TEOM® mass concentration can occur over several hours for $PM_{2.5}$ monitoring, but PM_{10} TEOM® measurements do not seem to be as significantly affected. It has been hypothesized that this noise is caused by changes in the equilibrium of particles on the TEOM filter when ambient pollutants or moisture is changing rapidly (Allen et al., 1997). Meyer et al. (1992) showed ~30% more PM_{10} mass was obtained with a 30 °C TEOM® sampling beside a 50 °C TEOM® in the woodburning-dominated environment at Mammoth Lakes, CA. R&P is currently testing modifications to the aerosol conditioning process that approximate the nominal filter equilibration conditions (~21 °C and ~35% relative humidity) to which FRM filters will be subjected prior to laboratory weighing.

3.1.2 Piezoelectric Microbalance

Piezoelectric crystals have mechanical resonances that can be excited by applying an alternating electrical voltage to the crystal. As the resonance frequencies are very well defined, such crystals (quartz in particular) have found applications as secondary time and frequency standards in clocks and watches. As for all mechanical resonators, the resonance frequency is a function of mass. Therefore, by monitoring the resonance frequency in comparison with a second crystal, one can continuously measure the mass deposited on the crystal (Sem et al., 1977; Bowers and Chuan, 1989; Ward and Buttry, 1990; Noel and Topart, 1994). Comparison with a second crystal largely compensates for the effect of temperature changes on the resonance frequency.

The piezoelectric principle has been used to measure particle mass by depositing the particles on the crystal surface either by electrostatic precipitation or by impaction (Olin and Sem, 1971). The collection efficiency of either mechanism has to be determined as function of particle size to achieve quantitative measurements. In addition, the mechanical coupling of large particles to the crystal is uncertain. Both single and multi-stage impactors have been used (Olin and Sem, 1971; Fairchild and Wheat, 1984). Quartz crystals have sensitivities of several hundred hertz per microgram. This sensitivity results in the ability to measure the mass concentration of a typical, 100 $\mu g/m^3$, aerosol to within a few percent in less than one minute (Olin and Sem, 1971).

3.1.3 Beta Attenuation Monitor (BAM)

Beta Attenuation Monitors (BAM) measure the loss of electrons as they penetrate a filter on which particles have been deposited (Nader and Allen, 1960; Spurny and Kubie, 1961; Lilienfeld and Dulchinos, 1972; Husar, 1974; Lilienfeld, 1975; Macias, 1976; Jaklevic et al., 1981; Klein et al., 1984; Wedding and Weigand, 1993). BAM technology has also recently been used to measure the liquid water content of aerosols (Speer et al., 1997).

Particles are collected on a spot of a filter tape. A radioactive (beta) source emits low-energy electrons. Electrons propagating through the tape are detected on the opposite side. Their intensity is attenuated by inelastic scattering with atomic electrons, including those of the particle deposit. The beta intensity is described, to a good approximation, by the Beer-Lambert relationship (Sem and Borgos, 1975; Cooper, 1976). If the beta attenuation coefficient per aerosol mass deposited on the filter is known, a continuous measurement of aerosol mass concentration becomes possible. Movement of the filter tape is needed when the aerosol loading on the deposition spot attenuates the beta intensity at the detector to near background levels (Cooper, 1975).

Lilienfeld (1975) identifies 13 different electron-emitting isotopes with half-lives in excess of one year, no significant emission of gamma radiation, and energies of less than 1 MeV. Carbon-14 (^{14}C) sources are most commonly used. The beta attenuation coefficient depends both on beta energy and on chemical composition of the aerosol. For a ^{14}C source and typical atmospheric aerosol, the attenuation coefficient is ~0.26 cm^2/mg (Macias, 1976). The dependence of the attenuation coefficient on the chemical aerosol composition (Macias, 1976; Jaklevic et al., 1981) is commonly assumed to be within measurement precision, but it may bias measurements when the composition of calibration standards differs substantially from the composition of the ambient aerosol. Measurement resolution and lower detection limit for modern instruments are on the order of a few $\mu g/m^3$ (Courtney et al., 1982).

Beta attenuation monitors are typically operated at ambient temperatures and relative humidity. While these conditions preserve the integrity of volatile nitrates and organic compounds, they also favor the sampling of liquid water associated with soluble species at high humidities. Under these conditions BAM concentrations are often larger than those of collocated filter samplers for which samples have been equilibrated at lower laboratory relative humidities prior to gravimetric analysis. Sampled air can be preceded by a diffusion dryer to remove water vapor, thereby encouraging the evaporation of liquid water associated with soluble components of suspended particles.

3.1.4 Pressure Drop Tape Sampler (CAMMS)

A continuous particle mass monitoring system, CAMMS (continuous ambient mass monitor system), based on measuring the pressure drop across a porous membrane filter (Fluoropore) has recently been developed at Harvard University (Babich et al., 1997). The pressure drop is linearly correlated to the particle mass deposited on the filter.

The filter face velocity is chosen such that pore obstruction by interception is the dominant cause of particle-related pressure drop change over time. The monitor consists of: 1) a Fluoropore filter tape to collect particles; 2) a filter tape transportation system to allow for several weeks of unattended particle sampling; 3) a system to measure the pressure drop across the filter; 4) a diffusion dryer to remove particle-bound water; and 5) an air sampling pump. The monitor exposes a new segment of filter tape every 20 to 60 minutes for particle collection. During this period, particles collected on the filter should remain in equilibrium with the sample air, since the composition of ambient air does not usually vary substantially over this short time period. Volatilization and adsorption artifacts are minimized because measurements are made at ambient temperature for short time periods and at a low face velocity. A diffusion dryer that removes water vapor could also be used to condition air, thereby encouraging the evaporation of liquid water associated with soluble components of suspended particles.

The CAMMS can detect concentrations as low as 2 $\mu g/m^3$ for hourly averages. Results from a Boston, MA, field study conducted during the summer of 1996 show good agreement between CAMMS and the Harvard Impactor, with a root mean square difference of less than 3 $\mu g/m^3$. Unpublished data (P. Koutrakis, personal communication) comparing CAMMS with the Harvard Impactor $PM_{2.5}$ filter sampler show R^2 for six individual sites ranges from 0.86 to 0.97. CAMMS is believed to be relatively insensitive to changes in aerosol composition between sites and over seasons.

3.2 Visible Light Scattering

Particle light scattering (b_{sp}) is determined by illuminating particles, individually or as a group, and measuring the scattered intensity at different orientations from the incident light source. The intensity of scattered light is related to mass concentration by electromagnetic theory or by comparison with a collocated filter measurement. Particle light scattering measurements from five different types of instruments are discussed in the following subsections.

3.2.1 Nephelometer

Nephelometers quantify particle light scattering. Integrating nephelometers quantify particle light scattering integrated over all directions. The original application of integrating nephelometers was to quantify airport visibility during World War II (Beuttell and Brewer, 1949). For visibility applications, scattering extinction serves as a surrogate for total light extinction which is related to visibility (Koschmieder, 1924). The basic integrating nephelometer design was developed by Beuttell and Brewer (1949), and has since been further perfected and automated (e.g., Ahlquist and Charlson, 1967; Charlson et al., 1967;

Quenzel, 1969a, 1969b; Ensor and Waggoner, 1970; Garland and Rae, 1970; Heintzenberg and Hänel, 1970; Rae and Garland, 1970; Rae, 1970a; Rae, 1970b; Ruppersberg, 1970; Heintzenberg and Quenzel, 1973a; Heintzenberg and Quenzel, 1973b; Rabinoff and Herman, 1973; Quenzel et al., 1975; Heintzenberg and Bhardwaja, 1976; Harrison, 1977a, 1977b; Heintzenberg and Witt, 1979; Ruby and Waggoner, 1981; Hasan and Lewis, 1983; Heintzenberg and Bäcklin, 1983; Hitzenberger et al., 1984; Gordon and Johnson, 1985; Ruby, 1985; Rood et al., 1987; Bodhaine et al., 1991; Horvath and Kaller, 1994; Mulholland and Bryner, 1994; Anderson et al., 1996; Rosen et al., 1997). A comprehensive review of nephelometer designs and applications is provided by Heintzenberg and Charlson (1996). The integrating nephelometer has been widely used to measure visibility in urban, non-urban, and background areas (e.g., Horvath and Noll, 1969; Harrison, 1979; Johnson, 1981; Malm et al., 1981; Ruby, 1985; White et al., 1994; Watson et al., 1996). Comparisons between calculated and measured aerosol light scattering have been made including its humidity dependence (e.g. Covert et al., 1972; Ensor et al., 1972; Winkler et al., 1981; Rood et al., 1985; Wilson et al., 1988; Eldering et al., 1994). Table 3-2 summarizes the operating characteristics of several available nephelometers.

Other applications of the integrating nephelometer include: 1) measurements of Rayleigh scattering coefficients (e.g., Bhardwaja et al., 1973; Bodhaine, 1979); 2) determination of aerosol size distributions (e.g. Ahlquist and Charlson, 1969; Thielke et al., 1972; Heintzenberg, 1975; Sverdrup and Whitby, 1977; Heintzenberg, 1980; Harrison and Mathai, 1981; Sloane et al., 1991) and refractive indices (e.g., Bhardwaja et al., 1974; Mathai and Harrison, 1980); 3) detection of sulfuric acid - ammonium sulfate aerosol (e.g., Charlson et al., 1974a; Charlson et al., 1974b; Larson et al., 1982; Waggoner et al., 1983); and 4) estimation of particle mass concentrations (e.g., Charlson et al., 1967; Charlson et al., 1968; Charlson et al., 1969; Borho, 1970; Thielke et al., 1972; Waggoner and Weiss, 1980; Waggoner et al., 1981; Moosmüller et al., 1998).

Nephelometer sampling procedures depend on the intended uses of the data. To determine visibility reduction, total light scattering is desired, including that caused by liquid water associated with soluble particles and that from the molecules in clean air. For this purpose the sensing chamber must have a minimal temperature differential with respect to ambient air and a particle-free baseline of ~10 Mm^{-1} is established. Internal ambient temperatures are maintained by a measurement chamber that is thermally insulated from the rest of the instrument and a large air inlet with motorized door that allows ambient air to flow unmodified over a short distance. Closing the inlet door allows for the introduction of a calibration gas. This passive sampling scheme alters the temperature of the air sample by less than 0.5 °C (Optec Inc., 1993).

Light scattering is often very high at relative humidities exceeding 80% because small particles grow to sizes that scatter light more efficiently as they acquire liquid water. As a result, ambient temperature nephelometers overestimate mass concentrations at high humidities when particles have a large soluble component. The air stream can be heated, similar to the TEOM air conditioning (see Section 3.1.1), to remove liquid water when an indicator of particle mass is desired (e.g., Waggoner and Weiss, 1980). Some systems control both temperature and humidity to characterize the hygroscopic properties of

Table 3-2
Operating Characteristics of Commercially Available Nephelometers

Manufacturer	Model	Scattering Type	Sampling	Time Resolution	Center Wavelength	Backscatter Feature
Belfort	1590	Integrating	Forced	2 min	530 nm	No
Optec	NGN-2	Integrating	Passive	≥ 2 min	550 nm	No
TSI	3551	Integrating	Forced	≥ 2 sec	550 nm	No
TSI	3563	Integrating	Forced	≥ 2 sec	450, 550, and 700 nm	Yes
Radiance	M903	Integrating	Forced	≥ 10 sec	530 nm	No
Grimm	DustCheck	Sideways	Forced	≥ 3 sec	780 nm	No
MIE	DataRam	Forward	Forced	≥ 1 sec	880 nm	No
MIE	personal DataRam	Forward	Passive	≥ 1 sec	880 nm	No
Met One Instruments	GT-640	Forward	Forced	≥ 1 min	781 nm	No
R&P	DustLite Model 3000	Forward	Forced	≥ 3 sec	880 nm	No
TSI	DustTrack Model 8520	Sideways	Forced	≥ 1 sec	780 nm	No

suspended particles (e.g., Covert et al., 1972; Rood et al., 1985; Rood et al., 1987). Heating prior to nephelometer sensing results in the same negative volatilization biases found for the heated TEOM air stream; the higher the temperature, the greater the volatilization of ammonium nitrate and volatile organic compounds.

Although light scattering is often highly correlated with mass concentrations, the relationship depends on several variables and may be different from location to location and for different seasons of the year. The light scattered per $\mu g/m^3$ (particle scattering efficiency, $\sigma_{sp,}$ usually expressed in m^2/g) depends on geometric particle diameter, real and imaginary parts of the refractive index, and particle shape. Particle scattering (b_{sp} in Mm^{-1}) is the product of the scattering efficiency and the particle concentration). For spherical particles of known compositions, scattering efficiencies can be calculated (e.g., Wiscombe, 1980; Barber and Hill, 1990; Lowenthal et al., 1995) based on Mie theory (Mie, 1908). An example of scattering efficiency as a function of particle diameter is given in Figure 3-1. For particles with diameters (d) less than the wavelength of light (λ), the scattering efficiency increases as function of diameter and reaches a maximum of ~4 m^2/g at a particle diameter comparable to the wavelength of the scattered light. For particles with diameters larger than the light wavelength, the scattering efficiency decreases proportional to 1/d and is modulated by an oscillation. This oscillation disappears as the particle diameter becomes much larger than the wavelength. This oscillation attenuates if non-monochromatic light is used and when a distribution of particle sizes and light wavelengths are present, as in ambient air.

Particle scattering measured by integrating nephelometers includes systematic errors owing to: 1) non-monochromatic light sources; 2) limits of the integration angle; and 3) and non-Lambertian light sources (e.g., Quenzel, 1969a, 1969b; Ensor and Waggoner, 1970; Heintzenberg and Quenzel, 1973a, 1973b; Rabinoff and Herman, 1973; Quenzel et al., 1975; Heintzenberg, 1978; Hasan and Lewis, 1983; Mulholland and Bryner, 1994; Anderson et al., 1996; Heintzenberg and Charlson, 1996; Rosen et al., 1997; Anderson and Ogren, 1998). Nephelometers can be designed to infer information about particle size, shape, and index of refraction by using several wavelengths and detection geometries (e.g., Heintzenberg and Bhardwaja, 1976; Bodhaine et al., 1991; Anderson et al., 1996; Heintzenberg and Charlson, 1996). Further modification of the nephelometer response can also be achieved by adding a size-selective inlet to the nephelometer air intake (e.g., Nyeki et al., 1992; White et al., 1994).

In practice, particle scattering efficiencies are empirically determined by collocating nephelometers with filter-based samplers and comparing their measurements. This approach has yielded a scattering efficiency of 2.6 m^2/g for TSP with 90% of a large number of measurements being within a factor of two from this value (e.g., Charlson et al., 1967; Charlson et al., 1968; Charlson et al., 1969). For a variety of locations classified as pristine, rural, residential, and industrial, the scattering efficiency was found to be 3.2 ± 0.2 m^2/g with correlations >0.95 for fine particles (~ $PM_{2.5}$) using a nephelometer with a heated air stream (Waggoner and Weiss, 1980; Waggoner et al., 1981). The constant scattering efficiency is due to the fact that the mass mean diameter of the fine particle mode is in the range of 0.4 to 1 µm where the scattering efficiency depends only weakly on the mass mean diameter. Trijonis et al. (1990) found scattering efficiencies of ~3 m^2/g for fine particles.

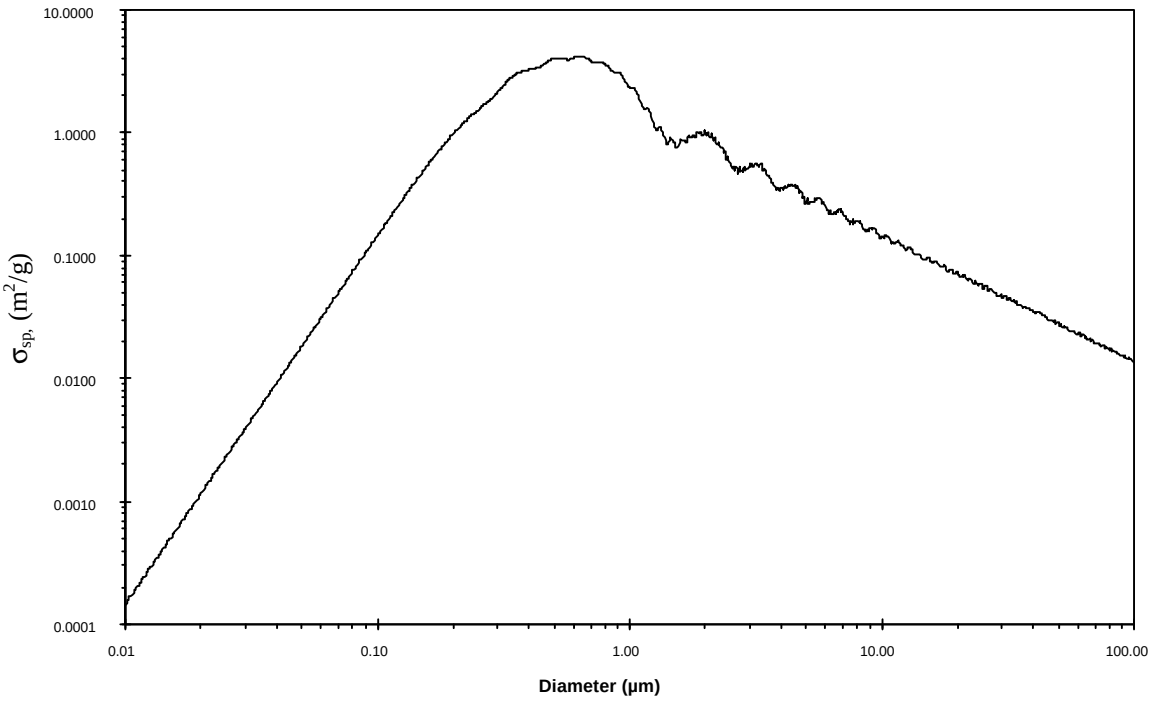

Figure 3-1. Particle scattering efficiency (σ_{sp}) as function of particle diameter for silica particles (δ = 2.2 g/cm^3, n = 1.46 at 550 nm) and monochromatic green light (λ = 550 nm).

Husar and Falke (1996) examined relationships between urban b_{sp} and $PM_{2.5}$ for five sites in Oregon, two sites in Missouri, and six sites in California, with R^2 ranging from 0.22 to 0.93. Linear regression slopes of b_{sp} vs. $PM_{2.5}$ ranged from 4.1 to 11.9 m^2/g. Most of the relationships were straight line with a few notable outliers.

3.2.2 Optical Particle Counter (OPC)

Optical Particle Counters (OPC) use light scattering to detect the size and number of individual particles (Gucker et al., 1947a; Gucker et al., 1947b; Gucker and Rose, 1954; Kerker, 1997; Fabiny, 1998). OPCs have long been used in aerosol research (e.g., Liu et al., 1974c; Heintzenberg, 1975; Heintzenberg, 1980; Eldering et al., 1994), thereby attaining a degree of reliability and ease of operation that allow them to be deployed in long-term monitoring networks. Some instruments analyze the spatial distribution of the scattered light to derive a shape parameter (e.g., Kaye et al., 1991) that can be used to determine deviations from sphericity.

In an OPC, a narrow air stream is directed through a small sensing zone, where it is illuminated by an intensive light beam, commonly a visible laser beam. Light scattered by an individual particle is sensed by a fast and sensitive detector, resulting in an electrical pulse. Particle size is determined from the pulse amplitude, and particle number is determined from the number of pulses (e.g., Whitby and Vomela, 1967; Mäkynen et al., 1982; Chen et al., 1984; Robinson and Lamb, 1986; Wen and Kasper, 1986). The size of particles that can be detected with OPCs ranges from about 0.05 to 50 μm (Fabiny, 1998), but it is more typically 0.2 to 30 μm.

Particle sizes and numbers are translated to mass concentration by assuming a spherical particle shape and a particle density. The sum over all particle size bins can be further related to mass loadings by comparison with a collocated filter sample. A few recently developed units allow a 47-mm filter to be placed in the exhaust stream so that the sensed particles can be collected for laboratory weighing and possible chemical characterization. This would allow at least an average calibration to be obtained for sampling periods that might last as long as one week.

The particle size measurement is commonly calibrated with a National Institute of Standards and Technology (NIST)-traceable, monodisperse distribution of polystyrene latex spheres (Whitby and Liu, 1968; Sloane et al., 1990). While size measurements with OPCs can be very precise (van der Meulen and van Elzakker, 1986), their accuracy depends on particle composition and shape (Buettner, 1990; Gebhart, 1991). These issues have been explored for atmospheric aerosols (e.g., Hindman et al., 1978; Hering and McMurry, 1991). Accuracy can be improved by simultaneous use of an integrating nephelometer with optical particle counters (Sloane et al., 1991).

3.2.3 Condensation Nuclei Counter (CNC)

Continuous-flow Condensation Nuclei Counters (CNC) sense ultrafine particles by causing them to grow to a size that is efficiently detected by light scattering (Sinclair and Hoopes, 1975; Bricard et al., 1976). Particles in a sampled air stream enter a saturator where

alcohol vapors at a temperature typically above ambient (e.g., 35 °C) create a saturated atmosphere. Particles then pass into a condenser tube at a temperature sufficiently below that of the saturator (e.g., 10 °C) (Miller and Bodhaine, 1982; Ahn and Liu, 1990). Alcohol vapor condenses on the particles causing them to grow, and they are detected and classified by an OPC. Table 3-3 summarizes the specifications of several representative CNCs.

CNCs detect particles with 0.003 to 1 µm diameters. For low particle concentrations, the instrument operates in a counting mode, registering individual light pulses. For concentrations above 1,000 particles/cm^3, the simultaneous presence of more than one particle in the viewing volume becomes frequent, and individual particles can no longer be counted. At this point, the CNC switches to the photometric mode where the power of the light scattered by all particles present in the viewing volume is measured (e.g., Agarwal and Sem, 1980). In the counting mode, a CNC can be very precise (e.g., Liu et al., 1982), but the counting efficiency for ultrafine particles depends substantially on the instrument design (Bartz et al., 1985; Su et al., 1990; McDermott et al., 1991; Stolzenburg and McMurry, 1991; Saros et al., 1996). In the photometric mode, the CNC must be calibrated with aerosol of known concentration (for example, by using an electrostatic classifier) (Liu and Pui, 1974). Response curves as a function of particle size, concentration, and different environmental conditions have been determined for several different CNCs (Liu et al., 1982; Noone and Hansson, 1990; Su et al., 1990; Zhang and Liu, 1990; Keston et al., 1991; Zhang and Liu, 1991).

CNCs are the most practical instruments for determining ultrafine particle concentrations, but they are not as accurate as other continuous methods for determining $PM_{2.5}$ or larger size fractions owing to the low upper limit of their size range.

3.2.4 Aerodynamic Particle Sizer (APS)

The Aerodynamic Particle Sizer (APS) measures light scattering as well as the time-of-flight of sampled particles (Wilson and Liu, 1980). The measured aerodynamic diameter can be converted to volume-equivalent diameter or mobility-equivalent diameter (Kasper, 1982).

The APS accelerates the air stream in a converging nozzle. Particles have a larger inertia than the gaseous component, and therefore lag in acceleration and speed behind the air stream. Particles with higher mass (as a result of higher density or larger size) achieve lower velocities than those with lower mass. Each particle is detected by laser scattering at the beginning and end of a fixed path length to determine the time taken to traverse this path (the "time-of-flight"). The flight times are related to particle mass. The APS measures particles with diameters of 0.5 to 30 µm (Peters et al., 1993).

The APS aerodynamic diameter differs from standard definition in Section 2 (the diameter of the unit density sphere that has the same settling velocity in still air). The APS aerodynamic diameter is adjusted (e.g., Rader et al., 1990) for particle density (Wilson and Liu, 1980; Baron, 1986; Wang and John, 1987; Ananth and Wilson, 1988; Brockmann et al., 1988; Wang and John, 1989; Chen et al., 1990), ambient gas density, and ambient air

Table 3-3
Comparison of Condensation Nuclei Counter Specifications

	TSI 3010	TSI 3022A	TSI 3025A
Minimum Particle Size (50% efficiency, nm)	10	7	3
Aerosol Flow Rate (cm^3/min)	1000	300	30
Upper Concentration Limit (particles/cm^3)	10^4	10^7	10^5
Lower Concentration Sensitivity (particles/cm^3)	0	0	0
False Count Rate (particles/cm^3)	< 0.0001	< 0.01	< 0.01
Response Time (95% response, sec)	< 5	< 13	1
Vacuum Source	External	Internal	Internal

viscosity (Chen et al., 1985; Lee et al., 1990). During the acceleration process, calibration and ambient particles can deform in different ways (i.e., flatten) depending on their viscosity (Baron, 1986; Griffiths et al., 1986; Chen et al., 1990). Nonspherical particles behave differently from spherical particles, necessitating additional adjustments (Chen and Crow, 1986; Brockmann and Rader, 1990; Cheng et al., 1990; Marshall et al., 1991; Cheng et al., 1993). Phantom particle counts may result from the time-of-flight laser detection system (Heitbrink et al., 1991; Heitbrink and Baron, 1992).

3.2.5 LIght Detection And Ranging (LIDAR)

LIight Detection And Ranging (LIDAR) measures light scattered in the direction of the light source ("backscattering") along a sight path (e.g., Measures, 1984; Grant, 1995). Aerosol lidar determines aerosol distributions while DIfferential Absorption Lidar (DIAL) can measure concentrations of several gases.

Basic single-wavelength aerosol lidar yields a semi-quantitative measurement of the backscatter coefficient. High-spectral-resolution and Raman lidars provide quantitative backscatter coefficients; these systems are very complex and currently not commercially available. The connection between backscatter coefficient and PM concentration is indirect and depends on particle size distribution and refractive index of the aerosol particles, similar to nephelometers. Aerosol lidars are more suitable for determining the spatial distribution of aerosol concentrations and its temporal development than for quantifying mass concentrations.

A basic aerosol lidar system consists of a transmitter and a receiver located next to each other. The transmitter, typically a pulsed laser, sends a short pulse of collimated light into the atmosphere. A small part of this light pulse is scattered back into the receiver by suspended particles and gas molecules. Light scattered at a distance r arrives at the receiver after a round trip time, $t = 2r/c$, where c is the speed of light. The lidar return signal S as a function of distance r depends both on the backscattering coefficient, $ß(r)$, at the distance r and the path integrated extinction, $\sigma(r)$, between lidar location r_0 and range r. For each measured signal, $S(r)$, there are two atmospheric parameters, $ß(r,\lambda)$ and $\sigma(r,\lambda)$, that need to be determined. The absolute system calibration is generally unknown. The lidar equation is, therefore, under-determined and cannot be solved without additional assumptions or data.

One approach to obtain semi-quantitative estimates of range-resolved atmospheric extinction and/or backscattering coefficients is to establish an empirical relationship between the backscattering coefficient, $ß(r)$, and the extinction coefficient, $\sigma(r)$ (e.g., Gibson, 1994), together with an estimate of a boundary condition for the extinction coefficient within the measurement range (Hitschfeld and Bordan, 1954; Fernald et al., 1972; Klett, 1981). The accuracy of the resulting backscattering and extinction data is highly dependent on the assumptions used (e.g., Kovalev, 1993; Kovalev and Moosmüller, 1994; Kovalev, 1995). Despite the semi-quantitative nature of these data, they are useful for the evaluation of aerosol sources and transport (e.g., McElroy and Smith, 1986; McElroy and McGown, 1992; Hoff et al., 1997).

Quantitative measurements of the atmospheric backscattering coefficient can be made by separately measuring the aerosol (Mie) backscattering and the gaseous (Rayleigh or Raman) backscattering. This dual measurement eliminates the extinction contribution to the lidar signal by normalizing the aerosol to the gaseous signals. This has been done by utilizing either inelastic gaseous scattering (i.e. Raman scattering) (Melfi, 1972; Cooney, 1975; Ansmann et al., 1992; Whiteman et al., 1992; Evans et al., 1997; Moosmüller and Wilkerson, 1997) or near-elastic gaseous scattering (i.e., Rayleigh scattering) (Fiocco et al., 1971; Alvarez II et al., 1990; Grund and Eloranta, 1991; She et al., 1992; Piironen and Eloranta, 1994).

DIAL measurements (Measures, 1984) are made at two different wavelengths with substantially different absorption coefficients for the gas of interest. DIAL may be a useful complement to other continuous measurements of aerosol precursor gases described in Section 3.6. The range resolved gas concentration is calculated from the ratio of the lidar signals at the two wavelengths. The laser line (wavelength) with the larger (smaller) absorption coefficient is referred to as "on-line" ("off-line").

DIAL has been used for the measurement of a number of relevant tropospheric trace gases including ozone (O_3) (e.g., Browell et al., 1983; Ancellet et al., 1989; Moosmüller et al., 1993; Kempfer et al., 1994; Zhao et al., 1994), sulfur dioxide (SO_2) (e.g., Woods and Jolliffe, 1978; Browell, 1982; Ancellet et al., 1987; Beniston et al., 1990), nitric oxide (NO) (e.g., Aldén et al., 1982; Edner et al., 1988; Kölsch et al., 1992), nitrogen dioxide (NO_2) (Rothe et al., 1974; Galle et al., 1988; de Jonge et al., 1991; Toriumi et al., 1996), ammonia (Force et al., 1985), and aromatic hydrocarbons (Milton et al., 1992). Though commercially available, lidar systems are expensive and must be individually designed or modified for each specific application.

3.3 Visible Light Absorption

Black carbon (BC) (sometimes termed "elemental carbon", "light-absorbing carbon", or "soot") is the dominant visible light-absorbing particulate species in the troposphere and mostly results from anthropogenic combustion sources (Horvath, 1993a). It is usually found in the nucleation or accumulation mode for particles well under 1 µm in equivalent dimensions (i.e., if chain aggregates were consolidated into a single sphere). Mass loadings range from a few ng/m^3 in remote pristine regions or over oceans distant from land, to a fraction of 1 $\mu g/m^3$ in rural regions of the continents, and exceed 1 $\mu g/m^3$ in many cities (Adams et al., 1990a, 1990b; Penner et al., 1993).

Continuous methods that monitor particle light absorption (b_{ap}) can also be used to measure the $PM_{2.5}$ component consisting of light absorbing particles. Attenuation of light through a filter and photoacoustic oscillation are detection principles used to quantify particle absorption as a surrogate for black carbon. Particle light absorption measurements from three different instruments are discussed in the following subsections.

3.3.1 Aethalometer and Particle Soot/Absorption Photometer

Light absorbing aerosol (e.g., BC) deposited on a filter can be quantified through the measurement of light transmission or reflection. As noted in Section 1, the British Smoke measurement (Mage, 1995) was first used in the early 1950s to visually characterize the reflectance of a filter sample. Coefficient of Haze (COH) measured by a paper tape sampler (Herrick et al., 1989) was the United States counterpart to the British Smoke measurement. A more quantitative method, the integrating sphere method (Fischer, 1973), measures aerosol light absorption by placing the loaded filter in an integrating sphere (Fussell, 1974; Labsphere Inc., 1994) and illuminating it. Light, both transmitted and scattered by the loaded filter, first reaches the diffusely reflecting surface of the sphere where it is homogenized, and then the light is detected by the photodetector. The difference between a clean filter and one loaded with particles gives the amount of light absorbed by the particles. Simplifications of the integrating sphere method, such as the integrating plate (Lin et al., 1973) or sandwich (Clarke, 1982b) methods are most often used for routine measurements.

Integrating plate methods have been used extensively for the measurement of aerosol light absorption as they are simple and cost-effective. Measurement accuracy is limited, however, due to the interaction of the scattering and absorption properties of the concentrated aerosol itself and of the aerosol with the filter medium. While some studies assure high accuracy, others determine an overestimation of *in-situ* aerosol light absorption by a factor of two to four (e.g., Szkarlat and Japar, 1981; Clarke, 1982a; Japar, 1984; Weiss and Waggoner, 1984; Horvath, 1993b; Campbell et al., 1995; Campbell and Cahill, 1996; Clarke et al., 1996; Horvath, 1997; Moosmüller et al., 1998).

A real-time version of the integrating plate method, the aethalometer (Hansen et al., 1984), continuously collects aerosol on a quartz-fiber filter tape. During the deposition process, the light attenuation through the aerosol collection spot and an unloaded reference spot are monitored. Their difference yields the absorption due to the integral of all light-absorbing materials collected on a particular spot. The time derivative of this quantity is a measure of the current aerosol light absorption. When the optical density of the aerosol spot reaches a certain value, the filter tape advances automatically. Time resolution available with the aethalometer varies from seconds or minutes in urban areas to ten minutes in rural locations and longer in very remote locations. One filter tape is sufficient for approximately 700 aerosol collection spots corresponding to one or more months of operation in urban areas, a year or more in rural areas.

The aethalometer converts the result of its filter attenuation measurement into BC mass concentration by a conversion factor of 19.2 m^2/g. Aethalometer BC agrees with collocated filter samples analyzed for elemental carbon (Hansen and McMurry, 1990). Applications of the aethalometer include air quality monitoring in urban (e.g., Hansen and Novakov, 1989; Hansen and Novakov, 1990) and more remote locations (e.g., Pirogov et al., 1994; Rosen et al., 1984), transport studies (e.g., Parungo et al., 1994), and source characterization (Hansen and Rosen, 1990).

The Particle Soot/Absorption Photometer (PSAP) (Bond et al., 1998) gives a filter-based, real-time measurement of aerosol light absorption. The PSAP produces

a continuous measurement of absorption by monitoring the change in transmittance across a filter (Pallflex E70-2075W) for two areas on the filter, a particle deposition area and a reference area. A light emitting diode (LED) operating at 550 nm, followed by an Opal glass, serves as light source. The absorption reported by the PSAP is calculated with a nonlinear equation correcting for the magnification of absorption by the filter medium and for response nonlinearities as the filter is loaded. Measurement time resolution can be as short as a few seconds to five minutes, depending on ambient aerosol light absorption. Applications of the PSAP include its use in ground-based monitoring by NOAA's Climate Monitoring and Diagnostics Laboratory (CMDL) and in field campaigns such as the Aerosol Characterization Experiment (ACE) of the International Global Atmospheric Chemistry (IGAC) program (e.g., Quinn et al., 1998).

3.3.2 Photoacoustic Spectroscopy

At atmospheric pressures, electromagnetic energy absorbed by particles changes to thermal energy, thereby heating the particles and the surrounding gases. Increased gas temperatures surrounding light-absorbing particles cause thermal expansion of the gas. When the light source power is modulated, the periodic expansion of the gas results in a sound wave at the modulation frequency, which may be detected with a microphone (Pao, 1977). This "photoacoustic" detection of particle light absorption (Bruce and Pinnick, 1977; Terhune and Anderson, 1977) can be related to the black carbon concentration.

Sensitive photoacoustic techniques use a power-modulated laser as light source. By placing the aerosol-laden air into an acoustic resonator, and modulating the laser power at its resonance frequency, the varying pressure disturbance (acoustic signal) is amplified by the buildup of a standing acoustic wave in the resonator. Related, but more sophisticated methods such as thermoacoustically amplified photoacoustic detection (Arnott et al., 1995; Bijnen et al., 1996) and interferometric detection (Lin and Campillo, 1985; Moosmüller and Arnott, 1996) have been discussed by Moosmüller et al. (1997).

Adams et al. (1989) used a water-cooled Argon ion laser operating at 514.5 nm (green) with an output power of 1 W. The detection limit of this system was b_{abs} = 4.7 Mm^{-1} or about 0.5 $\mu g/m^3$ BC, limited by window absorption. More modern systems apply solid-state lasers that greatly reduce system size and power consumption.

Petzold and Niessner (1995, 1996) developed a system with a detection limit of b_{abs} = 1.5 Mm^{-1}. It uses a 802 nm laser diode with 450 mW output power. The equivalent black carbon concentration was estimated to be 0.5 $\mu g/m^3$ (Petzold and Niessner, 1996). Decreasing aerosol absorption efficiency with increasing wavelength does not favor this design, nor does the fact that the 802-nm beam cannot be seen directly, which makes alignment difficult.

Arnott et al. (1998) and Moosmüller et al. (1998) use a diode-pumped, frequency-doubled Nd:YAG laser operating at 532 nm (green) with an output power of about 100 mW. Using an advanced acoustic design, window noise and flow noise were greatly reduced, resulting in a detection limit of about 0.5 Mm^{-1}, corresponding to about 0.05 $\mu g/m^3$ BC. Increasing the laser power in this system will proportionally improve the detection limit.

3.4 Electrical Mobility

Electrical mobility analyzers are applicable to particles smaller than 1 µm. They are the only practical alternative to the CNC instrument for quantifying the ultrafine fraction of the particle size distribution. The resulting particle size is known as mobility equivalent diameter, which can be converted to volume equivalent diameter or aerodynamic diameter (Kasper, 1982).

A basic electrical mobility analyzer consists of: 1) a charger to impart an electric charge to the particles (a diffusion charger that exposes particles to unipolar positive ions is commonly used); 2) a classifier that separates the particles by acting on their electrical charge and mass; and 3) a detector to monitor the separated particles.

Electrical mobility analyzers are often used together with aerodynamic particle sizers (see Section 3.2.4), with the electrical mobility analyzer capturing particles below 1 µm and the aerodynamic particle sizers measuring the larger particles (Peters et al., 1993). Particle number measurements with two different instruments are discussed in the following subsections.

3.4.1 Electrical Aerosol Analyzer (EAA)

The Electrical Aerosol Analyzer (EAA) (Whitby and Clark, 1966) has been widely applied and characterized in aerosol studies (Liu et al., 1974a, 1974b; Liu and Pui, 1975). Methods to translate EAA outputs to particle sizes and numbers have been developed (Helsper et al., 1982). EAAs are typically operated with about ten size channels covering the range from 0.01 to 1.0 µm with a measurement time on the order of a few minutes.

Positively charged aerosol enters a mobility tube consisting of two coaxial cylinders. The outer tube is grounded and a negative potential is applied to the inner tube. As the aerosol flows down the mobility tube, its mobile fraction is precipitated on the inner tube by electrical forces. The remaining aerosol is detected, commonly by an electrometer that measures the electrical current of the remaining aerosol. The potential of the inner cylinder is changed in steps. For each potential, a different fraction of the aerosol is precipitated. The resulting current-versus-voltage curve for an aerosol can be converted into a current-versus-size curve once the EAA has been calibrated with monodisperse aerosol of known size. Calibration of the current sensitivity is done by grounding the inner cylinder and measuring the aerosol current without precipitation losses.

3.4.2 Differential Mobility Particle Sizer (DMPS)

The Differential Mobility Particle Sizer (DMPS) (Knutson and Whitby, 1975a, 1975b) improves on the EAA by making measurements with much greater size resolution (e.g., 100 channels). Several DMPS configurations have been reported (e.g., Hoppel, 1978; Fissan et al., 1983; ten Brink et al., 1983; Kousaka et al., 1985) and data reduction has been studied extensively (e.g., Alofs and Balakumar, 1982; Hagen and Alofs, 1983; Birmili et al., 1997).

The DMPS is a modification of the EAA. The basic difference is that the DMPS produces a flow of aerosol consisting of particles with an electrical mobility between two closely spaced values (i.e., differential), while the EAA produces a flow consisting of particles with an electrical mobility above some value (i.e., integral). Instead of measuring the flow of particles missing the inner tube as in the EAA, a sample flow of aerosol is extracted through a slot in the inner tube. Only particles with mobilities within a limited range enter the sample stream for detection. As in the EAA, the voltage of the inner tube is stepped through a number of values and the DMPS directly yields the electrical mobility distribution without further differentiation.

Measurement times for DMPS with electrometers as detectors can be on the order of one hour. Operation with a CNC as detector can reduce the measurement time by an order of magnitude. A further order of magnitude reduction in averaging time can be achieved by scanning the inner tube voltage instead of stepping it discreetly (Wang and Flagan, 1990; Endo et al., 1997). This modification is referred to as Scanning Mobility Particle Analyzer (SMPA).

The conventional DMPS utilizing a cylindrical geometry is limited for ultrafine particles (< 0.020 µm) as its transmission efficiency drops dramatically below 0.02 µm due to diffusion losses (Reineking and Porstendörfer, 1986). The accessible size range can be extended down to 0.001 µm by either modifying the cylindrical DMPS (Reischl, 1991; Winklmayr et al., 1991) or by changing to a radial geometry (Zhang et al., 1995).

3.5 Chemical Components

If the carbonaceous, nitrate, sulfate, ammonium, and geological components of suspended particles could be determined continuously and *in situ*, a reliable speciated estimate of $PM_{2.5}$ or PM_{10} mass concentration could be derived. While most of these chemical-specific particle monitors are currently experimental, rapid technology advances will make them more available and more widely used within coming years. The following subsections introduce various versions of single particle mass spectrometers that measure particle size and chemical composition, along with single compound instruments to measure carbon, sulfur, and nitrate.

3.5.1 Single Particle Mass Spectrometers

Continuous versions of the LAser Microprobe Mass Spectrometer (LAMMS) have been developed as the Rapid Single particle Mass Spectrometer (RSMS) (Mansoori et al., 1994; Carson et al., 1995; Johnston and Drexler, 1995), Particle Analysis by Laser Mass Spectrometry (PALMS) (Murphy and Thomson, 1994, 1995), and Aerosol Time Of Flight Mass Spectrometry (ATOFMS) (Noble et al., 1994; Nordmeyer and Prather, 1994; Prather et al., 1994; Noble and Prather, 1996, 1998). These devices measure the size and chemical composition of individual particles. Portable instruments for ground based monitoring are becoming available (e.g., Gard et al., 1997), and an airborne instrument for measurements in the troposphere and lower stratosphere is being developed (Murphy and Schein, 1998).

Particles are introduced into a vacuum by a nozzle. The presence of particles is detected through light scattered from a visible laser beam. This scattering process is also used as an OPC (see Section 3.2.2) or APS (see Section 3.2.4) to determine the size and number of particles passing through the instrument. The presence of a particle triggers a high-energy pulsed laser which, with a single pulse, ablates particle material and ionizes part of it. The ions are detected and analyzed by a time-of-flight mass spectrometer. The time particles spend in the vacuum is on the order of microseconds, minimizing condensation, evaporation, and reactions.

The analysis rate is limited by the repetition rate of the pulsed laser. The presence of the OPC makes it possible to analyze a size selected fraction of the particles, however, it also imposes a lower limit on the particle size being analyzed, as very small particles are not detected by the OPC. Running a pulsed laser without triggering can acquire smaller particles, but at the expense of a lower duty cycle and no size selection. Because of the complicated ionization process, the technique is currently used to survey the chemical composition of particles than to yield quantitative mass concentrations of particle components.

These instruments have been recently developed and characterized with respect to ionization thresholds of aerosol particles (Thomson and Murphy, 1993; Thomson et al., 1997), trade-offs between aerodynamic particle sizing and OPC sizing coupled with mass spectroscopy (Salt et al., 1996), and the ability to determine surface and total composition of the aerosol particles (Carson et al., 1997). Applications of this technique have included characterizing aerosol composition in support of the 1993 OH experiment at Idaho Hill, CO (Murphy and Thomson, 1997a, 1997b), examining the purity of laboratory-generated sulfuric acid droplets (Middlebrook et al., 1997), determining halogen, (Murphy et al., 1997), speciating sulfur (Neubauer et al., 1996), studying matrix-assisted laser desorption/ionization (Mansoori et al., 1996), monitoring pyrotechnically derived aerosol in the troposphere (Liu et al., 1997), characterizing automotive emissions (Silva and Prather, 1997), measuring marine aerosols (Noble and Prather, 1997) and their radiative properties (Murphy et al., 1998), and observing heterogeneous chemistry (Gard et al., 1998).

3.5.2 Carbon Analyzer

The differentiation of organic carbon (OC) and elemental carbon (EC) based on their thermal properties followed by their detection as carbon dioxide (CO_2) or methane (CH_4) after combustion is commonly applied to filter deposits (e.g., Chow et al., 1993a). Turpin et al. (1990a, 1990b) pioneered the continuous thermal/optical carbon analyzer which provides *in-situ* time-resolved OC and EC measurements. Another version of the thermal method, the Ambient Carbon Particulate Monitor (ACPM, R&P Series 5400) (Rupprecht et al., 1995), consists of two aerosol collectors; one collector operates in the collection mode while the other one operates in the analysis mode at any given time. In the collection mode, particles are drawn through a size-selective inlet and deposited onto an impactor. The temperature of the collector in collection mode can be set either at or above ambient temperature. Once the pre-specified sampling period is achieved (typically one or more hours), the collector is switched into the analysis mode, while the second collector is switched from analysis to collection mode.

In the analysis mode, the ACPM first purges the analysis loop with filtered ambient air and measures a base line CO_2 concentration. The furnace surrounding the collector then heats the sample to the intermediate temperature level of 250 °C (default) while an infrared CO_2 detector measures the increase in CO_2 concentration due to carbon oxidation. An afterburner ensures that all volatile materials are fully oxidized. Once the temperature has stabilized and the CO_2 concentration has been measured, the oven heats to the final burn temperature of 750 °C (default) in the closed loop. The ACPM computes the OC and EC concentrations by dividing the measured amount of carbon released from the intermediate and final burn, respectively, by the air volume that passed through the instrument during sample collection.

The ACPM provides a continuous measure of OC and EC concentrations. However, its operational definitions of OC and EC and the selected combustion temperatures differ from those of commonly applied laboratory filter analysis protocols (e.g., Chow et al., 1993a).

3.5.3 Sulfur Analyzer

Continuous methods for the quantification of aerosol sulfur compounds first remove gaseous sulfur (e.g., SO_2, H_2S) from the sample stream by a diffusion tube denuder followed by the analysis of particulate sulfur (Cobourn et al., 1978; Durham et al., 1978; Huntzicker et al., 1978; Mueller and Collins, 1980; Tanner et al., 1980). Another approach is to measure total sulfur and gaseous sulfur separately by alternately removing particles from the sample stream, and aerosol sulfur is obtained as the difference between the total and gaseous sulfur (Kittelson et al., 1978). The total sulfur content is measured by a flame photometric detector (FPD) by introducing the sampling stream into a fuel-rich hydrogen-air flame (e.g., Stevens et al., 1969; Farwell and Rasmussen, 1976) that reduces sulfur compounds and measures the intensity of the S_2^* chemiluminescence.

Because the formation of S_2^* requires two sulfur atoms, the intensity of the chemiluminescence is theoretically proportional to the square of the concentration of molecules that contain a single sulfur atom. In practice, the relationship is between linear and square and depends on the sulfur compound being analyzed (Dagnall et al., 1967; Stevens et al., 1971). Calibrations are performed using both particles and gases as standards. The FPD can also be replaced by a chemiluminescent reaction with ozone that minimizes the potential for interference with a faster time response (Benner and Stedman, 1989, 1990).

Capabilities added to the basic system include *in-situ* thermal analysis (Cobourn et al., 1978; Huntzicker et al., 1978) and sulfuric acid (H_2SO_4) speciation (Tanner et al., 1980). Sensitivities for sulfur aerosols as low as 0.1 $\mu g/m^3$ with time resolution ranging from 1 to 30 minutes have been reported. Continuous measurements of aerosol sulfur content have also been obtained by on-line x-ray fluorescence analysis with a time resolution of 30 minutes or less (Jaklevic et al., 1980). During a field-intercomparison study of five different sulfur instruments, Camp et al. (1982) reported four out of five FPD systems agreed to within ±5% during a one-week sampling period.

3.5.4 Nitrate Analyzer

The Automated Particle Nitrate Monitor (APNM) is a new method being developed to provide high-time-resolution measurements of particle nitrate concentration (Hering, 1997; Chow et al., 1998b; Hering and Stolzenburg, 1998). It uses an integrated collection and vaporization cell whereby particles are collected by a humidified impaction process, and analyzed in place by flash vaporization. The approach is similar to the manual method for measuring the size distribution of sulfate aerosols (Roberts and Friedlander, 1976; Hering and Friedlander, 1982). The difference is that the particle collection and analysis has been combined into a single cell, allowing the system to be automated. Although the automated method that has been recently tested is specific to nitrate, the same technology could be applied for continuous sulfate measurements by using a sulfur detector instead of a nitric oxide detector.

Particles are humidified, and collected onto a metal strip by means of impaction. The humidification eliminates particle bounce from the collection surface without the use of grease (Winkler, 1974; Stein et al., 1994). Interference from vapors such as nitric acid is minimized with a denuder upstream of the humidifier. At the end of the 10-minute particle sampling period, a valve is switched to stop particle collection and to pass a carrier gas through the cell and into a gas analyzer. For nitrate, the deposited particles are analyzed by flash-vaporization in a nitrogen carrier gas, with quantification of the evolved gases by a chemiluminescent analyzer operated in NO_X mode (Yamamoto and Kosaka, 1994). The flow system is configured such that there are no valves on the aerosol sampling line. Time resolution of the instrument is on the order of 12 minutes, corresponding to a ten-minute collection followed by an analysis step of less than two minutes.

Field calibration and validation procedures include on-line checks of particle collection efficiency, calibration of aqueous standards, and determination of blanks by measurements of filtered ambient air. Particle collection efficiencies have been checked against an optical particle counter that operated between the collection cell and the pump. The analysis step of the monitor has been calibrated by application of aqueous standards (i.e., sodium nitrate and ammonium nitrate) directly onto the metal collection substrate. To ensure the absence of response to ammonium ion, standards of ammonium sulfate have also been applied. Field blanks are determined by placing a Teflon filter at the inlet of the system, collecting for the 10-minute sampling period, and then analyzing the strip exactly as done for a normal sample.

During the Northern Front Range Air Quality Study in Colorado (Watson et al., 1998a), the automated nitrate monitor captured the 12-minute time variability in fine particle nitrate concentrations with a precision of approximately ±0.5 $\mu g/m^3$ (Chow et al., 1998b). A comparison with denuded filter measurements followed by ion chromatographic analysis (Chow and Watson, 1998b) showed agreement within ±0.6 $\mu g/m^3$ for most of the measurements, but exhibited a discrepancy of a factor of two for the elevated nitrate periods.

More recent intercomparisons took place during the 1997 Southern California Ozone Study (SCOS97) in Riverside, CA. Comparisons with 14 days of 24-hour denuder-filter sampling gave a correlation coefficient of $R^2 = 0.87$, and showed no significant bias (i.e., the

regression slope is not significantly different from 1). As currently configured, the system has a detection limit of 0.7 μg/m^3, and a precision of 0.2 μg/m^3. Field operations with the system in Riverside showed that it was robust, providing nearly uninterrupted data over the six-week study period (S. Hering, personal communication).

3.5.5 Multi-Elemental Analyzer

Both streaker (PIXE International, Tallahassee, FL) and DRUM (Davis Rotating-drum Universal-size-cut Monitoring impactor) (University of California, Davis, CA) samplers provide continuous particle collection on filter substrates followed by laboratory elemental analysis with Particle-Induced X-Ray Emission (PIXE). This is a continuous, but not an *in-situ* real-time monitoring method due to the lag time between sample collection and chemical analysis in a laboratory. These samplers have a time resolution of ~ one hour, and can supply high-time-resolution elemental concentrations.

3.5.5.1 Streaker

Ambient particles in the streaker sampler are collected on two impaction stages and an after-filter (Hudson et al., 1980; Bauman et al., 1987; Annegarn et al., 1990). The first impaction stage has a 10-μm cutpoint and collects particles on an oiled frit that does not move. The particles collected on this stage are discarded. The second impaction stage has a 2.5-μm cutpoint and collects coarse particles (PM_{10} minus $PM_{2.5}$) on a rotating Kapton substrate that is coated with Vaseline to minimize particle bounce. The second impaction stage is followed by a 0.4-μm-pore-size Nuclepore polycarbonate-membrane filter (Chow, 1995) that has an 8-mm-long negative pressure orifice behind it to collect fine particles (nominally $PM_{2.5}$). The air flow rate through the streaker sampler is primarily controlled by the porosity of the filter and the area of the sucking orifice. A 1-mm-wide orifice can be set up to result in a flow rate of approximately 1 L/min and produce an annular deposit of 8 mm in width, with any point on the deposit collected during a one-hour time period.

The body of the streaker sampler has a cylindrical form with a diameter of approximately 10 cm and a length of about 20 cm. It contains a clock motor that advances two particle collection substrates mounted within the streaker. The streaker is mounted in the open air with the sample air inlet at the bottom to keep out very large particles (e.g., rain and drizzle). Sample air flow rates can be verified by a flow meter, temporarily attached to the inlet of the streaker sampler at the beginning and end of sampling on each substrate, or at times in between. Substrates of 168 mm in length had the capacity to accommodate a seven-day sampling period.

3.5.5.2 DRUM

The Davis Rotating-drum Universal-size-cut Monitoring impactor (DRUM) is an eight-stage cascade impactor. It collects particles on grease-coated mylar substrates that cover the outside circular surface of eight clock-driven slowly rotating cylinders or drums (one for each stage) (Raabe et al., 1988). The advantages of the DRUM sampler are its capability to operate for up to thirty days unattended and its use of the location of particle deposits along the drum substrate as a means to determine the time of their collection. The DRUM collects aerosol from 0.07 μm to 15 μm in diameter for eight size ranges (0.07 to

0.24, 0.24 to 0.34, 0.34 to 0.56, 0.56 to 1.15, 1.15 to 2.5, 2.5 to 5, 5 to 10, and 10 to 15 µm), followed by focused-beam PIXE analysis. DRUM samplers have been used in several visibility field studies to confirm assumptions about mass scattering efficiency dependence on sulfur size distributions (e.g., Pitchford and Green, 1997).

The DRUM sampler, and other Lundgren-type rotating drum impactors, are unique among size-segregating samplers in that they generate a continuous time history of aerosol component size distributions with short time resolution (e.g., hourly). Unlike the conventional aerosol size distribution data sets with at most a few dozen distributions that can be individually scrutinized, the DRUM produces hundreds of distributions. In addition, time series analysis, summary statistics, and multivariate analysis can be applied to concentrations measured on any or all stages of the DRUM sampler.

3.6 Precursor Gases

Continuous sulfur dioxide and oxides of nitrogen monitors have been available for decades, largely because these are regulated pollutants. These gases are important precursors to particulate sulfate and nitrate. Ammonia and nitric acid are other precursor gases for which concentrations are essential for understanding the equilibrium of particulate ammonium nitrate (Watson et al., 1994a). The following subsections discuss the instruments available to continuously measure ammonia and nitric acid.

3.6.1 Ammonia Analyzer

Ammonia gas can be quantified by fluorescence or by chemiluminescence methods. For the fluorescence method, sampled ammonia is removed from the airstream by a diffusion scrubber, dissolved in a buffered solution, and reacted with o-phtaldialdehyde and sulfite. The resulting i-sulfonatatoisoindole fluoresces when excited with 365-nm radiation, and the intensity of the 425-nm emission is monitored for quantification. The diffusion scrubber might be modified to pass particles while excluding ammonia gas to continuously quantify ammonium ions (Abbas and Tanner, 1981; Rapsomanikis et al., 1988; Genfa et al., 1989; Harrison and Msibi, 1994).

For the chemiluminescence method, oxides of nitrogen (NO_x) are first removed from an airstream, and ammonia is then oxidized to nitrogen oxide (NO) for detection by the same chemiluminscent detectors that are used to monitor ambient nitrogen oxide and nitrogen dioxide (NO_2) (e.g.,Breitenbach and Shelef, 1973; Braman et al., 1982; Keuken et al., 1989; Langford et al., 1989; Wyers et al., 1993; Sørensen et al., 1994; Jaeschke et al., 1998). Chemiluminescent ammonia analyzers convert ammonia to NO_x by thermal oxidation using a catalytic technique at high temperature. This type of continuous ammonia monitor has been used mostly in source emission testing rather than ambient monitoring in the past. Laboratory tests of TEI Model 42 (Thermo Environmental Instruments, Franklin, MA) during the Northern Front Range Air Quality Study (Chow et al., 1998b) show that: 1) typical response time is on the order of two or more hours for concentrations of 40 ppb to 400 ppb; 2) the instrument's detection limit is approximately 10 ppb (ambient concentration); 3) oxidizer efficiency is in the range of 50% to 75% and lower for NH_3 concentrations less

than 40 ppb; and 4) no effects upon ammonia concentrations could be identified by the changes in ambient relative humidity.

Other, less established methods to measure ammonia include photoacoustic spectroscopy (Rooth et al., 1990; Sauren et al., 1993), vacuum ultraviolet/photofragmentation laser-induced fluorescence (Schendel et al., 1990), Differential Optical Absorption Spectroscopy (DOAS) in the ultraviolet (Platt, 1994), DIfferential Absorption Lidar (DIAL, see section 3.2.5), and Fourier Transform Infrared (FTIR) spectroscopy (see section 3.6.3). Intercomparisons between different ammonia measurement methods have been conducted (Appel et al., 1988; Wiebe et al., 1990; Williams et al., 1992; Mennen et al., 1996).

3.6.2 Nitric Acid Analyzer

Atmospheric nitric acid (HNO_3) concentrations can be monitored by conversion of nitric acid to nitrogen dioxide (NO_2), followed by detection with a chemiluminescent analyzer (Kelly et al., 1979; Burkhardt et al., 1988; Harrison and Msibi, 1994). While conversion methods from nitric acid to nitrogen dioxide are not very selective, nylon filters have been used to remove nitric acid from a gas stream. The nitric acid concentration is therefore determined by the difference in NO_2 measurements with and without a nylon filter in the gas stream.

The sampled gas is initially passed through a Teflon filter to remove particles. This is followed by the nylon filter that removes more than 99% of the nitric acid and can be bypassed for using the difference method. Conversion from nitric acid to NO and NO_2 is achieved with a glass bead converter operating at high temperature (i.e., 350 to 400 °C). This is followed by a CrO_3 impregnated filter used to convert NO to NO_2 (Ripley et al., 1964). A chemiluminescence instrument (Fehsenfeld et al., 1990; Gregory et al., 1990) is used to measure the resulting NO_2 concentration, with luminol based instruments being particularly sensitive (Kelly et al., 1990).

These instruments have a sensitivity around 0.1 ppb with a time response of about 5 minutes (Harrison, 1994). Limitations of the technique are due to the sticking of nitric acid to walls and to the possible interference of high humidity and other nitrogen species with conversion processes (e.g., Burkhardt et al., 1988). These instruments have been tested in intercomparison studies (e.g., Fox et al., 1988; Hering et al., 1988; Gregory et al., 1990).

3.6.3 Fourier Transform Infrared (FTIR) Spectroscopy

Fourier Transform Infrared (FTIR) spectroscopy detects molecular gases (with the exception of homonuclear diatomic gases) by measuring the light absorption due to their rotational-vibrational transitions (Hanst and Hanst, 1994). For the measurement of the very polar nitric acid, this open-path technique mitigates the associated adsorption and desorption sampling problems. Nitric acid and ammonia have been measured with 1 to 1.5 km absorption path length folded into a 25-m long White cell (White, 1976) at wavenumbers of 879 and 967 cm^{-1} (nitric acid) and 932 and 967 cm^{-1} (ammonia) (Tuazon et al., 1978; Doyle et al., 1979; Tuazon et al., 1980; Tuazon et al., 1981; Hanst et al., 1982; Biermann et al., 1988). Sensitivities of 4 ppbv for nitric acid and 1.5 ppbv for ammonia have been achieved

with averaging times of about 5 minutes. This technique is not as sensitive as tunable diode laser techniques, but its sensitivity is sufficient for use in urban environments.

3.6.4 Other Nitric Acid Instruments

Tunable Diode Laser Absorption Spectroscopy (TDLAS) takes advantage of the high monochromaticity and rapid tunability of a lead salt diode laser to measure absorptions from single rotational-vibrational lines in the middle infrared spectrum of a molecule, since most gases absorb radiation in this spectral region. High spectral resolution is required to prevent interferences from other gases in the sampled air. The atmospheric sample is pumped rapidly at reduced pressure through a White cell, which also provides the long optical path lengths required to achieve the desired detection limits.

The tunable diode laser is a small lead crystal with variable amounts of tin, selenium, tellurium, or sulfur. The wavelength region at which the laser emits radiation is governed by the proportions of the three elements in the crystal. Techniques of measuring nitric acid by TDLAS at 1721 cm^{-1} and at 1314 cm^{-1} have been described (Schiff et al., 1983; Harris et al., 1987; Mackay et al., 1988; Schmidtke et al., 1988). The sensitivity of this technique is about 0.3 ppbv for 5-minute time resolution (a factor of 10 better than the long-path FTIR method). The time resolution is mostly limited by nitric acid sticking to surfaces as it is a very polar gas. The accuracy depends on the ability to measure the various flows and to determine the mixing ratio of the calibration standard. Several studies have compared TDLAS measurements with other nitric acid measurements (Anlauf et al., 1985, 1988; Fox et al., 1988; Hering et al., 1988; Fehsenfeld et al., 1998) and differences of about 30% have been reported. The lack of a direct nitric acid standard combined with sampling difficulties makes the interpretation of these intercomparisons difficult.

The mist chamber method samples nitric acid by efficiently scrubbing it from the atmosphere in a refluxing mist chamber followed by analysis of the scrubbing solution for NO_3^- by ion chromatography (Talbot et al., 1990). A sensitivity of 10 pptv for a 10-minute integration period has been reported.

Nitric acid concentrations have also been measured with the Laser-Photolysis Fragment-Fluorescence (LPFF) Method, which irradiates the air sample with ArF laser light (193 nm) resulting in the photolysis of nitric acid (Papenbrock and Stuhl, 1991). The resulting hydroxyl radical (OH) emits fluorescence at 309 nm which is taken as a measure of the nitric acid mixing ratio in air. A sensitivity of 0.1 ppbv and a time constant of 15 minutes limited by surface ad- and desorption have been reported. An intercomparison of this technique with a denuder technique was also reported.

Chemical Ionization Mass Spectrometry (CIMS) has been used for the sensitive (few pptv) and fast (second response) measurement of atmospheric nitric acid concentrations. Reagent ions formed by an ion source are mixed with the sampled air and react selectively with nitric acid. The ionic reaction product is detected with a mass spectrometer. Two different CIMS instruments have been described (Huey et al., 1998; Mauldin et al., 1998) and compared with an older, more established filter pack technique (Fehsenfeld et al., 1998).

3.7 Summary

All of the measurement methods identified in Table 3-1, and described generically above, show merit for particle monitoring. The most commonly available and widely used units range in cost from ~$10K to $30K for the TEOM, BAM, nephelometer, aethalometer, and carbon analyzer. Some continuous light scattering instruments can be purchased for as little as ~3K. These are comparable to the cost of continuous gas monitors for other criteria pollutants. These instruments are reliable and have benefited from feedback of a relatively large number of users. Their operating manuals and operating procedures are established. Most of these instruments have been evaluated in collocated tests with filter samplers, though the majority of these evaluations are for the PM_{10} rather than $PM_{2.5}$ size fraction.

Well-established research monitors include the APS, the OPC, the EAA, the DMPS, and the CNC. These are in the cost range of ~$20K to $50K. They are reliable and well-documented, but substantial skill is required to maintain and operate the equipment and to reduce the resulting data. Most of these instruments have also been evaluated in collocated tests with each other and with filter samplers, though once again there is a dearth of comparisons with $PM_{2.5}$ measurements.

The remaining devices are specialized technologies for which only a few units exist for application in special studies. Their costs range from ~$50K to $300K, their operating procedures are still being developed, and in many cases only the developer is currently competent to apply them. This situation will change in coming years, however, as the utility of these instruments is borne out in specialized studies. The information they acquire will be essential to accomplishing several of the objectives for continuous monitoring stated in Section 1.

The state of technology shows that several of the major chemical components can be adequately measured by continuous monitors. Organic and elemental carbon, sulfate, and nitrate each have continuous *in-situ* methods that have been proven, but need to be evaluated, accepted, and packaged. Continuous *in-situ* measurement methods for ammonium, crustal elements, and liquid water are still lacking (with the possible exception of the single particle mass spectrometers). Consideration needs to be given to ways in which these components might be practically quantified at intervals of one-hour duration or less. Continuous measurement methods for particle size, based on inertial, optical, electrical, and condensation properties, are also adequate to characterize the ultrafine as well as the accumulation modes of suspended particles.

The remainder of this document focuses on the equivalence and utility of the most commonly and widely used monitors that can be procured and operated within the fiscal and expertise constraints of most air pollution surveillance agencies at the present time. These are the most viable candidates for designation as Correlated Acceptable Continuous (CAC) monitoring status.

4. MEASUREMENT PREDICTABILITY, COMPARABILITY, AND EQUIVALENCE

This section provides example comparisons of collocated continuous particle monitors with each other and with filter-based aerosol samplers. Only a few of these are specific to the $PM_{2.5}$ size fraction, since few comparisons have been reported for this size fraction; most relate to PM_{10} sampling. Comparisons of continuous $PM_{2.5}$ monitors with $PM_{2.5}$ Federal Reference Method (FRM) samplers were unavailable for this guidance. These comparisons are intended to be illustrative rather than comprehensive. They are drawn from recent studies for which collocated measurements were readily available and quality assured.

$PM_{2.5}$ measurement predictability, comparability, and equivalence are defined as follows:

- **Predictability:** A consistent and reliable relationship can be established between a continuous particle monitor and a collocated FRM or FEM measurement that allows the FRM concentration to be consistently estimated from the continuous monitor measurements within acceptable precision intervals. Predictability does not require traceability to a $PM_{2.5}$ or PM_{10} mass concentration but it does require sufficient collocated measurements to establish the predictive relationship between the measured quantity and an FRM or FEM concentration. Light scattering or light absorption measurements are examples of continuously measured particle properties from which $PM_{2.5}$ concentrations might be predicted.

- **Comparability:** The predictability of a continuous particle monitor is established and the measurement is traceable to a $PM_{2.5}$ or PM_{10} mass calibration standard. A comparable monitor should provide readings in units of mass concentration, be equipped with a standardized size-selective inlet, and yield measurements that are the same as collocated FRM or FEM measurements. TEOM, BAM, and CAMMS are examples of instruments that are calibrated in units of $PM_{2.5}$ mass and are equipped with characterized inlets. Several of the particle sizing and light extinction methods could be comparable when particle shape, index of refraction, and density can be defined. A suite of the chemical specific monitors could also eventually estimate mass concentrations.

- **Equivalence:** The predictability and comparability of a continuous particle monitor is established and the requirements in Table 4-1 have been attained. Equivalence requires designation of the monitor as a Federal Equivalent Method, or FEM. Equivalence is more demanding than predictability or comparability in that it requires demonstration of comparability within high tolerances over a wide range of concentration loadings and measurement environments.

The following sub-sections examine the comparability and predictability of particle concentrations from selected field studies in order to determine the situations under which these attributes might be established for different types of monitors. They also examine different methods of quantifying comparability and predictability.

Table 4-1
Test Specifications for $PM_{2.5}$ Equivalence to Federal Reference Method[a]

Criteria	Specifications
Concentration Range	10 to 200 µg/m^3
Number of Test Sites	One for "Class I" monitors, two for "Class II" monitors. (More varied environments will be required for "Class III" continuous particle monitors.)
Number of Samplers	Three FRMs, three candidate samplers
Number of Samples	Class I 24-hour samples: R_j[b] > 40 µg/m^3 and R_j < 40 µg/m^3 Class I 48-hour samples: R_j > 30 µg/m^3 and R_j < 30 µg/m^3 Class II 24-hour samples: a. for $PM_{2.5}/PM_{10}$ ratio > 0.75: R_j > 40 µg/m^3 and R_j < 40 µg/m^3, b. for $PM_{2.5}/PM_{10}$ ratio < 0.40: R_j > 30 µg/m^3 and R_j < 30 µg/m^3, Class II 48-hour samples: a. for $PM_{2.5}/PM_{10}$ ratio > 0.75: R_j > 30 µg/m^3 and R_j < 30 µg/m^3, b. for $PM_{2.5}/PM_{10}$ ratio < 0.40: R_j > 20 µg/m^3 and R_j < 20 µg/m^3
Collocated Precision	2 µg/m^3 or 5% (largest)
Regression Slope	1 ± 0.05
Intercept	0 ± 1 µg/m^3
Correlation	≥ 0.97

[a] U.S. EPA (1997a).

[b] R_j = the minimum number of acceptable sample sets per site for $PM_{2.5}$. R_j must be equal to or greater than 3.

4.1 Measurement Comparability

There is a dearth of data available in the compliance monitoring network to evaluate the comparability between the U.S. EPA designated PM_{10} reference and equivalent methods and continuous PM monitors. Watson et al. (1997b) evaluated the quality and comparability of PM measurements from different networks between 1988 and 1993 in Central California. Figure 4-1 compares the high-volume size-selective-inlet (SSI) PM_{10} measurements with TEOM and BAM in Central California. The SSI measurements were 30% higher than those measured with the TEOM samplers, but they were nearly the same as those measured with the BAM samplers. There are notable outliers in each of these comparison plots, especially for the highest concentrations.

The TEOM data in Figure 4-1 show several values that compare well with the SSI, with nearly a one-to-one correspondence. These data were further divided for comparison into winter/fall and spring/summer subsets at the Bakersfield and Sacramento sites as shown in Figure 4-2. The spring/summer comparisons are good, with nearly a one-to-one correspondence. However, during the fall and winter, the TEOM read ~30% lower concentrations than the corresponding SSI PM_{10}. This is due to the higher content of volatile ammonium nitrate in fall and winter samples. The TEOM used in this example heated samples to 50 °C, well above the temperature at which ammonium nitrate can evaporate. The TEOM appears to be a good measurement of PM_{10} during other than fall and winter months when the aerosol is more stable.

Allen et al. (1995) reported similar TEOM versus SSI comparison results for the 61 data pairs collected at Rubidoux, California, with TEOM concentrations ~30% lower than the corresponding SSI PM_{10} concentrations. The Rubidoux site is well-known for having the highest nitrate levels in southern California (Solomon et al., 1989; Chow et al., 1992b; Chow et al., 1994a, 1994b), especially during fall and winter.

Several empirical and statistical approaches could have been used to make these comparisons (Mathai et al., 1990), although conclusions about sampler comparability are often subjective. Table 4-2 summarizes the collocated comparison between continuous and filter-based PM_{10} or $PM_{2.5}$ monitors from recent aerosol characterization studies.

Linear regression can be used to evaluate comparability between the X and Y samplers as well as predictability of one sampler's measurements from that of the other sampler (King, 1977). Regression slopes and intercepts with effective variance weighting (Watson et al., 1984) for each sampler pair, along with their standard errors, are given in Table 4-2. For each comparison, the X-sampler measurement was the independent variable and the Y-sampler measurement was the dependent variable. When the slope equals unity within three standard errors, when the intercept does not significantly differ from zero within three standard errors, and when the correlation coefficient also exceeds 0.9, the selection of independent and dependent variables is interchangeable (Berkson, 1950; Madansky, 1959; Kendall, 1951). When the correlation coefficient is greater than 0.9 but the slope and intercept criteria are not met, the dependent variable is predictable from the independent

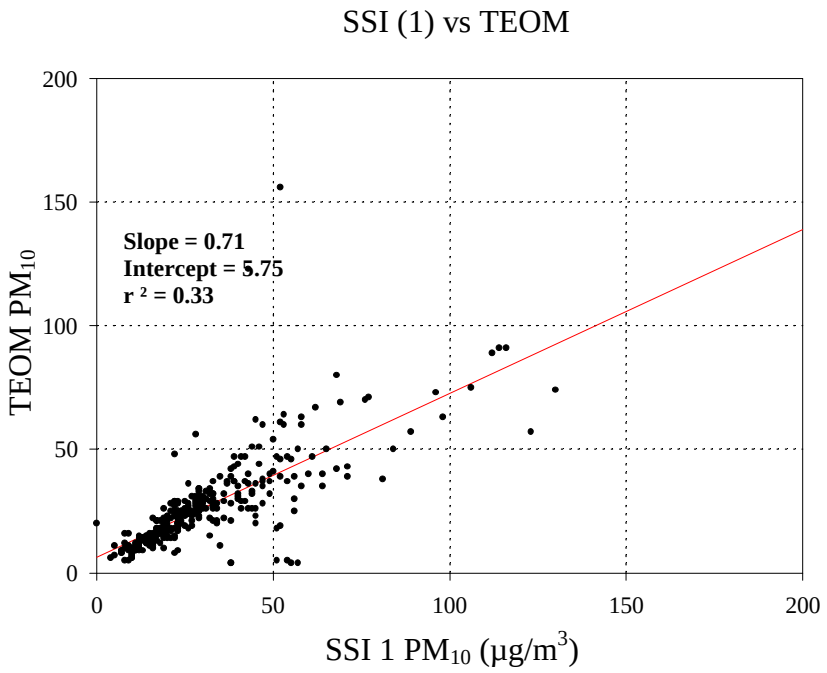

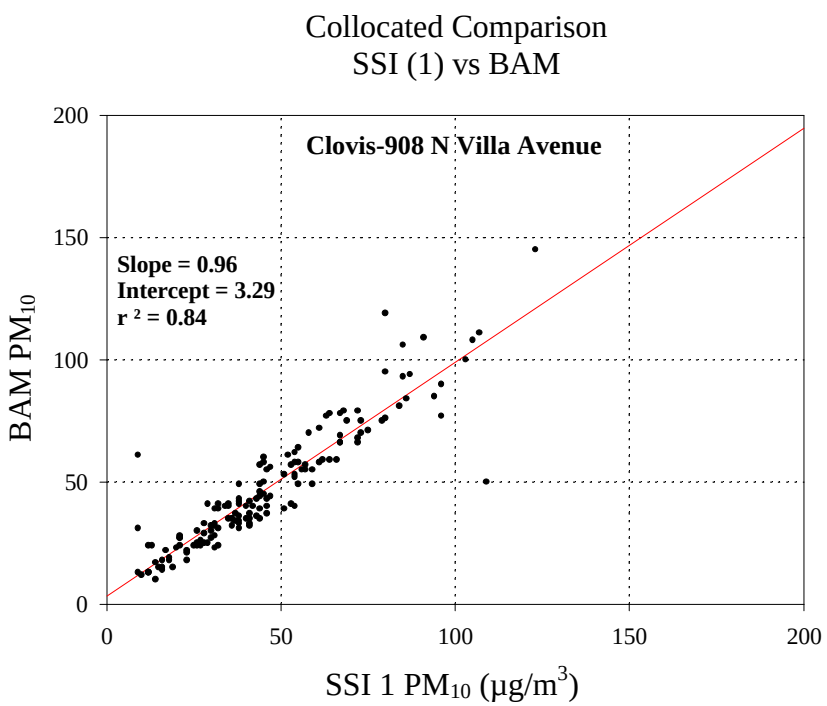

Figure 4-1. Collocated comparisons of 24-hour-averaged TEOM and BAM with high-volume SSI for PM_{10} measurements acquired in Central California between 1988 and 1993.

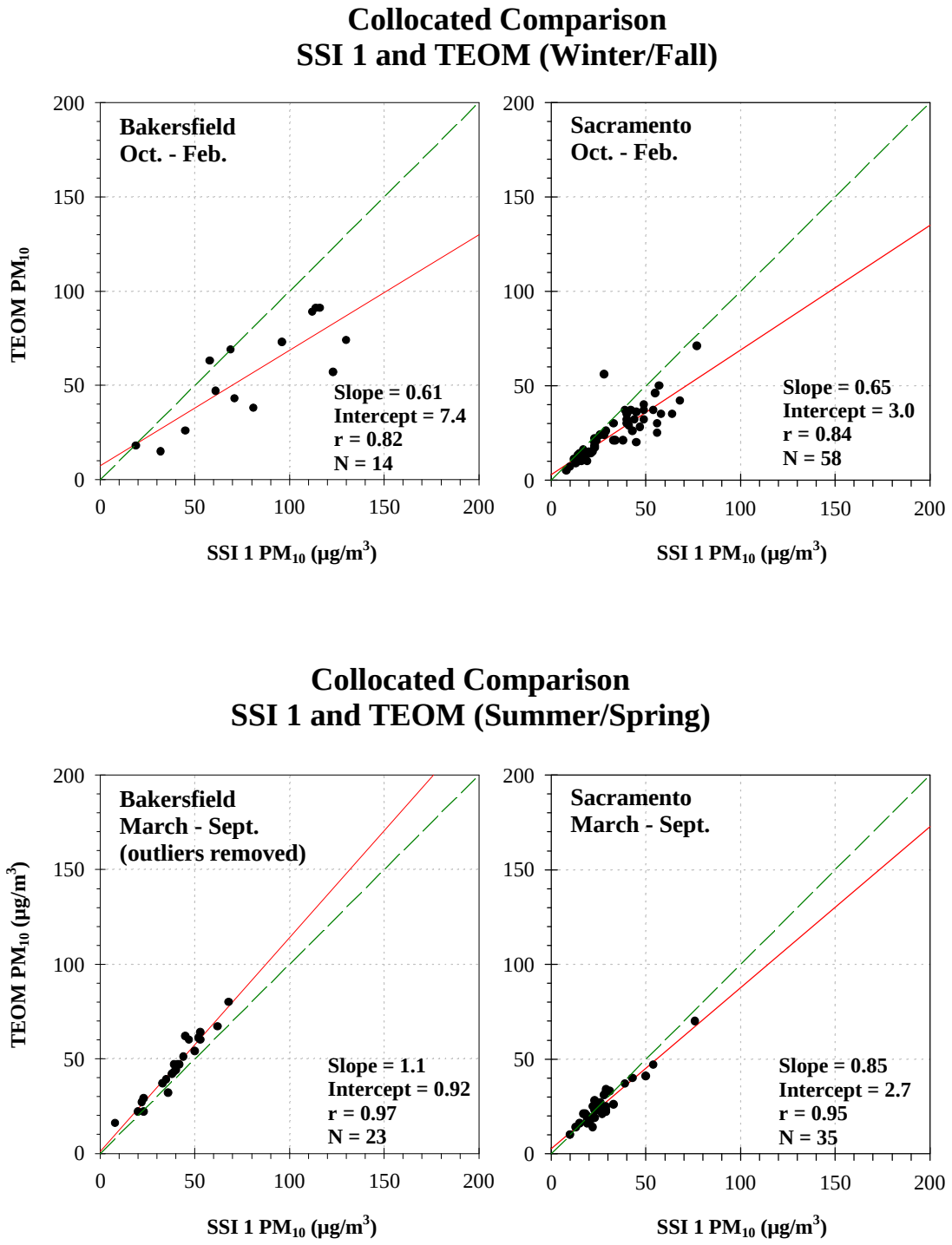

Figure 4-2. Collocated comparison of 24-hour-averaged TEOM and high-volume SSI PM_{10} during winter and summer at the Bakersfield and Sacramento sites in Central California between 1988 and 1993.

Table 4-2
Collocated Comparisons between Continuous and Filter-Based $PM_{2.5}$ or PM_{10} Monitors from Recent Aerosol Characterization Studies

Study Name	Study Area	Species	Sampler Y	Sampler X	Slope	Intercept ($\mu g/m^3$)	Correlation Coefficient	No. of Pairs	Average Ratio	Percent Distribution <1σ	1-2σ	2-3σ	>3σ	Average Difference ($\mu g/m^3$)	Precision Collocated	RMS	P>|T|
IMS95[a]	San Joaquin Valley, CA	$PM_{2.5}$ Mass	Bakersfield TEOM	Bakersfield 3-hr SFS	0.78±0.04	-1.8±13.5	0.82[b]	200	0.65±1.8	73	20	6	1	10.0	14.4	17.6	0.000
IMS95	San Joaquin Valley, CA	$PM_{2.5}$ Mass	Bakersfield Collocated TEOM	Bakersfield 3-hr SFS	0.93±0.04	-6.2±13.6	0.86[b]	200	0.59±1.9	75	21	3	1	8.8	13.7	16.2	0.000
IMS95	San Joaquin Valley, CA	$PM_{2.5}$ Mass	Chowchilla BAM	Chowchilla 3-hr SFS	0.32±0.03	2.3±4.6	0.69[b]	181	0.51±0.49	59	39	3	0	14.4	10.2	17.6	0.000
IMS95	San Joaquin Valley, CA	PM_{10} Mass	Chowchilla BAM	Chowchilla 3-hr SFS	0.57±0.03	1.1±7.3	0.78[b]	183	0.64±0.36	62	36	2	0	13.4	9.9	16.6	0.000
IMS95	San Joaquin Valley, CA	$PM_{2.5}$ Mass	Bakersfield Collocated TEOM	Bakersfield TEOM	0.85±0.01	3.9±9.3	0.94[b]	902	0.99±6.71	88	6	3	3	0.43	8.9	10.4	0.212
U.S./Mexico Transboundary Study[c]	Calexico, CA	PM_{10} Mass	Calexico BAM	Calexico 24-hr SFS	1.10±0.06	3.29±2.95	0.94[d]	45	1.20±0.27	47	31	4	18	7.63	9.63	6.63	0.0001
U.S./Mexico Transboundary Study	Calexico, CA	PM_{10} Mass	Calexico BAM	Calexico 24-hr POR	0.86±0.09	14.47±5.13	0.91[d]	21	1.34±0.40	24	52	10	14	7.78	13.76	7.65	0.02
U.S./Mexico Transboundary Study	Calexico, CA	PM_{10} Mass	Calexico BAM	Calexico 24-hr DIC	1.00±0.08	6.34±4.48	0.91[d]	34	1.14±0.26	56	32	3	9	6.43	10.82	7.56	0.0017
U.S./Mexico Transboundary Study	Calexico, CA	PM_{10} Mass	Calexico BAM	Calexico 24-hr SSI	0.89±0.06	4.21±4.21	0.93[d]	33	0.97±0.16	58	33	9	0	2.5	10.16	9.26	0.17
Las Vegas PM_{10} Study[e]	Las Vegas, NV	PM_{10} Mass	Bemis BAM	Bemis 24-hr SFS	0.66±0.14	23.92±5.28	0.44[f]	91	1.61±0.92	54	28	8	10	-13.6	29.3	5.7	0.000
Las Vegas PM_{10} Study	Las Vegas, NV	PM_{10} Mass	Bemis BAM	Bemis 24-hr POR	1.78±0.59	1.65±15.00	0.52[f]	26	2.06±1.78	73	19	0	8	-19.3	34.7	6.4	0.009
Las Vegas PM_{10} Study	Las Vegas, NV	PM_{10} Mass	East Charleston BAM	East Charleston 24-hr SFS	0.71±0.09	16.40±3.67	0.64[f]	93	1.30±0.51	72	18	2	8	-6.2	20.0	11.0	0.004
Las Vegas PM_{10} Study	Las Vegas, NV	PM_{10} Mass	East Charleston BAM	East Charleston 24-hr POR	0.54±0.19	19.97±5.61	0.5[f]	25	1.70±0.64	92	8	0	0	-9.3	18.6	4.8	0.019
NFRAQS[g]	Northern Front Range, CO (Winter 1995-96, 6-hr)	PM_{10} Mass	Welby PM_{10} BAM	Welby 6-hr and 12-hr SFS	0.82±0.04	1.87±1.27	0.93[h]	63	1.01±0.44	17	13	8	62	2.6	6.889	5.61	0.0035
NFRAQS	Northern Front Range, CO (Winter 1995-96, 12-hr)	PM_{10} Mass	Welby PM_{10} BAM	Welby 6-hr and 12-hr SFS	0.62±0.07	3.73±1.44	0.84[h]	37	0.94±0.42	15	10	11	64	3.3	5.199	2.45	0.0005
NFRAQS	Northern Front Range, CO (Summer 1996, 6-hr)	PM_{10} Mass	Welby PM_{10} BAM	Welby 6-hr and 12-hr SFS	0.62±0.07	9.02±1.99	0.72[h]	85	1.03±0.36	25	21	9	45	0.9	10.290	4.28	0.422
NFRAQS	Northern Front Range, CO (Summer 1996, 12-hr)	PM_{10} Mass	Welby PM_{10} BAM	Welby 6-hr and 12-hr SFS	0.81±0.09	5.53±1.85	0.80[h]	45	1.14±0.36	27	25	13	35	-1.8	3.861	2.27	0.003
Robbins Particulate Study[i]	Robbins, IL	PM_{10} Mass	Eisenhower BAM	Eisenhower 24-hr DICHOT	0.847±0.153	1.339±4.277	0.66[j]	41	0.93±0.40	8	17	7	68	2.7	9.1	2.9	0.066
Robbins Particulate Study	Robbins, IL	PM_{10} Mass	Eisenhower BAM	Eisenhower 24-hr SSI	0.760±0.107	0.108±3.574	0.75[j]	42	0.78±0.34	8	22	10	60	7.4	8.5	4.3	0.000

[x] Chow and Egami (1997), Chow et al. (1998a).
[b] See Figure 4-3.
[c] Chow and Watson (1997a).
[d] See Figure 4-4.
[e] Chow and Watson (1997b).
[f] See Figure 4-5.
[g] Chow et al. (1998b), Watson et al. (1998a).
[h] See Figure 4-6.
[i] Watson et al. (1997c).
[j] See Figure 4-7.

variable. These regression criteria for comparability are less stringent than those required for equivalence specified in Table 4-1

Table 4-2 also presents the average ratios and standard deviations of Y to X and the distribution differences (X minus Y) for <1σ, 1σ to 2σ, 2σ to 3σ, and >3σ precision intervals. Here, σ is the propagated precision of X minus Y, which is the square root of the sum of the squared uncertainties ($\sigma^2_x+\sigma^2_y$), where σ_x and σ_y are the reported precisions for the X or Y samples. Individual measurement uncertainties are calculated from replicate analyses, blank variabilities, and flow rate performance tests for each filter-based sampler. When hourly concentrations are integrated to calculate 24-hour average concentrations for comparison, the standard error of the mean is used to represent their associated uncertainties.

Table 4-2 gives the average of the paired differences (X-Y) between the X and Y samplers; the collocated precision, which is the standard deviation of the paired differences; and the root mean squared (RMS) precision (the square root of the mean squared precisions), which is essentially the average measurement uncertainty of "X-Y."

The average differences and collocated precisions can be used to test the statistical hypothesis that the difference between samplers X and Y is zero. A parametric test (Student's T-test) is performed for each pair of samplers to illustrate the paired differences. Table 4-2 gives the probability (P) for a greater absolute value of Student's T statistic. If P is less than 0.05, one can infer that one of the samplers gives a concentration that is larger or smaller than the other, depending on the sign of the average difference.

Chow and Egami (1997) and Chow et al. (1998a) compared three-hour filter-based $PM_{2.5}$ and PM_{10} samples with hourly TEOM and BAM measurements during winter, 1995 in California's San Joaquin Valley. Ammonium nitrate and woodburning have been found to be large wintertime particle contributors in this area (Chow et al., 1992a), and there were high humidities with fogs, cloud, and rain during the study period. None of these collocated measurements met the slope, intercept, and correlation criteria for comparability, as shown in the first five rows of Table 4-2.

Figure 4-3 shows that the collocated TEOMs operating with 30 °C heating of the air stream exhibit some data scatter, especially for $PM_{2.5}$ concentrations less than 50 μg/m^3. This conditioning temperature was purposefully set below the 50 °C temperature recommended by the manufacturer to minimize particle volatilization. The three-hour-average TEOM $PM_{2.5}$ mass fell below zero on several occasions. This probably occurred because some aerosol liquid water was present for high humidities during one three-hour period that subsequently evaporated when relative humidity decreased. On average, the 30 °C TEOM registered ~10 μg/m^3 less than the corresponding filter measurements in this challenging environment. The average ratio of TEOM versus filter-based (i.e., medium-volume Sequential Filter Sampler [SFS]) $PM_{2.5}$ was 0.65 ± 1.8 and 0.59 ± 1.9 for the two collocated TEOMs, implying that $PM_{2.5}$ mass concentrations acquired with the TEOMs were approximately 35% to 40% lower than those of gravimetric masses during this test. Ammonium nitrate constituted one-third to half of the $PM_{2.5}$ mass measured on a subset of samples during this test (Chow et al., 1998a).

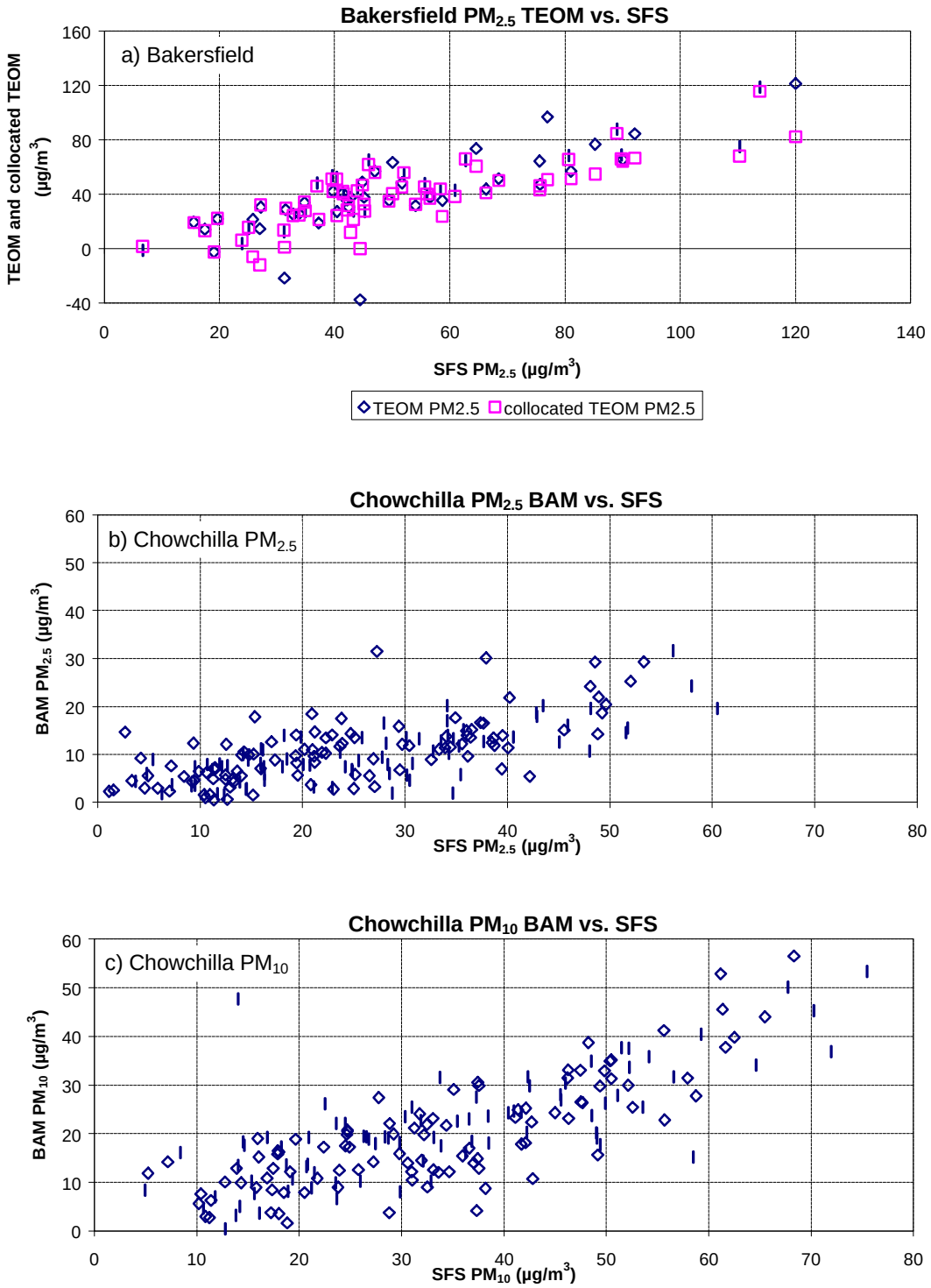

Figure 4-3. Collocated comparison of three-hour $PM_{2.5}$ SFS with $PM_{2.5}$ TEOM at the Bakersfield site, as well as $PM_{2.5}$ and PM_{10} SFS with BAM at the Chowchilla site in California's San Joaquin Valley between 12/09/95 and 01/06/96.

Similar observations were found for the $PM_{2.5}$ and PM_{10} BAM versus Sequential Filter Sampler (SFS) comparison. The average ratio of BAM versus SFS was 0.51 ± 0.49 for $PM_{2.5}$ and 0.64 ± 0.36 for PM_{10} measurements (Table 4-2). The correlations were moderate ($0.69 < r < 0.78$) for these measurements. The percent distribution in Table 4-2 shows that over 90% of the measurement differences fell within a $\pm 2\sigma$ interval, however. The two collocated $PM_{2.5}$ TEOM comparisons yielded a collocated precision of 8.9 $\mu g/m^3$. The correlation coefficient was 0.94, but the slope and intercept criteria were not met, indicating the Y sampler was predictable from the X sampler with 97% of measurement differences falling within a $\pm 3\sigma$ interval.

Chow and Watson (1997a), compared several PM_{10} filter samplers with BAM measurements at a site in California's Imperial Valley along the U.S./Mexican border from spring of 1992 through summer of 1993. Most of the suspended particles were composed of suspended dust and vehicle exhaust, with small quantities of nitrate. The high-volume size-selective inlet (SSI) and the dichotomous sampler (DIC) are designated PM_{10} reference methods while the BAM is a PM_{10} equivalent method (Chow, 1995). The SFS uses was similar, but not identical, to the Oregon Sequential Filter Sampler PM_{10} reference method. The Airmetrics portable (POR) PM_{10} monitor is used to determine zones of representation of fixed measurement locations. The Imperial Valley weather is warm throughout the year at this site.

As shown in the sixth through ninth rows of Table 4-2, the slope equals unity within three standard errors, the intercept is equal to zero within three standard errors, and the correlation coefficient is greater than 0.9. Table 4-2 shows that in all cases, 70% of the measurement differences lie within $\pm 2\sigma$, and more than 80% of the measurement differences lie within $\pm 3\sigma$. As shown in Figure 4-4, the differences between samplers are within the measurement error. Statistical comparability based on the pair-difference test is only valid for the BAM-SSI case. However, this rigorous test does not account for measurement uncertainty (i.e., if the samplers are different to within some multiple of the measurement uncertainty, they cannot realistically be considered different). Testing the hypothesis that the average ratio of "Y to X" (shown in Table 4-2) is equal to one indicates that for all sampler pairs, this ratio is different from unity at the 95% confidence interval except for BAM-SSI, which yielded an average ratio of 1.06 ± 0.18.

In this case, the BAM is as comparable to any filter-based sampler as these samplers are with each other. The sampled aerosol was relatively stable, non-hygroscopic, and humidities were low, providing stable conditions that favor a good comparison.

The remaining examples in Table 4-2 refer to: 1) year-long sampling in Las Vegas, NV, which is dry, dusty and hot (Chow and Watson, 1997a); 2) winter and summer sampling in the vicinity of Denver, CO (NFRAQS, Northern Front Range Air Quality Study) (Watson et al., 1998a; Chow et al., 1998b), where it is cold and moist during the winter and hot and dry during the summer; and 3) year-long sampling in southeastern Chicago, IL, where it is humid and warm in the summer and cold and wet during the winter (Watson et al., 1997c).

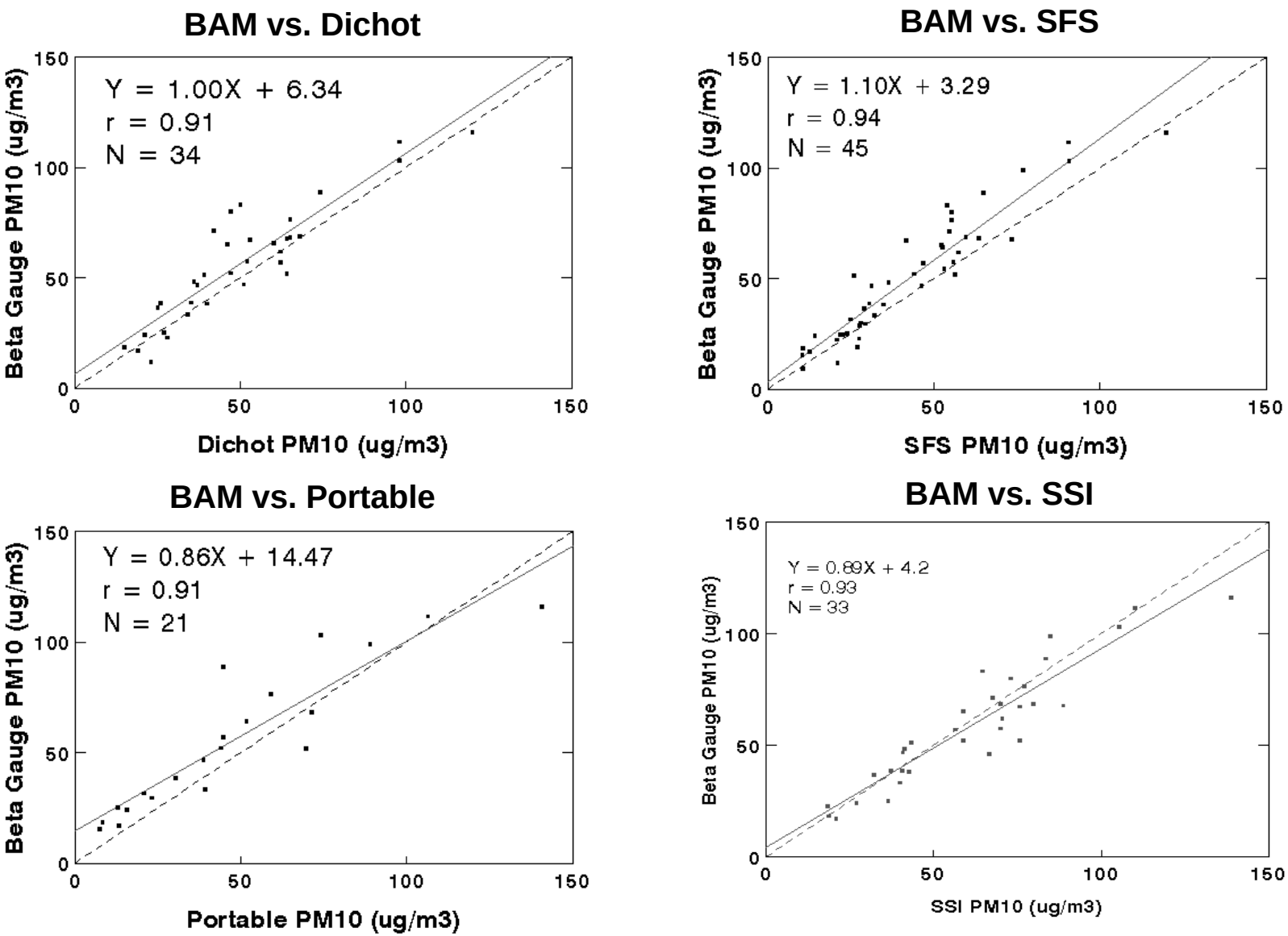

Figure 4-4. Collocated comparisons of 24-hour PM_{10} with BAM versus high-volume SSI, medium-volume SFS, low-volume dichotomous, and mini-volume portable samplers in Imperial Valley, CA, between 03/13/92 and 08/29/93.

For Las Vegas, collocated comparisons from 01/03/95 and 01/28/96 at the Bemis and East Charleston sites exhibit correlation coefficients less than 0.9, and filter measurements are not equivalent to continuous BAM measurements. The intercepts are quite large, ranging from 1.7 ± 15 μg/m^3 from the BAM versus portable PM_{10} survey sampler (POR) to 23.9 ± 5.3 μg/m^3 for the BAM versus SFS at the Bemis site. Figure 4-5 confirms that the BAM concentrations were generally higher than those obtained from the SFS or portable PM_{10} survey samplers, with average ratios ranging from 1.3 ± 0.51 (BAM versus SFS at the East Charleston site) to 2.06 ± 1.78 (BAM versus portable at the Bemis site). Table 4-2 shows that over 90% of all the pair comparisons lie within ±1σ for BAM versus POR at the East Charleston site, with more than 90% of the pair comparisons lying within ±2σ for BAM versus POR at the Bemis site. In all cases, over 80% of the paired differences lie within ±2σ, and over 90% of the measurements differ by no more than ±3σ. That is, in most cases, the differences between samplers are within the measurement errors. Table 4-2 indicates statistical comparability based on the pair-difference test is only valid for BAM versus POR at the East Charleston site. Overall, this comparison shows that BAM PM_{10} was systematically higher than the SFS and POR data (in the order of 30% to 100% on average) in the Las Vegas PM_{10} Study, even though the aerosol composition and climate was similar to that of the Imperial Valley, California.

At the Northern Front Range Air Quality Study (NFRAQS) Welby site just north of Denver, Table 4-2 shows the PM_{10} BAM measurements were lower than corresponding filter measurements, with slopes of 0.62 to 0.82 and large intercepts of 1.9 ± 1.3 to 9.0 ± 2.0 μg/m^3. The average ratios of BAM versus SFS PM_{10} were reasonable, ranging from 0.94 ± 0.42 to 1.14 ± 0.4. The correlations were variable (between 0.72 and 0.93), with higher correlations for measurements acquired during winter 1996. Figure 4-6 shows the extent of data scattering. The percent distribution in Table 4-2 shows that only 36% to 65% of the measurement differences fell within a ±3σ interval, however.

At the Eisenhower School site near Robbins IL, Table 4-2 shows correlation coefficients less than 0.9, and PM_{10} measurements from the collocated samplers are not equivalent to each other based on the pairwise comparison. While the regression statistics show that the slopes are equal to unity within three standard errors, the intercepts are variable (ranging from 0.11 ± 3.6 μg/m^3 for the BAM versus SSI pairs to 1.3 ± 4.2 μg/m^3 for the BAM versus DICHOT pairs). The correlations among these comparisons were low, being 0.66 and 0.75. Figure 4-7 confirms that the SSI PM_{10} concentrations were generally higher than those obtained from the BAM sampler in this Illinois study, in contrast to those observed in Central California. The BAM versus DICHOT comparisons meet the comparability criteria based on the parametric test. This comparison shows that over 70% of all the pair comparisons lie within a ±3σ interval. This percent distribution could be biased due to the estimated (rather than error-propagated) measurement uncertainties. The standard deviations associated with the average ratios are quite high, however, indicating some amount of data scattering. The average differences in PM_{10} measurements were 7.4 μg/m^3 for BAM versus SSI pairs and 2.7 μg/m^3 for BAM versus DICHOT pairs. The RMS precisions for PM_{10} mass comparisons are all less than 5 μg/m^3 in these comparisons.

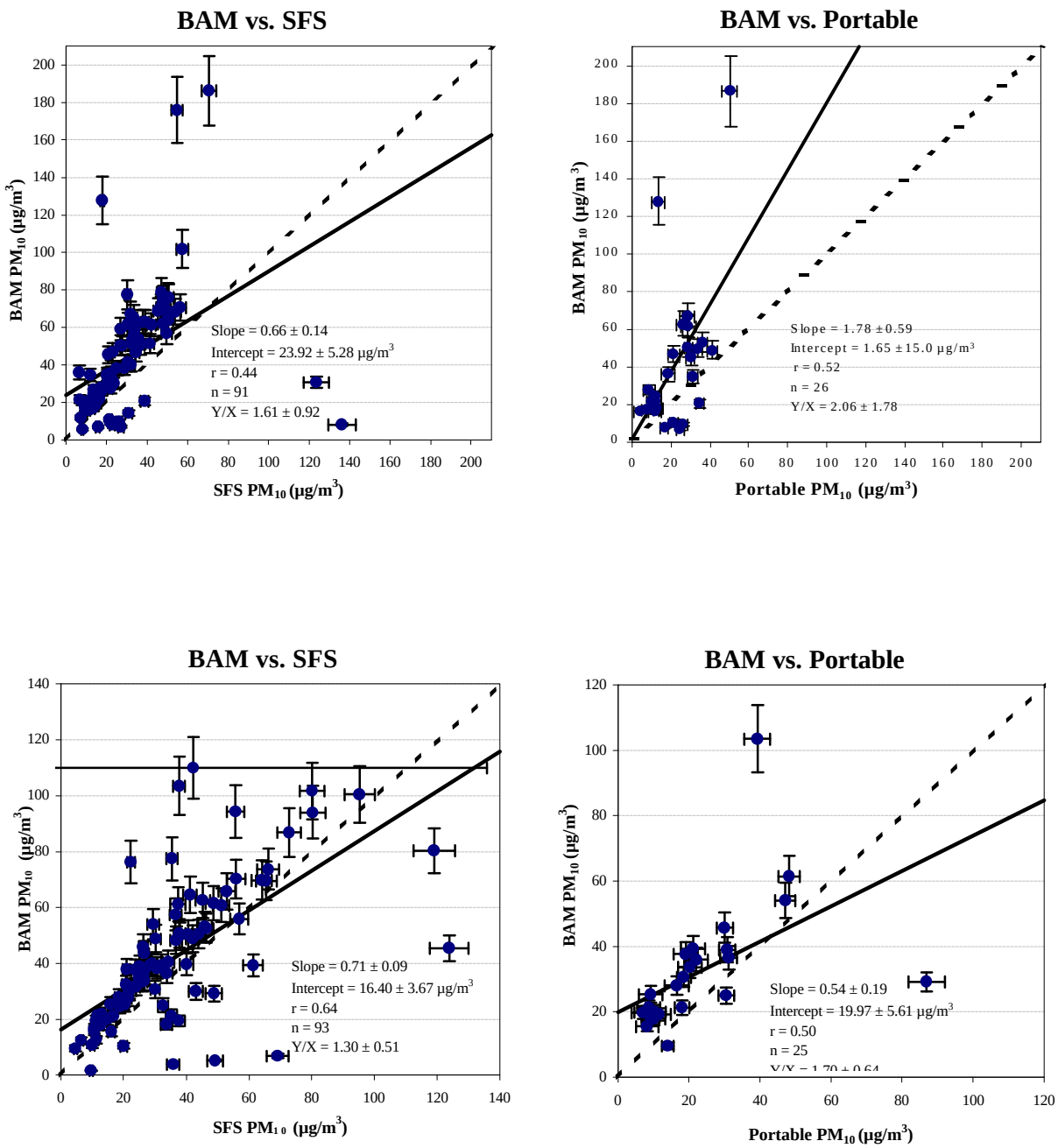

Figure 4-5. Collocated comparisons of 24-hour-averaged PM_{10} BAM versus SFS and portable samplers in Las Vegas Valley, NV, between 01/03/95 and 01/28/96.

Welby 6-hr

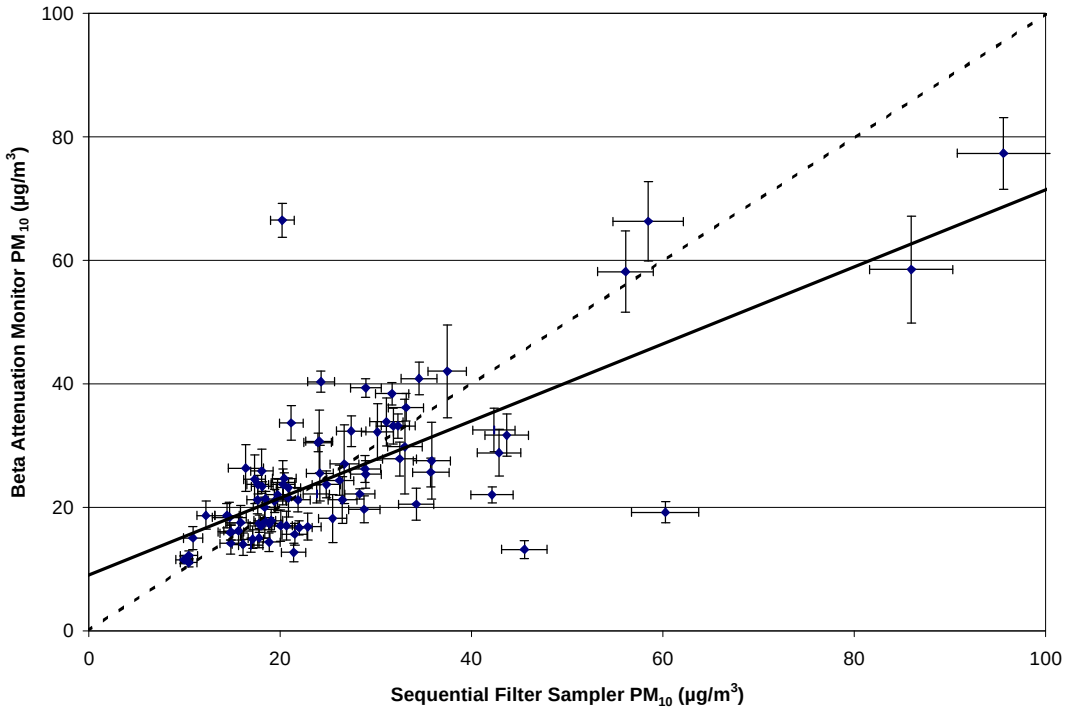

Welby 12-hr

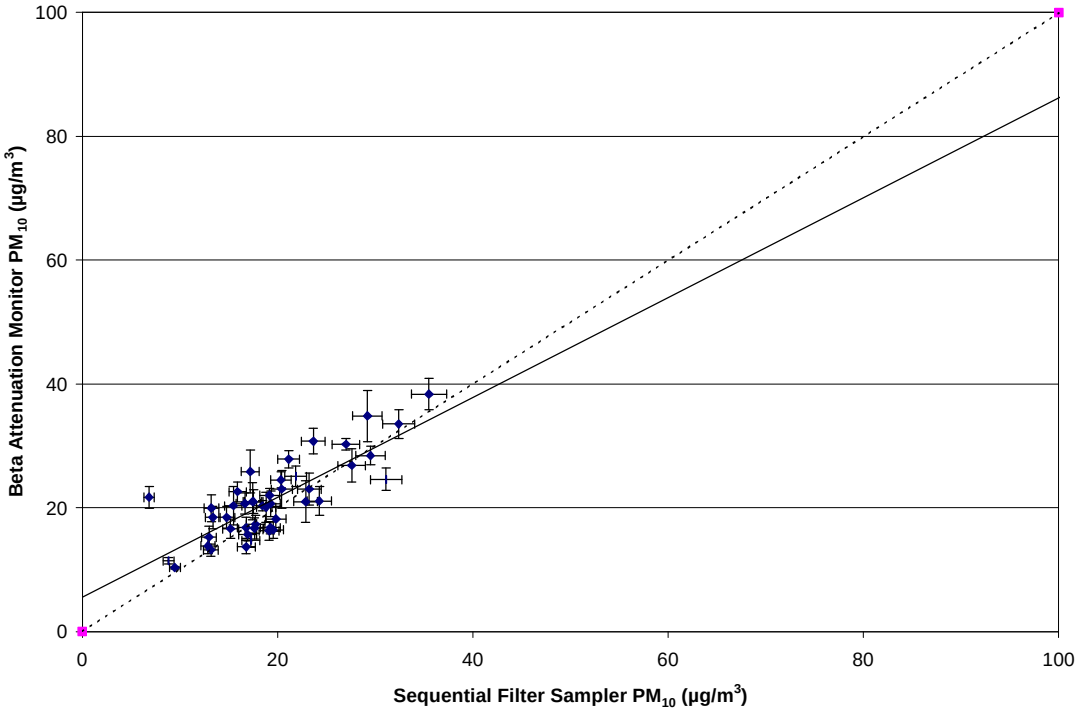

Figure 4-6. Collocated comparison of 6- and 12-hour PM_{10} BAM versus SFS in north Denver, CO, during winter and summer 1996.

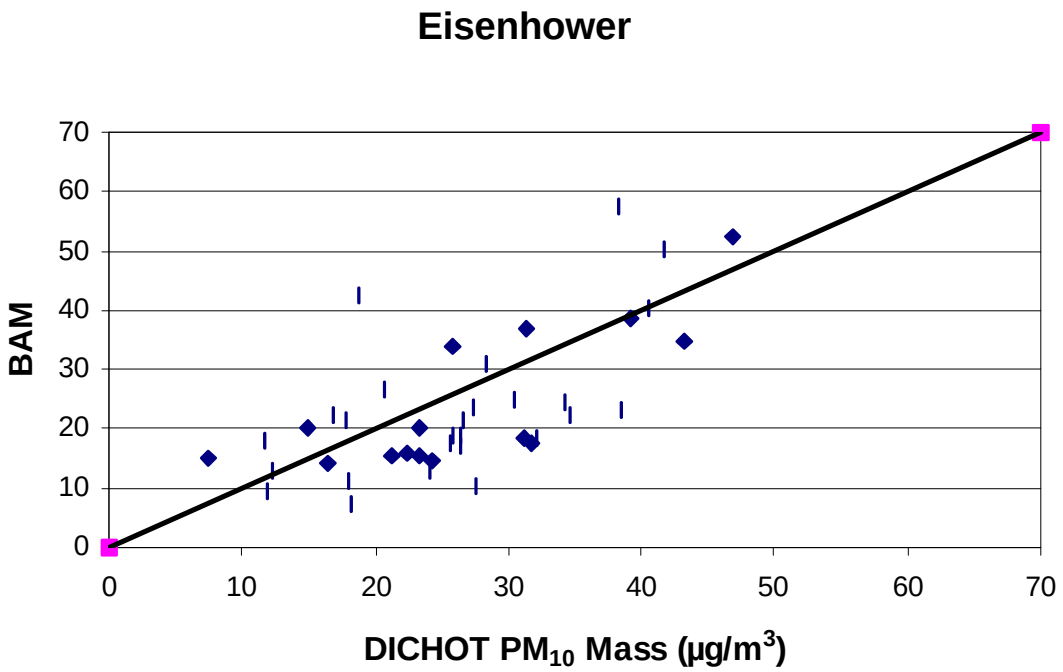

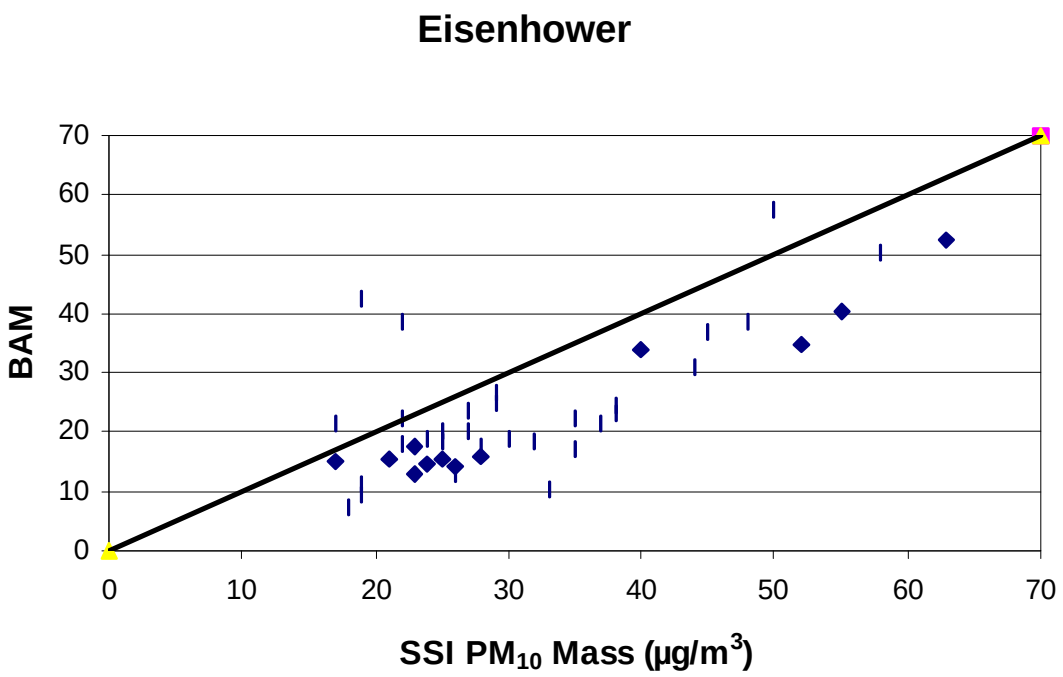

Figure 4-7. Collocated comparison of 24-hour PM_{10} BAM versus high-volume SSI and dichotomous samplers in southeastern Chicago, IL, between 10/12/95 and 09/30/96.

These comparisons show that comparability among the continuous BAM or TEOM measurements with 3-, 6-, 12-, or 24-hour filter measurements from MiniVol (i.e., portable PM_{10} survey sampler), low-volume (i.e., dichotomous sampler), medium-volume (i.e., SFS), or high-volume (i.e., SSI) samplers are highly variable, depending on the operating environments, and probably on the operating procedures. Reasonably good comparisons were found for TEOM-SSI during spring and summer only and BAM-SSI in Sacramento, Bakersfield, and Calexico, CA; and BAM-SFS, BAM-DICHOT, and BAM-portable PM_{10} in Calexico, CA; but comparability was not evident in Las Vegas, NV; Welby, CO; or Robbins, IL. The observed relationship between TEOM and filter-based methods varied widely depending on site location, time of year, range of particle concentrations, and conditioning temperature. TEOM measurements correlated well with filter-based measurements in urban areas along the East Coast during summer, but yielded much lower concentrations (and correlations) during winter (Allen et al., 1995). These measurement discrepancies could either be due to differences in inlet cleanliness, which affects the sampling efficiency (Watson et al., 1983); to differences in sampler calibration, which controls the sample volume; or to differences in filter handling and weighing for the conventional samplers.

These examples of sampler comparisons also show large discrepancies between different filter-based manual samplers for PM_{10}. In general, comparisons between the TEOM and BAM are no better or worse than comparisons among collocated PM_{10} filter samplers (Chow, 1995), many of which are designated PM_{10} reference methods.

4.2 Measurement Predictability

Though light scattering and absorption do not directly measure mass, they may provide reliable surrogates from which mass can be predicted once a correspondence has been established. As noted earlier, this empirical relationship is highly dependent on the consistency of aerosol composition measured at the monitoring site.

4.2.1 Particle Light Scattering and $PM_{2.5}$ Concentration

Chow and Egami (1997) examine relationships between particle scattering (b_{sp}) measured with the ambient temperature OPTEC NGN-2 nephelometer and a $PM_{2.5}$ Sequential Filter Sampler (SFS) in the high nitrate, foggy, and moist environment of the wintertime San Joaquin Valley, CA. When sampling during foggy conditions without preheating the sample stream, water vapor can condense on the NGN-2's optics, thereby affecting its response. Since water-soluble ammonium nitrate and ammonium sulfate particles can grow to many times their original size under high relative humidities, it is difficult to estimate the relationship between b_{sp} and $PM_{2.5}$ mass during these foggy conditions. It should also be noted that the nephelometer without a $PM_{2.5}$ size-selective inlet will also account for scattering by particles larger than 2.5 µm in diameter, though these were determined to be less than 20% of PM_{10} during the comparison. Figure 4-8 shows that particle scattering becomes dominated by liquid water at relative humidity (RH) above 80%, and that increased particle scattering can be detected at RH above 60%. These figures also show limitations of the relative humidity sensors that often are inaccurate at humidities above 90%; these limitations are especially noticeable at the Kern Wildlife Refuge site

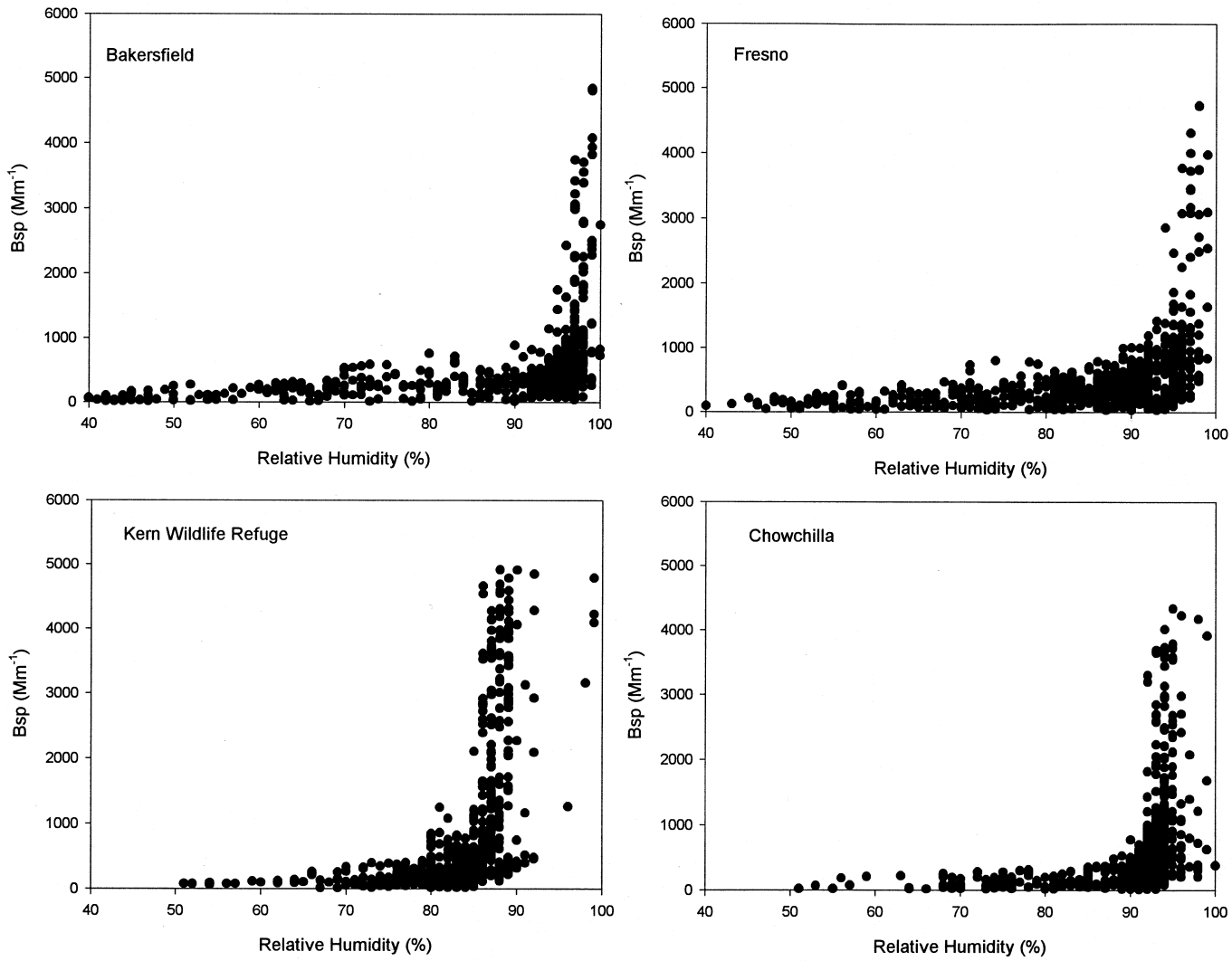

Figure 4-8. Relationship between hourly particle light scattering (b_{sp}) measured by nephelometer and ambient relative humidity in San Joaquin Valley, CA, between 12/09/95 and 01/06/96.

The $PM_{2.5}$ mass scattering efficiency is computed from the ratio of b_{sp} to $PM_{2.5}$ concentration, assuming that all particle light scattering is caused by particles smaller than 2.5 µm. While the hygroscopic growth properties of aerosols collected during the study are not known specifically, mass scattering efficiencies in similar environments change with 1/(1-RH) (Zhang et al., 1994). This is why b_{sp} and mass scattering efficiencies exhibit a similar upward pattern as RH above 80% or 90%.

Table 4-3 presents mass scattering efficiencies averaged by site as a function of relative humidity. Average mass scattering efficiencies ranged from 4.3 to 6.4 m^2/g for RH below 80%. Approximately 10% to 20% higher scattering efficiencies were estimated at the Kern Wildlife Refuge and Chowchilla sites for RH < 80%. These differences probably result from the higher proportion of ammonium sulfate and ammonium nitrate in $PM_{2.5}$ at the rural Kern Wildlife Refuge and Chowchilla sites. While ammonium nitrate and organic carbon are the dominant components of $PM_{2.5}$ at the urban sites, the relative abundance of organic carbon, which may be less hygroscopic than ammonium nitrate, is greatly diminished at the non-urban sites (Chow et al., 1998a).

Except at the Kern Wildlife Refuge site, mass scattering efficiency increased by ~30% to ~45% for RH between 80% and 90%, and increased by four- to ninefold for RH exceeding 90%. As noted earlier, high RH measurements at the Kern Wildlife Refuge site appear to be imprecise. Table 4-3 shows that recalculating mass scattering efficiency with adjusted RH at the two non-urban sites reduces the difference among the four sites. This analysis implies the importance of accurate on-site RH measurements and demonstrates that light scattering efficiency can only be derived for RH less than 80% or 90%.

4.2.2 Particle Light Absorption and Elemental Carbon Concentration

Chow and Egami (1997) measured light absorption (b_{ap}) on $PM_{2.5}$ Teflon-membrane filters with a densitometer standardized with photographers' neutral density filters. For each sample, the b_{ap} measurement on the Teflon-membrane filter was compared with light absorbing carbon or elemental carbon (EC) measured with Thermal/Optical Reflectance (TOR) analysis on a co-sampled quartz-fiber filter (Chow et al., 1993a), as shown in Figure 4-9. The overall correlation coefficient between b_{ap} and elemental carbon was 0.94. This suggests that nearly all of the fine-particle light absorption was due to elemental carbon. The average ratios and standard deviations of b_{ap} divided by elemental carbon concentration were 9.9 ± 2.1 m^2/g and 9.4 ± 2.6 m^2/g at the Bakersfield and Fresno urban sites, respectively; and 12.5 ± 3.2 m^2/g and 12.4 ± 4.1 m^2/g at the Kern Wildlife Refuge and Chowchilla non-urban sites, respectively. Note that in Figure 4-9, the standard deviations of the average ratios (which are influenced by the variations of individual data pairs) are approximately a factor of 10 higher than those derived with the effective variance weighted regression. Nevertheless, these absorption coefficients are within one standard deviation of the commonly accepted value of 10 m^2/g for the mass absorption efficiency of elemental carbon (Trijonis et al., 1988), but they differ from the most likely theoretical values shown in Section 2.

Three-hour average aethalometer BC concentrations are compared with Thermal/Optical Reflectance EC concentrations at the Bakersfield site in Figure 4-10a. The

Table 4-3
$PM_{2.5}$ Mass Scattering Efficiency (m^2/g) as a Function of Relative Humidity (%)

Site	Site Type	RH<80%	80%≤RH≤90%	RH>90%
Bakersfield	Urban	4.9±1.2	6.6±1.3	19.2±30.7
Fresno	Urban	5.4±1.2	7.7±2.2	27±42
Kern Wildlife Refuge	Non-urban	6.4±2.7	71±132	87±73
Kern Wildlife Refuge (RH+10%)	Non-urban	4.3±0.7	7.2±2.7	71±130
Chowchilla	Non-urban	5.7±0.9	8.2±3.9	56±106
Chowchilla (RH+5%)	Non-urban	5.1±0.6	6.8±1.8	49±99

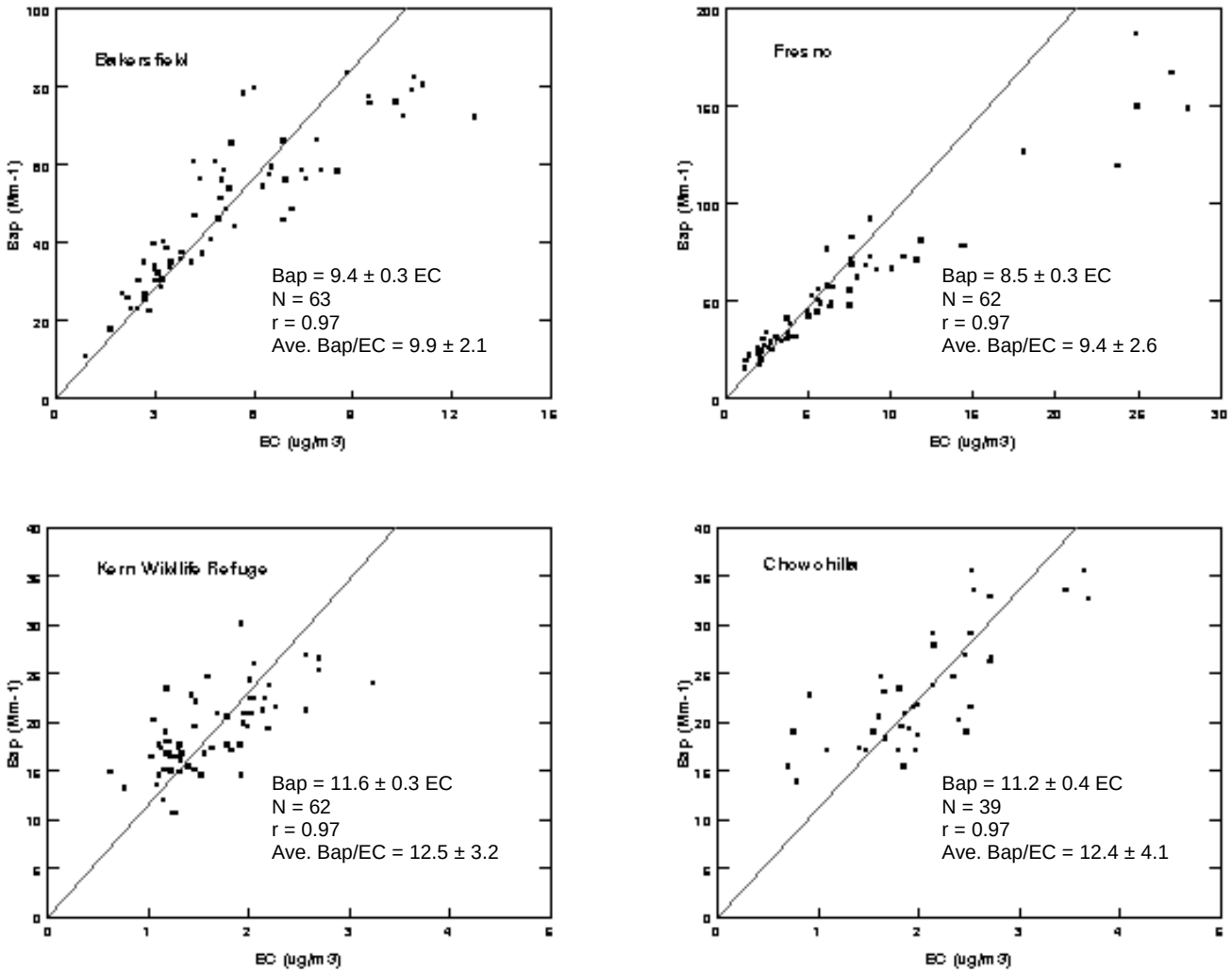

Figure 4-9. Relationship between $PM_{2.5}$ light absorption (b_{ap}) measured by densitometer on Teflon-membrane filter and elemental carbon measured by thermal/optical reflectance on a co-sampled quartz-fiber filter for three-hour samples acquired in San Joaquin Valley, CA, between 12/09/95 and 01/06/96.

a) Assumed value of 10 m^2/g absorption efficiency:

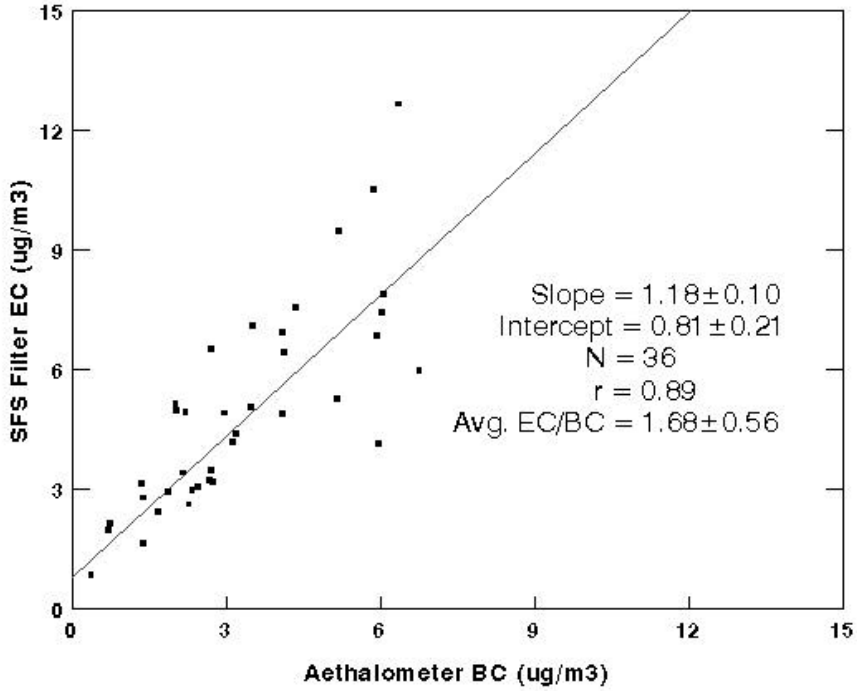

b) Calculated value of 9.4 m^2/g absorption efficiency:

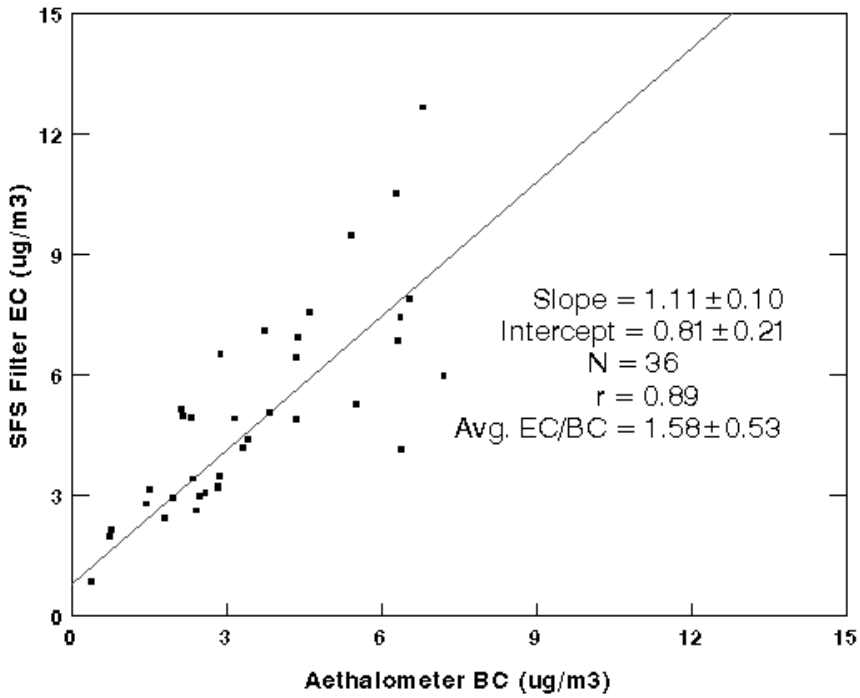

Figure 4-10. Relationship between filter-based $PM_{2.5}$ SFS elemental carbon (measured by thermal/optical reflectance on quartz-fiber filter) and aethalometer black carbon on three-hour samples acquired in the San Joaquin Valley between 12/09/95 and 01/06/96.

regression line was obtained using effective variance weighting assuming a 10% uncertainty in the BC measurements. The two measurements are well correlated (r = 0.89), but EC is systematically larger. This is indicated not only by the regression results (slope = 1.18 ± 0.10) and average ratio of EC/BC (1.68 ± 0.56), but also by a paired-difference t-test (Probability>|T| = 0.0001). This systematic difference is most likely due to bias built into the 19.2 m^2/g absorption efficiency that the aethalometer software uses to convert particle absorption to black carbon than to the variations in the chemical measurements. Figure 4-10b shows that average BC concentrations are within ±10% of EC measurements if 9.4 m^2/g (absorption efficiency derived at the Bakersfield site based on filter measurements of b_{ap} versus EC) instead of 10 m^2/g were used in this calculation.

4.2.3 Mass Concentration and Optical Measurements

Table 4-4 compares the comparability and predictability of particle light scattering measurements from nephelometers and particle light absorption measurements from aethalometers with collocated $PM_{2.5}$ concentrations for several environments.

The relationships between three-hour $PM_{2.5}$ and b_{sp} were well-defined at the four San Joaquin Valley (IMS95) sites with correlation coefficients (r) exceeding 0.93. The regression slopes of $PM_{2.5}$ versus b_{sp} were also consistent among the four sites (0.17 to 0.18). The correlations between b_{sp} and PM_{10} were reduced to 0.86 even though a majority (69% to 78%) of the PM_{10} was in the $PM_{2.5}$ fraction. The regression slopes for PM_{10} versus b_{sp} were similar to those derived from $PM_{2.5}$, in the range of 0.14 to 0.21. This reconfirms the fact that particle light scattering induced by coarse particles (PM_{10} minus $PM_{2.5}$) is insignificant during wintertime in the San Joaquin Valley, CA (Chow et al., 1993b).

There were many periods when relative humidity exceeded 90% in the San Joaquin Valley, CA, during the winter study, however. Because of increased b_{sp} due to liquid water growth under these conditions, the relationship between PM and b_{sp} breaks down over any sample averaging period containing periods of high relative humidity.

Table 4-4 indicates that relationships between b_{sp} and PM are less consistent with lower correlations for longer sample averaging times. For example, the correlations of b_{sp} with 12-hour $PM_{2.5}$ and PM_{10} concentrations at the Chowchilla, CA, site were 0.57 and 0.60, respectively. This deterioration is related to the inclusion of a few hours with high (>80%) RHs in the averages, even though the average humidities were <80%.

The relationships between b_{sp} and $PM_{2.5}$ were not as consistent for measurements in northern Colorado, with correlation coefficients ranging from 0.81 to 0.88 for 6- and 12-hour samples. The regression slope of 6-hour $PM_{2.5}$ versus b_{sp} varied a factor of two among these sites, ranging from 0.12 to 0.24. These values include the 0.17 or 0.18 slopes derived from three-hour IMS95 measurements.

The same relationships were not found for the Mt. Zirkel Wilderness Area in northwestern Colorado during the winter, summer, and fall seasons from 02/06/95 through 11/30/95 (Watson et al., 1996). The effects of liquid water on light scattering are apparent

Table 4-4
Relationships between Optical Measurements and PM Concentrations

Study	Sampling Duration (hours)	Site	X	Y	Slope[a]	Intercept[a] ($\mu g/m^3$)	r[b]	n[c]	$PM_{2.5}/PM_{10}$
IMS95[d]	3	Bakersfield, CA	b_{sp}[e] for RH<80%	$PM_{2.5}$	0.165 ± 0.005	2.2 ± 0.3	0.98	51	0.75 ± 0.42
IMS95	3	Fresno, CA	b_{sp} for RH<80%	$PM_{2.5}$	0.179 ± 0.008	0.120 ± 1.00	0.94	58	0.78 ± 0.12
IMS95	3	Kern Wildlife Refuge, CA	b_{sp} for RH<80%	$PM_{2.5}$	0.166 ± 0.012	0.74 ± 1.05	0.93	33	0.74 ± 0.22
IMS95	3	Chowchilla, CA	b_{sp} for RH<80%	$PM_{2.5}$	0.177 ± 0.010	0.32 ± 0.75	0.97	19	0.69 ± 0.15
IMS95	12[f]	Bakersfield, CA	b_{sp} for RH<80%	$PM_{2.5}$	0.135 ± 0.007	2.8 ± 0.4	0.98	14	0.75 ± 0.42
IMS95	12	Fresno, CA	b_{sp} for RH<80%	$PM_{2.5}$	0.146 ± 0.012	2.2 ± 2.5	0.95	18	0.78 ± 0.12
IMS95	12	Kern Wildlife Refuge, CA	b_{sp} for RH<80%	$PM_{2.5}$	0.032 ± 0.051	11.4 ± 13.7	0.84	7	0.74 ± 0.22
IMS95	12	Chowchilla, CA	b_{sp} for RH<80%	$PM_{2.5}$	0.055 ± 0.079	9.7 ± 16.4	0.57	3	0.69 ± 0.15
IMS95	24[g]	Bakersfield, CA	b_{sp} for RH<80% and n≥5	$PM_{2.5}$	0.106 ± 0.024	4.5 ± 1.6	0.93	5	0.75 ± 0.42
IMS95	24	Fresno, CA	b_{sp} for RH<80% and n≥5	$PM_{2.5}$	0.140 ± 0.031	3.1 ± 11.7	0.86	9	0.78 ± 0.12
IMS95	24	Bakersfield, CA	b_{sp} for RH<80%	$PM_{2.5}$	0.106 ± 0.024	4.5 ± 1.6	0.93	5	0.75 ± 0.42
IMS95	24	Fresno, CA	b_{sp} for RH<80%	$PM_{2.5}$	0.14 ± 0.031	3.1 ± 11.7	0.86	9	0.78 ± 0.12
IMS95	3	Bakersfield, CA	b_{sp} for RH<80%	PM_{10}	0.191 ± 0.014	6.9 ± 1.0	0.89	51	0.75 ± 0.42
IMS95	3	Fresno, CA	b_{sp} for RH<80%	PM_{10}	0.197 ± 0.012	6.9 ± 1.5	0.91	58	0.78 ± 0.12
IMS95	3	Kern Wildlife Refuge, CA	b_{sp} for RH<80%	PM_{10}	0.141 ± 0.015	9.2 ± 1.6	0.86	33	0.74 ± 0.22
IMS95	3	Chowchilla, CA	b_{sp} for RH<80%	PM_{10}	0.21 ± 0.02	5.2 ± 1.9	0.89	19	0.69 ± 0.15
IMS95	12	Bakersfield, CA	b_{sp} for RH<80%	PM_{10}	0.165 ± 0.026	2.5 ± 1.8	0.88	14	0.75 ± 0.42
IMS95	12	Fresno, CA	b_{sp} for RH<80%	PM_{10}	0.166 ± 0.014	8.0 ± 2.9	0.95	18	0.78 ± 0.12
IMS95	12	Kern Wildlife Refuge, CA	b_{sp} for RH<80%	PM_{10}	0.038 ± 0.051	14.8 ± 13.6	0.95	7	0.74 ± 0.22
IMS95	12	Chowchilla, CA	b_{sp} for RH<80%	PM_{10}	0.067 ± 0.090	13.3 ± 18.6	0.60	3	0.69 ± 0.15

Table 4-4 (continued)
Relationships between Optical Measurements and PM Concentrations

Study	Sampling Duration (hours)	Site	X	Y	Slope[a]	Intercept[a] ($\mu g/m^3$)	r[b]	n[c]	$PM_{2.5}/PM_{10}$
IMS95	24	Bakersfield, CA	b_{sp} for RH<80% and n≥5	PM_{10}	0.139 ± 0.065	11.0 ± 3.3	0.78	5	0.75 ± 0.42
IMS95	24	Fresno, CA	b_{sp} for RH<80% and n≥5	PM_{10}	0.172 ± 0.028	2.8 ± 10.4	0.92	9	0.78 ± 0.12
IMS95	24	Bakersfield, CA	b_{sp} for RH<80%	PM_{10}	0.139 ± 0.065	11.0 ± 3.3	0.78	5	0.78 ± 0.12
IMS95	24	Fresno, CA	b_{sp} for RH<80%	PM_{10}	0.172 ± 0.028	2.8 ± 10.4	0.92	9	0.78 ± 0.12
NFRAQS[h]	6	Brighton, CO	b_{sp}	$PM_{2.5}$	0.21 ± 0.02	2.0 ± 0.3	0.83	78	NA[i]
NFRAQS	6	Evans, CO	b_{sp}	$PM_{2.5}$	0.123 ± 0.009	2.8 ± 0.4	0.81	98	NA
NFRAQS	6	Welby, CO	b_{sp}	$PM_{2.5}$	0.24 ± 0.01	2.3 ± 0.4	0.85	97	NA
NFRAQS	12	Brighton, CO	b_{sp}	$PM_{2.5}$	0.148 ± 0.014	1.35 ± 0.24	0.88	36	NA
NFRAQS	12	Evans, CO	b_{sp}	$PM_{2.5}$	0.088 ± 0.009	1.73 ± 0.42	0.85	39	NA
NFRAQS	12	Welby, CO	b_{sp}	$PM_{2.5}$	0.189 ± 0.017	1.43 ± 0.43	0.87	40	NA
NFRAQS	6	Brighton, CO	$b_{sp2.5}$[j]	$PM_{2.5}$	0.23 ± 0.02	2.5 ± 0.3	0.83	72	NA
NFRAQS	6	Welby, CO	$b_{sp2.5}$	$PM_{2.5}$	0.26 ± 0.02	3.0 ± 0.4	0.83	99	NA
NFRAQS	12	Brighton, CO	$b_{sp2.5}$	$PM_{2.5}$	0.188 ± 0.019	1.41 ± 0.30	0.87	32	NA
NFRAQS	12	Welby, CO	$b_{sp2.5}$	$PM_{2.5}$	0.191 ± 0.020	2.1 ± 0.05	0.82	44	NA
Mt. Zirkel[k]	6	BAG1 BAGZ, CO	b_{sp} for RH<50%	$PM_{2.5}$	0.34 ± 0.04	0.59 ± 0.39	0.67	73	NA
Mt. Zirkel	6	BUF1 BUFZ, CO	b_{sp} for RH<50%	$PM_{2.5}$	0.33 ± 0.05	1.38 ± 0.34	0.73	38	NA
Mt. Zirkel	6	SEW1 SEWZ, CO	b_{sp} for RH<50%	$PM_{2.5}$	0.32 ± 0.04	0.76 ± 0.44	0.73	47	NA
Mt. Zirkel	6	VOR1 VORZ, CO	b_{sp} for RH<50%	$PM_{2.5}$	0.35 ± 0.06	2.0 ± 0.5	0.60	58	NA
Mt. Zirkel	6	JUN1 JUNZ, CO	b_{sp} for RH<50%	$PM_{2.5}$	0.23 ± 0.06	1.72 ± 0.49	0.54	42	NA

Table 4-4 (continued)
Relationships between Optical Measurements and PM Concentrations

Study	Sampling Duration (hours)	Site	X	Y	Slope[a]	Intercept[a] ($\mu g/m^3$)	r[b]	n[c]	$PM_{2.5}/PM_{10}$
Mt. Zirkel	12	BUF2 BUFZ, CO	b_{sp} for RH<50%	$PM_{2.5}$	0.33 ± 0.04	1.06 ± 0.19	0.80	34	NA
Mt. Zirkel	12	JUN2 JUNZ, CO	b_{sp} for RH<50%	$PM_{2.5}$	0.123 ± 0.056	1.97 ± 0.47	0.38	31	NA
Mt. Zirkel	12	GLC2 GLCZ, CO	b_{sp} for RH<50%	$PM_{2.5}$	0.37 ± 0.09	0.29 ± 0.83	0.46	62	NA
Mt. Zirkel	6	BAG1 BAGZ, CO	b_{sp} for RH<80%	$PM_{2.5}$	0.162 ± 0.029	1.69 ± 0.31	0.46	124	NA
Mt. Zirkel	6	BUF1 BUFZ, CO	b_{sp} for RH<80%	$PM_{2.5}$	0.31 ± 0.04	1.11 ± 0.25	0.69	73	NA
Mt. Zirkel	6	SEW1 SEWZ, CO	b_{sp} for RH<80%	$PM_{2.5}$	0.194 ± 0.025	1.77 ± 0.33	0.61	107	NA
Mt. Zirkel	6	VOR1 VORZ, CO	b_{sp} for RH<80%	$PM_{2.5}$	0.149 ± 0.042	3.2 ± 0.4	0.33	102	NA
Mt. Zirkel	6	JUN1 JUNZ, CO	b_{sp} for RH<80%	$PM_{2.5}$	0.043 ± 0.02	2.9 ± 0.3	0.24	75	NA
Mt. Zirkel	12	BUF2 BUFZ, CO	b_{sp} for RH<80%	$PM_{2.5}$	0.0022 ± 0.0041	2.6 ± 0.1	0.06	73	NA
Mt. Zirkel	12	JUN2 JUNZ, CO	b_{sp} for RH<80%	$PM_{2.5}$	-0.000021 ± 0.00089	2.5 ± 0.2	0.00	61	NA
Mt. Zirkel	12	GLC2 GLCZ, CO	b_{sp} for RH<80%	$PM_{2.5}$	0.0066 ± 0.0028	2.9 ± 0.2	0.20	138	NA
Mt. Zirkel	6	BUF3 BUFZ, CO	$b_{spg2.5}$[l] for RH<50% (heated inlet)	$PM_{2.5}$	0.31 ± 0.04	1.22 ± 0.37	0.59	93	NA
Mt. Zirkel	6	BUF3 BUFZ, CO	$b_{spg2.5}$ for RH<80% (heated inlet)	$PM_{2.5}$	0.32 ± 0.05	1.16 ± 0.41	0.56	95	NA
Mt. Zirkel	12	BUF6 BUFZ, CO	$b_{spg2.5}$ for RH<50% (heated inlet)	$PM_{2.5}$	0.31 ± 0.13	0.76 ± 0.80	0.53	16	NA
Mt. Zirkel	12	BUF6 BUFZ, CO	$b_{spg2.5}$ for RH<80% (heated inlet)	$PM_{2.5}$	0.31 ± 0.13	0.76 ± 0.80	0.53	16	NA
MOHAVE[m]	12	M2 (Summer 1992), AZ	b_{sp}	$PM_{2.5}$	0.25 ± 0.03	2.6 ± 0.4	0.62	89	0.40 ± 0.11
MOHAVE	12	M4 (Winter 1992), AZ	b_{sp}	$PM_{2.5}$	0.32 ± 0.07	-0.0112 ± 0.37	0.51	61	0.41 ± 0.25
MOHAVE	12	M1 (Summer 1992), AZ	$b_{sp2.5}$	$PM_{2.5}$	0.29 ± 0.04	2.8 ± 0.3	0.64	85	0.40 ± 0.11
MOHAVE	12	M3 (Summer 1992), AZ	b_{sp}	PM_{10}	0.78 ± 0.15	5.3 ± 1.6	0.48	88	0.40 ± 0.11
MOHAVE	12	M5 (Winter 1992), AZ	b_{sp}	PM_{10}	0.8 ± 0.12	-0.39 ± 0.58	0.66	61	0.41 ± 0.25

Table 4-4 (continued)
Relationships between Optical Measurements and PM Concentrations

Study	Sampling Duration (hours)	Site	X	Y	Slope[a]	Intercept[a] ($\mu g/m^3$)	r[b]	n[c]	$PM_{2.5}/PM_{10}$
Phoenix[n]	6	C1 CA, AZ	b_{sp} for RH<80%	$PM_{2.5}$	0.115 ± 0.009	6.2 ± 0.2	0.68	194	0.38 ± 0.21
Phoenix	6	S1 SC, AZ	b_{sp} for RH<80%	$PM_{2.5}$	0.115 ± 0.01	4.7 ± 0.6	0.68	178	0.38 ± 0.15
Phoenix	6	W1 WP, AZ	b_{sp} for RH<80%	$PM_{2.5}$	0.089 ± 0.007	6.5 ± 0.7	0.68	180	0.37 ± 0.20
Phoenix	6	V1 VA, AZ	b_{sp} for RH<80%	$PM_{2.5}$	0.104 ± 0.008	6 ± 0.5	0.69	172	0.41 ± 0.16
Phoenix	6	C3 CA, AZ	$b_{sp2.5}$ for RH<80%	$PM_{2.5}$	0.194 ± 0.021	7.1 ± 0.8	0.56	201	0.38 ± 0.21
Phoenix	6	C2 CA, AZ	b_{sp} for RH<80%	PM_{10}	0.33 ± 0.02	17.9 ± 1.3	0.72	189	0.38 ± 0.21
Phoenix	6	S2 SC, AZ	b_{sp} for RH<80%	PM_{10}	0.29 ± 0.03	13.7 ± 1.5	0.61	171	0.38 ± 0.15
Phoenix	6	W2 WP, AZ	b_{sp} for RH<80%	PM_{10}	0.192 ± 0.022	22 ± 2	0.54	181	0.37 ± 0.20
Phoenix	6	V2 VA, AZ	b_{sp} for RH<80%	PM_{10}	0.22 ± 0.03	17.2 ± 1.7	0.47	172	0.41 ± 0.16
Mexico[o]	6	M1 MER, MX	b_{sp} for RH<80%	$PM_{2.5}$	0.083 ± 0.003	17.8 ± 2.4	0.62	66	0.63 ± 0.18
Mexico	24	P1 PED, MX	b_{sp} for RH<80%	$PM_{2.5}$	0.16 ± 0.031	58 ± 2	0.87	11	0.56 ± 0.12
Mexico	6	M2 MER, MX	b_{sp} for RH<80%	PM_{10}	0.09 ± 0.005	37 ± 5	0.41	67	0.63 ± 0.18
Mexico	24	P2 PED, MX	b_{sp} for RH<80%	PM_{10}	0.24 ± 0.08	20 ± 6	0.72	11	0.56 ± 0.12
IMS95	3	Bakersfield, CA	b_{ap}[p] for RH<80%	$PM_{2.5}$	0.71 ± 0.08	1.40 ± 1.20	0.81	46	0.75 ± 0.42
IMS95	12	Bakersfield, CA	b_{ap} for RH<80%	$PM_{2.5}$	0.69 ± 0.11	0.89 ± 2.2	0.89	40	0.75 ± 0.42
IMS95	24	Bakersfield, CA	b_{ap} for RH<80% and n≥5	$PM_{2.5}$	0.58 ± 0.20	2.4 ± 4.8	0.86	5	0.75 ± 0.42
IMS95	24	Bakersfield, CA	b_{ap} for RH<80%	$PM_{2.5}$	0.58 ± 0.20	2.4 ± 4.8	0.86	5	0.75 ± 0.42
IMS95	3	Bakersfield, CA	b_{ap} for RH<80%	PM_{10}	0.86 ± 0.11	5.8 ± 1.8	0.76	46	0.75 ± 0.42
IMS95	12	Bakersfield, CA	b_{ap} for RH<80%	PM_{10}	0.83 ± 0.19	5.1 ± 3.8	0.81	12	0.75 ± 0.42
IMS95	24	Bakersfield, CA	b_{ap} for RH<80% and n≥5	PM_{10}	0.69 ± 0.25	6.3 ± 6.1	0.85	5	0.75 ± 0.42
IMS95	24	Bakersfield, CA	b_{ap} for RH<80%	PM_{10}	0.69 ± 0.25	6.3 ± 6.1	0.85	5	0.78 ± 0.12

Table 4-4 (continued)
Relationships between Optical Measurements and PM Concentrations

Study	Sampling Duration (hours)	Site	X	Y	Slope[a]	Intercept[a] ($\mu g/m^3$)	r[b]	n[c]	$PM_{2.5}/PM_{10}$
NFRAQS	6	Brighton, CO	b_{ap}	$PM_{2.5}$	0.41 ± 0.05	2.6 ± 0.6	0.64	82	NA
NFRAQS	6	Welby, CO	b_{ap}	$PM_{2.5}$	0.28 ± 0.06	4.0 ± 1.2	0.67	29	NA
NFRAQS	12	Brighton, CO	b_{ap}	$PM_{2.5}$	0.38 ± 0.09	1.41 ± 0.69	0.58	37	NA
NFRAQS	12	Welby, CO	b_{ap}	$PM_{2.5}$	0.155 ± 0.075	5.2 ± 1.4	0.53	13	NA
Mt. Zirkel	6	BUF4 BUFZ, CO	b_{ap} for RH<50% [h]	$PM_{2.5}$	1.33 ± 0.28	0.54 ± 0.73	0.61	41	NA
Mt. Zirkel	6	BUF4 BUFZ, CO	b_{ap} for RH<80%	$PM_{2.5}$	1.25 ± 0.2	0.76 ± 0.50	0.60	67	NA
Mt. Zirkel	12	BUF7 BUFZ, CO	b_{ap} for RH<50%	$PM_{2.5}$	1.19 ± 0.32	0.70 ± 0.47	0.63	22	NA
Mt. Zirkel	12	BUF7 BUFZ, CO	b_{ap} for RH<80%	$PM_{2.5}$	1.02 ± 0.18	1.00 ± 0.25	0.66	47	NA
Phoenix	6	C6 CA, AZ	b_{ap} for RH<80%	$PM_{2.5}$	0.56 ± 0.09	3.3 ± 1.6	0.71	39	0.38 ± 0.21
Phoenix	6	C7 CA, AZ	b_{ap} for RH<80%	PM_{10}	1.3 ± 0.2	9.6 ± 2.9	0.73	38	0.38 ± 0.21
Mexico	6	M3 MER, MX	b_{ap} * 19.2 for RH<80%	$PM_{2.5}$	0.175 ± 0.034	18.2 ± 2.6	0.47	96	0.63 ± 0.18
Mexico	24	P3 PED, MX	b_{ap} * 19.2 for RH<80%	$PM_{2.5}$	0.28 ± 0.08	7 ± 3.9	0.60	23	0.56 ± 0.12
Mexico	6	M4 MER, MX	b_{ap} * 19.2 for RH<80%	PM_{10}	0.174 ± 0.059	36 ± 5	0.30	95	0.63 ± 0.18
Mexico	24	P4 PED, MX	b_{ap} * 19.2 for RH<80%	PM_{10}	0.36 ± 0.17	18.7 ± 8.2	0.42	23	0.56 ± 0.12
IMS95	24	Bakersfield, CA	b_{ext}[q] = b_{sp} + b_{ap} for RH<80%	$PM_{2.5}$	0.091 ± 0.021	4.3 ± 2.3	0.93	5	0.75 ± 0.42
IMS95	24	Bakersfield, CA	b_{ext} = b_{sp} + b_{ap} for RH<80%	PM_{10}	0.117 ± 0.047	9.8 ± 3.4	0.82	5	0.78 ± 0.12
Mt. Zirkel	6	BUF5 BUFZ, CO	b_{ext} = b_{sp} + b_{ap} for RH<50%	$PM_{2.5}$	0.22 ± 0.05	1.69 ± 0.52	0.62	37	NA
Mt. Zirkel	12	BUF8 BUFZ, CO	b_{ext} = b_{sp} + b_{ap} for RH<50%	$PM_{2.5}$	0.26 ± 0.05	0.81 ± 0.26	0.77	22	NA
Mt. Zirkel	6	BUF5 BUFZ, CO	b_{ext} = b_{sp} + b_{ap} for RH<80%	$PM_{2.5}$	0.25 ± 0.03	1.19 ± 0.37	0.69	62	NA
Mt. Zirkel	12	BUF8 BUFZ, CO	b_{ext} = b_{sp} + b_{ap} for RH<80%	$PM_{2.5}$	0.166 ± 0.026	1.24 ± 0.19	0.69	45	NA

Table 4-4 (continued)
Relationships between Optical Measurements and PM Concentrations

Study	Sampling Duration (hours)	Site	X	Y	Slope[a]	Intercept[a] ($\mu g/m^3$)	r[b]	n[c]	$PM_{2.5}/PM_{10}$
Phoenix	6	C4 CA, AZ	$b_{ext} = b_{sp} + b_{ap}$ for RH<80%	$PM_{2.5}$	0.107 ± 0.009	2.6 ± 0.9	0.91	32	0.38 ± 0.21
Phoenix	6	C5 CA, AZ	$b_{ext} = b_{sp} + b_{ap}$ for RH<80%	PM_{10}	0.2 ± 0.04	10.2 ± 0.3	0.71	32	0.38 ± 0.21
Mexico	6	M5 MER, MX	$b_{ext} = b_{sp} + b_{ap}$ for RH<80%	$PM_{2.5}$	0.065 ± 0.01	16.4 ± 2.6	0.61	66	0.63 ± 0.18
Mexico	24	P5 PED, MX	$b_{ext} = b_{sp} + b_{ap}$ for RH<80%	$PM_{2.5}$	0.122 ± 0.025	3.6 ± 3.0	0.85	11	0.56 ± 0.12
Mexico	6	M6 MER, MX	$b_{ext} = b_{sp} + b_{ap}$ for RH<80%	PM_{10}	0.079 ± 0.019	34 ± 5	0.45	67	0.63 ± 0.18
Mexico	24	P6 PED, MX	$b_{ext} = b_{sp} + b_{ap}$ for RH<80%	PM_{10}	0.178 ± 0.054	16.8 ± 8.7	0.73	11	0.56 ± 0.12

[a] Effective variance weighted regression.
[b] Correlation coefficient.
[c] Number of sample pairs in the analysis.
[d] Integrated Monitoring Study (Chow and Egami, 1997; Chow et al., 1998a).
[e] Total particle light scattering.
[f] Averaging periods 0600–1800 and 1800–0600 PST.
[g] Averaging period 0000–2400 PST.
[h] Northern Front Range Air Quality Study (Chow et al., 1998b, Watson et al., 1998a).
[i] PM_{10} measurements were not acquired.
[j] $PM_{2.5}$ particle light scattering.
[k] Mt. Zirkel Visibility Study (Watson et al., 1996).
[l] Three-color nephelometer with $PM_{2.5}$ inlet (Chow et al., 1998b).
[m] Project MOHAVE Study (Watson et al., 1993).
[n] Phoenix Urban Haze Study (Watson et al., 1991).
[o] Mexico City Aerosol Characterization Study (Watson et al., 1998b).
[p] $PM_{2.5}$ particle light absorption.
[q] Particle light extinction = the sum of particle light scattering and particle light absorption.

for RH above 80%, resulting in a wide range of regression slopes. As the analyses were limited to samples with average RH < 50% for 6- and 12-hour measurements, the slope for $PM_{2.5}$ versus b_{sp} were 0.23 to 0.34 for 6-hour samples and 0.12 to 0.37 for 12-hour samples. Table 4-4 shows that correlations are quite variable, ranging from 0.54 to 0.73 for 6-hour averages and 0.38 to 0.80 for 12-hour averages. Because the multiwavelength nephelometer has a $PM_{2.5}$ inlet with elevated chamber temperature, its measurements ($b_{spg2.5}$ in Table 4-4) have a higher slope (0.31 to 0.32). Similar $PM_{2.5}$ versus b_{sp} slopes of 0.25 to 0.32 were found for the 12-hour samples acquired during the summer and winter of 1992 at a pristine location (Meadview, AZ, near the Grand Canyon) for Project MOHAVE (Watson et al., 1993), with moderate ($0.51 < r < 0.64$) correlations. Table 4-4 shows reasonable agreement between $PM_{2.5}$ and b_{sp} (slope of 0.09 to 0.19, correlation of 0.56 to 0.69) among the four urban sites in Arizona during the 1989/90 winter visibility study (Watson et al., 1991). Similar $PM_{2.5}$ versus b_{sp} slopes (0.08 to 0.16) were found in Mexico City's urban environment (Watson et al., 1998b).

Scattering by particles of all sizes (b_{sp}) and scattering by $PM_{2.5}$ ($b_{sp2.5}$, determined by installing a $PM_{2.5}$ inlet on the nephelometer) were compared in northern Colorado and central Arizona, and there was little difference between their outputs. This is due to low coarse particle concentrations during winter as well as a low scattering efficiency for those coarse particles that are present.

This analysis demonstrates the feasibility of using hourly nephelometer light scattering measurements to predict $PM_{2.5}$ concentrations as long as samples are taken at relative humidities less than 80% and site or region specific relationships can be established by collocation with filter samplers. Data from a variety of urban, non-urban, and pristine environments imply that each 100 Mm^{-1} of light scattering could potentially be associated with 8 to 34 $\mu g/m^3$ $PM_{2.5}$ in the atmosphere for 3- to 12-hour sampling durations. Preceding the nephelometer sensing chamber with a heatless dryer, such as a Nafion or Drierite denuder, and a $PM_{2.5}$ size-selective inlet may improve the nephelometer's utility as a surrogate for continuous $PM_{2.5}$ measurements.

Relationships between 3-hour $PM_{2.5}$ and PM_{10} and particle absorption (b_{ap}) measured with an aethalometer were good at the Bakersfield site, with correlation coefficients ranging from 0.81 to 0.89 for all but one sample-averaging periods ($r = 0.76$). The regression slopes of mass versus b_{ap} vary from 0.58 to 0.71 for $PM_{2.5}$ and 0.69 to 0.86 for PM_{10}. The relationships for the 6- and 12-hour measurements in northern and northwestern Colorado and central Arizona were not as consistent, with correlations ranging from 0.53 to 0.73. The regression slopes of $PM_{2.5}$ versus b_{ap} differed substantially from those derived at Bakersfield, CA, ranging from 0.16 to 1.3. Longer sample averaging times or ambient liquid water content appear to have little effect on the b_{ap} versus PM relationship, which is expected since relative humidity and particle growth have small effects on particle absorption. Higher correlations between light absorption and $PM_{2.5}$ at the Bakersfield site are mainly due to higher proportions of elemental carbon than those found at other locations.

Table 4-4 also compares the relationship between light extinction (derived from collocated nephelometers and aethalometers) and $PM_{2.5}$. A more narrow range of slopes

(between 0.09 and 0.26) and higher correlations (>0.7 in most cases) were found. Because the proportions of scattering and absorption may vary from sample to sample, more data is needed for comparison.

4.3 Summary

Comparisons with collocated filter samplers show that the TEOM and BAM have the capability of providing measurements comparable to filter samplers when air is dry and the sampled aerosol is stable. Inconsistencies found by some comparisons in similar environments are probably caused by differences in operating procedures rather than by inherent deficiencies of the instruments. Biases are evident when the sampled aerosol is volatile and when humidities are high, and these conditions often occur together.

Elevated sulfate and nitrate concentrations are often found in moist environments and absorb copious amounts of liquid water. TEOM heating evaporates volatile components, but lower temperatures allow liquid water to be collected along with particles. BAM monitors that sample at ambient temperatures and relative humidities may overestimate particle concentrations at high humidities owing to the liquid water associated with sampled particles. Sample conditioning that is similar to laboratory filter equilibration temperature and relative humidity conditions may alleviate these biases.

Relative humidity also affects the predictability of $PM_{2.5}$ from light scattering measured with a nephelometer because scattering increases substantially as RH climbs above 80%. Light absorption measured with an aethalometer is primarily sensitive to black carbon, and it will only be a good predictor of $PM_{2.5}$ when black carbon is a constant fraction of mass. The sum of nephelometer (b_{sp}) and aethalometer (b_{ap}) measurements, which is an indicator of particle light extinction (b_{ext}), gives slightly better correlations with $PM_{2.5}$ than b_{sp} and b_{ap} do individually. More comparison is needed before a reasonable relationship can be inferred. Again, sample conditioning that is similar to laboratory filter equilibration temperature and relative humidity conditions may alleviate these biases.

5. USES OF CONTINUOUS PM MEASUREMENTS

This section provides examples of how continuous particle measurements can be applied to achieve several of the objectives specified in Section 1. These purposes include:

- **Reduce site visits and network operation costs:** When a continuous particle monitor achieves FEM status, it can be used in place of a manual FRM or FEM, thereby reducing the frequency of site visits and the need for laboratory analysis. A proven CAC monitor can be operated alongside a manual FRM or FEM at a CORE site to reduce sampling frequency from daily to every third day (U.S. EPA, 1997b).

- **Identify the need to increase FRM/FEM sampling frequency:** Many $PM_{2.5}$ sites will have less than daily sampling frequency. A CAC monitor collocated with a manual $PM_{2.5}$ sampler at this site can be used to evaluate the extent to which this periodic sampling affects the annual average and 98th percentile $PM_{2.5}$ concentrations. The CAC data can be used to justify the lower sampling frequency or to demonstrate that more frequent manual sampling is needed to represent population exposures to outdoor air.

- **Evaluate real-time data to issue alerts or implement control strategies:** CAC measurements can be relayed via phone lines or satellites to a central facility where they can be evaluated as part of a public health strategy. These are particularly useful to detect pollution buildups under adverse meteorology or during unusual pollution events. Several communities currently use continuous particle and meteorological monitors to curtail residential wood combustion.

- **Evaluate diurnal variations in human exposures to outdoor air:** Although values for a 24-hour averaging time are required for comparison with standards, data bases with shorter time resolutions will provide better information for scientists investigating relationships to health end-points.

- **Define zones of representation of monitoring sites and zones of influence of pollution sources:** The portability and low cost of several continuous particle monitors, specifically a few of the nephelometers, facilitates their use in middle-scale and neighborhood-scale special purpose monitoring sites around CORE sites and at different downwind distances from suspected particle emitters. These data can be used to evaluate how well a CORE site represents population exposure and the distances at which individual source emissions significantly affect $PM_{2.5}$ levels. The width of $PM_{2.5}$ pulses in continuous measurements at a long-term $PM_{2.5}$ monitoring site also provides insight into the zone of representation. Short-duration (1 to 5 minutes) pulses often originate from nearby emitters and can distinguished from longer sample durations (>1 hour) that originate from urban and regional source mixtures.

- **Understand the physics, chemistry, and sources of high particle concentrations:** Short-duration particle measurements, especially those that are chemically specific, can be examined in conjunction with short-term

meteorological and gaseous air quality measurements to infer source origins, transport properties, and chemical transformation mechanisms.

The final continuous monitoring purpose offers a large range of possibilities. During a 24-hour day, wind directions and wind speed may change significantly. Some areas may experience several cycles of meteorological patterns with durations of a few hours. For example, the daytime sea-breeze and nighttime land-breeze are common occurrences in coastal areas, as are mountain-valley circulations in mountainous areas. With integrated 24-hour averaged PM data, changes in transport directions during the sampling period make it difficult to establish source-receptor relationships. Use of short-term or hourly particle, along with hourly meteorological observations, allows for a better understanding of receptor zones of representation and source zones of influence. High correlations of $PM_{2.5}$ with carbon monoxide and nitrogen oxide might indicate a large vehicle exhaust contribution, especially when coupled with wind directions from a major highway. Elevated elemental concentrations from a specific wind direction might indicate the location of a pollution source.

Sources that are sufficiently close to receptors often affect the measured concentrations on a scale of a few hours or less. These diurnal and episodic characteristics of $PM_{2.5}$ can also be used to investigate exposure patterns. A significant limitation of high-time-resolution PM data from instruments such as the BAM and TEOM and other continuous mass measurement methods is that they do not provide real-time chemical composition information. However, when used in conjunction with chemically speciated data averaged over longer time periods, these measurements can add to the understanding of the sources and behavior of atmospheric PM.

In arid regions, disturbances of the land surface can cause high concentrations of PM, especially during periods of high wind. Short-term PM and wind data can be used to determine "threshold velocities" above which high amounts of crustal material can be suspended. These threshold wind velocities could be used in control strategy development by mitigating the effects of certain activities when high winds are expected or are occurring. For example, clearing of land for construction activities or agricultural tilling could be restricted during periods of high winds.

Several possible uses of continuous particle measurements are illustrated by examples presented in the following sub-sections.

5.1 Diurnal Variations

By considering the diurnal pattern for PM, information may be obtained about factors that affect PM concentration. These diurnal patterns are also useful for better estimating human exposure, especially when they are available from locations near where people live, work, and play, as well as for periods when they are expected to be outdoors during commuting or exercise.

Figure 5-1 shows the 20th, 50th, and 80th percentile PM_{10} BAM data for a mixed light industrial/suburban site in the Las Vegas Valley, NV, during winter and summer

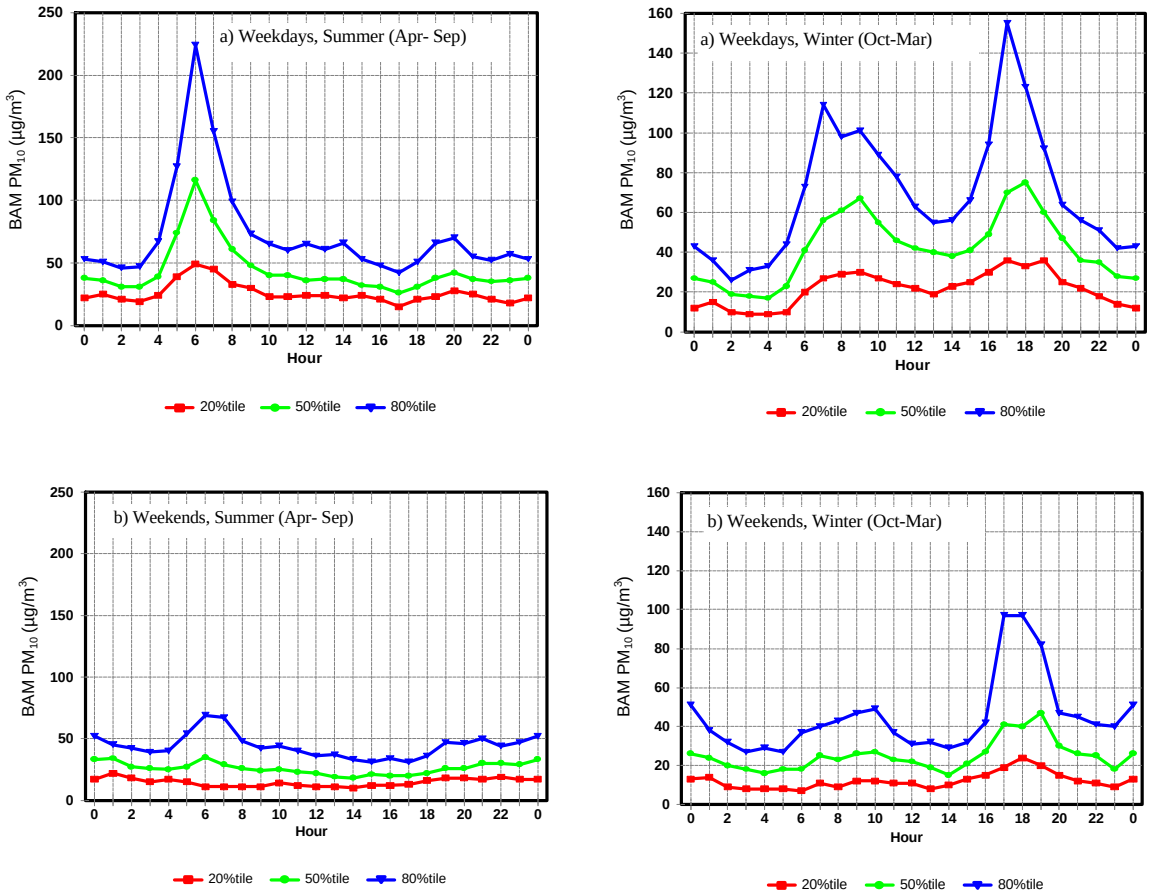

Figure 5-1. Winter weekday and weekend patterns in PM_{10} concentrations during summer (April to September 1995) and winter (October 1995 to March 1996) periods at a mixed light industrial/suburban site in the Las Vegas Valley, NV.

seasons, with comparisons of weekends and weekdays. Two distinguishable peaks occur on

correspond to periods of high traffic volume and low mixing heights. In the middle of the afternoon, deeper mixing depths caused by solar surface heating, along with somewhat reduced traffic volumes, result in a period with lower concentrations than during the morning and evening rush hours.

During summer weekdays, a large peak occurs in the early morning around 0600 to 0700 PST, and a smaller peak occurs in the early evening around 2000 PST. Lower concentrations occur during the intervening daytime hours due to dispersion associated with the deep mixing depths in summer. In fact, the evening peak in PM_{10} occurs well after peak traffic volumes, because during the rush hours deep mixing compensates for the increased traffic. The weekend patterns show a substantially reduced size of the morning peak. This may be explained by having fewer commuters traveling to work on weekend mornings.

Time-resolved PM data can also be used to understand differences between sites within the same urban area. Figure 5-2 shows diurnal patterns of winter 50th-percentile PM_{10} BAM concentrations for four sites in the Las Vegas Valley. The East Charleston and City Center sites are near the center of the Las Vegas urban area, while the Bemis and Walter Johnson sites are at the edge of the urban area. The two urban sites exhibit high PM_{10} concentrations until late in the evening (especially on weekends) due to higher traffic activities, while the two suburban sites have decreased concentrations after the evening rush hours. Each of these sites shows a characteristic morning traffic peak on weekdays that is attenuated on weekends. The apparent relationships between traffic level and PM_{10} concentration in Las Vegas are consistent with contributions from emissions along roadways, including both direct vehicle emissions and dust resuspended by vehicles traveling on (mostly) paved roads.

Figure 5-3 illustrates the diurnal cycle of PM_{10} concentrations at a site in Calexico, CA, along the U.S./Mexico border, a location close to vehicle exhaust and paved road dust sources. These patterns have many of the same features as the Las Vegas measurements, but the timing is different. The median and 95th percentile data show peaks at about 0800 PST as well as 1900 to 2000 PST. The evening peak at the 95th percentile level is about twice as high as the morning peak. In Las Vegas, the morning peak is associated with increased traffic and low mixing heights. The evening peak is consistent with a collapse in the mixing depth at sunset that traps vehicle emissions at the end of the evening rush hours. Traffic is heavy at the nearby border crossing late into the evening, and this is reflected in diurnal maxima that occur a few hours later in the evening.

5.2 Wind Speed and PM Relationships

Figures 5-4 and 5-5 show average PM_{10} corresponding to different wind speed categories at the Calexico, CA, site for winds from the north (Figure 5-4) and from the south (Figure 5-5). Higher PM_{10} concentrations occur for wind flow from the south (i.e., Mexico) at all wind speeds. Higher concentrations occur at very low and high wind speeds as

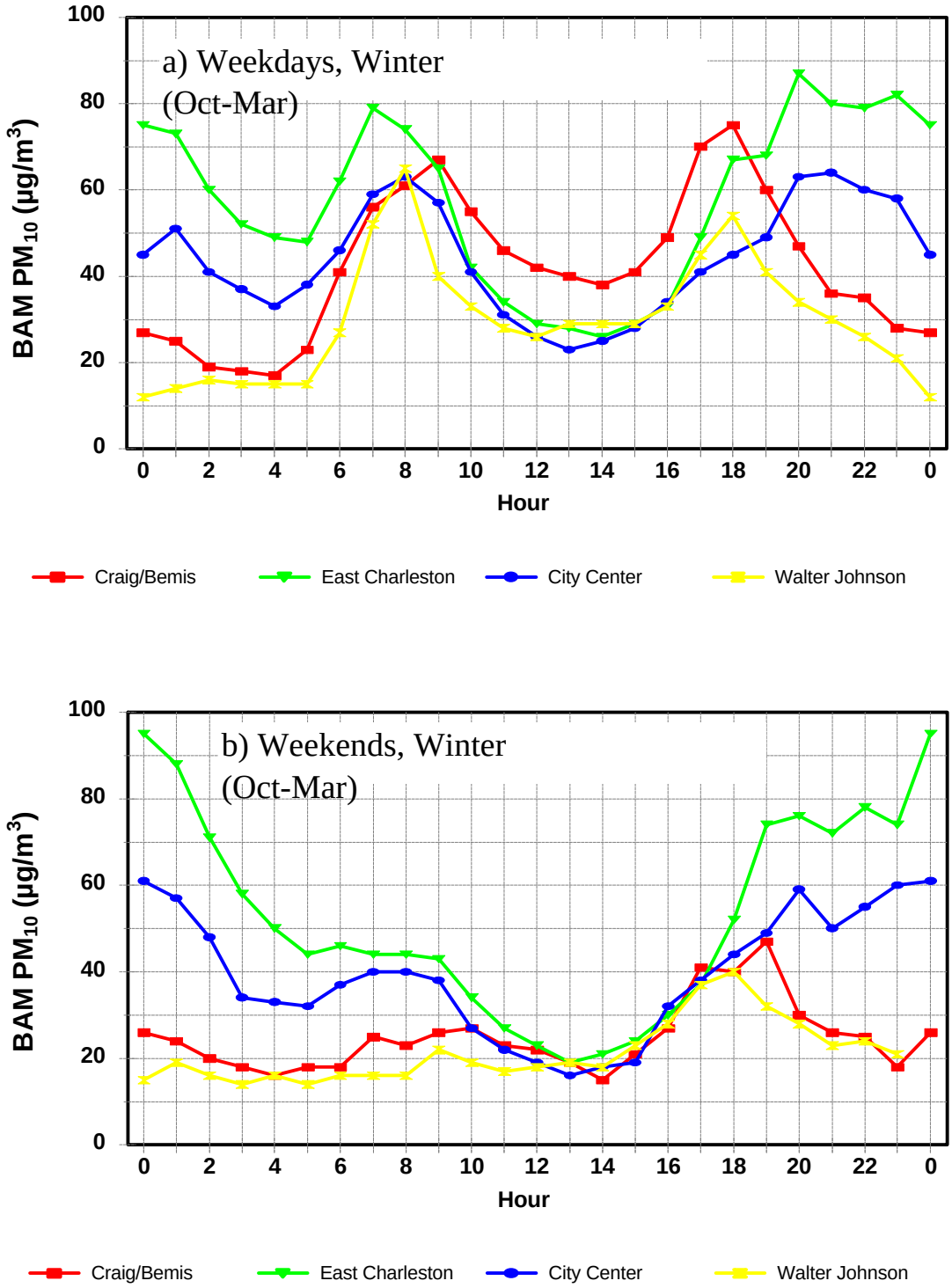

Figure 5-2. Weekday and weekend patterns for 50th percentile PM_{10} concentrations at the City Center and East Charleston (Microscale) urban center sites and Bemis/Craig and Walter Johnson urban periphery sites during Winter 1995 in the Las Vegas Valley, NV.

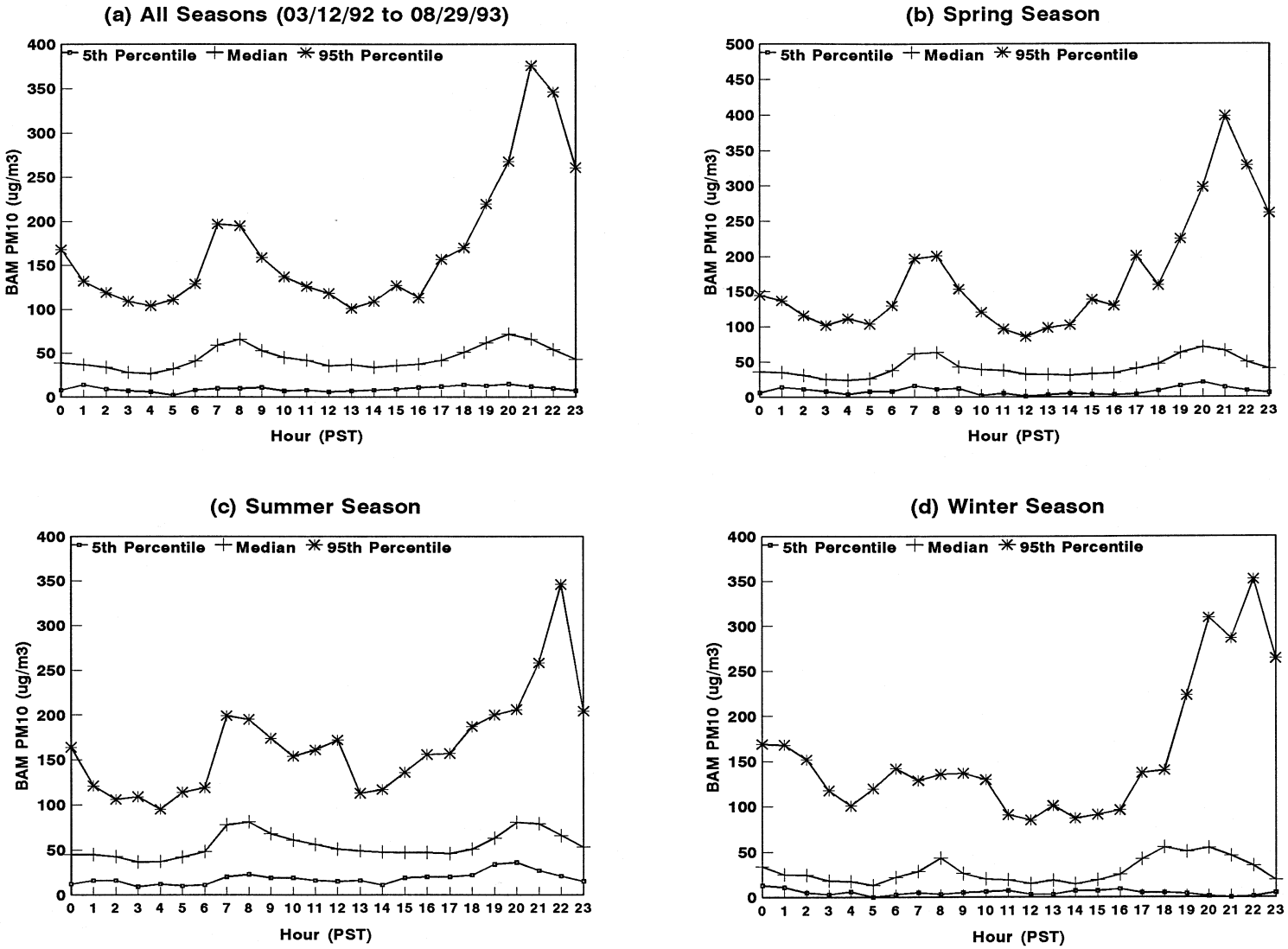

Figure 5-3. Diurnal variations of hourly BAM PM_{10} concentrations at a monitoring site in Calexico, CA, near the U.S./Mexico border during 03/12/92 to 08/29/93.

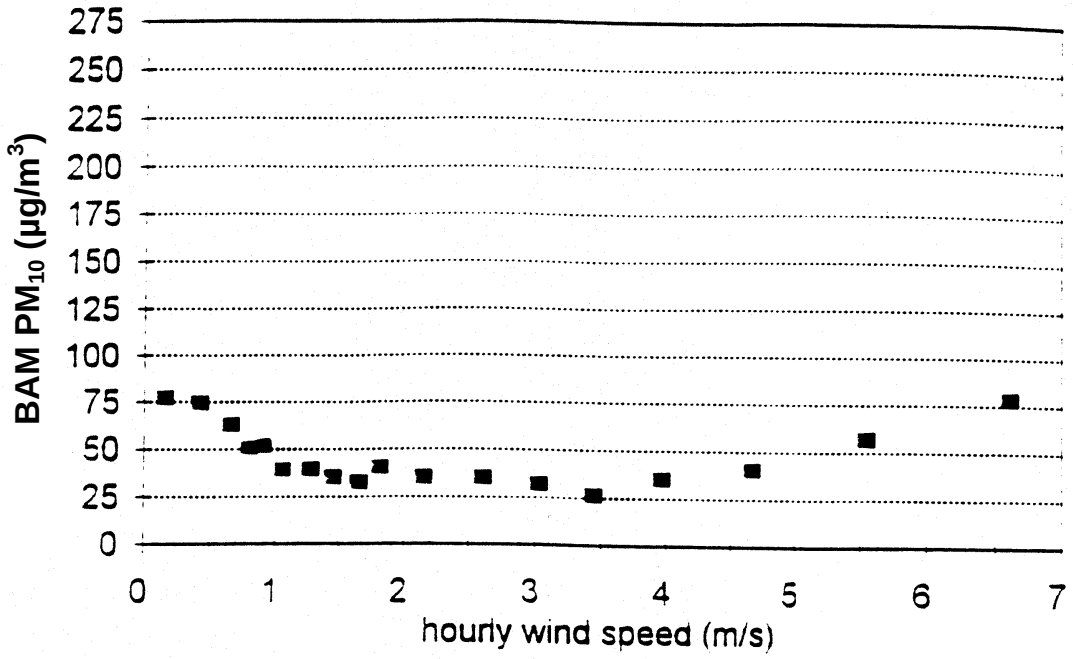

Figure 5-4. Relationships between BAM PM_{10} and wind speed for northerly flow.

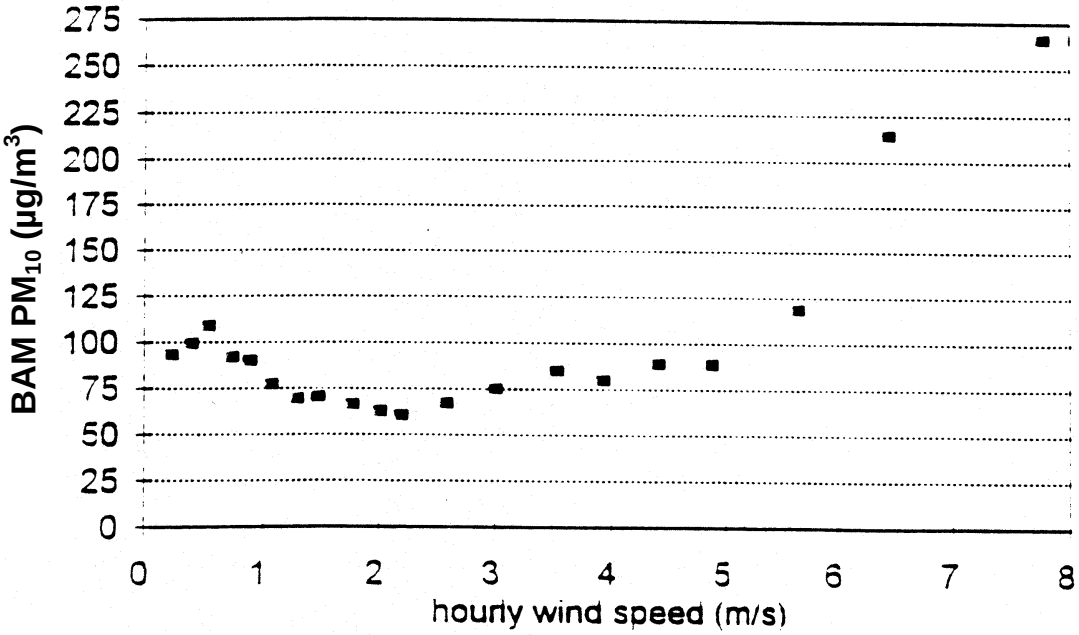

Figure 5-5. Relationships between BAM PM_{10} and wind speed for southerly flow.

compared to intermediate wind speeds. At low wind speeds, stagnation allows buildup of locally generated pollutants. As wind speed increases, increased transport and dispersion leads to lower concentrations. At yet higher wind speeds, especially above ~7 m/s, PM_{10} increases rapidly with increased wind speed due to resuspended dust.

A similar pattern between wind speed and PM_{10} concentrations is found in Las Vegas (Chow and Watson, 1997b), as shown in Figure 5-6. Concentrations are relatively high at very low wind speeds, reach a minimum at about 4 m/s, and begin increasing above ~6 m/s, with a sharp increase above 10 m/s.

Figure 5-7 shows the hour-by-hour relationship between PM_{10} and wind speed at a Las Vegas Valley site on a day with high PM_{10} concentrations. A rise in wind speed from 4 to 14 m/s is accompanied by an increase in PM_{10} from less than 50 $\mu g/m^3$ to over 1,000 $\mu g/m^3$ during an hour, clearly demonstrating the effect of increased wind speed on dust suspension. Figure 5-7 also shows that peak PM_{10} concentrations dropped rapidly even though wind speeds stayed high (>10 m/s) for several hours. This suggests that the "reservoir" of material available for suspension was largely depleted by the initial gusts (Chow and Watson, 1994).

Figure 5-8 shows similar variations with wind speed for data acquired at a southeastern Chicago (Eisenhower) site near Robbins, IL. At moderate wind speeds of 1.5 to 4 m/s, PM_{10} concentrations reach their lowest levels due to greater dispersion. When wind speeds exceed 7 m/s, PM_{10} concentrations increase due to wind-raised particulate matter. The third quarter reported higher PM_{10} levels because lower wind speeds were more frequent than during the other quarters. It appears that threshold suspension velocities may be ~2 m/s lower during the third quarter (summer) than during the other two quarters, possibly due to drier conditions that allow dust to be more easily suspended by wind.

5.3 Source Directionality

The Imperial Valley examples in Figures 5-4 and 5-5 (Chow and Watson, 1997a) demonstrate how continuous data can be coupled with wind direction measurements to determine transport fluxes. This will be an important use of continuous $PM_{2.5}$ at transport sites that are intended to determine the effect of one Metropolitan Planning Area (MPA) on other MPAs (Watson et al., 1997a). Cross-border fluxes of PM_{10} at the Calexico site are shown in Table 5-1. Mean fluxes were calculated by multiplying average wind speed with average PM_{10} concentration for each flow direction (U.S to Mexico and Mexico to U.S). For periods of flow from Mexico, cross-border fluxes were three times as large as for flows from the U.S. However, because flow was more frequently from the U.S., the total flux from Mexico was only about 45% higher than the total flux from the U.S.

Figure 5-9 shows PM_{10} concentrations at various percentiles as a function of wind direction for the Eisenhower site in southeastern Chicago, IL (Watson et al., 1997c). In the first calendar quarter of 1996, PM_{10} concentrations were highest for transport from the east and south, although directional differences were not pronounced. In the second calendar quarter of 1996, PM_{10} concentrations were highest with transport from the southwest and

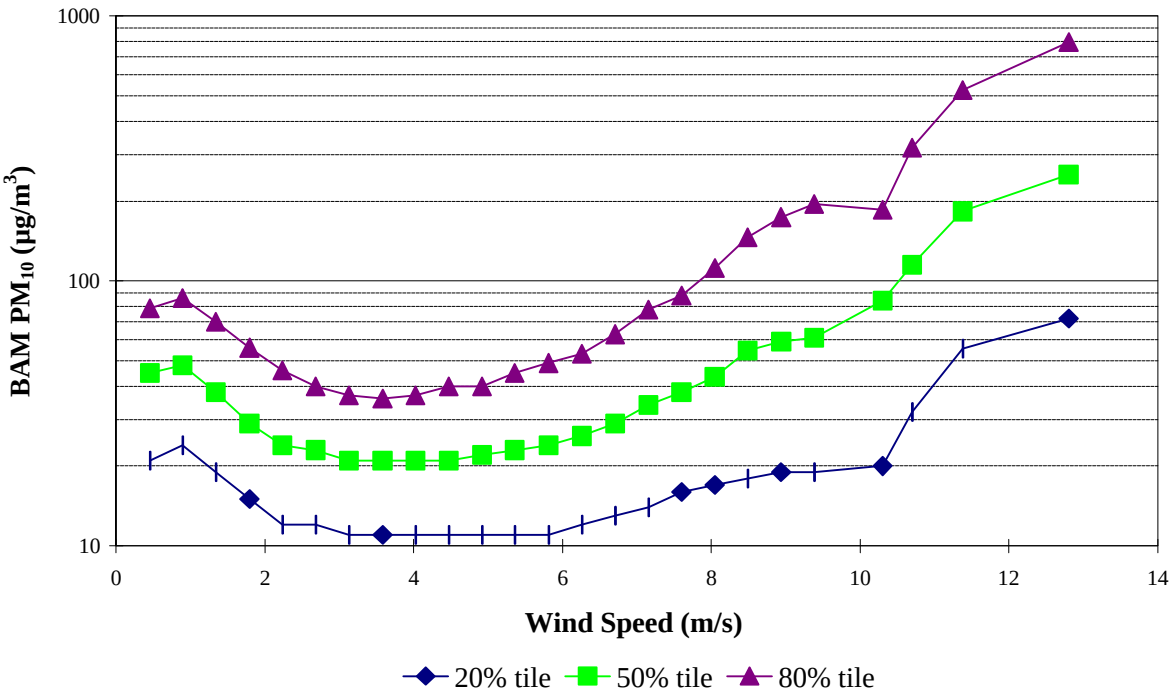

Figure 5-6. Distribution of hourly BAM PM_{10} as a function of wind speed at 14 meteorological sites in the Las Vegas Valley, NV, monitoring network between 01/01/95 and 01/31/96.

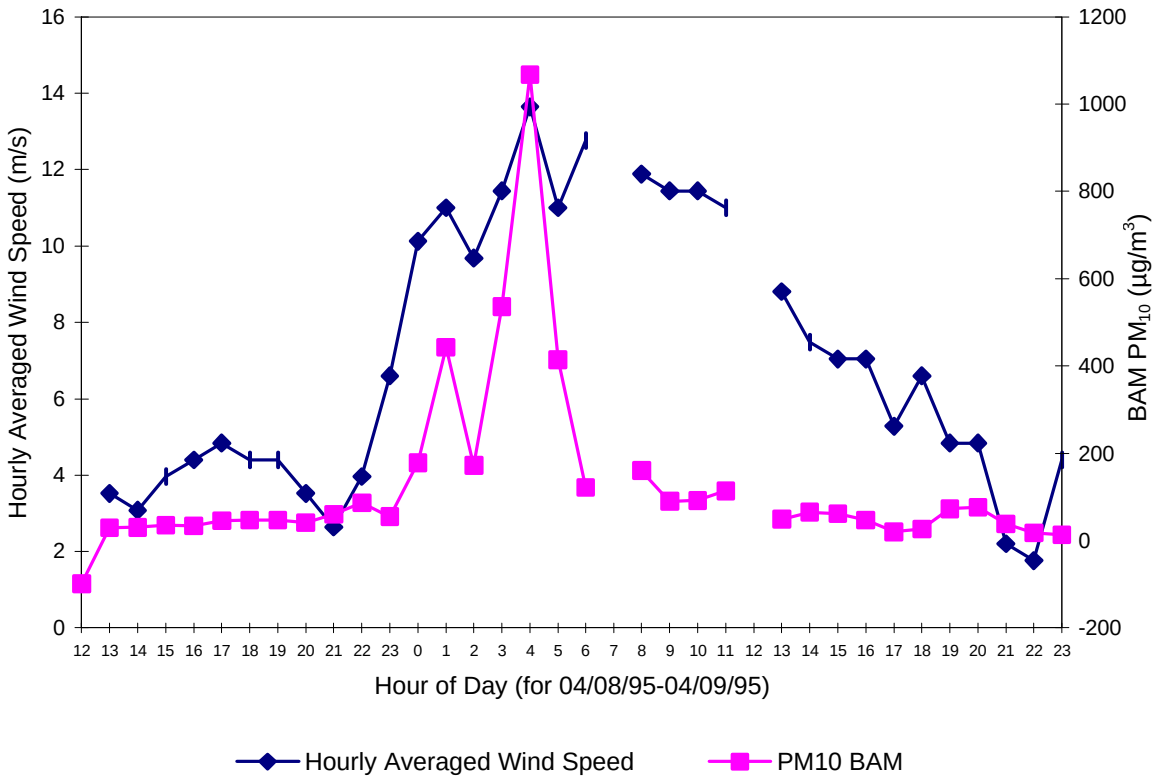

Figure 5-7. Relationship between hourly averaged wind speed and PM_{10} concentrations at a North Las Vegas, NV, site (Bemis) during the period of 04/08/95 to 04/09/95.

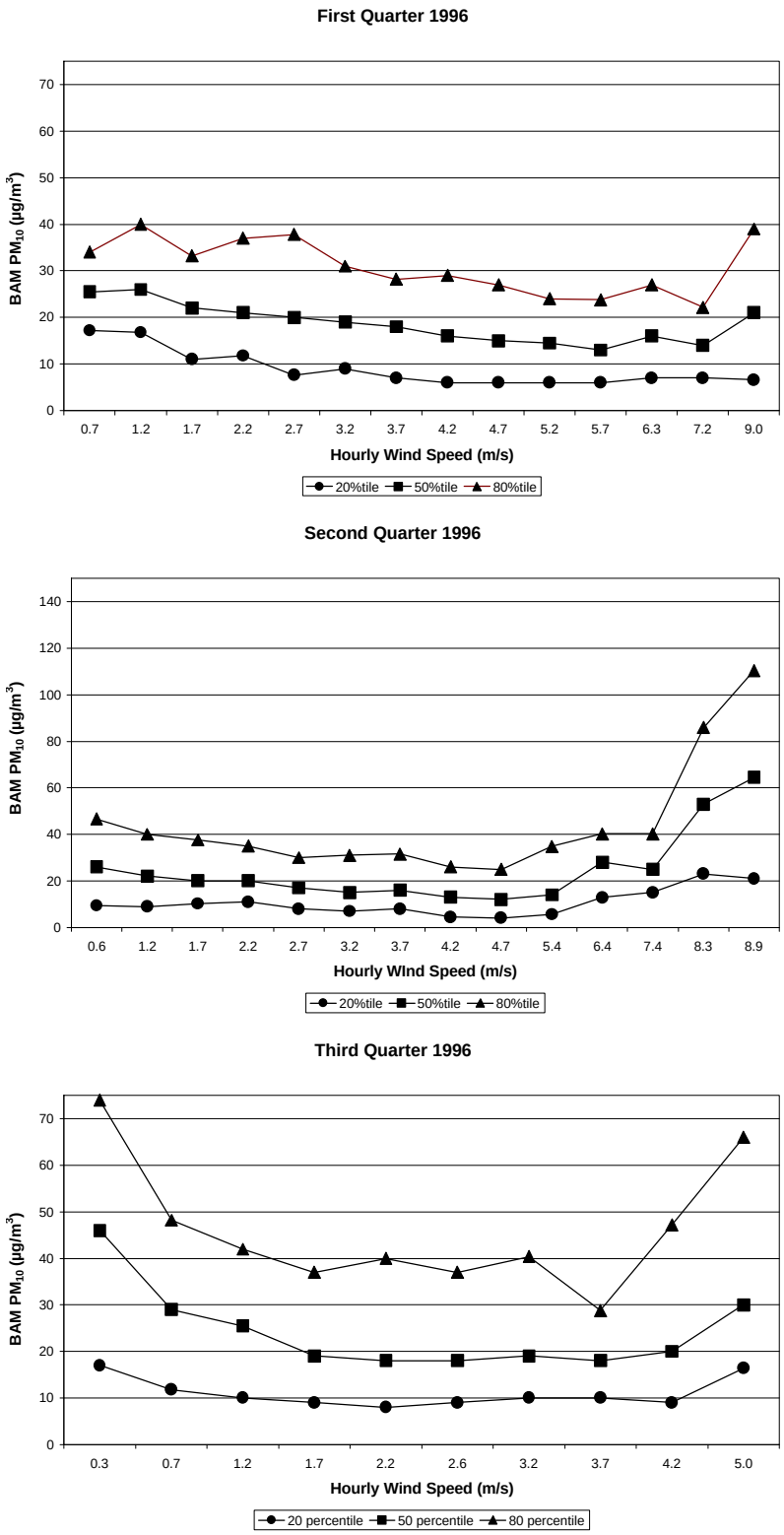

Figure 5-8. Distribution of hourly PM_{10} concentrations as a function of wind speed at a southeastern Chicago, IL, site (Eisenhower) during the first three quarters of 1996.

Table 5-1
Cross-Border Fluxes at the Calexico Site

	Northerly Flow (from the United States)	Southerly Flow (from Mexico)
Mean Flux	52 $\mu g/m^2$-s	156 $\mu g/m^2$-s
Total Flux (μg-hr/m^2-s)	213,367 μg-hr/m^2-s	308,430 μg-hr/m^2-s

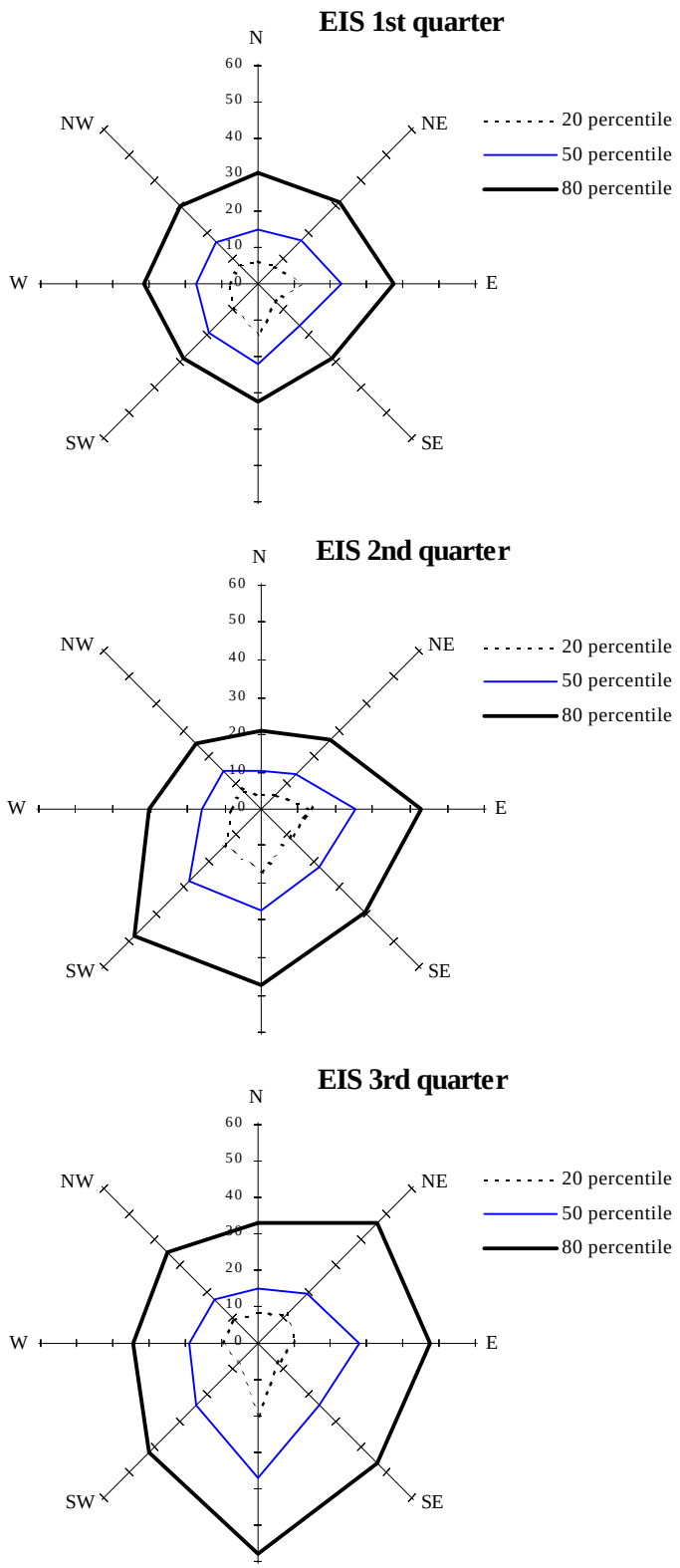

Figure 5-9. PM_{10} concentrations at the 20th, 50th, and 80th percentiles at a southeastern Chicago, IL, site (Eisenhower) during the first three quarters of 1996.

south, then from the east, and lowest for northerly transport. PM_{10} concentrations during the second quarter were higher than those from the first quarter in most directions except for the north. The third quarter exhibited the highest PM_{10} concentrations with transport from the south.

Table 5-2 shows how continuous particle measurements can be associated with wind direction and continuous precursor gas measurements, in this case sulfur dioxide (SO_2). Average wind speeds in each wind direction were highest in the first quarter and lowest in the third quarter. At the 50th percentile, PM_{10} concentrations during the third quarter of 1996 were 10 to 15 $\mu g/m^3$ higher than during the first two quarters of 1996. The higher PM_{10} concentrations in the third quarter are associated with lower wind speeds that limit dilution of local emissions.

Higher PM_{10} concentrations during the third quarter may also be due to more photochemically produced PM. Sulfate and some of the organic carbon components are derived from this photochemistry, and these may originate in emissions from other populated areas. Major population centers, as well as large sulfur dioxide emitters in the Ohio River Valley, are in the northeastern to southern direction with respect to northeastern Illinois. During all three quarters, average hourly SO_2 concentrations were highest when transport was from the south. The highest SO_2 values were observed with a narrow range of wind directions (about 200 degrees), which is precisely the direction of a nearby oil refinery.

When continuous particle chemistry measurements are available, even more specificity can be obtained from the correspondence between concentration and wind direction. Figure 5-10 shows the directionality of selected elemental concentrations determined from a streaker sampler at three southeastern Chicago sites along a north/south line of ~10 km length (the Meadowlane [MEA] site is ~1.5 km north of the Eisenhower [EIS] site, and the Breman [BRE] site is ~8 km south of the Eisenhower site). A large number of industrial sources are located between these sites, and even larger complexes are located to the east and northeast of the Robbins, IL, neighborhood.

Wind-sector averages of $PM_{2.5}$ aluminum (Al), silicon (Si), calcium (Ca), potassium (K), iron (Fe), manganese (Mn), lead (Pb), sulfur (S), zinc (Zn), chromium (Cr), calcium (Ca), and bromine (Br) are plotted in Figure 5-10. A marker on each axis in these figures represents the average concentration for the 45-degree sector from which the designated element originates. Similar directionality and magnitude for an element at all sites indicates transport from sources in that direction outside of the study domain. Lack of directionality at any site indicates a widespread area-type source. Large directionality and magnitude at a single site that is not observed at the other sites indicates a nearby emitter with a small (~<5 km) zone of influence. A high directionality in a northerly or southerly direction at some sites, but in the opposite direction at other sites, indicates a source within the domain between the sites. The source is probably closer to the site with the highest directional average. Each sector average is a combination of contributions from areawide, distant point, and nearby emitters. Contributions from sources near an individual site manifest themselves as larger concentration increments over those measured from the same wind direction at other sites.

Table 5-2
Distribution of Hourly PM_{10} and SO_2 Concentrations at Robbins, IL, as a Function of Wind Speed and Wind Direction

Wind Direction	Distribution of PM_{10} Concentrations ($\mu g/m^3$) 20th Percentile	50th Percentile	80th Percentile	Average Wind Speed (m/s)	Average PM_{10} ($\mu g/m^3$)	Average SO_2 (ppb)
First Quarter 1996						
N	6.2	15.0	30.0	3.9	20.1	1.3
NE	7.0	17.0	31.0	3.3	22.1	2.3
E	12.0	23.0	37.0	2.3	25.9	7.1
SE	7.0	16.0	29.0	3.1	19.7	6.7
S	14.0	22.0	32.0	3.8	25.7	15.1
SW	10.0	19.0	29.0	4.1	21.1	10.2
W	8.0	17.0	31.0	6.7	21.1	5.0
NW	7.0	16.0	30.0	3.5	19.0	4.7
Second Quarter 1996						
N	4.0	10.0	21.0	2.4	13.6	1.0
NE	6.0	13.0	26.0	2.2	19.3	1.5
E	13.6	25.0	42.4	2.2	30.3	5.8
SE	11.0	22.0	38.6	2.2	25.3	4.0
S	17.0	27.0	47.0	3.4	32.6	11.5
SW	13.4	27.0	48.0	4.0	33.9	5.9
W	8.0	16.0	30.0	3.4	20.2	2.1
NW	7.0	14.0	24.6	2.9	18.2	0.8
Third Quarter 1996						
N	8.4	15.0	32.6	1.8	23.3	3.7
NE	11.0	19.0	46.0	1.5	28.8	4.7
E	10.0	28.0	47.2	1.9	32.1	9.3
SE	8.0	24.0	46.4	1.6	29.2	5.1
S	20.0	36.5	57.4	2.3	40.6	10.3
SW	8.0	24.0	42.0	2.3	26.5	6.3
W	10.0	19.0	34.0	2.3	23.5	4.2
NW	9.0	17.0	35.0	1.9	22.8	3.7

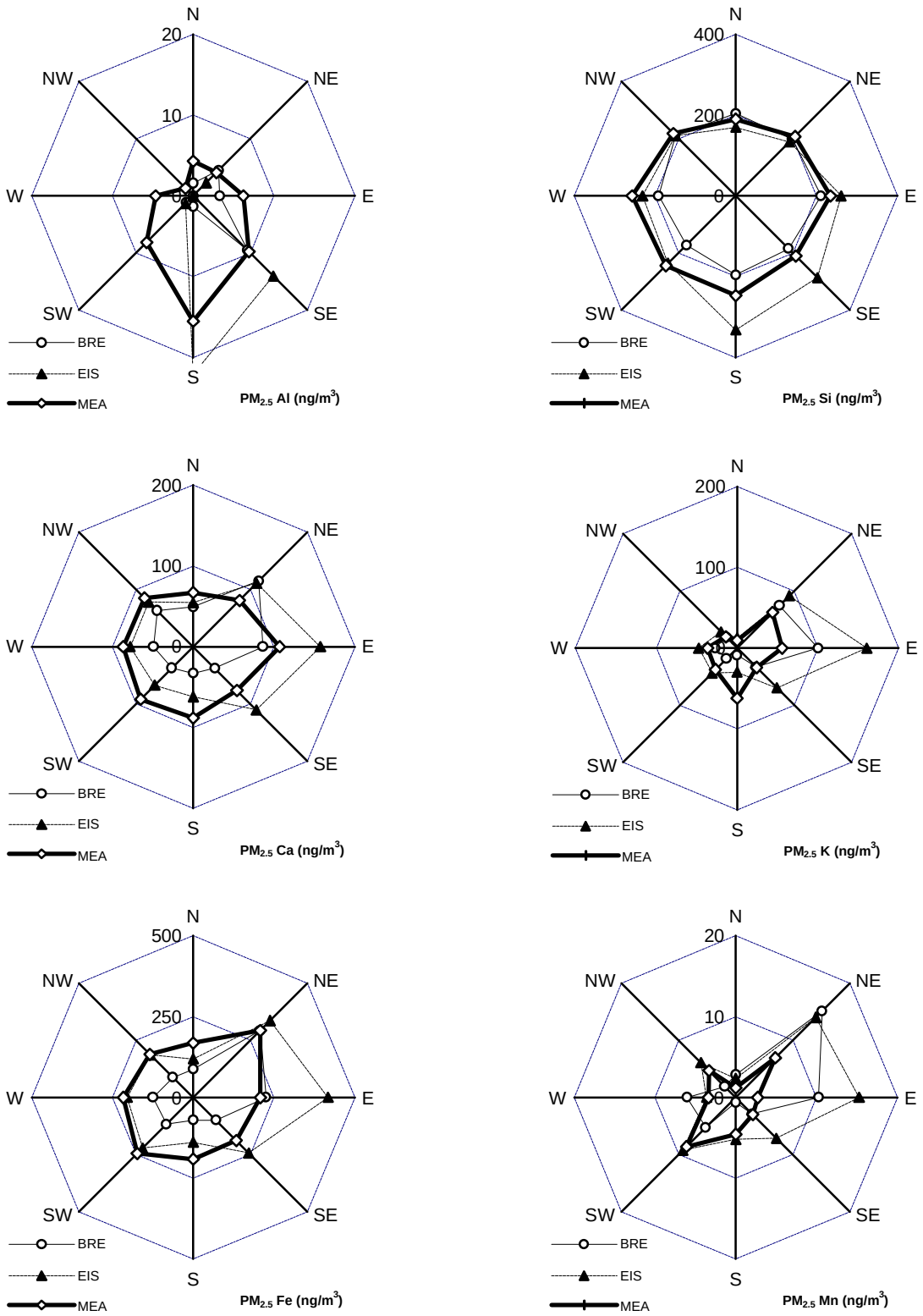

Figure 5-10. Hourly $PM_{2.5}$ elemental concentrations (ng/m^3) at three southeastern Chicago, IL, sites near Robbins, IL, averaged by wind sector for one week apiece during the first three calendar quarters of 1996.

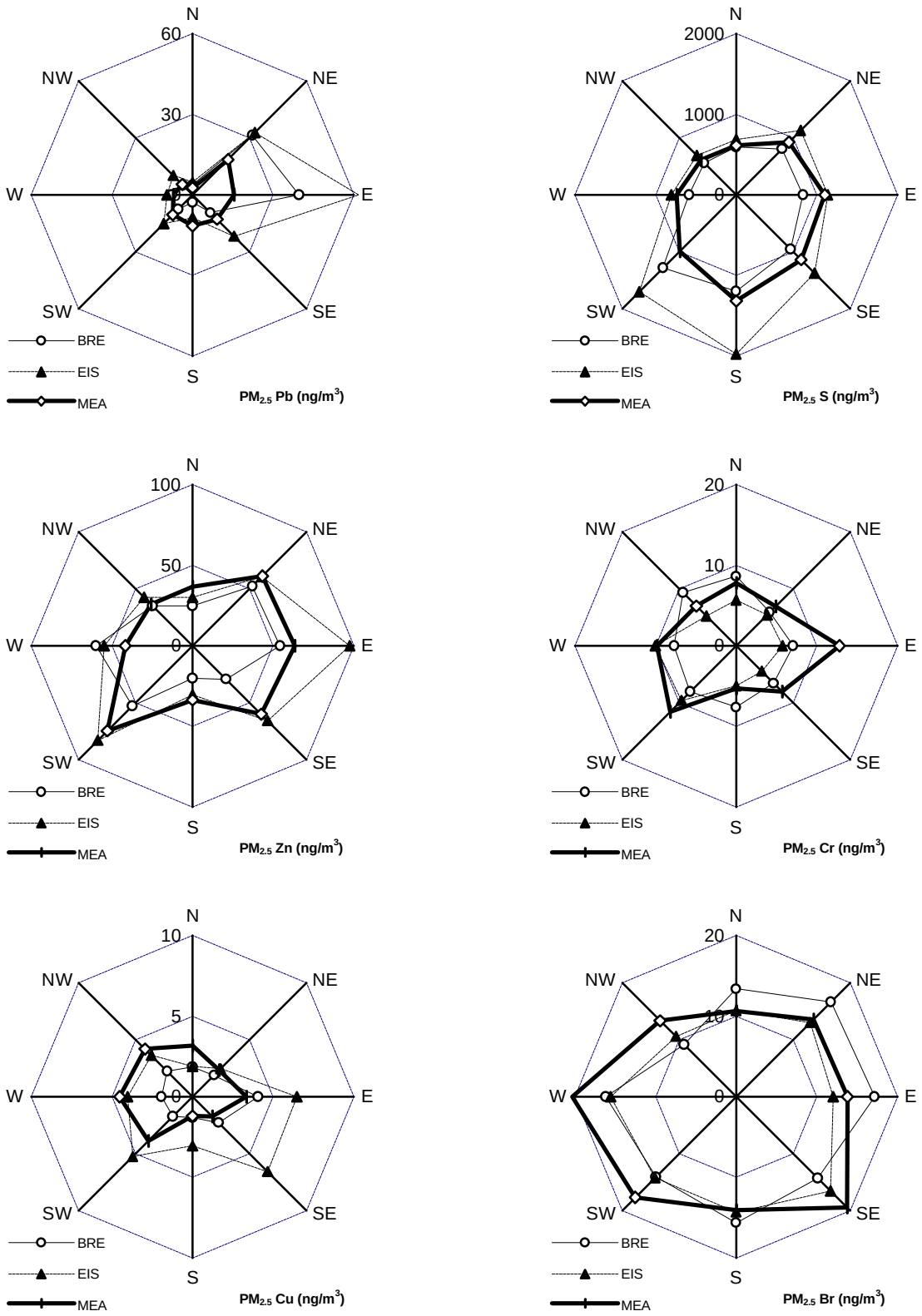

Figure 5-10. (continued)

Silicon (Si) is a good indicator for suspended road dust and windblown geological sources that are ubiquitous in most urban areas. The $PM_{2.5}$ Si homogeneity in all wind directions at the residential (Breman and Meadowlane) sites is consistent with an areawide source. This homogeneity also indicates that average dilution of emissions does not significantly differ as a function of wind direction. At the Eisenhower site, however, Si levels are slightly higher for the southern and southeastern directions, while $PM_{2.5}$ Si concentrations from remaining directions are comparable to those at the other sites. Even the Meadowlane site shows slightly higher Si levels from the south. This indicates a Si point source lying south of the Eisenhower and Meadowlane sites that is not south of the Breman site.

$PM_{2.5}$ aluminum (Al) concentrations show a distinct southerly source contributing to the Eisenhower and Meadowlane sites, but not to the Breman site. A slight southeasterly aluminum source affects the Breman location.

The Eisenhower site also shows higher particulate sulfur (S) concentrations deriving from the southern and southwestern directions that are not evident at the other two sites. For the most part, average particle sulfur concentrations are about twice as high from the northeastern to southeastern directions as they are from the remaining sectors, consistent with the locations of large sulfur emitters in the Midwest. The incremental particle sulfur measured at the Eisenhower site is most probably from a nearby oil refinery.

$PM_{2.5}$ calcium (Ca), potassium (K), iron (Fe), manganese (Mn), and lead (Pb) each have strong northeasterly to easterly components. A steel mill is located ~6 km to the east and there are other steel mills further to the northeast and east of the study network. Sector-averaged iron concentrations are comparable at the Breman and Meadowlane sites, as are the manganese concentrations, consistent with contributions from more distant Indiana sources. Large increments in iron and manganese concentrations at the Eisenhower site are consistent with contributions from a steel mill.

Lead (Pb) also appears to derive from distant and nearby sources to the east and northeast. Lead concentrations at the Meadowlane site represent contributions from the more distant sources. A nearby lead source to the east of Eisenhower affects that site and the Breman site, but not the Meadowlane site. The Eisenhower site also measures large incremental calcium and potassium concentrations in the eastern sector with respect to the other sites, while there is no indication of excessive calcium or other minerals from the southern sector at the Meadowlane site, even though stone cutting and polishing take place within 100 m south of the sampler.

Zinc (Zn), chromium (Cr), and copper (Cu) patterns are variable between the elements and the measurement locations. Concentrations are highest in the eastern, western, and southwestern sectors. There is a strong local copper influence to the southeast of the Eisenhower site that may originate from several nearby plating and metal handling industries. The common directionality for these metals at the different sites indicates that a major fraction of their contributions originate from sources outside of the study domain.

5.4 Receptor Zones of Representation and Source Zones of Representation

The directional analyses shown in Figure 5-10 demonstrates similarities and differences among nearby sites. The proximity of a pollution source can also be estimated from the width of a pulse received at a receptor. This is illustrated in Figure 5-11 for which five-minute average black carbon concentrations are plotted for a downtown site (MER) in Mexico City located on a single-story rooftop near a heavily traveled roadway and for a suburban residential site (PED) in Mexico City located in a schoolyard more than 200 m from a major highway. These sites are separated by ~15 km, typical of an urban-scale network.

The overall diurnal pattern represents a daily buildup starting at 0500 CST at the downtown (MER) site and at ~0800 CST at the suburban (PED) site. The concentrations become similar after the morning surface inversion breaks at ~1000 CST. The short-duration spikes at the downtown (MER) site are probably from passing trucks and buses that emit substantial quantities of black carbon.

Smaller spikes are evident at the suburban (PED) site, but they are not as prominent or as frequent as those detected at the downtown (MER) site. The integral of these spikes at the downtown (MER) site constitutes a substantial fraction of the 24-hour black carbon concentration. These could be filtered out of the time-resolved measurements to obtain a larger zone of representation of this site. Comparison of the 0500 to 1000 CST concentrations at the downtown (MER) and suburban (PED) sites shows that nearly half of the black carbon accumulates within the neighborhood surrounding the downtown (MER) site, probably owing to traffic emissions into a stable morning layer. Aside from the spikes at the downtown (MER) site, the black carbon measured at either site appears to represent black carbon concentrations over a large portion of Mexico City. This analysis indicates that when continuous monitors are operated and have sufficient sensitivity over short monitoring periods, they can acquire high-resolution measurements that allow a single site to quantify the superposition of particles from middle-scale, neighborhood-scale, and urban-scale particle influences.

5.5 Summary

The examples in the previous subsections show that continuous particle monitoring provides perspectives on particle concentrations that cannot be inferred from 24-hour average filter samplers. Hourly particle measurements elucidate the times of day when high and low concentrations occur, and these can often be related to emissions patterns, such as those from traffic, and to atmospheric mixing characteristics, such as the breakup of a morning inversion.

In addition to indicating the origins of particles, these diurnal cycles show those periods when people are most likely to be exposed to the highest and lowest PM concentrations. Relationships to changes in wind direction and wind speed help to locate source areas and to determine interactions between the atmosphere and emissions. This is especially important for intermittent sources, such as windblown dust, that are not well

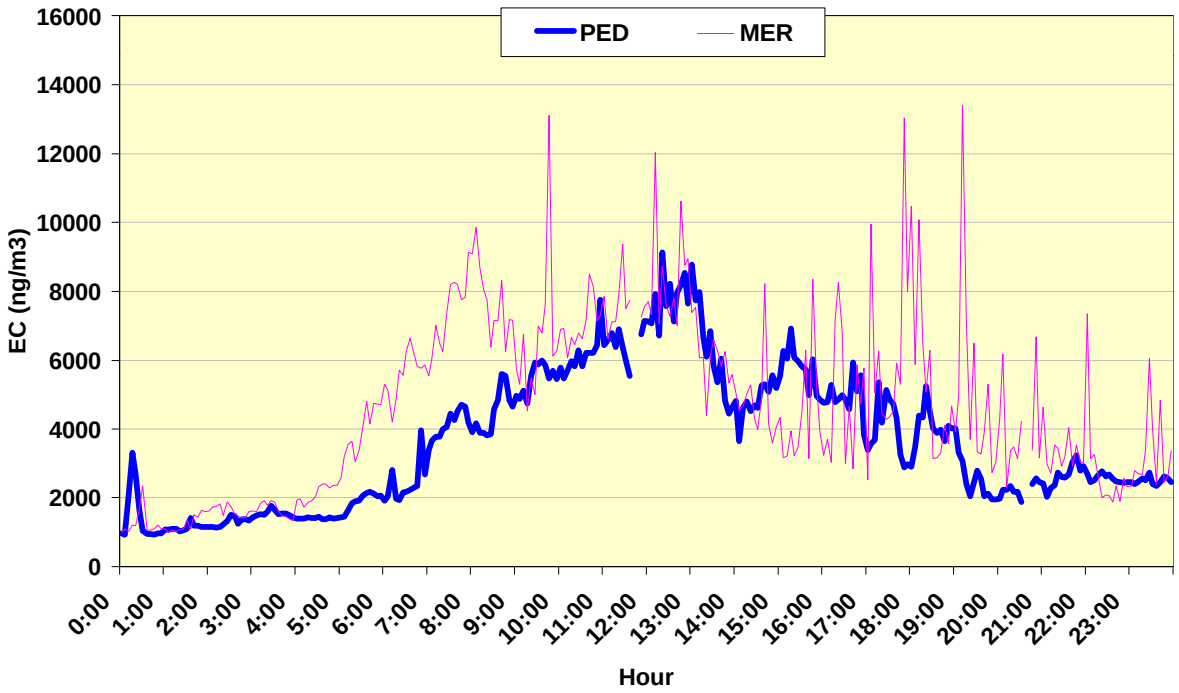

Figure 5-11. Five-minute-average aethalometer black carbon measurements at a downtown (MER) site and a suburban (PED) site in Mexico City. The short-term spikes correspond to contributions from very nearby sources, such as diesel exhaust plumes from trucks and buses.

represented in emissions inventories. With chemical-specific methods, more source specificity can be obtained. Very short averaging times (~5 minutes) allow estimates to be placed on contributions from nearby, local, or distant emitters from measurements at one or two sites. This information will be especially important for evaluating Community Monitoring Zones (CMZ) within which $PM_{2.5}$ concentrations may be averaged to determine compliance with the annual standard.

These examples show how measurements from widely used monitors can be used for fairly simple analyses. More complex combinations of instruments described in Section 3 will allow the science of particle formation and transport to be understood. Condensation nuclei counter (CNC), electrical aerosol analyzer (EAA), and differential mobility particle sizer (DMPS) monitors can quantify the ultrafine fraction that may be a future indicator of adverse health effects (Oberdorster et al., 1995).

Simultaneous continuous measurements of sulfate, nitrate, nitric acid, and ammonia will provide more accurate estimates of changes in equilibrium with changes in temperature and relative humidity than are currently possible with filter/denuder sampling and analysis. The time-width of nitrate, sulfate, sulfur dioxide, and oxides of nitrogen pulses will permit distant and nearby sources of secondary aerosol contributions to be distinguished from each other, similar to the example for primary carbon shown in Figure 5-11. This concept has been tested to some extent in recent $PM_{2.5}$ studies (Watson et al., 1996, 1998a), and shows large potential once the operation of these instruments is perfected.

As noted above, the examples given here should be considered illustrative, but not comprehensive. They show the potential of continuous particle monitors to address certain problems. Creative combinations of continuous measurements and data analysis methods are needed to address specific particle pollution issues.

6. CONTINUOUS PARTICLE MONITORING IN $PM_{2.5}$ NETWORKS

This section discusses how continuous particle measurements complement, and possibly substitute for, filter sampling in $PM_{2.5}$ networks. It examines the issues involved in designating Correlated Acceptable Continuous (CAC) monitors and specifies reasonable tests for a CAC monitor. CAC monitors are not required to attain FEM designation, but they should show comparability to FRM or FEM measurements in the monitored environment. The CAC monitor's predictability for $PM_{2.5}$ concentrations may be considered sufficient for certain situations, but traceability to $PM_{2.5}$ mass concentration standards is preferred.

6.1 $PM_{2.5}$ Network Site Types

CAC monitors are a subset of continuous particle monitors that are to be used at Community Representative (CORE) $PM_{2.5}$ monitoring sites. These CORE sites are located where people live, work, and play rather than at the expected maximum impact point for specific source emissions. CORE sites are used to determine NAAQS compliance for both annual and 24-hour $PM_{2.5}$ standards within a Community Monitoring Zone (CMZ), the spatial zone of representation of the site. $PM_{2.5}$ concentrations may be spatially averaged among several sites within a CMZ when the annual average $PM_{2.5}$ at each Core site is within ±20% of the spatial average on a yearly basis.

CORE sites have a zone of representation of at least neighborhood scale (> 0.5 km). For a neighborhood scale, this means that the 24-hour concentrations should vary by no more than ±10% within an area whose diameter is between 0.5 and 4 km. For urban scale, the concentrations would be similar for distances greater than 4 km. In some monitoring areas, a site with a smaller spatially representative scale (microscale [~100 m] or middle scale [a few hundred m]) may represent many such small scale sites in the general area.

At least two CORE sites in each metropolitan area with more than 500,000 people are required to sample every day with Federal Reference Method (FRM) or Federal Equivalent Method (FEM) samplers. The regulations allow sampling frequency to be reduced to once in three days if the sampler is collocated with a continuous analyzer whose measurements are correlated with those of the FRM. A continuous monitor can be used as a CAC monitor for this purpose when the FRM $PM_{2.5}$ is predicable from the CAC measurements.

Hot spot sites do not represent community-oriented monitoring and would be located near an emitter with a microscale or middle-scale zone of influence. Data from population-oriented hot spot sites would only be compared to the 24-hour standard. Everyday sampling is not specifically required at hot spot locations. CAC monitors will not be routinely operated at hot spot $PM_{2.5}$ sites.

Special Purpose Monitors (SPM) may be used to understand the nature and causes of excessive concentrations measured at core or hot spot compliance monitoring sites. Any or all of the continuous particle measurement methods described in Section 3, or ones that may be invented in the future, qualify as SPMs as long as they contributes to knowledge about the nature, sources, and/or health effects of suspended particles. SPM sites do not need to use FRMs, FEMs, or CACs. They do not necessarily need to show comparability or

predictability of $PM_{2.5}$ mass concentrations, though they must have sufficient accuracy, precision, validity, and reliability to meet special purpose monitoring objectives. SPMs may be operated over short periods of time at different locations, and they can be discontinued within their first two years of operation without prejudice when monitoring purposes have been achieved.

6.2 Federal Reference and Equivalent Methods

The Federal Reference Method (FRM) specifies sampler design, performance characteristics, operational requirements, and quality assurance applicable to the $PM_{2.5}$ FRM in 40 CFR part 50, Appendix L; 40 CFR part 53, Subpart E; and 40 CFR part 58, Appendices A and C. $PM_{2.5}$ FRMs are intended to acquire deposits over 24-hour periods on Teflon-membrane filters from air drawn at a controlled flow rate through the WINS (Well Impactor Ninety Six) $PM_{2.5}$ inlet. The inlet and size separation components, filter types, filter cassettes, and internal configurations of the filter holder assemblies are specified by design, with drawings and manufacturing tolerances published in 40 CFR part 53 (U.S. EPA, 1997b).

Other sampler components and procedures, such as flow rate control, operator interface controls, exterior housing, data acquisition) are specified by performance characteristics, with specific test methods to assess that performance. Chow and Watson (1998a) provide more detail on FRM and equivalent filter sampling systems.

Design specifications of the FRM samplers include a modified SA-246 PM_{10} inlet that has previously been wind tunnel tested and approved for PM_{10} compliance monitoring. The inlet cover has been extended by 2.5 inches and bent 45° downward to minimize water penetration during rainstorms. Sample air enters the inlet and is drawn through the WINS inlet that removes particles with aerodynamic diameters greater than 2.5 µm by impacting them on the bottom of an open-topped aluminum cylindrical container.

Impacted particles are trapped at the bottom of the well on an oil-impregnated filter (35 to 37 mm borosilicate glass-fiber) impregnated with a low vapor-pressure oil (tetramethyl tetraphenyltrisiloxane, maximum vapor pressure 2×10^{-8} mm Hg, density 1.06 to 1.07 g/cm^3, 32 to 40 centistoke viscosity at 25 °C). More than 50% of the particles with aerodynamic diameters less than 2.5 µm follow the air flow through the WINS, which turns up and out of the well and is directed back down to a Teflon-membrane filter where the particles are removed by filtration. Internal surfaces exposed to sample air prior to the Teflon-membrane filter are treated electrolytically in a sulfuric acid bath to produce a clear, uniformly anodized coating (at least 1.08 mg/cm^2 in accordance with military standard specifications).

CAC monitors should be adapted, to the greatest extent possible, to comply with these inlet characteristics so that the size fraction they measure is equivalent to that measured by the FRM. This may not always be possible, owing to differences in flow rate and sample configuration. In this case, other inlets that have been demonstrated as equivalent (as described below) should receive first preference.

FRM performance specifications require constant volumetric flow rates (16.67 ± 0.83 L/min) to be monitored and recorded continuously with temperature and pressure of the sample air entering the inlet and near the filter. FRMs are required to maintain the temperature of the filter during and after sampling within ±5 °C of concurrent ambient temperatures regardless of heating and cooling from direct sun or shade during and after sampling. This specification intends to minimize losses from volatile particles such as ammonium nitrate and some organic compounds. Potential FRM designs use active ventilation of the enclosure that surrounds the filter holder and WINS impactor to attain these temperature performance specifications.

FRMs from different manufacturers may vary in appearance, but their principles of operation and resulting $PM_{2.5}$ mass measurements should be the same within reasonable measurement precisions. Though they may follow the published design specifications, $PM_{2.5}$ samplers are not FRMs until they have demonstrated attainment of the published specifications (U.S. EPA, 1997b) and assigned an FRM number published in the Federal Register.

As stated in Section 1, Federal Equivalent Methods (FEMs) are divided into several classes in order to encourage innovation and provide monitoring flexibility. This is especially important for continuous particle monitors, as it provides a means for them to be accepted as CAC monitors, or even as FEMs.

Class I FEMs meet nearly all FRM specifications, with minor design changes that permit sequential sampling without operator intervention and different filter media in parallel or in series. Flow rate, inlets, and temperature requirements are identical for FRMs and Class I FEMs. Particles losses in flow diversion tubes are to be quantified and must be in compliance with Class I FEM tolerances specified in 40 CFR part 53, Subpart E.

Class II FEMs include samplers that acquire 24-hour integrated filter deposits for gravimetric analysis, but that differ substantially in design from the reference-method instruments. These might include dichotomous samplers, and high-volume samplers with $PM_{2.5}$ size-selective inlets. More extensive performance testing is required for Class II FEMs than for FRMs or Class I FEMs, as described in 40 CFR part 53, Subpart F. Key requirements for Class I and Class II FEM equivalence tests are summarized in Table 4-1.

Class III FEMs include samplers that do not qualify as Class I or Class II FEMS. This category is intended to encourage the development of and to evaluate new monitoring technologies that increase the specificity of $PM_{2.5}$ measurements or decrease the costs of acquiring a large number of measurements. Class III FEMs may either be filter-based integrated samplers or filter- or non-filter-based *in-situ* continuous or semi-continuous samplers, including many of those described in Section 3. Test procedures and performance requirements for Class III candidate instruments will be determined on a case-by-case basis. Performance criteria for Class III FEMs will be the most restrictive, because equivalency to reference methods must be demonstrated over a wide range of particle size distributions and aerosol compositions.

FEM applications require the following:

- A detailed description of measurement principles and procedures, manufacturer's name, model number, schematic diagrams of components, design drawings, and apparatus description;
- A comprehensive instrument manual documenting operational, maintenance, and calibration procedures;
- A statement of the method, analyzer, or sampler being tested; and
- A description of quality systems that will be utilized as well as the durability characteristics of the sampler.

Candidate sampler inlets differing from those already tested are to be evaluated in a wind tunnel test at wind speeds of 2 and 24 km/hr for monodisperse aerosol between 1.5 ± 0.25 µm and 4.0 ± 0.5 µm. In addition, tests for inlet aspiration, static fractionation, loading, and volatility are also specified in 40 CFR part 53, Subpart F, as procedures to test performance characteristics of Class II equivalent method for $PM_{2.5}$.

Requirements for $PM_{2.5}$ Class III FEMs have not been specified owing to ". . . the wide range of non-filter-based measurement technologies that could be applied and the likelihood that these requirements will have to be specifically adapted for each such type of technology. Specific requirements will be developed as needed and may include selected requirements from Subpart C, E, or F as described for Class II FEM . . ." (U.S. EPA, 1997b).

6.3 Potential Tolerances for FEM and CAC Monitor Designation

Given the comparison results shown in Section 4, Class III FEM designation will be difficult to attain for all sampling sites and monitoring periods likely to be encountered in $PM_{2.5}$ monitoring networks. The specifications in Table 4-1 should be attained for Class III FEMs, but the types of measurement environments needs to be more than two. These environments should include: 1) stable, non-hygroscopic aerosol in low relative humidity, such as that found in summertime Las Vegas, NV or Phoenix, AZ; 2) stable, hygroscopic aerosol in moderate to high relative humidity, such as that found in summertime Birmingham, AL or Chicago, IL; 3) unstable, hygroscopic aerosol, under variable humidity, such as that found in wintertime Fresno, CA or Washington D.C.; 4) unstable, non-hygroscopic aerosol, such as that found in wood-smoke-dominated environments such as Medford, OR, or Mammoth Lakes, CA; and 5) a complex photochemical environment with a combination of stable and unstable aerosol within and outside of a moist marine layer, such as that found during early fall in Riverside, CA.

Aerosol volatility and liquid water sampling are the major impediments for FEM designation of continuous particulate monitors. Until methods are perfected to compensate for these interferences, such as equilibrating the sampled air stream to conditions comparable to those of the FRM filter equilibration, continuous particle monitors will not be universally equivalent to filter-based measurements. A filter/gravimetric $PM_{2.5}$ mass fraction has been

established as the NAAQS, and continuous FEMs must be equivalent, within acceptable bounds, to these concentrations as operationally defined by an FRM.

It is also evident from the comparisons in Section 4 and from other published comparisons (e.g. Husar and Falke, 1996) that reasonable $PM_{2.5}$ estimates can be obtained from certain continuous particle monitors, and that these monitors can be used as CAC monitors. The main criteria selecting a CAC monitor should be: 1) measurement precision; 2) correlation with FRMs and FEMs; 3) consistency of relationships with FRMs; and 4) frequency of deviation. The performance measures applied in Section 4 address each of these issues.

With respect to measurement precision, CAC monitors, cannot be expected to compare with FRMs or FEMs better than collocated $PM_{2.5}$ FRM monitors. Several $PM_{2.5}$ samplers using the WINS and other $PM_{2.5}$ inlets were collocated in a variety of environments from November 1996 through May 1997 (Pitchford et al., 1997) and demonstrated collocated precisions of ~0.5 to 1.0 $\mu g/m^3$ among the WINS samplers. A reasonable lower bound on collocated precision is, therefore, ±1 $\mu g/m^3$.

As an upper limit, the annual $PM_{2.5}$ NAAQS allow measurements at a single site in a Community Monitoring Zone to deviate from the spatial average of Core sites within that zone by up to 20%. For $PM_{2.5}$ concentrations near the annual standard of 15 $\mu g/m^3$, this is a maximum difference of ±3 $\mu g/m^3$. This tolerance is not as stringent as the tolerances for collocated samplers because annual averages can be quite similar even though specific samples in those averages may be markedly different.

A precision requirement for collocated CAC monitors should be between these extremes. Table 4-1 allows a collocated precision of ±2 $\mu g/m^3$ for Class I or Class II FEMs, and this (or its equivalent) should be retained as precision requirement for collocated CAC monitors.

CAC monitors are intended to be used alongside FRMs or FEMs, so sufficient data sets will be acquired from $PM_{2.5}$ networks to evaluate correlations between their output and 24-hour $PM_{2.5}$ concentrations in a variety of environments. Table 4-1 specifies 0.97 as the correlation coefficient required for FEM status. This is intended for specialized testing under controlled conditions. Section 4 demonstrates that a correlation coefficient in excess of 0.90 is probably more realistic for routine operating conditions. This is more consistent with correlation coefficients found for collocated PM_{10} samplers.

The linear relationship between CAC monitor output and collocated FRMs or FEMs needs to be consistent, although Section 4 shows that this relationship may differ for different environments. The 1.0 ±0.05 slope requirement in Table 4-1 will probably not be attained by potential CAC monitors that are not calibrated or traceable to $PM_{2.5}$ mass. The ±5% standard error on the slope that is attained should be retained for the environments to which the relationship is to apply. Similarly the 0±1 $\mu g/m^3$ intercept is not applicable to all potential CAC monitors, but its $\mu g/m^3$ equivalent should be.

CAC monitors can be used to reduce FRM monitoring frequencies after sufficient daily data have been acquired to establish their $PM_{2.5}$ comparability or predictability at a CORE sites. The initial reduction could be from every day to every third day. In some cases, FRM sampling might be less frequent, possibly every sixth day, during spring and summer in the California's San Joaquin Valley when the arid climate and non-volatile aerosol allow TEOM and BAM measurements to approximate filter $PM_{2.5}$ samples.

In areas that are shown to have low humidities and low abundances of volatile aerosol throughout the year, such as Las Vegas, NV, and California's Imperial Valley, CAC monitors might be shown to meet the FEM requirements all of the time and could completely replace filter/gravimetric samplers. This might also be found in certain parts of the midwestern and eastern U.S., such as Robbins, IL, where the sulfate aerosol is stable, and heating of the sampled airstream to evaporate liquid water will not necessarily volatilize significant fractions of the $PM_{2.5}$. It is more likely, however, that the Class III FEM designation will be reserved for monitors that meet Class II FEM requirements for a large number of environments.

7. REFERENCES

Abbas, R. and Tanner, R.L. (1981). Continuous determination of gaseous ammonia in the ambient atmosphere using fluorescence derivatization. *Atmos.Environ.* **15:**277-81.

Adams, K.M. (1989). Real-time *in situ* measurements of atmospheric optical absorption in the visible via photoacoustic spectroscopy I: Evaluation of photoacoustic cells. *Appl.Opt.* **27:**4052-6.

Adams, K.M., Davis, L.I., Jr., Japar, S.M., Pierson, W.R. (1989). Real time, *in situ* measurements of atmospheric optical absorption in the visible via photoacoustic spectroscopy - II. Validation for atmospheric elemental carbon aerosol. *Atmos.Environ.* **23:**693-700.

Adams, K.M., Davis, L.I., Jr., Japar, S.M., Finley, D.R., Cary, R.A. (1990a). Measurement of atmospheric elemental carbon: Real-time data for Los Angeles during summer 1987. *Atmos.Environ.* **24A:**597-604.

Adams, K.M., Davis, L.I., Jr., Japar, S.M., Finley, D.R. (1990b). Real-time *in situ* measurements of atmospheric optical absorption in the visibile via photoacoustic spectroscopy - IV. Visibility degradation and aerosol optical properties in Los Angeles. *Atmos.Environ.* **24A:**605-10.

Agarwal, J.K. and Sem, G.J. (1980). Continuous flow, single-particle-counting condensation nucleus counter. *J.Aerosol Sci.* **11:**343-57.

Ahlquist, N.C. and Charlson, R.J. (1967). A new instrument for evaluating the visual quality of air. *JAPCA* **17:**467-9.

Ahlquist, N.C. and Charlson, R.J. (1969). Measurement of the wavelength dependence of atmospheric extinction due to scatter. *Atmos.Environ.* **3:**551-64.

Ahn, K.H. and Liu, B.Y.H. (1990). Particle activation and droplet growth processes in condensation nucleus counter I. Theoretical background. *J.Aerosol Sci.* **21:**263-76.

Aldén, M., Edner, H., Svanberg, S. (1982). Laser monitoring of atmospheric NO using ultraviolet differential-absorption techniques. *Opt.Lett.* **7:**543-5.

Allen, A.G., Harrison, R.M., Erisman, J.W. (1989). Field measurements of the dissociation of ammonium nitrate and ammonium chloride aerosols. *Atmos.Environ.* **23:**1591-9.

Allen, G.A., Turner, W.A., Wolfeson, J.M., Spengler, J.D. (1984). Description of a continuous sulfuric acid sulfate monitor. *4th Annual National Symposium; Recent Advances in Pollutant Monitoring of Ambient Air and Stationary Sources, Raleigh, NC, 1984,* Raleigh,NC.

Allen, A.G. and Miguel, A.H. (1995). Biomass burning in the Amazon: Characterization of the ionic component of aerosols generated from flaming and smouldering rainforest and savannah. *Environ.Sci.Technol.* **29:**486-93.

Allen, G.A., Sioutas, C., Koutrakis, P., Reiss, R., Lurmann, F.W., Roberts, P.T. (1997). Evaluation of the TEOM method for measurement of ambient particulate mass in urban areas. *JAWMA* **47:**682-9.

Alofs, D.J. and Balakumar, P. (1982). Inversion to obtain aerosol size distributions from measurements with a differential mobility analyzer. *J.Aerosol Sci.* **13:**513-27.

Alvarez, R.J.Jr., Caldwell, L.M., Li, Y.H., Krueger, D.A., She, C.Y. (1990). High-spectral resolution lidar measurement of tropospheric backscatter ratio using barium atomic blocking filters. *J.Atmos.Oceanic Technol.* **7:**876-81.

Ananth, G. and Wilson, J.C. (1988). Theoretical analysis of the performance of the TSI aerodynamic particle sizer. *Aerosol Sci.Technol.* **9:**189-99.

Ancellet, G., Megie, G., Pelon, J., Capitini, R., Renaut, D. (1987). Lidar measurements of sulfur dioxide and ozone in the boundary layer during the 1983 Fos Berre campaign. *Atmos.Environ.* **21:**2215-26.

Ancellet, G., Papayannis, A., Pelon, J., Megie, G. (1989). DIAL tropospheric ozone measurement using a Nd:YAG laser and the Raman shifting technique. *J.Atmos.Oceanic Technol.* **6:**832-9.

Anderson, T.L., Covert, D.S., Marshall, S.F., Laucks, M.L., Charlson, R.J., Waggoner, A.P., Ogren, J.A., Caldow, R., Holm, R.L., Quant, F.R., Sem, G.J., Wiedensohler, A., Ahlquist, N.C., Bates, T.S. (1996). Performance characteristics of a high-sensitivity, three-wavelength, total scatter/backscatter nephelometer. *J.Atmos.Oceanic Technol.* **13:**967-86.

Anderson, T.L. and Ogren, J.A. Determining aerosol radiative properties using the TSI 3563 integrating nephelometer. [In Press] Aerosol Sci.Technol. (1998).

Anlauf, K.G., Fellin, P., Wiebe, H.A., Schiff, H.I., Mackay, G.I., Braman, R.S., Gilbert, R. (1985). A comparison of three methods for measurements of atmospheric nitric acid and aerosol nitrate and ammonium. *Atmos.Environ.* **19:**325-33.

Anlauf, K.G., MacTavish, D.C., Wiebe, H.A., Schiff, H.I., Mackay, G.I. (1988). Measurements of atmospheric nitric acid by the filter method and comparison with the tuneable diode laser and other methods. *Atmos.Environ.* **22:**1579-86.

Annegarn, H.J., Zucchiatti, A., Cereda, E., Braga Marcazzan, G.M. (1990). Source profiles by unique ratios (SPUR) analysis: interpretation of time-sequence PIXE aerosol data. In *Nuclear Instruments and Methods in Physics Research,* Elsevier Science, Amsterdam. p. 372-5.

Ansmann, A., Riebesell, M., Wandinger, U., Weitkamp, C., Voss, E., Lahmann, W., Michaelis, W. (1992). Combined raman elastic-backscatter lidar for vertical profiling of moisture, aerosol extinction, backscatter, and lidar ratio. *Appl.Phys.* **B55:**18-28.

Appel, B.R., Tokiwa, Y., Kothny, E.L., Wu, R., Povard, V. (1988). Evaluation of procedures for measuring atmospheric nitric acid and ammonia. *Atmos.Environ.* **22:**1565-73.

Arnold, S.H., Hague, W., Pierce, G., Sheetz, R. (1992). The use of beta gauge monitors for PSI and every day SIP monitoring - An overview of the Denver experience. In *Transactions: PM_{10} Standards and Nontraditional Particulate Source Controls,* Chow, J.C. and Ono, D.M., editors. AWMA, Pittsburgh, PA. p. 13-23.

Arnott, W.P., Moosmüller, H., Abbott, R.E., Ossofsky, M.D. (1995). Thermoacoustic enhancement of photoacoustic spectroscopy: theory and measurements of the signal to noise ratio. *Rev.Sci.Instrum.* **66:**4827-33.

Arnott, W.P., Moosmüller, H., Rogers, C.F., Jin, T., Bruch, R. Photoacoustic spectrometer for measuring light absorption by aerosol: instrument description. [In Press] Atmos.Environ. (1998).

ASTM (1985). Standard method of test for particulate matter in the atmosphere: optical density of filtered deposit. In *ASTM Methods,* American Society for Testing Materials, Philadelphia, PA. p. 1704-78.

Babich, P., Wang, P.Y., Sioutas, C., Koutrakis, P. (1997). Continuous Ambient Mass Monitor (CAMM). *Emerging Air Issues for the 21st Century: The Need for Multidisciplinary Management,* Calgary,Alberta.

Ball, D.J. and Hume, R. (1977). The relative importance of vehicular and domestic emissions of dark smoke in greater London in the mid-1970's, the significance of smoke shade measurements, and an explanation of the relationship of smoke shade to gravimetric measurements of particulate. *Atmos.Environ.* **11:**1065-73.

Barber, P.W. and Hill, S.C. (1990). *Light Scattering by Particles: Computational Methods.* World Scientific Publishing Co., Teaneck, NJ.

Barnes, R.A. (1973). Duplicate measurements of low concentrations of smoke and sulphur dioxide using two "National Survey" samplers with a common inlet. *Atmos.Environ.* **7:**901-4.

Baron, P.A. (1986). Calibration and use of aerodynamic particle sizer (APS 3300). *Aerosol Sci.Technol.* **5:**55-67.

Baron, P.A., Mazumder, M.K., Cheng, Y.S. (1993). Direct-reading techniques using optical particle detection. In *Aerosol Measurement: Principles, Techniques and Applications,* Willeke, K. and Baron, P.A., editors. Van Nostrand Reinhold, New York,NY. p. 381-409.

Bartz, H., Fissan, H., Helsper, C., Kousaka, Y., Okuyama, K., Fukushima, N., Keady, P.B., Kerrigan, S., Fruin, S.A., McMurry, P.H., Pui, D.Y.H., Stolzenburg, M.R. (1985). Response characterization for four different condensation nucleus counters to particles in the 3-50 nm diameter range. *J.Aerosol Sci.* **16:**443-56.

Bauman, S.E., Houmere, P.D., Nelson, J.W. (1987). Local events in atmospheric aerosol concentrations. In *Nuclear Instruments and Methods in Physics Research,* Elsevier Science, Amsterdam. p. 322-4.

Beniston, M., Wolf, J.P., Beniston-Rebetez, M., Kölsch, H.J., Rairoux, P., Wöste, L. (1990). Use of lidar measurements and numerical models in air pollution research. *J.Geophys.Res.* **95:**9879-94.

Benner, R.L. and Stedman, D.H. (1989). Universal sulfur detection by chemiluminescence. *Analytical Chemistry* **61:**1268-71.

Benner, R.L. and Stedman, D.H. (1990). Field evaluation of the sulfur chemiluminescence detector. *Environ.Sci.Technol.* **24:**1592-6.

Berkson, J. (1950). Are there two regression? *J.Am.Stat.Assoc.* **45:**164-80.

Beuttell, R.G. and Brewer, A.W. (1949). Instruments for the measurement of the visual range. *J.Sci.Instrum.* **26:**357-9.

Bhardwaja, P.S., Charlson, R.J., Waggoner, A.P., Ahlquist, N.C. (1973). Rayleigh scattering coefficients of freon-12, freon-22, and CO_2 relative to that of air. *Appl.Opt.* **12:**135-6.

Bhardwaja, P.S., Herbert, J., Charlson, R.J. (1974). Refractive index of atmospheric particulate matter: an *in situ* method for determination. *Appl.Opt.* **13:**731-4.

Biermann, H.W., Tuazon, E.C., Winer, A.M., Wallington, T.J., Pitts, J.N., Jr. (1988). Simultaneous absolute measurements of gaseous nitrogen species in urban ambient air by long pathlength infrared and ultraviolet-visible spectrocsopy. *Atmos.Environ.* 1541-4.

Bijnen, F.G.C., Dongen, J.v., Reuss, J., Harren, F.J.M. (1996). Thermoacoustic amplification of photoacoustic signal. *Rev.Sci.Instrum.* **67:**2317-24.

Birmili, W., Stratmann, F., Wiedensohler, A., Covert, D., Russell, L.M., Berg, O. (1997). Determination of differential mobility analyzer transfer functions using identical instruments in series. *Aerosol Sci.Technol.* **27:**215-23.

Bodhaine, B.A. (1979). Measurement of the Rayleigh scattering properties of some gases with a nephelometer. *Appl.Opt.* **18:**121-5.

Bodhaine, B.A., Ahlquist, N.C., Schnell, R.C. (1991). Three-wavelength nephelometer suitable for aircraft measurement of background aerosol scattering coefficient. *Atmos.Environ.* **25A:**2267-76.

Bond, T.C., Charlson, R.J., Heintzenberg, J. (1998). Quantifying the emission of light-absorbing particles: measurements tailored to climate studies. *Geophysical Research Letters* **25:**337-40.

Borho, K. (1970). A scattered-light measuring instrument for high dust concentrations. *Staub-Reinhaltl.Luft* **30:**45-9.

Bowers, W.D. and Chuan, R.L. (1989). Surface acoustic-wave piezoelectric crystal aerosol mass monitor. *Rev.Sci.Instrum.* **60:**1297-302.

Braman, R.S., Shelley, T.J., McClenny, W.A. (1982). Tungstic acid for preconcentration and determination of gaseous and particulate ammonia and nitric acid in ambient air. *Analytical Chemistry* **54:**358-64.

Breitenbach, L.P. and Shelef, M. (1973). Development of a method for the analysis of NO_2 and NH_3 by NO-measuring instruments. *JAPCA* **23:**128-31.

Bricard, J., Delattre, P., Madelaine, G., Pourprix, M. (1976). Detection of ultra-fine particles by means of a continuous flux condensation nuclei counter. In *Fine Particles,* Liu, B.Y.H., editor. Academic Press, New York. p. 566-80.

Brimblecombe, P. (1987). *The Big Smoke: A History of Air Pollution in London since Medieval Times.* Methuen, London.

Brockmann, J.E., Yamano, N., Lucero, D. (1988). Calibration of the aerodynamic particle sizer 3310 (APS-3310) with polystyrene latex monodisperse spheres and oleic acid monodisperse particles. *Aerosol Sci.Technol.* **8:**279-81.

Brockmann, J.E. and Rader, D.J. (1990). APS response to nonspherical particles and experimental determination of dynamic shape factor. *Aerosol Sci.Technol.* **13:**162-72.

Browell, E.V. (1982). Lidar measurements of tropospheric gases. *Opt.Eng.* **21:**128-32.

Browell, E.V., Carter, A.F., Shipley, S.T., Allen, R.J., Butler, C.F., Mayo, M.N., Siviter, J.H., Jr., Hall, W.M. (1983). NASA multipurpose airborne DIAL system and measurements of ozone and aerosol profiles. *Appl.Opt.* **22:**522-34.

Bruce, C.W. and Pinnick, R.G. (1977). *In-situ* measurements of aerosol absorption with a resonant CW laser spectrophone. *Appl.Opt.* **16:**1762-5.

Buettner, H. (1990). Measurement of the size distribution of fine nonspherical particles with a light-scattering particle counter. *Aerosol Sci.Technol.* **12:**413-21.

Burkhardt, M.R., Buhr, M.P., Ray, J.D., Stedman, D.H. (1988). A continuous monitor for nitric acid. *Atmos.Environ.* **22:**1575-8.

Camp, D.C., Stevens, R.K., Cobourn, W.G., Husar, R.B., Collins, J.F., Huntzicker, J.J., Husar, J.D., Jaklevic, J.M., McKenzie, R.L., Tanner, R.L., Tesch, J.W. (1982). Intercomparison of concentration results from fine particle sulfur monitors. *Atmos.Environ.* **16:**911-6.

Campbell, D.S., Copeland, S., Cahill, T.A. (1995). Measurement of aerosol absorption coefficient from Teflon filters using integrating plate and integrating sphere techniques. *Aerosol Sci.Technol.* **22:**287-92.

Campbell, D.S. and Cahill, C. (1996). Response to "Comment on measurement of aerosol coefficient from Teflon filters using integrating plate and integrating sphere techniques" by D. Campbell, S. Copeland, and T. Cahill. *Aerosol Sci.Technol.* **24:**225-9.

Carson, P.G., Neubauer, K.R., Johnston, M.V., Wexler, A.S. (1995). On-line chemical analysis of aerosols by rapid single-particle mass spectrometry. *Aerosol Sci.Technol.* **26:**535-45.

Carson, P.G., Johnston, M.V., Wexler, A.S. (1997). Real-time monitoring of the surface and total composition of aerosol particles. *Aerosol Sci.Technol.* **26:**291-300.

Charlson, R.J., Horvath, H., Pueschel, R.F. (1967). The direct measurement of atmospheric light scattering coefficient for studies of visibility and pollution. *Atmos.Environ.* **1:**469-78.

Charlson, R.J., Ahlquist, N.C., Horvath, H. (1968). On the generality of correlation of atmospheric aerosol mass concentration and light scatter. *Atmos.Environ.* **2:**455-64.

Charlson, R.J., Ahlquist, N.C., Selvidge, H., MacCready, P.B. (1969). Monitoring of atmospheric aerosol parameters with the integrating nephelometer. *JAPCA* **19:**937-42.

Charlson, R.J., Vanderpol, A.H., Covert, D.S., Waggoner, A.R., Ahlquist, N.C. (1974a). $H_2SO_4/(NH_4)_2SO_4$ background aerosol: optical detection in St. Louis region. *Atmos.Environ.* **8:**1257-67.

Charlson, R.J., Vanderpol, A.H., Covert, D.S., Waggoner, A.P., Ahlquist, N.C. (1974b). Sulfuric acid-ammonium sulfate aerosol: optical detection in the St. Louis region. *Science* **184:**156-8.

Chen, B.T., Cheng, Y.S., Yeh, H.C. (1984). Experimental response of two optical particle counters. *J.Aerosol Sci.* **15:**457-64.

Chen, B.T., Cheng, Y.S., Yeh, H.C. (1985). Performance of a TSI aerodynamic particle sizer. *Aerosol Sci.Technol.* **4:**89-97.

Chen, B.T. and Crow, D.J. (1986). Use of an aerodynamic particle sizer as a real-time monitor in generation of ideal solid aerosols. *J.Aerosol Sci.* **17:**963-72.

Chen, B.T., Yeh, H.C., Cheng, Y.S. (1986). Performance of a modified virtual impactor. *Aerosol Sci.Technol.* **5:**369-76.

Chen, B.T., Cheng, Y.S., Yeh, H.C. (1990). A study of density effect and droplet deformation in the TSI aerodynamic particle sizer. *Aerosol Sci.Technol.* **12:**278-85.

Cheng, Y.S., Chen, B.T., Yeh, H.C. (1990). Behaviour of isometric nonspherical aerosol particles in the aerodynamic particle sizer. *J.Aerosol Sci.* **21:**701-10.

Cheng, Y.S. (1993). Condensation detection and diffusion size separation techniques. In *Aerosol Measurement: Principles,Techniques and Applications,* Willeke, K. and Baron, P.A., editors. Van Nostran Reinhold, New York,NY. p. 427-48.

Cheng, Y.S., Chen, B.T., Yeh, H.C., Marshall, I.A., Mitchell, J.P., Griffiths, W.D. (1993). Behaviour of compact nonspherical aerosol particles in the TSI aerodynamic particle sizer model APS33B: ultra-stokesian drag forces. *Aerosol Sci.Technol.* **19:**255-67.

Chow, J.C., Watson, J.G., Lowenthal, D.H., Solomon, P.A., Magliano, K.L., Ziman, S.D., Richards, L.W. (1992a). PM_{10} source apportionment in California's San Joaquin Valley. *Atmos.Environ.* **26A:**3335-54.

Chow, J.C., Liu, C.S., Cassmassi, J.C., Watson, J.G., Lu, Z., Pritchett, L.C. (1992b). A neighborhood-scale study of PM_{10} source contributions in Rubidoux, California. *Atmos.Environ.* **26A:**693-706.

Chow, J.C. and Watson, J.G. (1992). Fugitive emissions add to air pollution. *Environ.Protect.* **3:**26-31.

Chow, J.C., Watson, J.G., Pritchett, L.C., Pierson, W.R., Frazier, C.A., Purcell, R.G. (1993a). The DRI Thermal/Optical Reflectance Carbon Analysis System: Description, evaluation and applications in U.S. air quality studies. *Atmos.Environ.* **27A:**1185-202.

Chow, J.C., Watson, J.G., Lowenthal, D.H., Solomon, P.A., Magliano, K.L., Zinman, S.D., Richards, L.W. (1993b). PM_{10} and $PM_{2.5}$ compositions in California's San Joaquin Valley. *Aerosol Sci.Technol.* **18:**105-28.

Chow, J.C., Watson, J.G., Bowen, J.L., Gertler, A.W., Frazier, C.A., Fung, K.K., Ashbaugh, L.L. (1993c). A sampling system for reactive species in the western U.S. Winegar, E., editor. American Chemical Society, Washington, DC. p. 209-28.

Chow, J.C. and Watson, J.G. (1994). Guidelines for PM_{10} sampling and analysis applicable to receptor modeling. Report No. EPA-452/R-94-009**,** U.S. EPA, Research Triangle Park, NC.

Chow, J.C., Fujita, E.M., Watson, J.G., Lu, Z., Lawson, D.R., Ashbaugh, L.L. (1994a). Evaluation of filter-based aerosol measurements during the 1987 Southern California Air Quality Study. *Environmental Monitoring and Assessment* **30:**49-80.

Chow, J.C., Watson, J.G., Fujita, E.M., Lu, Z., Lawson, D.R., Ashbaugh, L.L. (1994b). Temporal and spatial variations of $PM_{2.5}$ and PM_{10} aerosol in the Southern California Air Quality Study. *Atmos.Environ.* **28:**2061-80.

Chow, J.C., Watson, J.G., Houck, J.E., Pritchett, L.C., Rogers, C.F., Frazier, C.A., Egami, R.T., Ball, B.M. (1994c). A laboratory resuspension chamber to measure fugitive dust size distributions and chemical compositions. *Atmos.Environ.* **28:**3463-81.

Chow, J.C. (1995). Critical review: Measurement methods to determine compliance with ambient air quality standards for suspended particles. *JAWMA* **45:**320-82.

Chow, J.C., Watson, J.G., Lu, Z., Lowenthal, D.H., Frazier, C.A., Solomon, P.A., Thuillier, R.H., Magliano, K.L. (1996). Descriptive analysis of $PM_{2.5}$ and PM_{10} at regionally representative locations during SJVAQS/AUSPEX. *Atmos.Environ.* **30:**2079-112.

Chow, J.C. and Watson, J.G. (1997a). Imperial Valley/Mexicali Cross Border PM_{10} Transport Study. Report No. 4692.1D1**,** Desert Research Institute, Reno, NV.

Chow, J.C. and Watson, J.G. (1997b). Fugitive dust and other source contributions to PM_{10} in Nevada's Las Vegas Valley. Report No. DRI Document No. 4039.1F**,** Desert Research Institute, Reno, NV. Prepared for Clark County Department of Comprehensive Planning, Las Vegas, NV.

Chow, J.C. and Egami, R.T. (1997). San Joaquin Valley Integrated Monitoring Study: Documentation, evaluation, and descriptive analysis of PM and PM, and precursor gas measurements - Technical Support Studies No. 4 and No. 8 - Final report. Desert Research Institute, Reno, NV. Prepared for California Regional Particulate Air Quality Study, California Air Resources Board, Sacramento, CA.

Chow, J.C. and Watson, J.G. (1998a). Guideline on speciated particulate monitoring. Desert Research Institute, Reno, NV. Prepared for U.S. EPA, Research Triangle Park, NC.

Chow, J.C. and Watson, J.G. (1998b). Ion chromatography. In *Elemental Analysis of Airborne Particles,* Landsberger, S. and Creatchman, M., editors. Gordon and Breach, Newark.

Chow, J.C., Watson, J.G., Lowenthal, D.H., Egami, R.T., Hackney, R., Magliano, K.L. (1998a). Temporal variations of PM_{10}, $PM_{2.5}$ and gaseous precursors during the Integrated Monitoring Study in Central California. [In Press] JAWMA

Chow, J.C., Zielinska, B., Watson, J.G., Fujita, E.M., Richards, H.W., Neff, W., Dietrich, D., Hering, S. (1998b). Northern Front Range Air Quality Study. Volume A: Ambient Measurements. Desert Research Institute, Reno, NV. Prepared for Colorado State University, Cooperative Institute for Research in the Atmosphere, Fort Collins, CO.

Clarke, A.D. (1982a). Effects of filter internal reflection coefficient on light absorption measurements using the integrating plate method. *Appl.Opt.* **21:**3021-31.

Clarke, A.D. (1982b). Integrating sandwich: a new method of measurement of the light absorption coefficient for atmospheric particles. *Appl.Opt.* **21:**3011-20.

Clarke, A.D., Ogre, J., Charlson, R. (1996). Comment on "Measurement of aerosol absorption coefficient from Teflon filters using the integrating plate and integrating sphere techniques" by D. Campbell, S. Copeland, and T. Cahill. *Aerosol Sci.Technol.* **24:**221-4.

Cobourn, W.G., Husar, R.B., Husar, J.D. (1978). Continuous *in situ* monitoring of ambient particulate sulfur using flame photometry and thermal analysis. *Atmos.Environ.* **12:**89-98.

Cooney, J. (1975). Normalization of elastic lidar returns by use of Raman Rotational Backscatter. *Appl.Opt.* **14:**270-1.

Cooper, D.W. (1975). Statistical errors in beta absorption measurements of particulate mass concentration. *JAPCA* **25:**1154-5.

Cooper, D.W. (1976). Significant relationships concerning exponential transmission or penetration. *JAPCA* **26:**366-7.

Courtney, W.J., Shaw, R.W., Dzubay, T.G. (1982). Precision and accuracy of a beta-gauge for aerosol mass determination. *Environ.Sci.Technol.* **16:**236-8.

Covert, D.S., Charlson, R.J., Ahlquist, N.C. (1972). A study of the relationship of chemical composition and humidity to light scattering by aerosols. *J.Appl.Meteorol.* **11:**968-76.

Dagnall, R.M., Thompson, K.C., West, T.S. (1967). Molecular emission in cool flames I. *Analyst* **92:**506-12.

de Jonge, C.N., Bergwerff, J.B., Swart Using DIAL to measure freeway traffic NO_2 emissions. Technica Optical Society of America. (1991). 18**:** 250-252. Washington, D.C.

Dixon, J.K. (1940). The absorption coefficient of nitrogen dioxide in the visible spectrum. *J.Chem.Phys.* **8:**157-60.

Doyle, G.J., Tuazon, E.C., Graham, R.A., Mischke, T.M., Winer, A.M., Pitts, J.N. (1979). Simultaneous concentrations of ammonia and nitric acid in a polluted atmosphere and their equilibrium relationship to particulate ammonium nitrate. *Environ.Sci.Technol.* **13:**1416-9.

Durham, J.L., Wilson, W.E., Bailey, E.B. (1978). Application of an SO_2 denuder for continuous measurement of sulfur in submicrometric aerosols. *Atmos.Environ.* **12:**883-6.

Edlen, B. (1953). The dispersion of standard air. *J.Opt.Soc.Am.* **43:**339-44.

Edner, H., Sunesson, A., Svanberg, S. (1988). NO plume mapping by laser-radar techniques. *Opt.Lett.* **13:**704-6.

Edwards, J.D., Ogren, J.A., Weiss, R.E., Charlson, R.J. (1984). Particulate air pollutants: a comparison of British `Smoke' with optical absorption coefficients and elemental carbon concentration. *Atmos.Environ.* **17:**2337-41.

Eldering, A., Cass, G.R., Moon, K.C. (1994). An air monitoring network using continuous particle size distribution monitors: connecting pollutant properties to visibility via Mie scattering calculations. *Atmos.Environ.* **28:**2733-50.

Endo, Y., Fukushima, N., Tashiro, S., Kousaka, Y. (1997). Performance of a scanning differential mobility analyzer. *Aerosol Sci.Technol.* **26:**43-50.

Ensor, D.S. and Waggoner, A.P. (1970). Angular truncation error in the integrating nephelometer. *Atmos.Environ.* **4:**481-7.

Ensor, D.S., Charlson, R.J., Ahlquist, N.C., Whitby, K.T., Husar, R.B., Liu, B.Y.H. (1972). Multi-wavelength nephelometer measurements in Los Angeles smog aerosol I: Comparison of calculated and measured light scattering. *J.Colloid Interface Sci.* **39:**240-51.

Evans, K.D., Melfi, S.H., Ferrare, R.A., Whiteman, D.N. (1997). Upper tropospheric temperature measurements with the use of a Raman lidar. *Appl.Opt.* **36:**2594-602.

Fabiny, L. (1998). Sensing rogue particles with optical scattering. *Opt.Photon.News* **9:**34-8.

Fairchild, C.I. and Wheat, L.D. (1984). Calibration and evaluation of a real-time cascade impactor. *Am.Indus.Hyg.Assoc.J.* **45:**205-11.

Farwell, S.O. and Rasmussen, R.A. (1976). Limitations of the FPD and ECD in atmospheric analysis: a review. *J.Chromatogr.Sci.* **14:**224-34.

Fehsenfeld, F.C., Dickerson, R.R., Hübler, G., Luke, W.T., Nunnermacker, L., Williams, E.J., Roberts, J.M., Calvert, J.G., Curran, C.M., Delany, A.C., Eubank, C.S., Fahey, D.W., Fried, A., Gandrud, B.W., Langford, A.O., et al. (1987). A ground-based intercomparison of NO, NO_x, NO_y measurement techniques. *J.Geophys.Res.* **92:**14710-22.

Fehsenfeld, F.C., Drummond, J.W., Roychowdhury, U.K., Galvin, P.J., Williams, E.J., Buhr, M.P., Parrish, D.D., Hübler, G., Langford, A.O., Calvert, J.G., Ridley, B.A., Grahek, F., Heikes, B.G., Kok, G.L., Shetter, J.D., et al. (1990). Intercomparison of NO_2 measurement techniques. *J.Geophys.Res.* **95:**3579-97.

Fehsenfeld, F.C., Huey, L.G., Sueper, D.T., Norton, R.B., Williams, E.J., Eisele, F.L., Mauldin, R.L., III, Tanner, D.J. (1998). Ground-based intercomparison of nitric acid measurement techniques. *J.Geophys.Res.* **103:**3343-54.

Fernald, F.G., Herman, B.M., Reagan, J.A. (1972). Determination of aerosol height distributions by lidar. *J.Appl.Meteorol.* **11:**482-9.

Finlay, W.H., Stapleton, K.W., Zuberbuhler, P. (1997). Fine particle fraction as a measure of mass depositing in the lung during inhalation of nearly isotonic nebulized aerosols. *Journal of Aerosol Science* **28:**1301-10.

Fiocco, G., Benedetti-Michelangeli, G., Maischberger, K., Madonna, E. (1971). Measurement of temperature and aerosol to molecule ratio in the troposphere by optical radar. *Nature Phys.Science* **229:**78-9.

Fischer, K. (1973). Mass absorption coefficients of natural aerosol particles in the 0.4 to 2.4 μm wavelength interval. *Contrib.Atmos.Phys.* **46:**89-100.

Fissan, H.J., Helsper, C., Thielen, H.J. (1983). Determination of particle size distributions by means of an electrostatic classifier. *J.Aerosol Sci.* **14:**354-7.

Force, A.P., Killinger, D.K., Defeo, W.E., Menyuk, N. (1985). Laser remote sensing of ammonia using a CO_2 lidar system. *Appl.Opt.* **24:**2837-41.

Fox, D.L., Stockburger, J., Weathers, W., Spicer, C.W., Mackay, G.I., Schiff, H.I., Eatough, D.J., Mortensen, F., Hansen, L.D., Shepson, P.B., Kleindienst, T.E., Edney, E.O. (1988). Intercomparison of nitric acid diffusion denuder methods with tunable diode laser absorption spectroscopy. *Atmos.Environ.* **22:**575-85.

Fuchs, N.A. (1964). *Mechanics of Aerosols.* Pergamon Press, New York, NY.

Fussell, W.B. (1974). Approximate theory of the integrating sphere. Report No. 594-7**,** National Bureau of Standards, Gaithersburg, MD.

Galle, B., Sunesson, A., Wendt, W. (1988). NO_2 mapping using laser-radar techniques. *Atmos.Environ.* **22:**569-73.

Gard, E.E., Mayer, J.E., Prather, K.A. (1997). Real-time analysis of individual atmospheric particles: design and performance of a portable ATOFMS. *Analytical Chemistry* **69:**4083-91.

Gard, E.E., Kleeman, M.J., Gross, D.S., Hughes, L.S., Allen, J.O., Morrical, B.D., Fergenson, D.P., Dienes, T., Gälli, M.E., Johnson, R.J., Cass, G.R., Prather, K.A. (1998). Direct observation of heterogeneous chemistry in the atmosphere. *Science* **279:**1184-7.

Garland, J.A. and Rae, J.B. (1970). An integrating nephelometer for atmospheric studies and visibility warning devices. *J.Phys.E: Sci.Instrum.* **3:**275-80.

Gebhart, J. (1991). Response of single-particle optical counters to particles of irregular shape. *Part.Syst.Charact.* **8:**40-7.

Gebhart, J. (1993). Optical direct-reading techniques: light intensity systems. In *Aerosol Measurement: Principles, Techniques, and Applications,* Willeke, K. and Baron, P.A., editors. Van Nostrand Reinhold, New York. p. 313-44.

Genfa, Z., Dasgupta, P.K., Dong, S. (1989). Measurement of atmospheric ammonia. *Environ.Sci.Technol.* **23:**1467-74.

Gibson, F.W. (1994). Variability in atmospheric light-scattering properties with altitude. *Appl.Opt.* **33:**4919-29.

Gordon, J.I. and Johnson, R.W. (1985). Integrating nephelometer: theory and implications. *Appl.Opt.* **24:**2721-30.

Grant, W.B. (1995). Lidar for atmospheric and hydrospheric studies. In *Tunable Laser Applications,* Duarte, F., editor. Marcel Dekker, New York. p. 213-305.

Gregory, G.L., Hoell, J.M., Jr., Huebert, B.J., van Bramer, S.E., LeBel, P.J., Vau, S.A., Marinaro, R.M., Schiff, H.I., Hastie, D.R., Mackay, G.I., Karecki, D.R. (1990). An intercomparison of airborne nitric acid measurements. *J.Geophys.Res.* **95:**10089-102.

Griffiths, W.D., Iles, P.J., Vaughan, N.P. (1986). The behavior of liquid droplet aerosols in an APS 3300. *J.Aerosol Sci.* **17:**921-30.

Grund, C.J. and Eloranta, E.W. (1991). University of Wisconsin high spectral resolution lidar. *Opt.Eng.* **30:**6-12.

Gucker, F.T., Jr., O'Konski, C.T., Pickard, H.B., Pitts, J.N., Jr. (1947a). A photoelectronic counter for colloidal particles. *J.Am.Chem.Soc.* **69:**422-28.

Gucker, F.T., Jr., Pickard, H.B., O'Konski, C.T. (1947b). A photoelectric instrument for comparing concentrations of very dilute aerosols and measuring very low light intensities. *J.Am.Chem.Soc.* **69:**429-38.

Gucker, F.T., Jr. and Rose, D.G. (1954). A photoelectronic instrument for counting and sizing aerosol particles. *Brit.J.Appl.Phys.* S138-S143.

Hagen, D.E. and Alofs, D.J. (1983). Linear inversion method to obtain aerosol size distributions from measurements with a differential mobility analyzer. *Aerosol Sci.Technol.* **2:**465-75.

Hansen, A.D.A., Bodhaine, B.A., Dutton, E.G., Schnell, R.C. (1988). Aerosol and black carbon measurements at the South Pole: initial results, 1986-1987. *Geophysical Research Letters* **15:**1193-6.

Hansen, A.D.A., Conway, T.J., Steele, L.P., Bodhaine, B.A., Thoning, K.W., Tans, P., Novakov, T. (1989). Correlations among combustion effluent species at Barrow, Alaska: aerosol black carbon, carbon dioxide, and methane. *Journal of Atmospheric Chemistry* **9:**283-300.

Hansen, A.D.A. and Novakov, T. (1989). Aerosol black carbon measurements in the Arctic haze during AGASP-II. *Journal of Atmospheric Chemistry* **9:**347-62.

Hansen, A.D.A. and McMurry, P.H. (1990). An intercomparison of measurements of aerosol elemental carbon during the 1986 Carbonaceous Species Method Comparison Study. *JAWMA* **40:**894-5.

Hansen, A.D.A. and Novakov, T. (1990). Real-time measurement of aerosol black carbon during the Carbonaceous Species Methods Comparison Study. *Aerosol Sci.Technol.* **12:**194-9.

Hansen, A.D.A. and Rosen, H. (1990). Individual measurements of the emission factor of aerosol black carbon in automobile plumes. *JAWMA* **40:**1654-7.

Hanst, P.H. and Hanst, S.T. (1994). Gas measurements in the fundamental infrared region. In *Air Monitoring by Spectroscopic Techniques,* Sigrist, M.W., editor. Wiley, New York. p. 335-470.

Hanst, P.L., Wong, N.W., Bragin, J. (1982). A long-path infra-red study of Los Angeles smog. *Atmos.Environ.* **16:**969-81.

Harris, G.W., Mackay, G.I., Iguchi, T., Schiff, H.I., Schuetzle, D. (1987). Measurements of NO_2 and HNO_3 in diesel exhaust gas by tunable diode laser absorption spectrometry. *Environ.Sci.Technol.* **21:**299-304.

Harrison, A.W. (1977a). An automatic scanning integrating spectronephelometer. *Can.J.Phys.* **55:**1399-406.

Harrison, A.W. (1977b). Rayleigh volume scattering coefficients for freon-12, freon-22, and sulphur hexafluoride. *Canadian J.Phys.* **55:**1989-01.

Harrison, A.W. (1979). Nephelometer estimates of visual range. *Atmos.Environ.* **13:**645-52.

Harrison, A.W. and Mathai, C.V. (1981). Comparison of telephotometer and nephelometer measurements of atmospheric attenuation and its relationship to aerosol size distribution. *Atmos.Environ.* **15:**2625-30.

Harrison, R.M. and Msibi, I.M. (1994). Validation of techniques for fast response measurement of HNO_3 and NH_3 and determination of the $[NH_3]$ $[HNO_3]$ concentration product. *Atmos.Environ.* **28:**247-56.

Hasan, H. and Lewis, C.W. (1983). Integrating nephelometer response corrections for bimodal size distributions. *Aerosol Sci.Technol.* **2:**443-53.

Heintzenberg, J. and Hänel, G. (1970). A stabilized integrating nephelometer for visibility studies 1. Technical aspects. *Atmos.Environ.* **4:**585-7.

Heintzenberg, J. and Quenzel, H. (1973a). Calculations on the determination of the scattering coefficient of turbid air with integrating nephelometers. *Atmos.Environ.* **7:**509-19.

Heintzenberg, J. and Quenzel, H. (1973b). On the effect of the loss of large particles on the determination of scattering coefficients with integrating nephelometers. *Atmos.Environ.* **7:**503-7.

Heintzenberg, J. (1975). Determination *in situ* of the size distribution of the atmospheric aerosol. *J.Aerosol Sci.* **6:**291-303.

Heintzenberg, J. and Bhardwaja, P.S. (1976). On the accuracy of the backward hemispheric integrating nephelometer. *J.Appl.Meteorol.* **15:**1092-6.

Heintzenberg, J. (1978). The angular calibration of the total scatter/backscatter nephelometer, consequences and applications. *Staub-Reinhaltl.Luft* **38:**62-3.

Heintzenberg, J. and Witt, G. (1979). Extension of atmospheric light scattering measurements into the UV region. *Appl.Opt.* **18:**1281-3.

Heintzenberg, J. (1980). Particle size distribution and optical properties of Arctic haze. *Tellus* **32:**251-60.

Heintzenberg, J. and Bäcklin, L. (1983). A high sensitivity integrating nephelometer for airborne air pollution studies. *Atmos.Environ.* **17:**433-6.

Heintzenberg, J. and Charlson, R.J. (1996). Design and application of the integrating nephelometer: a review. *J.Atmos.Oceanic Technol.* **13:**987-1000.

Heitbrink, W.A., Baron, P.A., Willeke, K. (1991). Coincidence in time-of-flight spectrometers: phantom particle creation. *Aerosol Sci.Technol.* **14:**112-26.

Heitbrink, W.A. and Baron, P.A. (1992). An approach to evaluating and correcting Aerodynamic Particle Sizer measurements for phantom particle count creation. *Am.Indus.Hyg.Assoc.J.* **53:**427-31.

Helsper, C., Fissan, H., Kapadia, A., Liu, B.Y.H. (1982). Data inversion by simplex minimization for the electrical aerosol analyzer. *Aerosol Sci.Technol.* **1:**135-46.

Hemeon, W.C., Haines, G.F., Jr., Ide, H.M. (1953). Determination of haze and smoke concentrations by filter paper samples. *Air Repair* **3:**22-8.

Hemeon, W.C. (1973). A critical review of regulations for the control of particulate e missions. *JAPCA* **23:** 376-87.

Hering, S.V. and Friedlander, S.K. (1982). Origins of aerosol sulfur size distributions in the Los Angeles basin. *Atmos.Environ.* **16:**2647-56.

Hering, S.V., Lawson, D.R., Allegrini, I., Febo, A., Perrino, C., Possanzini, M., Sickles, J.E., II, Anlauf, K.G., Wiebe, A., Appel, B.R., John, W., Ondo, J.L., Wall, W., Braman, R.S., Sutton, R., et al. (1988). The nitric acid shootout: Field comparison of measurement methods. *Atmos.Environ.* **22:**1519-39.

Hering, S.V. and McMurry, P.H. (1991). Optical counter response to monodisperse atmospheric aerosols. *Atmos.Environ.* **25A:**463-8.

Hering, S.V. (1997). Automated, high-time resolution measurement of fine particle nitrate concentrations for the Northern Front Range Air Quality Study. Final Report to EPRI, Palo Alto, CA.

Hering, S.V. and Stolzenburg, M.R. (1998). Proceedings: A new method for the automated high-time resolution measurement of $PM_{2.5}$ nitrate. *AWM&A Conference $PM_{2.5}$: A Fine Particulate Standard*, Chow, J., and Koutrakis, P., editors. Long Beach, CA.

Hering, S.V. (1998). Personal communication. Aerosol Dynamics, Berkeley, CA.

Herrick, R.A., Kinsman, S., Lodge, J.P., Lundgren, D.A., Phillips, C.R., Sholtes, R.S., Stein, E., Wagman, J., Watson, J.G. (1989). Continuous tape sampling of coefficient of haze; intersociety committee method 502. In *Methods of Air Sampling and Analysis*, Lodge, J.P., editor. Intersociety Committee, Lewis Publishers, Chelsea, MI. p. 446-9.

Hill, A.S.G. (1936). Measurement of the optical densities of smokestains of filter papers. *Trans.Faraday Soc.* **32:**1125-31.

Hindman, E.E., Trusty, G.L., Hudson, J.G., Fitzgerald, J.W., Rogers, C.F. (1978). Field comparisons of optical particle counters. *Atmos.Environ.* **12:**1195-200.

Hinds, W.C. (1982). *Aerosol Technology: Properties, Behavior, and Measurement of Airborne Particles.* John Wiley & Sons, New York, NY.

Hitschfeld, W. and Bordan, J. (1954). Errors inherent in the radar measurement of rainfall at attenuating wavelengths. *J.Meteorol.* **11:**58-67.

Hitzenberger, R.M., Husar, R.B., Horvath, H. (1984). An intercomparison of measurements by a telephotometer and an integrating nephelometer. *Atmos.Environ.* **18:**1239-42.

Hodkinson, J.R. (1966). The optical measurement of aerosols. In *Aerosol Science,* Davies, C.N., editor. Academic Press, London and New York. p. 287-358.

Hoff, R.M., Harwood, M., Sheppard, A., Froude, F., Martin, J.B., Strapp, W. (1997). Use of airborne lidar to determine aerosol sources and movement in the Lower Fraser Valley (LFV), BC. *Atmos.Environ.* **31:**2123-34.

Hoppel, W.A. (1978). Determination of the aerosol size distribution from the mobility distribution of the charged fraction of aerosols. *J.Aerosol Sci.* **9:**41-54.

Horvath, H. and Noll, K.E. (1969). The relationship between atmospheric light scattering coefficient and visibility. *Atmos.Environ.* **3:**543-52.

Horvath, H. and Trier, A. (1993). A Study of the Aerosol of Santiago de Chile - I. Light Extinction Coefficients. *Atmos.Environ.* **27a:**371-84.

Horvath, H. (1993a). Atmospheric light absorption - a review. *Atmos.Environ.* **27A:**293-317.

Horvath, H. (1993b). Comparison of measurements of aerosol optical absorption by filter collection and a transmissometric method. *Atmos.Environ.* **27A:**319-25.

Horvath, H. and Kaller, W. (1994). Calibration of integrating nephelometers in the post-halocarbon era. *Atmos.Environ.* **28:**1219-24.

Horvath, H. (1997). Experimental calibration for aerosol light absorption measurements using the integrating plate method - summary of the data. *J.Aerosol Sci.* **28:**1149-61.

Houck, J.E., Goulet, J.M., Chow, J.C., Watson, J.G., Pritchett, L.C. (1990). Chemical characterization of emission sources contributing to light extinction. In *Transactions, Visibility and Fine Particles,* Mathai, C.V., editor. Air and Waste Management Association, Pittsburgh, PA. p. 437-46.

Hudson, G.M., Kaufmann, H.C., Nelson, J.W., Ronacci, M.A. (1980). Advances in the Use of PIXE and PESA for Air Pollution Sampling. In *Nuclear Instruments and Methods,* North Holland Publishing, Amsterdam. p. 259-63.

Huey, L.G., Dunlea, E.J., Lovejoy, E.R., Hanson, D.R., Norton, R.B., Fehsenfeld, F.C., Howard, C.J. (1998). Fast time response measurements of HNO_3 in air with a chemical ionization mass spectrometer. *J.Geophys.Res.* **103:**3355-60.

Huntzicker, J.J., Hoffman, R.S., Ling, C.S. (1978). Continuous measurement and speciation of sulfur containing aerosols by flame photometry. *Atmos.Environ.* **12:**83-8.

Husar, R.B. (1974). Atmospheric particulate mass monitoring with a beta radiation detector. *Atmos.Environ.* **8:**183-8.

Husar, R.B. and Falke, S.R. (1996). The relationship between aerosol light scattering and fine mass. Report No. CX 824179-01**,** Center for Air Pollution Impact and Trend Analysis, St. Louis, MO. Prepared for U.S. Environmental Protection Agency, Research Triangle Park, NC.

Ingram, W.J. and Golden, J. (1973). Smoke curve calibration. *JAPCA* **23:**110-5.

Jaeschke, W., Dierssen, J.P., Günther, A., Schumann, M. (1998). Phase partitioning of ammonia and ammonium in a multiphase system studied using a new vertical wet denuder technique. *Atmos.Environ.* **32:**365-71.

Jaklevic, J.M., Loo, B.W., Fujita, T.Y. (1980). Automatic particulate sulfur measurements with a dichotomous sampler and on-line x-ray fluorescence analysis. Report No. LBL-10882**,** Lawrence Berkeley National Laboratory, Berkeley, CA.

Jaklevic, J.M., Gatti, R.C., Goulding, F.S., Loo, B.W. (1981). A beta-gauge method applied to aerosol samples. *Environ.Sci.Technol.* **15:**680-6.

Japar, S.M. (1984). A comparison of optical methods for the measurement of elemental carbon in combustion aerosols. In *Aerosols,* Liu, Y.H., Pui, D.Y.H., Fissan, H.J., editors. Elsevier Science Publishing, p. 401-5.

Jennings, S.G. and Pinnick, R.G. (1980). Relationship between visible extinction, absorption and mass concentration of carbonaceous smokes. *Atmos.Environ.* **14:**1123-9.

Johnson, R.W. (1981). Daytime visibility and nephelometer measurements related to Its determination. *Atmos.Environ.* **15:**1835-46.

Johnston, M.V. and Drexler, A.S. (1995). MS of individual aerosol particles. *Analytical Chemistry* **67:**721A-6A.

Kasper, G. (1982). Dynamics and measurement of smokes. I. *Aerosol Sci.Technol.* **1:**187-99.

Kaye, P.H., Eyles, N.A., Ludlow, I.K., Clark, J.M. (1991). An instrument for the classification of airborne particles on the basis of size, shape, and count frequency. *Atmos.Environ.* **25A:**645-54.

Kelly, T., Stedman, D.H., Kok, G. (1979). Measurements of H_2O_2 and HNO_3. *Geophysical Research Letters* **6:**375-8.

Kelly, T.J., Spicer, C.W., Ward, G.F. (1990). An assessment of the luminol chemiluminescence technique for measurement of NO_2 in ambient air. *Atmos.Environ.* **24A:**2397-403.

Kempfer, U., Carnuth, W., Lotz, R., Trickl, T. (1994). A wide-range ultraviolet lidar system for tropospheric ozone measurements: development and application. *Rev.Sci.Instrum.* **65:**3145-64.

Kendall, M.G. (1951). Regressions, structure and functional relationship, Part II. *Biometrika* **39:**96-108.

Kerker, M. (1997). Light scattering instrumentation for aerosol studies: an historical overview. *Aerosol Sci.Technol.* **27:**522-40.

Keston, J., Reineking, A., Porstendorfer, I. (1991). Calibration of a TSI Model 3025 ultrafine condensation nucleus counter. *Aerosol Sci.Technol.* **15:**107-11.

Keuken, M.P., Wayers-IJpelaan, A., Mols, J.J., Otjes, R.P., Slanina, J. (1989). The determination of ammonia in ambient air by an automated thermodenuder system. *Atmos.Chemi.* **8:**359-76.

Kim, Y.P., Seinfeld, J.H., Saxena, P. (1993a). Atmospheric gas-aerosol equilibrium I. Thermodynamic model. *Aerosol Sci.Technol.* **19:**157-81.

Kim, Y.P., Seinfeld, J.H., Saxena, P. (1993b). Atmospheric gas-aerosol equilibrium II. Analysis of common approximations and activity coefficient calculation methods. *Aerosol Sci.Technol.* **19:**182-98.

Kim, Y.P. and Seinfeld, J.H. (1995). Atmospheric gas-aerosol equilibrium III. Thermodynamics of crustal elements Ca^{2+}, K^{+}, and Mg^{2+}. *Aerosol Sci.Technol.* **22:**93-110.

King, D.E. (1977). Evaluation of interlaboratory comparison data on linear regression analysis. In *Methods and Standards for Environmental Measurement,* Kirchoff, W.H., editor. NBS Publication 464, Gaithersburg, MD.

Kittelson, D.B., McKenzie, R.L., Vermeersch, M., Dorman, F., Pui, D.Y.H., Linne, M., Liu, B.Y.H., Whitby, K.T. (1978). Total sulfur aerosol concentration with an electrostatically pulsed flame photometric detector system. *Atmos.Environ.* **12:**105-11.

Klein, F., Ranty, C., Sowa, L. (1984). New examinations of the validity of the principle of beta radiation absorption for determinations of ambient air dust concentrations. *J.Aerosol Sci.* **15:**391-4.

Klett, J.D. (1981). Stable analytical inversion solution for processing lidar returns. *Appl.Opt.* **20:**211-20.

Knutson, E.O. and Whitby, K.T. (1975a). Aerosol classification by electric mobility: apparatus, theory, and applications. *J.Aerosol Sci.* **6:**443-51.

Knutson, E.O. and Whitby, K.T. (1975b). Accurate measurement of aerosol electric mobility moments. *J.Aerosol Sci.* **6:**453-60.

Koschmieder, H. (1924). Theorie der horizontalen sichtweite. *H.Beit.Phys.Freien.Atm.* **12:**171-81.

Kousaka, Y., Okuyama, K., Adachi, M. (1985). Determination of particle size distribution of ultra-fine aerosols using a differential mobility analyzer. *Aerosol Sci.Technol.* **4:**209-25.

Koutrakis, P. (1998). Personal communication. Harvard School of Public Health, Boston, MA.

Kovalev, V.A. (1993). Lidar measurement of the vertical aerosol extinction profiles with range-dependent backscatter-to-extinction ratios. *Appl.Opt.* **32:**6053-65.

Kovalev, V.A. and Moosmüller, H. (1994). Distortion of particulate extinction profiles measured by lidar in a two-component atmosphere. *Appl.Opt.* **33:**6499-507.

Kovalev, V.A. (1995). Sensitivity of the lidar solution to errors of the aerosol backscatter-to-extinction ratio: influence of a monotonic change in the aerosol extinction coefficient. *Appl.Opt.* **34:**3457-62.

Kölsch, H.J., Rairoux, P., Wolf, J.P., Wöste, L. (1992). Comparative study of nitric oxide immission in the cities of Lyon, Geneva, and Stuttgart using a mobile differential absorption LIDAR system. *Appl.Phys.* **B54:**89-94.

Labsphere (1994). A guide to integrating sphere photometry and radiometry.

Langford, A.O., Goldan, P.D., Fehsenfeld, F.C. (1989). A molybdenum oxide annular denuder system for gas phase ambient ammonia measurements. *Journal of Atmospheric Chemistry* **8:**359-76.

Larson, T.V., Ahlquist, N.C., Weiss, R.E., Covert, D.C., Waggoner, A.P. (1982). Chemical speciation of $H_2SO_4(NH_4)_2SO_4$ particles using temperature and humidity controlled nephelometry. *Atmos.Environ.* **16:**1587-90.

Lawson, D.R. (1990). The Southern California Air Quality Study. *JAWMA* **40:**156-65.

Lee, K.W., Kim, J.C., Han, D.S. (1990). Effects of gas density and viscosity on response of aerodynamic particle sizer. *Aerosol Sci.Technol.* **13:**203-12.

Lee, R.E., Caldwell, J.S., Morgan, G.B. (1972). The evaluation of methods for measuring suspended particulates in air. *Atmos.Environ.* **6:**593-622.

Lillienfeld, P. and Dulchinos, J. (1972). Portable instantaneous mass monitoring for coal mine dust. *Am.Indus.Hyg.Assoc.J.* **33:**136-45.

Lilienfeld, P. (1975). Design and operation of dust measuring instrumentation based on the beta-radiation method. *Staub-Reinhaltl.Luft* **35:**458.

Lin, C.I., Baker, M.B., Charlson, R.J. (1973). Absorption coefficient of atmospheric aerosol: a method for measurement. *Appl.Opt.* **12:**1356-63.

Lin, H.B. and Campillo, A.B. (1985). Photothermal aerosol absorption spectroscopy. *Appl.Opt.* **24:**422-33.

Liu, B.Y.H., Whitby, K.T., Pui, D.Y.H. (1974a). A portable electrical analyzer for size distribution measurement of submicron aerosols. *JAPCA* **24:**1067-72.

Liu, B.Y.H., Marple, V.A., Whitby, K.T., Barsic, N.J. (1974b). Size distribution measurement of airborne coal dust by optical particle counters. *Am.Indus.Hyg.Assoc.J.* **8:**443-51.

Liu, B.Y.H., Berglund, R.N., Agarwal, J.K. (1974c). Experimental studies of optical particle counters. *Atmos.Environ.* **8:**717-32.

Liu, B.Y.H. and Pui, D.Y.H. (1974). A submicron aerosol standard and the primary, absolute calibration of the condensation nuclei counter. *J.Colloid Interface Sci.* **47:**155-71.

Liu, B.Y.H. and Pui, D.Y.H. (1975). On the performance of the electrical aerosol analyzer. *J.Aerosol Sci.* **6:**249-64.

Liu, B.Y.H., Pui, D.Y.H., McKenzie, R.L., Agarwal, J.K., Jaenicke, R., Pohl, F.G., Preining, O., Reischl, G., Szymanski, W., Wagner, P.E. (1982). Intercomparison of different "absolute" instruments for measurement of aerosol number concentration. *J.Aerosol Sci.* **13:**429-50.

Liu, D.Y., Rutherford, D., Kinsey, M., Prather, K.A. (1997). Real-time monitoring of pyrotechnically derived aerosol particles in the troposphere. *Analytical Chemistry* **69:**1808-14.

Lodge, J.P., Waggoner, A.P., Klodt, D.T., Crain, C.N. (1981). Non-health effects of airborne particulate matter. *Atmos.Environ.* **15:**431-82.

Lodge, J.P. (1989). *Methods of Air Sampling and Analysis.* Lewis Publishers, Inc., Chelsea, MI.

Lowenthal, D.H., Rogers, C.F., Saxena, P., Watson, J.G., Chow, J.C. (1995). Sensitivity of estimated light extinction coefficients to model assumptions and measurement errors. *Atmos.Environ.* **29:**751-66.

Macias, E.S. and Husar, R.B. (1976). Atmospheric particulate mass measurement with beta attenuation mass monitor. *Environ.Sci.Technol.* **10:**904-7.

Mackay, G.I., Schiff, H.I., Wiebe, A., Anlauf, K.G. (1988). Measurements of NO_2, H_2CO and HNO_3 by tunable diode laser absorption spectroscopy during the 1985 Claremont intercomparison study. *Atmos.Environ.* 1555-64.

Madansky, A. (1959). The fitting of straight lines when both variables are subject to error. *J.Am.Stat.Assoc.* **54:**173-205.

Mage, D.T. (1995). The relationship between total suspended particulate matter (TSP) and British smoke measurements in London: development of a simple model. *JAWMA* **45:**737-9.

Malm, W.C. (1979). Considerations in the measurement of visibility. *JAPCA* **29:**1042-52.

Malm, W.C., Pitchford, A., Tree, R., Walther, E.G., Pearson, M.J., Archer, S. (1981). The visual air quality predicted by conventional and scanning teleradiometers and an integrating nephelometer. *Atmos.Environ.* **15:**2547-54.

Malm, W.C., Sisler, J.F., Huffman, D., Eldred, R.A., Cahill, T.A. (1994). Spatial and seasonal trends in particle concentration and optical extinction in the United States. *J.Geophys.Res.* **99:**1347-70.

Mansoori, B.A., Johnston, M.V., Wexler, A.S. (1994). Quantitation of ionic species in single microdroplets by on-line laser desorption/ionization. *Anal.Chem.* **66:**3681-7.

Mansoori, B.A., Johnston, M.V., Wexler, A.S. (1996). Matrix-assisted laser desorption/ionization of size- and composition-selected aerosol particles. *Analytical Chemistry* **68:**3595-601.

Marshall, I.A., Mitchell, J.P., Griffiths, W.D. (1991). The behaviour of regular-shaped non-spherical particles in a TSI Aerodynamic Particle Sizer. *J.Aerosol Sci.* **22:**73-89.

Mathai, C.V. and Harrison, A.W. (1980). Estimation of Atmospheric Aerosol Refractive Index. *Atmos.Environ.* **14:**1131-5.

Mathai, C.V., Watson, J.G., Rogers, F.A., Chow, J.C., Tombach, I.H., Zwicker, J.O., Cahill, T.A., Feeney, P.J., Eldred, R.A., Pitchford, M.L., Mueller, P.K. (1990). Intercomparison of ambient aerosol samplers used in western visibility and air quality studies. *Environ.Sci.Technol.* **24:**1090-9.

Mauldin, R.L., III, Tanner, D.J., Eisele, F.L. (1998). A new chemical ionization mass spectrometer technique for the fast measurement of gas phase nitric acid in the atmosphere. *J.Geophys.Res.* **103:**3361-7.

Mäkynen, J., Hakulinen, J., Kivistö, T., Lektimäki, M. (1982). Optical particle counters: Response, resolution and counting efficiency. *J.Aerosol Sci.* **13:**529-35.

McDermott, W.T., Ockovic, R.C., Stolzenburg, M.R. (1991). Counting efficiency of an improved 30A condensation nucleus counter. *Aerosol Sci.Technol.* **14:**278-87.

McElroy, J.L. and Smith, T.B. (1986). Vertical pollutant distributions and boundary layer structure observed by airborne lidar near the complex southern California coastline. *Atmos.Environ.* **20:**1555-66.

McElroy, J.L. and McGown, M.R. (1992). Application of airborne lidar in particulate air quality problem delineation, monitoring network design and control strategy development. *JAWMA* **42:** 1186-92.

McFarland, A.R. (1979). Wind tunnel evaluation of British Smoke Shade Sampler: test report. Report No. Rep #3565/05/79/ARM**,** Texas A&M University, College Station, TX.

Measures, R.M. (1984). *Laser Remote Sensing.* John Wiley & Sons, Inc., New York.

Melfi, S.H. (1972). Remote measurements of the atmosphere using raman scattering. *Appl.Opt.* **11:**1605-10.

Meng, Z., Seinfeld, J.H., Saxena, P., Kim, Y.P. (1995). Atmospheric gas-aerosol equilibrium IV. Thermodynamics of carbonates. *Aerosol Sci.Technol.* **23:**131-54.

Mennen, M.G., van Elzakker, B.G., Van Putten, E.M., Uiterwijk, J.W., Regts, T.A., Van Hellemond, J., Wyers, G.P., Otjes, R.P., Verhage, A.J.L., Wouters, L.W., Heffels, C.J.G., Römer, F.G., Van Den Beld, L., Tetteroo, J.E.H. (1996). Evaluation of automatic ammonia monitors for applications in an air quality monitoring network. *Atmos.Environ.* **30:**3239-56.

Meyer, M.B., Lijek, J., Ono, D.M. (1992). Continuous PM_{10} measurements in a woodsmoke environment. In *Transactions: PM_{10} Standards and Nontraditional Particulate Source Controls,* Chow, J.C. and Ono, D.M., editors. AWMA, Pittsburgh, PA. p. 24-38.

Middlebrook, A.M., Thomson, D.S., Murphy, D.M. (1997). On the purity of laboratory-generated sulfuric acid droplets and ambient particles studied by laser mass spectrometry. *Aerosol Sci.Technol.* **27:**293-307.

Mie, G. (1908). Beiträge zur optik trüber medien. *Annalen Der Physik* **4:**377-445.

Miller, S.W. and Bodhaine, B.A. (1982). Supersaturation and expansion ratios in condensation nuclei counters: an historical perspective. *J.Aerosol Sci.* **13:**481-90.

Milton, M.J.T., Woods, P.T., Jolliffe, B.W., Swann, N.R.W., McIlveen, T.J. (1992). Measurements of toluene and other aromatic hydrocarbons by differential-absorption lidar in the near-ultraviolet. *Appl.Phys.* **55:**41-5.

Moosmüller, H., Alvarez, R.J.Jr., Edmonds, C.M., Turner, R.M., Bundy, D.H., McElroy, J.L. (1993). Airborne ozone measurements with the USEPA UV-DIAL. In *Optical Remote Sensing of the Atmosphere Technical Digest,* Optical Society of America, Washington, DC. p. 176-9.

Moosmüller, H. and Arnott, W.P. (1996). Folded Jamin interferometer: a stable instrument for refractive-index measurements. *Opt.Lett.* **21:**438-40.

Moosmüller, H. and Wilkerson, T.D. (1997). Combined raman-elastic backscatter lidar method for the measurement of backscatter ratios. *Appl.Opt.* **36:**5144-7.

Moosmüller, H., Arnott, W.P., Rogers, C.F. (1997). Methods for real-time, in situ measurement of aerosol light absorption. *JAWMA* **47:**157-66.

Moosmüller, H., Arnott, W.P., Rogers, C.F., Chow, J.C., Frazier, C.A., Sherman, L.E., Dietrich, D.L. (1998). Photoacoustic and filter measurements related to aerosol light absorption during the Northern Front Range Air Quality Study (Colorado 1996/1997). *J.Geophys.Res.*

Motallebi, M., Pederson, J., Croes, B.E., VanCuren, T., Hering, S.V., Prather, K.A., Allan, M.A. (1998). To be presented: The 1997 Southern California Ozone Study-NARSTO: Aerosol program and radiation study. *A&WMA's 91st Annual Meeting and Exhibition,* San Diego, CA.

Mueller, P.K. and Collins, J.F. (1980). Development of a particulate sulfate analyzer. Report No. P-1382F**,** ERT, Westlake Village, CA. Prepared for Electric Power Research Institute, Palo Alto, CA.

Mulholland, G.W. and Bryner, N.P. (1994). Radiometric model of the transmission cell-reciprocal nephelometer. *Atmos.Environ.* **28:**873-87.

Murphy, D.M. and Thomson, D.S. (1994). Analyzing single aerosol particles in real time. *Aerosol Science* **24:**30-5.

Murphy, D.M. and Thomson, D.S. (1995). Laser ionization mass spectroscopy of single aerosol particles. *Aerosol Sci.Technol.* **22:**237-49.

Murphy, D.M. and Thomson, D.S. (1997a). Chemical composition of single aerosol particles at Idaho Hill: Positive ion measurements. *J.Geophys.Res.* **102:**6341-52.

Murphy, D.M. and Thomson, D.S. (1997b). Chemical composition of single aerosol particles at Idaho Hill: Negative ion measurements. *J.Geophys.Res.* **102:**6353-68.

Murphy, D.M., Thomson, D.S., Middlebrook, A.M. (1997). Bromine, iodine, and chlorine in single aerosol particles at Cape Grimm. *Geophysical Research Letters* **24:**3197-200.

Murphy, D.M., Anderson, J.R., Quinn, P.K., McInnes, L.M., Brechtel, F.J., Kreidenweis, S.M. (1998). Influence of sea-salt on aerosol radiative properties in the southern ocean marine boundary layer. *Nature* **392:**62-5.

Murphy, D.M. and Schein, M.E. (1998). Wind tunnel tests of a shrouded aircraft inlet. *Aerosol Sci.Technol.* **28:**33-9.

Nader, J.S. and Allen, R. (1960). A mass loading and radioactivity analyser for atmospheric particulates. *Am.Indus.Hyg.Assoc.J.* **21:**300-7.

Neubauer, K.R., Sum, S.T., Johnston, M.V., Wexler, A.S. (1996). Sulfur speciation in individual aerosol particles. *J.Geophys.Res.* **101:**18701-8.

Noble, C.A., Nordmeyer, T., Salt, K., Morrical, B., Prather, K.A. (1994). Aerosol characterization using mass spectrometry. *Trends in Analytical Chemistry* **13:**218-22.

Noble, C.A. and Prather, K.A. (1996). Real-time measurement of correlated size and composition profiles of individual atmospheric aerosol particles. *Environ.Sci.Technol.* **30:**2667-80.

Noble, C.A. and Prather, K.A. (1997). Real-time single particle monitoring of a relative increase in marine aerosol concentration during winter rainstorms. *Geophysical Research Letters* **24:**2753-6.

Noble, C. and Prather, K.A. (1998). Air pollution: the role of particles. *Phys.World* **11:**39-43.

Noel, M.A. and Topart, P.A. (1994). High-frequency impedance analysis of quartz crystal microbalances. 1. General considerations. *Analytical Chemistry* **66:**484-91.

Noone, K.J. and Hansson, H.C. (1990). Calibration of the TSI 3760 condensation nucleus counter for nonstandard operating conditions. *Aerosol Sci.Technol.* **13:**478-85.

Nordmeyer, T. and Prather, K.A. (1994). Real-time measurement capabilities using aerosol time-of-flight mass spectrometry. *Analytical Chemistry* **66:**3540-2.

Norton, T., Tucker, S., Smith, R.E., Lawson, D.R. (1998). The Northern Front Range Air Quality Study. *EM* 13-9, January.

Nyeki, S.A.P., Colbeck, I., Harrison, R.M. (1992). A portable aerosol sampler to measure real-time atmospheric mass loadings. *J.Aerosol Sci.* **23:**S687-S690.

Oberdörster, G., Gelein, R., Ferin, J., Weiss, B. (1995). Association of particulate air pollution and acute mortality: involvement of ultrafine particles? *Inhalation Toxicology* **7:**111-24.

Olin, J.G. and Sem, G.J. (1971). Piezoelectric microbalance for monitoring the mass concentration of suspended particles. *Atmos.Environ.* **5:**653-68.

Optec Inc. Model NGN-2 Open-Air Integrating Nephelometer: Technical Manual for Theory of Operation and Operating Procedures. (1993).

Pandis, S.N., Harley, R.A., Cass, G.R., Seinfeld, J.H. (1992). Secondary organic aerosol formation and transport. *Atmos.Environ.* **26A:**2269-82.

Pao, Y.H. (1977). *Optoacoustic Spectroscopy and Detection.* Academic Press, New York, NY.

Papenbrock, T. and Stuhl, F. (1991). Measurement of gaseous nitric acid by a laser-photolysis fragment-fluorescence (LPFF) method in the Black Forest and at the North Sea coast. *Atmos.Environ.* **25A:**2223-8.

Parungo, F.P., Nagamoto, C.T., Zhou, M.Y., Hansen, A.D.A., Harris, J. (1994). Aeolian transport of aerosol black carbon from China to the ocean. *Atmos.Environ.* **28:**3251-60.

Patashnick, H. and Hemenway, C.L. (1969). Oscillating fiber microbalance. *Rev.Sci.Instrum.* **40:**1008-11.

Patashnick, H. (1987). On-line, real-time instrumentation for diesel particulate testing. *Diesel Prog.N.Amer.* **53:**43-4.

Patashnick, H. and Rupprecht, E.G. (1991). Continuous PM_{10} measurements using the tapered element oscillating microbalance. *JAWMA* **41:**1079-83.

Penndorf, R. (1957). Tables of the refractive index for standard air and the Rayleigh scattering coefficient for the spectral region between 0.2 and 20 μm and their applications to atmosphere optics. *J.Opt.Soc.Am.* **47:**176-82.

Penner, J.E., Eddleman, H., Novakov, T. (1993). Towards the development of a global inventory for black carbon emissions. *Atmos.Environ.* **27A:**1277-95.

Peters, T.M., Chein, H.M., Lundgren, D.A., Keady, P.B. (1993). Comparison and combination of aerosol size distributions measured with a low pressure impactor, differential mobility particle sizer, electrical aerosol analyzer, and aerodynamic particle sizer. *Aerosol Sci.Technol.* **19:**396-405.

Petzold, A. and Niessner, R. (1995). Novel design of a resonant photoacoustic spectrophone for elemental carbon mass monitoring. *Appl.Phys.Lett.* **66:**1285-7.

Petzold, A. and Niessner, R. (1996). Photoacoustic soot sensor for *in-situ* black carbon monitoring. *Appl.Phys.* **B63:**191-7.

Phalen, R.F., Cuddihy, R.G., Fisher, G.L., Moss, O.R., Schlessinger, R.B., Swift, D.L., Yeh, H.C. (1991). Main Features of the Proposed NCRP Respiratory Tract Model. *Radiat.Protect.Dosim.* **38:**179-84.

Piironen, P. and Eloranta, E.W. (1994). Demonstration of a high-spectral-resolution lidar based on an iodine absorption filter. *Opt.Lett.* **19:**234-6.

Pilinis, C., Seinfeld, J.H., Seigneur, C. (1987). Mathematical modeling of the dynamics of multicomponent atmospheric aerosols. *Atmos.Environ.* **21:**943-55.

Pirogov, S.M., Korneyev, A.A., Hansen, A.D.A. (1994). Absorbing aerosol of the Pacific equatorial zone as measured in the SAGA 3 experiment. *Phys.Atmos.Ocean* **29:**633-5.

Pitchford, M.L. and Green, M. (1997). Analyses of sulfur aerosol size distributions for a forty day period in summer, 1992 at Meadview, Arizona. *JAWMA* **47:**136-46.

Pitchford, M.L., Chow, J.C., Watson, J.G., Moore, C.T., Campbell, D.H., Eldred, R.A., Vanderpool, R.W., Ouchida, P., Hering, S.V., Frank, N.H. (1997). Prototype $PM_{2.5}$ federal reference method field studies report-an EPA staff report. U.S. EPA, Las Vegas, NV. Prepared for U.S. EPA, Research Triangle Park, NC.

Platt, U. (1994). Differential optical absorption spectroscopy (DOAS). In *Air Monitoring by Spectroscopic Techniques,* Sigrist, M.W., editor. Wiley, New York. p. 27-84.

Pollak, L.W. and Metnieks, A.L. (1959). New calibration of photo-electric nucleus counters. *Geofis.Pura Applicata* **43:**285-301.

Prather, K.A., Nordmeyer, T., Salt, K. (1994). Real-time characterization of individual aerosol particles using time-of-flight mass spectrometry. *Analytical Chemistry* **66:**1403-7.

Pruppacher, H.R. and Klett, J.D. (1978). *Microphysics of Clouds and Precipitation.* D. Reidel Publishing Co, Boston, MA.

Pui, D.Y.H. and Swift, D.L. (1995). Direct-reading instruments for airborne particles. In *Air Sampling Instruments for Evaluation of Atmospheric Contaminants,* Cohen, B.S. and Hering, S.V., editors. American Conference of Governmental Industrial Hygienists, Cincinnati, OH. p. 337-68.

Pytkowicz, R.M. and Kester, D.R. (1971). The physical chemistry of sea water. *Oceanogr.Mar.Biol.* **9:**11-60.

Quenzel, H. (1969a). Der einfluss der aerosolgröβenverteilung auf die messgenauigkeit von streulichtmessern. *Gerlands Beitr.Geophys.* **78:**251-63.

Quenzel, H. (1969b). Influence of refractive index on the accuracy of size determination of aerosol particles with light-scattering aerosol counters. *Appl.Opt.* **8:**165-9.

Quenzel, H., Ruppersberg, G.H., Schellhase, R. (1975). Calculations about the systematic error of visibility-meters measuring scattered light. *Atmos.Environ.* **9:**587-601.

Quinn, P.K., Coffman, D.J., Kapustin, V.N., Bates, T.S., Covert, D.S. Aerosol optics in the marine boundary layer during ACE-1 and the underlying chemical and physical aerosol properties. [In Press] J.Geophys.Res. (1998).

Raabe, O.G., Braaten, D.A., Axelbaum, R.L., Teague, S.V., Cahill, T.A. (1988). Calibration studies of the DRUM impactor. *J.Aerosol Sci.* **19:**183-95.

Rabinoff, R.A. and Herman, B.M. (1973). Effect of aerosol size distribution on the accuracy of the integrating nephelometer. *Journal of Applied Meteorology* **12:**184-6.

Rader, D.J., Brockmann, J.E., Ceman, D.L., Lucero, D.A. (1990). A method to employ the APS factory calibration under different operating conditions. *Aerosol Sci.Technol.* **13:**514-21.

Rader, D.J. and O'Hern, T.J. (1993). Optical direct-reading techniques: i*n situ* sensing. In *Aerosol Measurement: Principles, Techniques and Applications,* Willeke, K. and Baron, P.A., editors. Van Nostrand Reinhold, New York, NY. p. 345-80.

Rae, J.B. (1970a). Author's reply to Heintzenberg and Hänel: A stabilized integrating nephelometer for visibility studies. *Atmos.Environ.* **4:**586.

Rae, J.B. (1970b). Author's reply to Ruppersberg: a stabilized integrating nephelometer for visibility studies. *Atmos.Environ.* **4:**587.

Rae, J.B. and Garland, J.A. (1970). A stabilized integrating nephelometer for visibility studies. *Atmos.Environ.* **4:**219-23.

Rapsomanikis, S., Wake, M., Kitto, A.M.N., Harrison, R.M. (1988). Analysis of atmospheric ammonia and particulate ammonium by a sensitive fluorescence method. *Environ.Sci.Technol.* **22:**948-52.

Reineking, A. and Porstendörfer, J. (1986). Measurements of particle loss functions in a differential mobility analyzer (TSI, Model 3071) for different flow rates. *Aerosol Sci.Technol.* **5:**483-6.

Reischl, G.P. (1991). Measurement of ambient aerosols by the differential mobility analyzer method: concepts and realization criteria for the size range between 2 and 500 nm. *Aerosol Sci.Technol.* **14:**5-24.

Ripley, D., Clingenpeel, J., Hurn, R. (1964). Continuous determination of nitrogen oxides in air and exhaust gases. *Int.J.Air Water Pollut.Control* **8:**455-63.

Roberts, P.T. and Friedlander, S.K. (1976). Analysis of sulfur in deposited aerosol particles by vaporization and flame photometric detection. *Atmos.Environ.* **10:**403-8.

Robinson, N.F. and Lamb, D. (1986). On the calibration of an optical particle counter. *Aerosol Sci.Technol.* **5:**113-6.

Rogge, W.F., Hildemann, L.M., Mazurek, M.A., Cass, G.R. (1991). Sources of fine organic aerosol. 1. Charbroilers and meat cooking operations. *Environ.Sci.Technol.* **25:**1112-25.

Rogge, W.F., Hildemann, L.M., Mazurek, M.A., Cass, G.R., Simoneit, B.R.T. (1993a). Sources of fine organic aerosol. 2. Noncatalyst and catalyst-equipped automobiles and heavy-duty diesel trucks. *Environ.Sci.Technol.* **27:**636-51.

Rogge, W.F., Hildemann, L.M., Mazurek, M.A., Cass, G.R., Simoneit, B.R.T. (1993b). Sources of fine organic aerosol. 5. Natural gas home appliances. *Environ.Sci.Technol.* **27:**2736-44.

Rogge, W.F., Mazurek, M.A., Hildemann, L.M., Cass, G.R., Simoneit, B.R.T. (1993c). Quantification of urban organic aerosols at a molecular level: identification, abundance and seasonal variation. *Atmos.Environ.* **27A:**1309-30.

Rogge, W.F., Hildemann, L.M., Mazurek, M.A., Cass, G.R., Simoneit, B.R.T. (1997). Sources of fine organic aerosol. 8. Boilers burning No. 2 distillate fuel oil. *Environ.Sci.Technol.* **31:**2731-7.

Rogge, W.F., Hildemann, L.M., Mazurek, M.A., Cass, G.R., Simoneit, B.R.T. (1998). Sources of fine organic aerosol. 9. Pine, oak, and synthetic log combustion in residential fireplaces. *Environ.Sci.Technol.* 13-22.

Rood, M.J., Larson, T.V., Covert, D.S., Ahlquist, N.C. (1985). Measurement of laboratory and ambient aerosols with temperature and humidity controlled nephelometry. *Atmos.Environ.* **19:**1181-90.

Rood, M.J., Covert, D.S., Larson, T.V. (1987). Temperature and humidity controlled nephelometry: improvements and calibration. *Aerosol Sci.Technol.* **7:**57-65.

Rooth, R.A., Verhage, A.J.L., Wouters, L.W. (1990). Photoacoustic measurement of ammonia in the atmosphere: Influence of water vapor and carbon dioxide. *Appl.Opt.* **29:**3643-53.

Rosen, H., Hansen, A.D.A., Novakov, T. (1984). Role of graphitic carbon particles in radiative transfer in the Arctic haze. *Sci.Total Environ.* **36:**103-10.

Rosen, J.M., Pinnick, R.G., Garvey, D.M. (1997). Nephelometer optical response model for the interpretation of atmospheric aerosol measurements. *Appl.Opt.* **36:**2642-9.

Rothe, K.W., Brinkmann, U., Walther, H. (1974). Remote measurement of NO_2 emission from a chemical factory by the differential absorption technique. *Appl.Phys.* **4:**181-2.

Ruby, M.G. and Waggoner, A.P. (1981). Intercomparison of integrating nephelometer measurements. *Environ.Sci.Technol.* **15:**109-13.

Ruby, M.G. (1985). Visibility measurement methods: I. Integrating nephelometer. *JAPCA* **35:**244-8.

Ruppersberg, G.H. (1970). Discussions: a stabilized integrating nephelometer for visibility studies. *Atmos.Environ.* **4:**586.

Rupprecht, E.G., Meyer, M., Patashnick, H. The Tapered Element Oscillating Microbalance as a tool for measuring ambient particulate concentrations in real time. (1992). Oxford, UK.

Rupprecht, G., Patashnick, H., Beeson, D.E., Green, R.N., Meyer, M.B. (1995). A new automated monitor for the measurement of particulate carbon in the atmosphere. *Particulate Matter: Health and Regulatory Issues,* Pittsburgh, PA.

Salt, K., Noble, C.A., Prather, K.A. (1996). Aerodynamic particle sizing versus light scattering intensity measurement as methods for particle sizing coupled with a time-of- flight mass spectrometer. *Analytical Chemistry* **68:**230-4.

Saros, M.T., Weber, R.J., Marti, J.J., McMurry, P.H. (1996). Ultrafine aerosol measurement using a condensation nucleus counter with pulse height analysis. *Aerosol Sci.Technol.* **25:**200-13.

Sauren, H., Gerkema, E., Bic'anic', D., Jalink, H. (1993). Real-time and *in situ* determination of ammonia concentrations in the atmosphere by means of intermodulated stark resonant CO_2 laser photoacoustic spectroscopy. *Atmos.Environ.* **27A:**109-12.

Saxena, P. and Hildemann, L.M. (1997). Water absorption by organics: survey of laboratory evidence and evaluation of UNIFAC for estimating water activity. *Environ.Sci.Technol.* **31:**3318-24.

Schendel, J.S., Stickel, R.E., van Dijk, C.A., Sandholm, S.T., Davis, D.D., Bradshaw, J.D. (1990). Atmospheric ammonia measurement using a VUV/Photofragmentation laser-induced fluorescence technique. *Appl.Opt.* **29:**4924-37.

Schiff, H.I., Hastu, D.R., Mackay, G.I., Iguchi, T., Ridley, B.A. (1983). Tunable diode laser systems for measuring trace gases in tropospheric air. *Environ.Sci.Technol.* **17:**352A-64A.

Schmidtke, G., Kohn, W., Klocke, U., Knothe, M., Riedel, W.J., Wolf, H. (1988). Diode laser spectrometer for monitoring up to five atmospheric trace gases in unattended operation. *Appl.Opt.* **28:**3665-70.

Seinfeld, J.H. and Pandis, S.N. (1997). *Atmospheric Chemistry and Physics: From Air Pollution to Climate Change.* John Wiley & Sons, New York, NY.

Sem, G.J. and Borgos, J.W. (1975). Experimental investigation of the exponential attenuation of beta radiation for dust measurements. *Staub-Reinhaltl.Luft* **35:**5-9.

Sem, G.J., Tsurubayashi, K., Homma, K. (1977). Performance of the piezoelectric microbalance respirable aerosol sensor. *J.Am.Ind.Hyg.Assoc.* **38:**580-8.

She, C.Y., Alvarez, R.J.Jr., Caldwell, L.M., Krueger, D.A. (1992). High-spectral-resolution Rayleigh-Mie lidar measurement of vertical aerosol and atmospheric profiles. *Appl.Phys.* **B55:**154-8.

Shimp, D.R. (1988). Field comparison of beta attenuation PM_{10} sampler and high-volume PM_{10} sampler. In *Transactions, PM_{10}: Implementation of Standards,* Mathai, C.V. and Stonefield, D.H., editors. Air Pollution Control Association, Pittsburgh, PA. p. 171-8.

Silva, P.J. and Prather, K.A. (1997). On-line characterization of individual particles from automobile emissions. *Environ.Sci.Technol.* **31:**3074-80.

Sinclair, D. and Hoopes, G.S. (1975). A continuous flow condensation nucleus counter. *J.Aerosol Sci.* **6:**1-7.

Sloane, C.S., Watson, J.G., Chow, J.C., Pritchett, L.C., Richards, L.W. (1990). Size distribution and optical properties of the Denver Brown Cloud. In *Transactions, Visibility and Fine Particles,* Mathai, C.V., editor. Air & Waste Management Association, Pittsburgh, PA. p. 384-93.

Sloane, C.S., Rood, M.J., Rogers, C.F. (1991). Measurements of aerosol particle size: improved precision by simultaneous use of optical particle counter and nephelometer. *Aerosol Sci.Technol.* **14:**289-301.

Solomon, P.A., Fall, T., Salmon, L., Cass, G.R., Gray, H.A., Davidson, A. (1989). Chemical characteristics of PM_{10} aerosols collected in the Los Angeles a rea. *JAPCA* **39:**154-63.

Sørensen, L.L., Granby, K., Nielsen, H., Asman, W.A.H. (1994). Diffusion scrubber technique used for measurements of atmospheric ammonia. *Atmos.Environ.* **28:**3637-45.

Speer, R.E., Barnes, H.M., Brown, R. (1997). An instrument for measuring the liquid water content of aerosols. *Aerosol Sci.Technol.* **27:**50-61.

Spurny, K. and Kubie, G. (1961). Analytische methoden zur bestimmung von aerosolen unter verwendung von membranultrafiltern: v. herstellung und anwendung von mit radioaktivem ^{63}nickel-isotop markierten membranultrafiltern. *Coll.Czechoslovak Chem.Commun.* **26:**1991-8.

Stein, S.W., Turpin, B.J., Cai, X., Huang, P.F., McMurry, P.H. (1994). Measurements of relative humidity-dependent bounce and density for atmospheric particles using the DMA-impactor technique. *Atmos.Environ.* **28:**1739-46.

Stelson, A.W. and Seinfeld, J.H. (1982a). Relative humidity and temperature dependence of the ammonium nitrate dissociation constant. *Atmos.Environ.* **16:**983-92.

Stelson, A.W. and Seinfeld, J.H. (1982b). Thermodynamic prediction of the water activity, NH_4HO_3 dissociation constant, density and refractive index for the NH_4NO_3-$(NH_4)_2SO_4H_2O$ system at 25°C. *Atmos.Environ.* **16:**2507-14.

Stevens, R.K., O'Keefe, A.E., Ortman, G.C. (1969). Absolute calibration of a flame photometric detector to volatile sulfur compounds at sub-part-per-million levels. *Environ.Sci.Technol.* **3:**652-5.

Stevens, R.K., Mulik, J.D., O'Keeffe, A.E., Krost, K.J. (1971). Gas chromatography of reactive sulfur gases in air at the parts-per-billon level. *Analytical Chemistry* **43:**827-31.

Stolzenburg, M.R. and McMurry, P.H. (1991). An ultrafine aerosol condensation nucleus counter. *Aerosol Sci.Technol.* **14:**48-65.

Su, Y.F., Cheng, Y.S., Newton, G.J., Yeh, H.C. (1990). Counting efficiency of the TSI Model 3020 condensation nucleus counter. *Aerosol Sci.Technol.* **12:**1050-4.

Sverdrup, G.M. and Whitby, K.T. (1977). Determination of submicron aerosol size distribution by use of continuous analog sensors. *Environ.Sci.Technol.* **11:**1171-6.

Szkarlat, A.C. and Japar, S.M. (1981). Light absorption by airborne aerosols: comparison of integrating plate and spectrophone techniques. *Appl.Opt.* **20:**1151-5.

Talbot, R.W., Vijgen, A.S., Harris, R.C. (1990). Measuring tropospheric HNO_3: Problems and prospects for nylon filter and mist chamber techniques. *J.Geophys.Res.* **95:**7553-61.

Tang, I.N., Munkelwitz, H.R., Davis, J.G. (1977a). Aerosol growth studies II: Preparation and growth measurements of monodisperse salt aerosols. *J.Aerosol Sci.* **8:**149-59.

Tang, I.N. and Munkelwitz, H.R. (1977b). Aerosol growth studies III: Ammonium bisulfate aerosols in a moist atmosphere. *J.Aerosol Sci.* **8:**321-30.

Tang, I.N. (1980). Deliquescence properties and particle size change of hygroscopic aerosols. In *Generation of Aerosols and Facilities for Exposure Experiments,* Willeke, K., editor. Ann Arbor Science Publishers, Inc., Ann Arbor, MI.

Tanner, R.L., D'Ottavio, T., Garber, R.W., Newmann, L. (1980). Determination of ambient aerosol sulfur using a continuous flame photometric detection system. Part I, Sampling system for aerosol sulfate and sulfuric acid. *Atmos.Environ.* **14:**121-7.

ten Brink, H.M., Plomp, A., Spoelstra, H., van de Vate, J.F. (1983). A high-resolution electrical mobility aerosol spectrometer (MAS). *J.Aerosol Sci.* **5:**589-97.

Terhune, R.W. and Anderson, J.E. (1977). Spectrophone measurements of the absorption of visibile light by aerosols in the atmosphere. *Opt.Lett.* **1:**70-2.

Thielke, J.F., Charlson, R.J., Winter, J.W., Ahlquist, N.C., Whitby, K.T., Husar, R.B., Liu, B.Y.H. (1972). Multiwavelength nephelometer measurements in Los Angeles smog aerosols. II. Correlation with size distributions, volume concentrations. *J.Colloid Interface Sci.* **39:**252-9.

Thomson, D.S. and Murphy, D.M. (1993). Laser-induced ion formation thresholds of aerosol particles in a vacuum. *Appl.Opt.* **32:**6818-26.

Thomson, D.S., Middlebrook, A.M., Murphy, D.M. (1997). Thresholds for laser-induced ion formation from aerosols in a vacuum using ultraviolet and vacuum-ultraviolet laser wavelengths. *Aerosol Sci.Technol.* **26:**544-59.

Thornes, J. (1978). London's Changing Meteorology. In *Changing London,* University Tutorial Press, London.

Toriumi, R., Tai, H., Takeuchi, N. (1996). Tunable solid-state blue laser differential absorption lidar system for NO_2 monitoring. *Opt.Eng.* **35:**2371-5.

Trijonis, J.C., McGown, M., Pitchford, M.L., Blumenthal, D.L., Roberts, P.T., White, W.H., Macias, E.S., Weiss, R.E., Waggoner, A., Watson, J.G., Chow, J.C., Flocchini, R.G. (1988). The RESOLVE project: visibility conditions and causes of visibility degradation in the Mojave desert of California. Santa Fe Research Corporation, Sante Fe, NM. Prepared for Sante Fe Research Corp., Sante Fe, NM, Naval Weapons Center/China Lake.

Trijonis, J.C., Malm, W.C., Pitchford, M.L., White, W.H., Charlson, R., Husar, R. (1990). Visibility: existing and historical conditions - causes and effects. National Acid Precipitation Assessment Program (NAPAP), Washington D.C.

Tsai, C.J. and Cheng, Y.H. (1996). Comparison of two ambient beta gauge PM_{10} samplers. *JAWMA* **46:**142-7.

Tuazon, E.C., Graham, R.A., Winer, A.M., Easton, R.R., Pitts, J.R., Hanst, P.L. (1978). A kilometer pathlength Fourier-transform infrared system for the study of trace pollutants in ambient and synthetic atmospheres. *Atmos.Environ.* **12:**865-75.

Tuazon, E.C., Winer, A.M., Graham, R.A., Pitts, J.N., Jr. (1980). Atmospheric measurements of trace pollutants by kilometer pathlength FTIR spectroscopy. *Adv.Environ.Sci.Technol.* **10:**259-300.

Tuazon, E.C., Winer, A.M., Pitts, J.N. (1981). Trace pollutant concentrations in a multi-day smog episode in the California South Coast Air Basin by long pathlength FT-IR spectroscopy. *Environ.Sci.Technol.* **15:**1232-7.

Turpin, B.J., Huntzicker, J.J., Adams, K.M. (1990a). Intercomparison of photoacoustic and thermal-optical methods for the measurement of atmospheric elemental carbon. *Atmos.Environ.* **24A:**1831-5.

Turpin, B.J., Cary, R.A., Huntzicker, J.J. (1990b). An *in-situ*, time-resolved analyzer for aerosol organic and elemental carbon. *Aerosol Sci.Technol.* **12:**161-71.

Turpin, B.J. and Huntzicker, J.J. (1991). Secondary formation of organic aerosol in the Los Angeles Basin: a descriptive analysis of organic and elemental carbon concentrations. *Atmos.Environ.* **25A:**207-15.

U.S.Dept.HEW (1969). Air quality criteria for particulate matter. U.S. Government Printing Office, Washington, D.C.

U.S.EPA (1982). Air quality criteria for particulate matter and sulfur oxides, Volumes I and II. Report No. EPA-600/8-82-029a**,** EPA,U.S., Research Triangle Park, NC.

U.S.EPA (1987). Revisions to the national ambient air quality standards for particulate matter. *Federal Register* **52:**24634.

U.S.EPA (1990). Compilation of air pollutant emission factors. Volume I: Stationary point and area sources. U. S. Environmental Protection Agency, Office of Air and Radiation, Office of Air Quality Planning and Standards, Research Triangle Park, NC.

U.S.EPA (1991). Technical assistance document for sampling and analysis of ozone precursors. Report No. EPA 600/8-91-215**,** U.S. Environmental Protection Agency, Atmospheric Research and Exposure Assessment Laboratory, Research Triangle Park, NC.

U.S.EPA (1996). Air quality criteria for particulate matter. Report No. EPA/600/P-95/001abcF**,** U.S. EPA, Research Triangle Park, NC.

U.S.EPA (1997a). Revised requirements for designation of reference and equivalent methods for $PM_{2.5}$ and ambient air quality surveillance for particulate matter – final rule. 40 CFR part 58. *Federal Register*, **62**(138):38830-38854. July 18, 1997.

U.S.EPA (1997b). Revised requirements for designation of reference and equivalent methods for $PM_{2.5}$ and ambient air quality surveillance for particulate matter – final rule. 40 CFR part 53. *Federal Register*, **62**(138):38763-38830. July 18, 1997.

U.S.EPA (1997c). National ambient air quality standards for particulate matter – final rule. 40 CFR part 50. *Federal Register*, **62**(138):38651-38760. July 18, 1997.

U.S.EPA (1997d). National ambient air quality standards for particulate matter; availability of supplemental information and request for comments – final rule. 40 CFR part 50. *Federal Register*, **62**(138):38761-38762. July 18, 1997.

van der Meulen, A. and van Elzakker, B.G. (1986). Size resolution of laser optical particle counters. *Aerosol Sci.Technol.* **5:**313-24.

van Elzakker, B.G. and van der Meulen, A. (1989). Performance characteristics of various beta-dust monitors: intercomparison. *Journal of Aerosol Science* **20:**1549-52.

Vedal, S. (1997). Critical review - Ambient particles and health: lines that divide. *JAWMA* **47:**551-81.

Waggoner, A.P. and Weiss, R.E. (1980). Comparison of fine particle mass concentration and light scattering extinction in ambient aerosol. *Atmos.Environ.* **14:**623-6.

Waggoner, A.P., Weiss, R.E., Ahlquist, N.C., Covert, D.S., Will, S., Charlson, R.J. (1981). Optical characteristics of atmospheric aerosols. *Atmos.Environ.* **15:**1891-909.

Waggoner, A.P., Weiss, R.E., Ahlquist, N.C. (1983). *In situ*, rapid response measurement of $H_2SO_4/(NH_4)_2SO_4$ in urban Houston: a comparison with rural Virginia. *Atmos.Environ.* **17:**1723-31.

Waller, R.E. (1963). Acid droplets in town air. *Int.J.Air Water Pollut.Control* **7:**773-8.

Wang, H. and John, W. (1989). A simple iteration procedure to correct for the density effect in the aerodynamic particle sizer. *Aerosol Sci.Technol.* **10:**501-5.

Wang, J.C. and John, W. (1987). Particle density correction for the aerodynamic particle sizer. *Aerosol Sci.Technol.* **6:**191-8.

Wang, S.C. and Flagan, R.C. (1990). Scanning electrical mobility spectrometer. *Aerosol Sci.Technol.* **13:**230-40.

Ward, M.D. and Buttry, D.A. (1990). *In situ* interfacial mass detection with piezoelectric transducers. *Science* **249:**1000-7.

Watson, J.G., Chow, J.C., Shah, J.J., Pace, T.G. (1983). The effect of sampling inlets on the PM_{10} and PM_{15} to TSP concentration ratios. *JAPCA* **33:**114-9.

Watson, J.G., Cooper, J.A., Huntzicker, J.J. (1984). The effective variance weighting for least squares calculations applied to the mass balance receptor model. *Atmos.Environ.* **18:**1347-55.

Watson, J.G., Chow, J.C., Richards, L.W., Haase, D.L., McDade, C., Dietrich, D.L., Moon, D., Sloane, C.S. (1991). The 1989-90 Phoenix, AZ Urban Haze Study Volume II: The apportionment of light extinction to sources appendices. Final report. Report No. DRI 8931.5F2**,** Desert Research Institute, Reno, NV. Arizona Department of Environmental Quality.

Watson, J.G., Green, M.C., Hoffer, T.E., Lawson, D.R., Eatough, D.J., Farber, R.J., Malm, W.C., McDade, C., Pitchford, M.L. (1993). Project MOHAVE data analysis plan. *86th Annual Meeting of the Air and Waste Management Association,* Denver, CO.

Watson, J.G. and Chow, J.C. (1994). Clear sky visibility as a challenge for society. *Annual Rev.Energy Environ.* **19:**241-66.

Watson, J.G., Chow, J.C., Lurmann, F.W., Musarra, S. (1994a). Ammonium nitrate, nitric acid, and ammonia equilibrium in wintertime Phoenix, Arizona. *JAWMA* **44:**405-12.

Watson, J.G., Chow, J.C., Lu, Z., Fujita, E.M., Lowenthal, D.H., Lawson, D.R. (1994b). Chemical mass balance source apportionment of PM_{10} during the Southern California Air Quality Study. *Aerosol Sci.Technol.* **21:**1-36.

Watson, J.G., Chow, J.C., Fujita, E.M., Lu, S.L., Heisler, S.L., Moore, T.A. (1994c). Wintertime source contributions to light extinction in Tucson, AZ. *International Specialty Conference on Aerosols and Atmospheric Optics: Radiative Balance and Visual Air Quality,* Pittsburgh.

Watson, J.G., Chow, J.C., Fujita, E.M., Frazier, C.A., Lu, Z., Heisler, S.L., Moore, C.T. (1994d). Aerosol data validation for the 1992-93 Tucson Urban Haze Study. *87th Annual Meeting,* Cincinnati, OH.

Watson, J.G., Blumenthal, D.L., Chow, J.C., Cahill, C., Richards, L.W., Dietrich, D., Morris, R., Houck, J., Dickson, R.J., Anderson, S.R. (1996). Mt. Zirkel Wilderness Area Reasonable Attribution Study of Visibility Impairment - Volume II: Results of data analysis and modeling. Desert Research Institute, Reno, NV. Prepared for Colorado Department of Public Health and Environment, Denver, CO.

Watson, J.G., Chow, J.C., DuBois, D.W., Green, M.C., Frank, N.H., Pitchford, M.L. (1997a). Guidance for network design and optimal site exposure for $PM_{2.5}$ and PM_{10}. Desert Research Institute, Reno, NV. Prepared for U.S. EPA, Research Triangle Park, NC.

Watson, J.G., Chow, J.C., Rogers, C.F., Dubois, D., Cahill, C. (1997b). Analysis of historical PM_{10} and $PM_{2.5}$ measurements in Central California. Draft report. Desert Research Institute, Reno, NV. Prepared for California Regional Particulate Air Quality Study, California Air Resources Board, Sacramento, CA.

Watson, J.G., Chow, J.C., Rogers, C.F., Green, M.C., Kohl, S.D., Frazier, C.A., Robinson, N.F., Dubois, D. (1997c). Annual report for the Robbins Particulate Study - October 1995 through September 1996. Report No. 7100.3F2**,** Desert Research Institute, Reno, NV.

Watson, J.G., Fujita, E.M., Chow, J.C., Richards, L.W., Neff, W.D., Dietrich, D.L., Hering, S.V. (1998a). Northern Front Range Air Quality Study final report. Desert Research Institute, Reno, NV. Prepared for Colorado State University.

Watson, J.G., Chow, J.C., Edgerton, S.A., Ruíz, M.E. (1998b). Program plan for the Mexico City Aerosol Characterization Study. Desert Research Institute, Reno, NV. Prepared for U.S. Department of Energy, Washington, D.C.

Wedding, J.B. and Weigand, M.A. (1993). An automatic particle sampler with beta gauging. *JAWMA* **43:**475-9.

Weiss, R.E. and Waggoner, A.P. (1984). Aerosol optical absorption: accuracy of filter measurement by comparison with *in-situ* extinction. In *Aerosols: Science, Technology, and Industrial Applications of Airborne Particles,* Liu, B.Y.H., Pui, D.Y.H., Fissan, H.J., editors. Elsevier Science Publishing Co., New York, NY. p. 397-400.

Wen, H.Y. and Kasper, G. (1986). Counting efficiencies of six commercial particle counters. *J.Aerosol Sci.* **17:**947-61.

Wernisch, J. (1985). Quantitative electron microprobe analysis without standard. *X-Ray Spectrometry* **14:**109-19.

Wexler, A.S. and Seinfeld, J.H. (1991). Second-generation inorganic aerosol model. *Atmos.Environ.* **25A:**2731-48.

Whitby, K.T. and Clark, W.E. (1966). Electrical aerosol particle counting and size distribution measuring system for the 0.015 to 1.0 μm size range. *Tellus* **18:**573-86.

Whitby, K.T. and Vomela, R.A. (1967). Response of single particle optical counters to non-ideal particles. *Environ.Sci.Technol.* **1:**801-14.

Whitby, K.T. and Liu, B.Y.H. (1968). Polystyrene aerosols - electrical charge and residue size distribution. *Atmos.Environ.* **2:**103-16.

White, J.U. (1976). Very long optical paths in air. *J.Opt.Soc.Am.* **66:**411-6.

White, W.H., Macias, E.S., Nininger, R.C., Schorran, D.E. (1994). Size-resolved measurements of light scattering by ambient particles in the southwestern U.S.A. *Atmos.Environ.* **28:**909-22.

Whiteman, D.N., Melfi, S.H., Ferrare, R.A. (1992). Raman lidar system for the measurement of water vapor and aerosols in the Earth's atmosphere. *Appl.Opt.* **31:**3068-82.

Wiebe, H.A., Anlauf, K.G., Tuazon, E.C., Winer, A.M., Biermann, H.W., Appel, B.R., Solomon, P.A., Cass, G.R., Ellestad, T.G., Knapp, K.T., Peake, E., Spicer, C.W., Lawson, D.R. (1990). A comparison of measurements of atmospheric ammonia by filter packs, transition-flow reactors, simple and annular denuders and Fourier transform infrared spectroscopy. *Atmos.Environ.* **24A:**1019-28.

Williams, E.J., Sandholm, S.T., Bradshaw, J.D., Schendel, J.S., Langford, A.O., Quinn, P.K., LeBel, P.J., Vay, S.A., Roberts, P.D., Norton, R.B., Watkins, B.A., Buhr, M.P., Parrish, D.D., Calvert, J.G., Fehsenfeld, F.C. (1992). An intercomparison of five ammonia measurement techniques. *J.Geophys.Res.* **97:**11591-611.

Williams, K.R., Fairchild, C.I., Jaklevic, J. (1993). Dynamic mass measurement techniques. In *Aerosol Measurement: Principles, Techniques and Applications,* Willeke, K. and Baron, P.A., editors. Van Nostrand Reinhold, New York, NY. p. 296-312.

Wilson, J.C. and Liu, B.Y.H. (1980). Aerodynamic particle size measurement by laser-Doppler velocimetry. *Journal of Aerosol Science* **11:**139-50.

Wilson, J.C., Gupta, A., Whitby, K.T., Wilson, W.E. (1988). Measured aerosol light scattering coefficients compared with values calculated from EAA and optical particle counter measurements: improving the utility of the comparison. *Atmos.Environ.* **22:**789-93.

Winkler, P. (1974). Relative humidity and the adhesion of atmospheric particles to the plates of impactors. *J.Aerosol Sci.* **5:**235-40.

Winkler, P., Heintzenberg, J., Covert, D. (1981). Vergleich zweier Meβverfahren zur bestimmung der quellung von aerosolpartikeln mit der relativen feuchte. *Meteorol.Rdsch.* **34:**114-9.

Winklmayr, W., Reischl, G.P., Lindner, A.O., Berner, A. (1991). A new electromobility spectrometer for the measurement of aerosol size distribution in the size range from 1 to 1000 nm. *J.Aerosol Sci.* **22:**289-96.

Wiscombe, W.J. (1980). Improved Mie scattering algorithms. *Appl.Opt.* **19:**1505-9.

Woods, P.T. and Jolliffe, B.W. (1978). Experimental and theoretical studies related to a dye laser differential lidar system for the determination of atmospheric SO_2 and NO_2 concentrations. *Opt.Laser Techn.* 25-8.

Wyers, G.P., Otjes, R.P., Slanina, J. (1993). A continuous-flow denuder for the measurement of ambient concentrations and surface-exchange fluxes of ammonia. *Atmos.Environ.* **27A:**2085-90.

Yamamoto, M. and Kosaka, H. (1994). Determination of nitrate in deposited aerosol particles by thermal decomposition and chemiluminescence. *Analytical Chemistry* **66:**362-7.

Yeh, H.C. (1993). Electrical techniques. In *Aerosol Measurement: Principles, Techniques and Applications,* Willeke, K. and Baron, P.A., editors. Van Nostrand Reinhold, New York, NY. p. 410-25.

Zhang, S.H., Akutsu, Y., Russell, L.M., Flagan, R.C., Seinfeld, J.H. (1995). Radial differential mobility analyzer. *Aerosol Sci.Technol.* **23:**357-72.

Zhang, Z.Q. and Liu, B.Y.H. (1990). Dependence of the performance of TSI 3020 condensation nucleus counter on pressure, flow rate and temperature. *Aerosol Sci.Technol.* **13:**493-504.

Zhang, Z.Q. and Liu, B.Y.H. (1991). Performance of TSI 3760 condensation nuclei counter at reduced pressures and flow rates. *Aerosol Sci.Technol.* **15:**228-38.

Zhang, X.Q., Turpin, B.J., McMurry, P.H., Hering, S.V., Stolzenburg, M.R. (1994). Mie theory evaluation of species contributions to 1990 wintertime visibility reduction in the Grand Canyon. *JAWMA* **44:**153-62.

Zhao, Y., Hardesty, R.M., Gaynor, J.E. (1994). Demonstration of a new and innovative ozone Lidar's capability to measure vertical profiles of ozone concentration and aerosol in the lower troposphere. Report No. ARB-R-92-328**,** National Oceanic and Atmospheric Administration, Environmental Technology Laboratory, Atmospheric Lidar Division,

APPENDIX A: CONTINUOUS MEASUREMENT DATA SETS

This appendix provides a brief description of current aerosol characterization studies with collocated filter and continuous PM measurements, preferably chemical speciation. A description of study periods, sampling sites, sources affecting sites, composition of sampled aerosol, and measurements available for comparison are summarized.

A.1 Southern California Air Quality Study (SCAQS)

The SCAQS was conducted during the summer (06/19/87 to 09/03/87, with 5 episodes, 11 days total) and fall (11/11/87 to 12/11/87, with 3 episodes, 6 days total) periods. Meteorological, air quality, and visibility measurements were acquired simultaneously at more than 40 locations throughout California's South Coast Air Basin (Lawson, 1990). Aerosol and gaseous measurements at nine sites (termed "B sites") included:

- Hourly gaseous data (O_3, NO/NO_x, CO, and SO_2);
- Hourly meteorological data (temperature, dew point, wind speed, wind direction, and ultraviolet radiation intensity);
- Nephelometer measurements of light scattering;
- Five samples per episode day (4-, 5-, and 7-hour durations during summer and 4- and 6-hour durations during fall) for $PM_{2.5}$ and PM_{10} mass, chemistry, and precursor gases (HNO_3, NH_3, SO_2) (Chow et al., 1994a, 1994b); and
- Three samples per day during the summer and fall periods for carbonyl compounds and hydrocarbons (C_1 to C_{12}).

Continuous measurements of aerosol mass and chemistry included:

- Hourly PM_{10} mass measurements by beta gauge sampler;
- Hourly sulfur and sulfate measurements by continuous sulfur analyzer with flame photometric detector (FPD);
- Hourly organic and elemental carbon measurements by in-situ carbon analyzer;
- Hourly black carbon measurements by photoacoustic spectroscopy; and
- Hourly black carbon measurements by aethalometer.

A.2 1995 Integrated Monitoring Study (IMS95)

The IMS95 Study domain in central California extends from the city of Merced to south of Bakersfield and from the coastal mountains to 1,000 m elevation in the Sierra Nevadas. IMS95 included a 11/01/95 to 11/14/95 saturation monitoring network (the fall study) in the Corcoran/Hanford area and a 12/09/95 to 01/06/96 monitoring network (the winter study) that included saturation sampling for aerosols and reactive aerosol precursor gases, high-time-resolution aerosol measurements, fog chemistry measurements, surface- and upper-air measurements, and micrometeorological surface measurements. $PM_{2.5}$ tapered element oscillating microbalance (TEOM), PM_{10} and $PM_{2.5}$ beta attenuation monitor (BAM), 5-minute aethalometer, 5-minute nephelometer, 3-hour-average $PM_{2.5}$ and PM_{10} filter measurements under high-nitrate and high- and low-relative-humidity (RH) conditions with meteorological data are available (Chow and Egami, 1997).

- Hourly Optec NGN-2 nephelometer measurements (SWC, BFC, FEI and KWR) for particle light scattering (b_{sp}) from 12/09/95 through 01/06/96.
- Hourly meteorological data (12/09/95 to 01/06/96).
- Hourly visibility data (12/09/95 to 01/06/96).
- Hourly $PM_{2.5}$ TEOM at Bakersfield during winter study (12/09/95 to 01/06/96).
- Hourly collocated PM_{10} and $PM_{2.5}$ BAM, at Chowchilla during winter study (12/09/95 to 01/06/96).
- Daily 3-hour $PM_{2.5}$ and PM_{10} mass and b_{abs} (12/09/95 to 01/06/96).
- 3-hour $PM_{2.5}$ mass, light absorption (b_{abs}), and chemistry data for the three core sites (on selected 9 days).
- 3-hour PM_{10} mass, b_{abs}, chemistry data for the three core sites (on selected 9 days).

A.3 1997 Southern California Ozone Study (SCOS97) – North American Research Strategy for Tropospheric Ozone (NARSTO)

The SCOS97-NARSTO was conducted from 06/16/97 through 10/15/97 and consisted of extensive monitoring of emissions activity, meteorology, and air quality in Southern California (Motallebi et al., 1998). Filter-pack and continuous measurements of fine particles and precursor gases included:

- $PM_{2.5}$ and PM_{10} mass and chemistry measurements taken 5 times/day at 6 sites;
- $PM_{2.5}$ organic species measurements taken 5 times/day at 6 sites;

- Measurements of precursor gases (NH_3, HNO_3) with filter packs taken 5 times/day at 6 sites;

- Size-resolved measurements of aerosol (mass, ions, and carbon) by 8-stage Micro-Orifice Uniform Deposit Impactor (MOUDI) at 6 sites;

- Continuous $PM_{2.5}$ mass measurements by beta attenuation monitor (BAM), tapered element oscillating microbalance (TEOM, sandwich and desiccation prototypes) and continuous ambient mass monitoring system (CAMMS) at 1 site;

- Continuous particle number and size measurements by electrical aerosol analyzer (EAA), differential mobility particle sizer (DMPS), and optical particle counter (OPC) at 6 sites;

- Continuous size and chemical composition measurements by aerosol time-of-flight mass spectrometer (ATOFMS) at 6 sites;

- Continuous nitric acid and ammonia measurements by TECO 42CV analyzer, denuder diffusion method, and long-path Fourier transform spectrometer at 5 sites;

- Continuous light absorption measurements by aethalometer and continuous light scattering measurements with nephelometer at 3 sites; and

- Continuous nitrate measurements with automated particle nitrate monitor (APNM) at 1 site.

A.4 San Joaquin Valley Compliance Network

Bakersfield and Fresno sites with PM_{10} TEOM and BAM collocated with PM_{10} high-volume size-selective inlet (SSI), dichotomous, and California Acid Deposition Monitoring Program (CADMP) measurements (Watson et al., 1997b). San Joaquin Valley meteorological data other than 1995 is currently being processed and will be available from California Air Resources Board (CARB), Sacramento, CA.

- Hourly BAM PM_{10} network at four sites from 1994 to 1996.

- Hourly TEOM PM_{10} data at 30 sites (currently) from 1992 to 1996.

- Hourly nephelometer (b_{scat}) network data at 11 sites from 1991 to 1996.

- Hourly Coefficient of Haze data arranged by quarter at 43 sites during 1995.

- Hourly meteorological data averaged by quarter at 40 sites for 1995.

- Every-sixth-day 24-hour compliance PM_{10} SSI mass and chemistry data at 58 sites from 1991 to 1996.

- Every-sixth-day 12-hour mass, ion, and precursor gas data from California Acid Deposition Monitoring Program network at 11 sites from 1990 to 1996.

A.5 Imperial Valley/Mexicali Cross Border PM_{10} Transport Study

The ambient sampling program acquired PM_{10} measurements at two base sites in the U.S. and Mexico near the international border between 03/13/92 and 08/29/93, on an every-sixth-day sampling schedule. A saturation monitoring network consisting of 20 to 30 sampling sites was operated for the summer (08/21/92 to 08/27/92), winter (12/11/92 to 12/20/92), and spring (05/13/93 to 05/19/93) periods. Source emissions for fugitive dust, motor vehicle exhaust, field burning, charcoal cooking, and industrial sources were sampled and chemically characterized. The data were supplemented with: 1) hourly average BAM PM_{10} mass measured on the U.S. side of the border by the CARB, 2) high-volume SSI PM_{10} at sites in the cities of Brawley, El Centro, and Calexico, operated by the Imperial County Air Pollution Control District (ICAPCD), and 3) meteorological data from the California Irrigation Management Information System (CIMIS) and several industrial permitting stations located in Imperial County, California. Collocated PM_{10} SSI, BAM, dichotomous, sequential filter sampler (SFS), and Minivol portable PM_{10} survey sampler with meteorology was measured at the Calexico site (Chow and Watson, 1997a).

- Hourly BAM PM_{10} at the Grant Fire Station site from 03/07/92 to 08/29/93.

- Every-sixth-day dichotomous fine, coarse, and PM_{10} at the El Centro and Grant Fire Station sites from 01/01/92 to 08/29/92.

- Every-sixth-day TSP mass at the Laidlaw Environmental Services site from 01/04/89 to 06/29/91.

- Every-sixth-day high-volume SSI PM_{10} mass at the Brawley, Grant Fire Station, El Centro, and Calexico Police and Fire Station sites from 01/02/92 to 08/29/93.

- Every-sixth-day 24-hour portable PM_{10} mass, b_{abs}, and elements at the Calexico (Grant Fire Station) and Mexicali (SEDESOL) sites from 03/18/92 to 08/29/92.

- Every-sixth-day 24-hour SFS PM_{10} mass, b_{abs}, elements, and ions at the Calexico (Grant Fire Station) and Mexicali (SEDESOL) sites from 02/19/92 to 08/29/92, and daily during summer (08/21/92 to 08/27/92), winter (12/11/92 to 12/20/92), and spring (05/13/93 to 05/19/93) periods.

- Daily 24-hour PM_{10} mass, b_{abs}, and elements at the Calexico (Grant Fire Station) and Mexicali (SEDESOL) sites, and at 20 satellite sites during summer (08/21/92

to 08/27/92), winter (12/11/92 to 12/20/92), and spring (05/13/93 to 05/19/93) periods.

- Daily 6-hour, 4-times-per-day, SFS PM_{10} mass, b_{abs}, elements, organic and elemental carbon, and ions collected at the Calexico (Grant Fire Station) and Mexicali (SEDESOL) sites during summer (08/21/92 to 08/27/92), winter (12/11/92 to 12/20/92), and spring (05/13/93 to 05/19/93) periods.

A.6 Washoe County (Nevada) Compliance Network

Collocated SSI and BAM PM_{10} with meteorology at the Sparks (NV) Post Office site. This site was selected for its high wood smoke influence during the winter.

- Hourly meteorology and photochemical data from 1995 to 1997.

- Hourly BAM PM_{10} and collocated 24-hour high-volume SSI PM_{10} data from 1995 to 1997.

A.7 Las Vegas PM_{10} Study

The Las Vegas Valley PM_{10} Study was conducted during 1995 and 1996 to determine the contributions to PM_{10} aerosol from fugitive dust, motor vehicle exhaust, residential wood combustion, and secondary aerosol sources. In addition to monitoring with BAMs, 24-hour samples were taken at two neighborhood-scale sites every sixth day. Five week-long intensive saturation studies were conducted over a middle-scale subregion that contained many construction projects emitting fugitive dust (Chow and Watson, 1997b).

- Hourly PM_{10} data from 14 sites (including one compliance monitoring site with PM_{10} high-volume SSI, six compliance monitoring sites with BAMs, and seven special purpose sites with BAMs) from 01/03/95 to 01/28/96.

- Hourly meteorological data from 10-m towers at 17 sites from 01/03/95 to 01/28/96.

- Every-sixth-day 24-hour SFS PM_{10} data from two sites (one in Las Vegas, NV [East Charleston] and the other in North Las Vegas [Bemis]) from 01/03/95 to 01/28/96.

- Daily 24-hour battery-powered mini-volume portable survey sampler PM_{10} data from 30 satellite sites from 01/03/95 to 01/28/96 during the intensive monitoring period.

- PM_{10} elements, ions, and carbon on a selected subset of samples.

A.8 Northern Front Range Air Quality Study (NFRAQS)

The Northern Front Range Air Quality Study (Watson et al., 1998a, Chow et al., 1998b) was executed as three intensive field campaigns. These three field campaigns were;

- Winter 96 Campaign: This 44 day intensive field campaign was conducted between 01/16/96 and 02/29/96. This was a pilot study that was used to design the Winter 97 study. It also provides a contrast between different wintertime periods along the Northern Front Range. Measurements taken during this campaign include:
  - Hourly Optec NGN-2 measurements at one site;
  - Hourly particle light absorption by aethalometer at one site;
  - Upper air and surface meteorological measurements at seven sites; and
  - Daily $PM_{2.5}$, PM_{10}, nitric acid, and ammonia measurements of 3- to 24-hour durations at one site.
- Summer 96 Campaign: This 45-day intensive field campaign was conducted between 07/16/96 and 08/31/96. It was intended to provide baseline measurements for summer $PM_{2.5}$ and to provide a contrast to wintertime levels. Few detailed summertime particulate measurements are available from the Northern Front Range. Measurements taken during this campaign include:
  - Hourly PM_{10} BAM at one site;
  - Hourly Optec NGN-2 measurements at one site;
  - Hourly particle light absorption by aethalometer at one site;
  - Upper air and surface meteorological measurements at seven sites; and
  - Daily $PM_{2.5}$, PM_{10}, nitric acid, and ammonia measurements of 3- to 24-hour durations at three sites.
- Winter 97 Campaign: This 60-day intensive field campaign was conducted between 12/09/96 and 02/07/97 over a large domain along the Northern Front Range in Colorado. The most complete set of measurements was acquired during this period. Measurements taken during this campaign include:
  - Hourly particle light absorption by aethalometer at three sites;
  - Hourly light extinction by transmissometer at two sites;
  - Hourly nitrate measurements by automated particle nitrate monitor at one site;
  - Hourly total particle light absorption by photoacoustic spectrometer at one site;
  - Continuous scene measurements at five sites;

- Hourly PM_{10} BAM measurements at three sites;
- Hourly Optec NGN-2 measurements at five sites;
- Hourly $PM_{2.5}$ size cut NGN-2 measurements at two sites;
- Hourly $PM_{2.5}$ particle light scattering by TSI three-color nephelometer at one site; and
- Daily $PM_{2.5}$, ammonia, and nitric acid measurements of 3- to 24-hour durations at nine sites.

A.9 Mount Zirkel Visibility Study

Ambient measurements were taken for a one-year period from 12/01/94 through 11/30/95. Twelve-hour-average (0600 to 1800 MST) aerosol and sulfur dioxide filter sampling did not commence until 02/06/95 and continued every day through 11/30/95 at the Buffalo Pass, Gilpin Creek, and Juniper Mountian sites (Watson et al., 1996). Embedded in the annual measurements were three intensive monitoring periods. These included winter (02/06/95 to 03/02/95), summer (08/03/95 to 09/02/95), and fall (09/15/95 to 10/15/95). Morning (0600 to 1200 MST) and afternoon (1200 to 1800 MST) aerosol and sulfur dioxide measurements were taken a the Buffalo Pass, Juniper Mountain, Baggs, Hayden VOR, and Hayden Waste Water sites during these periods. Morning and afternoon denuder-difference filter-based measurements of nitric acid and ammonia precursor gases were acquired at the Buffalo Pass, Juniper Mountian, and Hayden VOR sites. Continuous sulfur dioxide, sulfate, and optical absorption measurements were taken during the intensives at the Buffalo Pass site.

- Hourly Optec NGN-2 nephelometer measurements from 12/01/94 to 11/30/95 at six sites.
- Hourly Magee Scientific aethelometer measurements from 12/01/94 to 11/30/95 at one site.
- Hourly meteorological measurements from 12/01/94 to 11/30/95 at eight sites.
- Hourly TSI three-color nephelometer measurements during summer (08/03/95 to 09/02/95) and fall (09/15/95 to 10/15/95) intensive monitoring periods at two sites.
- 12-hour $PM_{2.5}$ filter measurements for particle mass, light absorption, elements, ions, and carbon during annual period on selected days at three sites.
- 6-hour $PM_{2.5}$ filter measurements for particle mass, light absorption, elements, ions, and carbon during intensive monitoring periods on selected days at five sites.

A.10 Robbins Particulate Study

The Robbins Particulate Study (RPS) began in October 1996 will continue for five years in order to characterize $PM_{2.5}$ and PM_{10} mass and chemical concentrations, as well as source contributions in neighborhoods surrounding the Robbins Waste-to-Energy (WTE) power station (south Chicago, IL) (Watson et al., 1997c). BAM PM_{10}, collocated SSI PM_{10}, and dichotomous data at the Eisenhower site were assembled. Meteorological data was measured from the nearby Alsip site.

- Hourly wind measurements at the Alsip site from 10/01/95 to 09/30/96.
- Hourly BAM PM_{10} at the Eisenhower site from 01/0196 to 09/30/96.
- Every-sixth-day dichotomous and high-volume SSI PM_{10} and $PM_{2.5}$ at the Eisenhower site from 10/12/95 to 09/30/96.
- $PM_{2.5}$ and coarse elements, ions, and carbon on a selected subset of samples from the Alsip, Breman, Meadowlane, and Eisenhower sites.

A.11 Birmingham (Alabama) Compliance Network

- Hourly wind speed and wind direction data at the Birmingham Airport site from 1989 to 1992.
- Hourly TEOM PM_{10} and collocated SSI PM_{10} at the North Birmingham site during 1993.
- Every-sixth-day high-volume SSI PM_{10} data at the North Birmingham site from 1990 to 1995.

A.12 Mexico City Aerosol Characterization Study

The Mexico City Aerosol Characterization Study is a two-year study with a duration from 01/01/97 through 12/31/98. The first year consisted of planning and executing a major field study in Mexico City from 02/23/97 through 03/22/97. This study is a cooperative project sponsored by PEMEX through the Instituto Mexicano del Petroleo (IMP) and by U.S. Department of Energy (DOE) through national laboratories and universities (Watson et al., 1998b).

- Five-minute aethalometer measurements from 02/23/97 to 03/22/97 at two sites (Merced and Pedregal).
- Hourly nephelometer measurements from 02/23/97 to 03/22/97 at two sites (Merced and Pedregal).

- Hourly TEOM PM_{10} from 02/2/97 to 03/22/97 at ten RAMA particulate monitoring sites (Merced, Xalostoc, Pedregal, Tlalnepantla, Nezahuatcoyotl, Cerro de Estrella, Tultitlan, La Villa, Coacalco, and Tlahuac).

- Hourly temperature, relative humidity, and wind measurements from 02/23/97 to 03/22/97 at ten RAMA meteorological monitoring sites (Merced, Xalostoc, Pedregal, Tlalnepantla, Cerro de Estrella, ENAP Acatalan, Hangares, San Augustin, and Plateros).

- Daily 24-hour portable PM_{10} mass, b_{abs}, elements, ions, carbon, and ammonia from 03/02/97 to 03/19/97 at 25 satellite sites.

- Daily 6-hour PM_{10} mass, b_{abs}, elements, ions, and carbon from 03/02/97 to 03/19/97 at three super-core sites.

- Daily 24-hour PM_{10} mass, b_{abs}, elements, ions, and carbon from 03/02/97 to 03/19/97 at three core sites.